2019

ISSN 1512-1887

ANNALS OF AGRARIAN SCIENCE

Vol. 17 No. 2

EDITORIAL BOARD

Annals of Agrarian Science

Volume 17, Number 2, June 2019

Aims and Scope

The aim of "Annals of Agrarian Science" is to overview problems of the following main disciplines and subjects: Agricultural and Biological Sciences, Biochemistry, Genetics and Molecular Biology, Engineering, Environmental Science. The Journal will publish research papers, review articles, book reviews and conference reports for the above mentioned subjects.

ANNALS OF AGRARIAN SCIENCE

Volume 17, Number 2 June 2019

CONTENTS

Annals of Agrarian Science

Journal homepage: http://journals.org.ge/index.php

Application of Blue-green Alga Spirulina for removing Caesium ions from polluted water

M. Kurashvili*, G. Adamia, T. Varazi, G. Khatisashvili, G. Gigolashvili, M. Pruidze, L. Chokheli, S. Japharashvili

Durmishidze Institute of Biochemistry and Biotechnology of Agricultural University of Georgia, 240, David Agmashenebeli, Alley, Tbilisi, 0159, Georgia;

Received: 23 October 2018; accepted: 12 December 2018

A B S T R A C T

The presented work concerns studying a possibility of using blue-green alga (cyanobacteria) Spirulina (*Spirulina platensis)* for removal of Caesium ions form polluted waters. For this aim, tolerance of alga to Cs^+ ions, in particular, influence of different concentrations of heavy metal on ultrastructure of Spirulina cells, as well as on biomass production by Spirulina and chlorophyll accumulation in alga cells have been studied. According to obtained data, the highest concentration of Cs^+ (100 ppm) blocked biomass formation only by 25%, and the content of chlorophyll decreased by 20%. This concentration of heavy metal caused only an increase of hydrocarbons-containing space between lamella in Spirulina cells, which can be a result of accumulation of Cs^+ ions in alga cells. Thus, 100 ppm concentration of Cs^+ ions has been chosen for testing possibility of using Spirulina to clean artificially polluted water in the model large-scale experiment. The obtained data have shown that Spirulina has capability to assimilate up to 90% of Cs^+ ions from polluted water during 15 days. These results indicate that Spirulina is potentially useful for cleaning waters polluted with nonradioactive Cs^+ ions as well as with $^{137}Cs^+$ ions.

Keywords: Phytoremediation, *Spirulina platensis*, Water pollution, Heavy metals, Caesium ions, Radioactive and Stable Cesium.

*Corresponding author: Maritca Kurashvili, E-mail address: m.kurashvili@agruni.edu.ge

1. Introduction

Nowadays, water pollution by different chemicals especially by hazardous heavy metals and radionuclides is one of the most important ecological problem. Among them ^{137}Cs is very dangerous. Nonradioactive Caesium ions that occur in nature and are released into environment through mining and milling of ores, are only mildly toxic [1]. Both radioactive and stable cesium, when they occur in human or animal body, act the same way [2].

Presented work devotes to elaboration of method for cleaning water contaminated with Cs^+ ions by using blue-green alga Spirulina (*Spirulina platensis)*. Spirulina (*Spirulina platensis*) should have prospects for phytoremediation of waters polluted by different toxic compounds. Spirulina has unique chemical content and biological properties. This blue-green alga is characterized by reproduction and fast biomass formation in extreme conditions. Spirulina cells have rich content of proteins and peptides, and these compounds should be chelating ions of heavy metals. During the aging, the vacuoles of Spirulina cells inflate with air bubbles and as a result, Spirulina colonies float onto the water surface. As a result, Spirulina biomass will be easily (mechanically) separated from cleared water body after remediation. These factors have attracted our interest in Spirulina as to potential phytoremediator agent. It is known the information about using of algae for cleaning the environment polluted with such toxicants as heavy metals [3-

8], radioactive elements [9], fluoride ions [10] and others. There is only limited data concerning using Spirulina as a phytoremediator agent in case of water pollution with Cs^+ ions, but for this aim, Spirulina seems to have prospects, because there is a lot of information about heavy metals uptake processes by Spirulina [3-5].

In presented work, potential of Spirulina to uptake of Cs^+ ions from water solutions has been evaluated. For this aim, tolerance of alga to Cs^+ ions, in particular, the influence of different concentrations of heavy metal on ultrastructure of Spirulina cells, as well as on biomass formation and chlorophyll accumulation by Spirulina have been studied. According to the obtained data, the phytoremediation technology for cleaning of water polluted with Caesium based on application of Spirulina have been elaborated and tested via model experiments.

2. Materials and methods

2.1 Materials

The biomass of Spirulina platensis obtained via cultivation in standard Zarrouk's medium (pH – 8.7; content in g/L: $NaHCO_3$ – 16.8, K_2HPO_4 - 0.5, $NaNO_3$ – 2.5, K_2SO_4 – 1.0, NaCl – 1.0, $MgSO_4 \cdot 7H_2O$ – 0.2, $CaCl_2 \cdot 2H_2O$ – 0.04, $FeSO_4 \cdot 7H_2O$ – 0.01, EDTA – 0.08; and microelements kit A5 – 1 mL) were used in the experiments. Incubation was carried out with permanent air barbotage (rate of air flow 2 L/min), at temperature 25°C, and under following illumination conditions: a photoperiod of lighting 16L/8D (16 hours of light: 8 hours of dark), a total photosynthetic photon flux density (PPFD) of ≈15 μmol · m^{-2} · s^{-1}.

2.2 Methods

For measurement of fresh biomass productivity and chlorophyll formation by Spirulina, the following method was elaborated: the incubation medium was centrifuged at 1000 g during 20 min and obtained pellet was weighted. The obtained fresh biomass was treated by acetone and the content of chlorophyll was determined spectrophotometrically at 652 nm according to standard method [11].

The biomass of Spirulina in incubation medium have been measured spectrophotometrically at 750 nm [12].

The content of Cs^+ ions in the samples was determined by the method of atomic absorption (flame emission) analysis [13]. Conditions for analysis are the following: Instrument – PerkinElmer HGA900 Graphite Furnace; wavelength – 852.1 nm; slit – 0.2/0.4 nm; flame – air-acetylene; stock standard solution – CESIUM 1000 mg/L; light source – EDL; interfence – ionization controlled by addition of 0.1% KCl.

To study the influence of Cs^+ ions on cell ultrastructure, biomass of Spirulina was fixed in 2.5% glutaraldehyde and then in 1% OsO_4. After dehydration in ethanol of increasing concentrations, the samples were embedded in Epon–Araldite resin (1.5: 1.0) and poured into gelatin capsules [14]. Thin serial sections (50–60 nm) were made using an LKB III ultra-microtome, stained with 2% uranyl acetate, and analyzed by electron microscope Tesla BS 500 (Czech Republic) (specifics, transmission; resolution, 0.8 nm).

2.3 Experimental design

For estimation of influence of different concentrations of Cs^+ on growing parameters of Spirulina, alga was cultivated in standard Zarrouk's media (volume 50 mL) containing different concentrations of Cs^+ (1, 10 or 100 ppm). The initial biomass of Spirulina was 3-4 g/L. The incubation was carried out in flasks during 72 h (120 h for ultrastructural investigations), at temperature 25°C, without air barbotage, a photoperiod of lighting 16L/8D, PPFD ≈15 μmol · m^{-2} · s^{-1}. After incubation the biomass productivity by Spirulina and chlorophyll content in cells by above mentioned methods were determined. The ultrastructure analysis was carried out in same samples.

The model large-scale experiment was carried out in following conditions: Spirulina was preliminary growing in Zarrouk's medium (volume 20 L) and after 7 days 20 L of Cs^+ containing solution was added. The volume of incubation medium in the beggining of incubation of Spirulina with Cs^+ was 40 L. At that moment, the biomass of Spirulina was 3.5 g/L and Cs^+ concentration was 100 ppm. The incubation was carried out in a glass container with sizes 60 x 21 x 40 (in cm, length x width x height), with permanent air barbotage (rate of air flow 2 L/min), at temperature 25°C, under following illumination conditions: a 24-h lighting (24L/0D), PPFD ≈15 μmol · m^{-2} · s^{-1}. In the control variant instead of Cs^+ solution 20 L of water was added. The content of Cs^+ ions and biomass of Spirulina were determined after 5, 10 and 15 days from addition of heavy metal ions.

3. Results and Discussion

3.1. The influence of Cs^+ on Spirulina cells

The influence of different concentrations of Caesium ions (1, 10 and 100 ppm) on biomass and chlorophyll accumulation by Spirulina has been studied. The obtained results are given in Fig. 1.

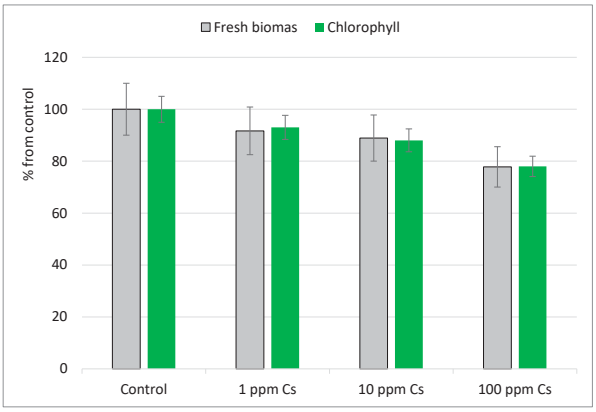

Fig. 1. *The influence of different concentrations of ceasium ions on biomass formation and chlorophyll accumulation by Spirulina. Incubation conditions are described in part 2.3.*

According to the obtained results, low concentrations of heavy metal revealed insignificant effect on Spirulina vital processes - reduction of biomass formation (by 5-6%) and chlorophyll content (by 8-9%). The high concentration of Cs^+ (100 ppm) blocked biomass production by 25%, and the content of chlorophyll decreased by 20%. According to the obtained results, Spirulina revealed tolerance to all tested concentrations of Cs^+ ions.

3.2. Study of penetration and localization of Cs^+ in Spirulina

On the next stage, the influence of Cs^+ ions on ultrastructure of Spirulina cells using electron microscopic method has been studied (Fig. 2 A-D).

As Fig. 2 shows, the influence of the highest concentration of Cs^+ ions (100 ppm) caused only an increase of hydrocarbons-containing space between lamella in Spirulina cells, which can be a result of accumulation of heavy metal ions. Thus, 100 ppm concentration of Cs^+ ions has been chosen for the model experiments.

3.3. The results of model experiment

The model experiments for elaboration new approach of phytoremediation technology for cleaning water polluted by Cs^+ ions have been carried out. For this aim, Spirulina cultivated in water artificially polluted with 100 ppm Cs^+ ions. The obtained data are given in Fig. 3.

As it seen from Fig. 3, Spirulina has capability to assimilate up to 90% of heavy metal ions from polluted water during 15 days. At the same time biomass of alga decreases by 25%. These results indicate that Spirulina is potentially usable for cleaning of waters polluted with nonradioactive Cs^+ ions as well as with $^{137}Cs^+$ ions.

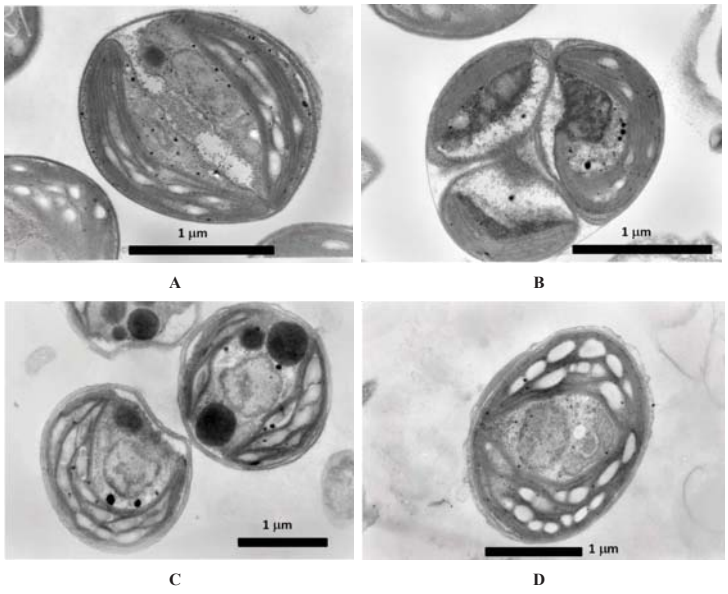

Fig. 2. *Electron micrographs of cells of Spirulina, cultivated on Zarrouk's medium without Cs^+ ions (A and B), and with 100 pm of Cs^+ ions. Incubation conditions are described in part 2.3.*

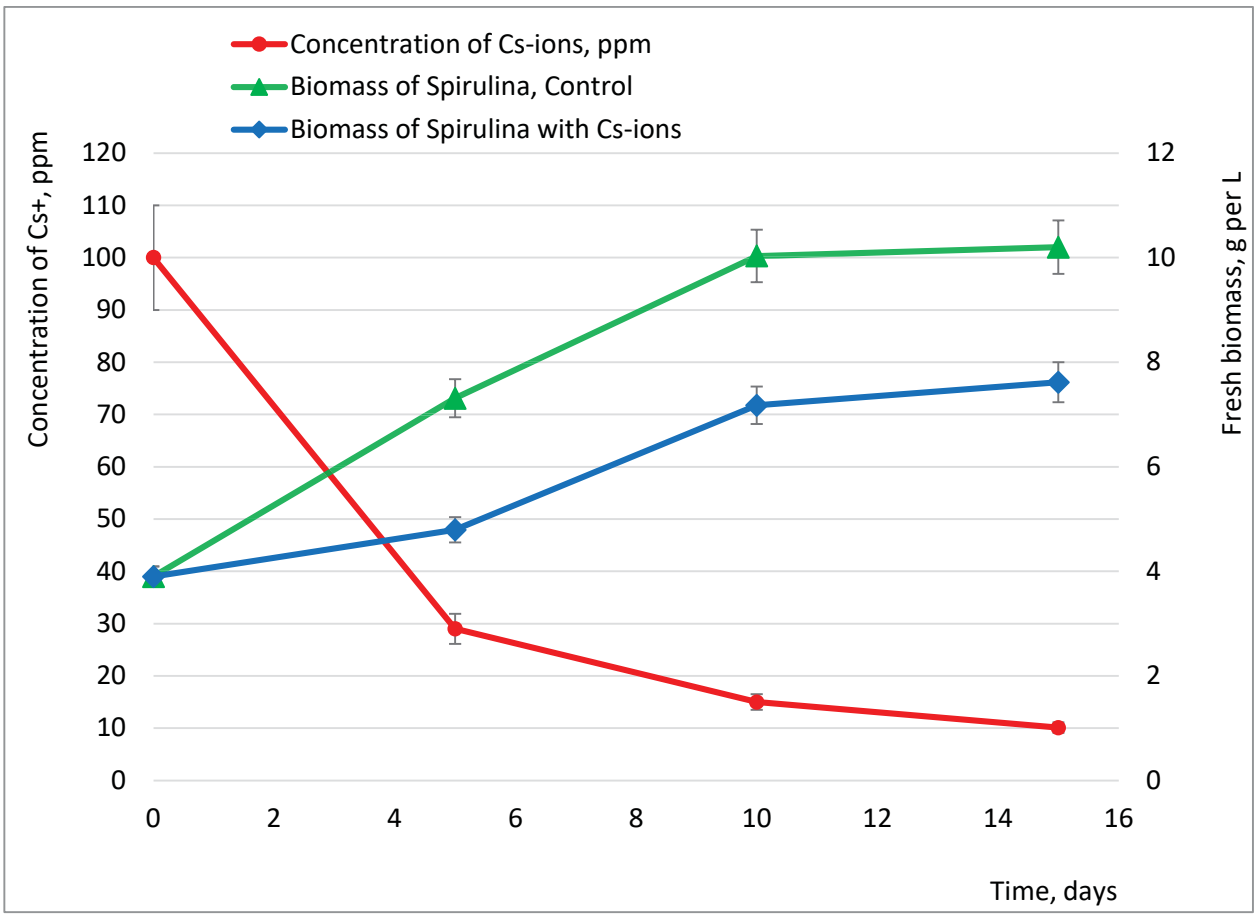

Fig. 3. *The results of model experiment for cleaning Cs^+ containing water by using Spirulina. The conditions of experiment are described in part 2.3.*

5. Conclusions

Thus, the work carried out has shown that Spirulina cells have an ability to effectively remove Cs^+ ions from artificially polluted water. These results can become a basis for development of a new phytoremediation technology for cleaning waters polluted with radioactive Caesium ions ($^{137}Cs^+$) based on application of Spirulina.

6. Acknowledgment

This work was supported by Shota Rustaveli National Science Foundation (SRNSF), with cofounding by Georgian Agricultural University - Applied Research Grant # 216944 and SRNSF - CNR # 04/51.

References

[1] C. Pinsky, R. Bose, J.R. Taylor, J. McKee, C. Lapointe, J. Birchall, Cesium in mammals: Acute toxicity, organ changes and tissue accumulation, ". J. Environ. Sci. Health. Part A, 16 (1981) 549–567.

[2] J. Rundo, A Survey of the Metabolism of Caesium in Man, British J. Radiol. 37 (1964) 108–114.

[3] A. Ahmad, R. Ghufran, Z.A. Wahid, Cd, As, Cu, and Zn Transfer through Dry to Rehydrated Biomass of Spirulina *Platensis* from Wastewater, Polish J. Environ. Stud. 19 (2010) 887-893.

[4] H. Chen, S. Pan, Bioremediation potential of spirulina: toxicity and biosorption studies of lead, J. Zhejiang Univ. Sci. B. 6 (2005) 171-174.

[5] O. Murali, S. Mehar. Bioremediation of heavy metals using Spirulina. Int. J. Geology, Earth and Environ. Sci. 4 (2014) 244-249.

[6] K. Suresh Kumar, H.-U. Dahms, E.-J. Won, J.-S. Lee, K.-H. Shin, Microalgae – A promising tool for heavy metal remediation, Ecotoxicol. Environ. Saf. 113 (2015) 329–352.

[7] A.H. Mahvi, Cadmium Biosorption from Wastewater by Ulmus Leaves and Their Ash, Europ. J. Scient. Res. 23 (2008) 197-203.
[8] A. Maleki, A.H. Mahvi, M.A. Zazouli, H. Izanloo, A.H. Barati, Aqueous Cadmium Removal by Adsorption on Barley Hull and Barley Hull Ash, Asian J. Chem. 23 (2011) 1373-1376.
[9] S. Fukuda, K. Lwamoto, M. Asumi, A. Yokoyama, T. Nakayama, K. Ishida, I. Inouye, Y. Shraiwa, Global searches for microalgae and aquatic plants that can eliminate radioactive cesium, iodine and strontium from the radio-polluted aquatic environment, J. Plant Res. 127 (2014) 79-89.
[10] M.A. Zazouli, A.H. Mahvi, S. Dobaradaran, M. Barafrashtehpour, Y. Mahdavi, D. Balarak, Adsorption of fluoride from aqueous solution by modified Azolla filiculoides, Fluoride 47 (2014) 349-358.
[11] D.I. Arnon, Copper enzymes in isolated chloroplasts, Polyphenoxidase in Beta Vulgaris. Plant Physiol. 24 (1949) 1-15.
[12] C. Butterwick, S.I. Heaney, J.F. Talling. A comparison of eight methods for estimating the biomass and growth of planktonic algae, British Phycol.J., 17, (1982) 69-79.
[13] L.V. Guba, I.I. Dovgyy, M.A. Rizhkova, Method of measuring of cesium by flame emission photometry method. Scientific Notes of Taurida V.Vernadsky National University. Series: Biol. Chem. 25 (2012) 284-288.
[14] O. Buadze, T. Sadunishvili, G. Kvesitadze, The effect of 1,2-benzanthracene and 3,4-benzpyrene on the ultrastructure of maize cells, Int. Biodeter. Biodegr. 44 (1998) 49–54.

Annals of Agrarian Science

Journal homepage: http://journals.org.ge/index.php

Quality assessment of the aquatic habitat of mountain streams in the period of minimal flow using the ichthyofauna as a bioindicator

Zuzana Štefunková[a*], Viliam Macura[a], Igor Kondé[b]

[a]Department of Land and Water Resources Management, Faculty of Civil Engineering, Slovak University of Technology Bratislava, 11, Radlinského, Bratislava, 813 68, Slovak Republic

[b]Department of Landscape Engineering, Faculty of Horticulture and Landscape Engineering, Slovak University of Agriculture in Nitra, 7, Tulipánová, Nitra, 949 76, Slovak Republic.

Received: 22 February 2019; accepted: 14 May 2019

A B S T R A C T

This paper describes the IFIM methodology (Instream Flow Incremental Methodology) for determining the minimum discharge, which, in addition to hydrological parameters, takes hydraulic, morphological and ichthyologic parameters into account as well. The basic principle of the method is the relationship between the fish population and its habitat, i.e., that most fish species prefer certain combinations of depths, stream velocities, and bed materials. If the values for a species living in a section of the river investigated are known, the minimum discharge for each fish species may be determined. This method was verified on reference sections of the Teplá River in the town of Sklené Teplice.

Keywords: IFIM Method (Instream Flow Incremental Methodology), Low flow characteristics, Stream Regulation, Abundance, Bioindication, Ichthyomass, WUA - Weighted Usable Area.

*Corresponding author: Zuzana Štefunková; E-mail address: zuzana_stefunkova@stuba.sk

Introduction

In Europe, it is gradually becoming a standard to model the ecological water quality based on the Instream Flow Incremental Methodology (IFIM) [1]. IFIM is an interdisciplinary decision-making system that assists landscape engineers to consider the benefits and consequences of different water management solutions [2]. IFIM methodology was developed in the United States by the U.S. Fish and Wildlife Service (USFWS) to determine the effect of water management projects on the natural environment by quantifying the aquatic environment [3,4]. The basis of the IFIM methodology is the Physical Habitat Simulation System (PHABSIM), which is used to analyse the relationship between the flow and biotic components of the environment. This relationship is a continuous flow function [5]. This method can also be used to predict the impact of climate change on the quality of the aquatic habitat [7]. Climate change has a negative impact on the biota of the flow similarly as contamination of flow [7].

The quality of the aquatic habitats of mountain and piedmont streams was evaluated using the Instream Flow Incremental Methodology (IFIM) decision-making tool. IFIM is based on the knowledge that most fish species prefer certain combinations of water depths, flow velocities [8, 9], availability of cover, and bed materials [10]. IFIM can provide robust assessments of the quality of a river when sufficient data are available. One of the most considerable advantages of IFIM over alternative methods (CCA, RDA, GLM, and related-analyses) is the fact that it incorporates a spatially distributed model in any desired detail.

In the case of morphological changes, the biotic component of the environment represents fish as

the most crucial element standing at the top of the food pyramid of aquatic biota. Because of their longevity, their mobility and their sensitivity to habitat modification, fish are good bioindicators [11-13], and they are often used for the assessment of the ecological integrity of rivers [11, 14-16].

In the IFIM methodology, the basic parameters of the flow habitat are divided into abiotic and biotic. A more detailed analysis between abiotic and biotic characteristics is given in the basic abiotic characteristics are depth and flow velocity. The relationship of the abiotic and biotic characteristics of the aquatic area is represented by the suitability curves of individual fish species. A detailed analysis of the relation of the suitability curves to the hydraulics of flow was confirmed mainly in relation to the flow depth [17]. The river regulation changes mainly the morphology of the river bed, which is reflected in the change in depth and flow velocity. For this purpose, the Riverine HABitat Simulation model (RHABSIM) is used to generate quantitative results representing the quality of the aquatic habitat. Habitat quality is determined by depth and velocity parameters, which are derived from suitability curves that represent habitat preference for individual fish species [18]. The habitat quality is represented by the WUA -Weighted Usable Area. WUA expresses the functional relationship between the flow and the surface of the flow.

The following procedure was chosen for the determination of the quality of the aquatic habitat for reference sections of 20 different representative Rivers in Hron River basin:

- measurement of topographic parameters of the reference sections,
- measurement of the velocity field,
- evaluation of the grain-size distribution of the bottom material,
- ichthyological research,
- evaluation of the results in the IFIM model.

The results of the measurements were then evaluated for the selected reference sections of the Teplá River in the town of Sklené Teplice using the RHABSIM model and then compared with the model developed by the authors of this paper.

Topographic measurement of the reference sections

The topography of the reference sections was characterized by cross-sections set at fixed points, which permitted the repeating of measurements in the same profile. The measurements were made by leveling, which has a higher precision for hydraulic modeling.

Measurement of the velocity field

The discharge was measured in a representative measuring profile using hydrometric devices. The velocity field was set by point measurements in each cross section. The distance between the verticals ranged from 1 to 2 meters. The measurement was made in within the ichthyological survey and then separately for different water stages to verify the hydraulic model.

Grain-size distribution of the bottom material

The grain size was analyzed using a sieve directly in the field. Sieves with circular meshes were used. The weight of the samples ranged from 120 kg to 240 kg.

Ichthyological survey

The reference sections of the rivers were blocked at each end by nets with a mesh size of 10x10 mm. Fish were caught using an electric aggregate and put afterward into a fish tank located in the river below the lower net, beyond the reach of the electric field. Three catches were made in each of the blocked sections, whereby the second and third catches were made 45 minutes after the previous ones. After each catch, every fish species was counted separately, and the fish were measured, weighed and let out into the river below the last net. The calculated values, combined with the mean weight of the respective species, were applied to the calculation of the biomass of the individual species and total ichthyomass. At the same time, the mean weight of each species was calculated, and this weight was compared with the number of fish in each of the length groups.

The abundance expresses the number of fish of the respective species. The abundance is given in fish per hectare; the ichthyomass expresses the aggregate weight of the entire fish population and is given in $kg.ha^{-1}$.

Results and discussion

We tried to confine ourselves to an examination of the quantifiable basic parameters of a river, which

would implicitly include ecologically relevant information. The width, depth, water level area, velocity field, water temperature and characteristics of the ichthyic fauna as indicators of the quality of the biological environment in a river may be considered as the basic parameters of a river.

An analysis of the morphometric, hydraulic and ichthyological parameters has been made for all selected reference sections in the Hron River basin. This paper contains the basic results obtained from the reference sections of the Teplá River in the town of Sklené Teplice.

Basic characteristics of the Teplá River

Catchment area = 172 km^2, stationing 127 km. Water gauge altitude = 287.00 m above sea level, $Q_{max\ (1941\text{-}2017)}$ = 72 m^3.s^{-1}, $Q_{min\ (1941\text{-}2017)}$ = 0.17 m^3.s^{-1}.

Table.1. *Overrun of average daily discharges*

M-days	30	90	180	270	330	335	364
Discharge [m^3.s^{-1}]	5.65	2.73	1.52	1.05	0.68	0.53	0.32

Water quality in the Teplá River in the town of Sklené Teplice

In the profile situated in the town of Sklené Teplice, the effect of the local municipal pollution was demonstrated by the usual increase in the number of coliform (class IV - fairly clean) and psychrophile bacteria (class V - waters are not classified in class 1-4), especially in 2016. The organic pollution expressed by BOD already exceeds the class II (very clean) limit value. COD-Mn remains in class II of the classification under standard ČSN 75 7221. The dissolved oxygen complies with class I (extra clean). The biological activity of the river expressed by the saprogenic index of biosestone corresponds to class III (medium clean).

Characterization of the riverbed of the reference sections of the Teplá River

Three reference sections were chosen on the Teplá River in the town of Sklené Teplice, and these sections follow one another; therefore, they may be documented in one longitudinal section. The numbering of the sections is identical with the designation of the cross sections; hence, the sections are numbered upstream.

Section No. 1 is in the town of Sklené Teplice. It is 52.58 m long (the stationing of the section in figure 1 starts at 0.00 and ends at 52.58 m). The riverbed bottom is dissected only to a small extent with unmarked alterations of the depth; it consists of gravel sand. This section represents the flow area. The topography of the riverbed bottom in all three sections is partially documented by the longitudinal section in figure 1.

Section No. 2 is 83 m long (the stationing of the section in figure 1 starts at 52.58 and ends at 135.60 m). The riverbed bottom is dissected; trees and shrubs cover the banks. This section represents the flow shadow area.

Section No. 3 is 33.3 m long (the stationing of the section in figure 1 starts at 135.60 and ends at 168.90 m). The riverbed bottom is dissected only to a small extent. Trees and shrubs cover the banks. The longitudinal slope of the water level is large (0.93%), which means greater flow velocities and small depths. This section represents the fording area with small depths and higher flow velocities.

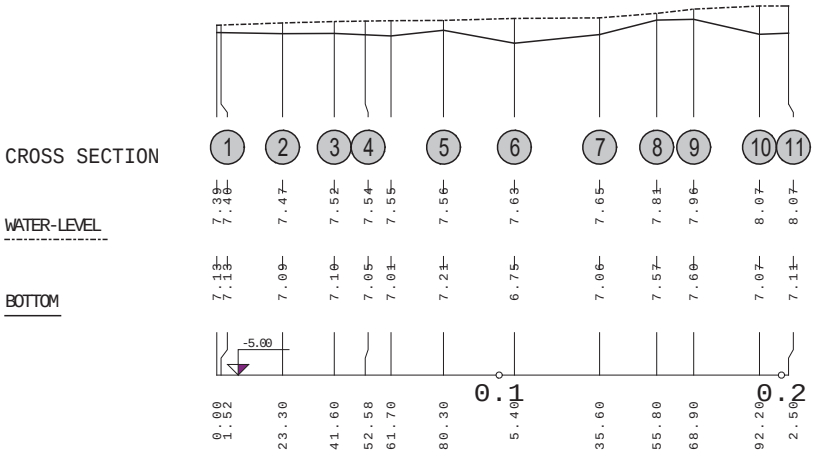

Fig. 1. *Longitudinal section of reference sections 1-3 of the Teplá River in the town of Sklené Teplice*

Basic abundance and ichthyomass data are given in Figures 2 and 3; the list of fish found in the reference sections of the Teplá River is given in Table 2.

Table 2. *List of fish species found in the reference sections of the Teplá River*

Fish name	Scientific name
Barbel	Barbus barbus
Brown trout	Salmo labrax m.fario
Chub	Leuciscus cephalus
Eel	Anguilla anguilla
Grayling	Thymallus thymallus
Gudgeon	Gobio gobio

Fish name	Scientific name
Minnow	Phoxinus phoxinus
Perch	Perca fluviatilis
Picke	Exox lucius
Roach	Rutilus rutilus
Spirling	Alburnoides bipunctatus
Stoneloach	Barbatula barbatula

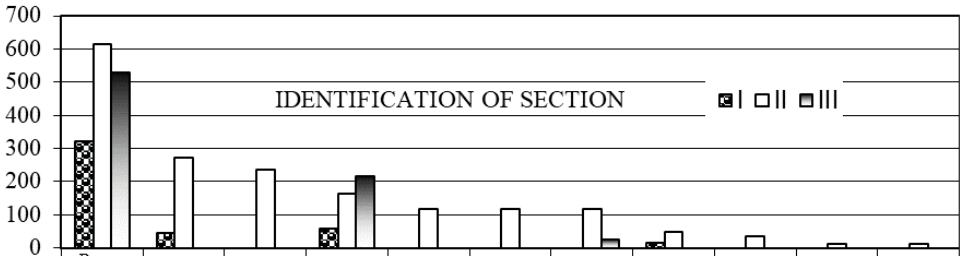

	Brown trout	Grayling	Spirling	Stoneloch	Chub	Gudgeon	Minnow	Roach	Barbel	Eel	Picke
I	323	44	0	59	0	0	0	15	0	0	0
II	614	272	236	165	118	118	118	47	35	12	12
III	529	0	0	217	0	0	24	0	0	0	0

Fig. 2. *Abundance [fish.ha^{-1}] in the reference sections of the Teplá River in the town of Sklené Teplice*

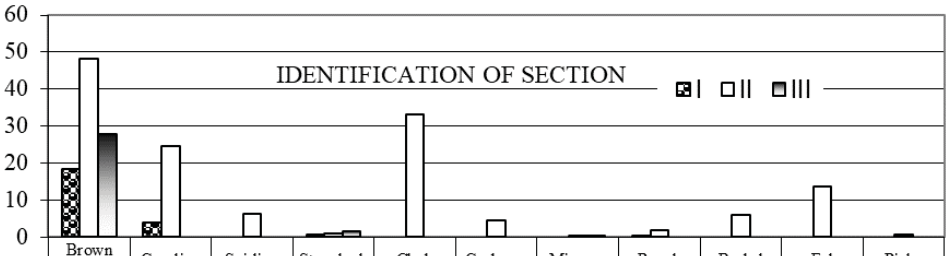

	Brown trout	Grayling	Spirling	Stoneloch	Chub	Gudgeon	Minnow	Roach	Barbel	Eel	Picke
I	18.4	4	0	0.7	0	0	0	0.4	0	0	0
II	48.3	24.7	6.2	1.1	33	4.4	0.14	1.7	6	13.6	0.8
III	27.8	0	0	1.4	0	0	0.03	0	0	0	0

Fig. 3. *Ichthyoses [kg.ha^{-1}] in the reference sections of the Teplá River in the town of Sklené Teplice*

Hydraulic and topographic parameters of the reference sections in the Teplá River in the town of Sklené Teplice

The hydraulic model of all reference sections was developed in a two-dimensional program. The purpose of the model was to complement the velocity field and water level for the selected discharges.

The velocity field of the reference sections in the Teplá River in the town of Sklené Teplice was measured twice: 20th July 2017, at a discharge of 1.85 m^3.s^{-1} and on 7th September 2017, at a discharge of 0.5 m^3.s^{-1}. Two discharges were modeled: 0.32 m^3.s^{-1} (Q_{365} = 0.32 m^3.s^{-1}) and 0.15 m3.s-1 ($Q_{min\ (1941\text{-}1997)}$ = 0.17 m^3.s^{-1}). The basic hydraulic characteristics, water depth, and the velocity field, for reference sections 1 to 3 at a discharge of 0.5 m^3.s^{-1} are shown in Figure 4.

The expected hydrobiological changes in the river may be simulated by changing the basic hydraulic parameters using the suitability curve.

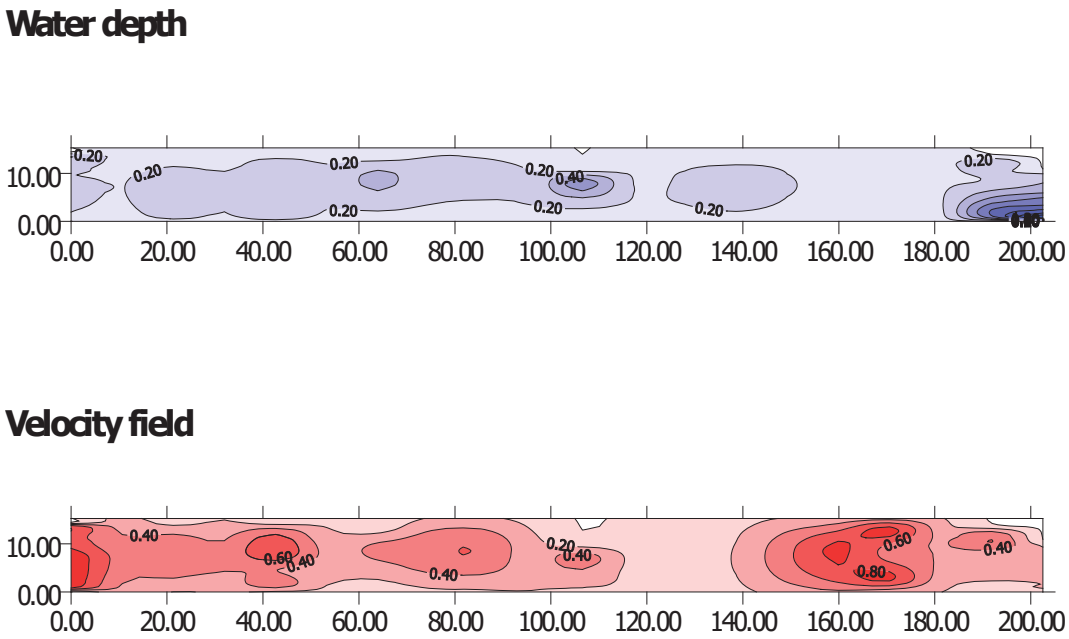

Fig. 4. *Water depths [m] and flow velocities [m.s^{-1}] in the reference sections Teplá River in the town of Sklené Teplice*

Habitat Suitability Curves

The Habitat Suitability Curves (HSCs) represent the main abiotic components of the microhabitat (flow velocity, water depth, and hiding places) preferred by the individual fish species. HSCs express a preference of each species for various habitats. The curves are based on the assumption that every fish species prefers certain combinations of abiotic environmental parameters [19]. Suitability curves for the Teplá River for water depth are given in figure 5.

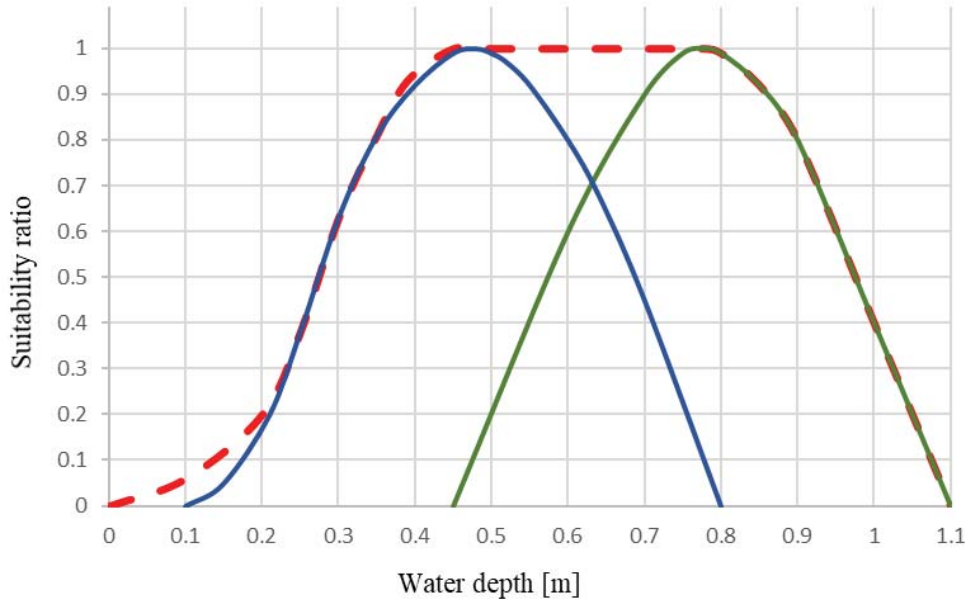

Fig. 5. *Suitability curves of brown trout (salmo trutta m. fario) for the water depth evaluated at two discharges (blue at 0.03 m^3.s^{-1} and green at 1.5 m^3.s^{-1}) with the generalized curve (red dashed)*

Evaluation of the relation between the depth, velocity and water level area

The relation between the depth, velocity and water level area was quantified using two methods.

First method was a method of means of the RHABSIM software, which simplifies the evaluation of parameters. Depths and velocities are evaluated independently; therefore, the results remain constant from one river profile to another (two-dimensional solution model). The depth and velocity values are multiplied individually by parameters from the suitability curves for the individual fish species, while when applying the second method, these values are multiplied by one value, which is the intersection of the depth and flow velocity with a standard weight.

The second method was developed by the authors of this paper, mainly as a reference method for the verification of standard models; therefore, accuracy was the primary criterion. The modeling of the habitat's degree of accessibility is based on the physical essence of the individual phenomena without simplification. It may be assumed that the results of such a model are of high quality and are substantially suitable for the verification of other models; therefore, in the further text, the term of the reference model for this methodic will be used. The measurement and hydraulic modeling results are not evaluated two-dimensionally, but as a three-dimensional contour plan, which was used for the evaluation of the velocity field and water depth intersection areas at a specific flow. The intersection areas were corrected by the parameters of the suitability curves with the same weight. The evaluation of the habitat quality assumes that a function defined as WUA may characterize the degree of accessibility of the physical habitat of the targeted fish species. WUA for the reference section of Teplá River in the town of Sklené Teplice is given in figure.

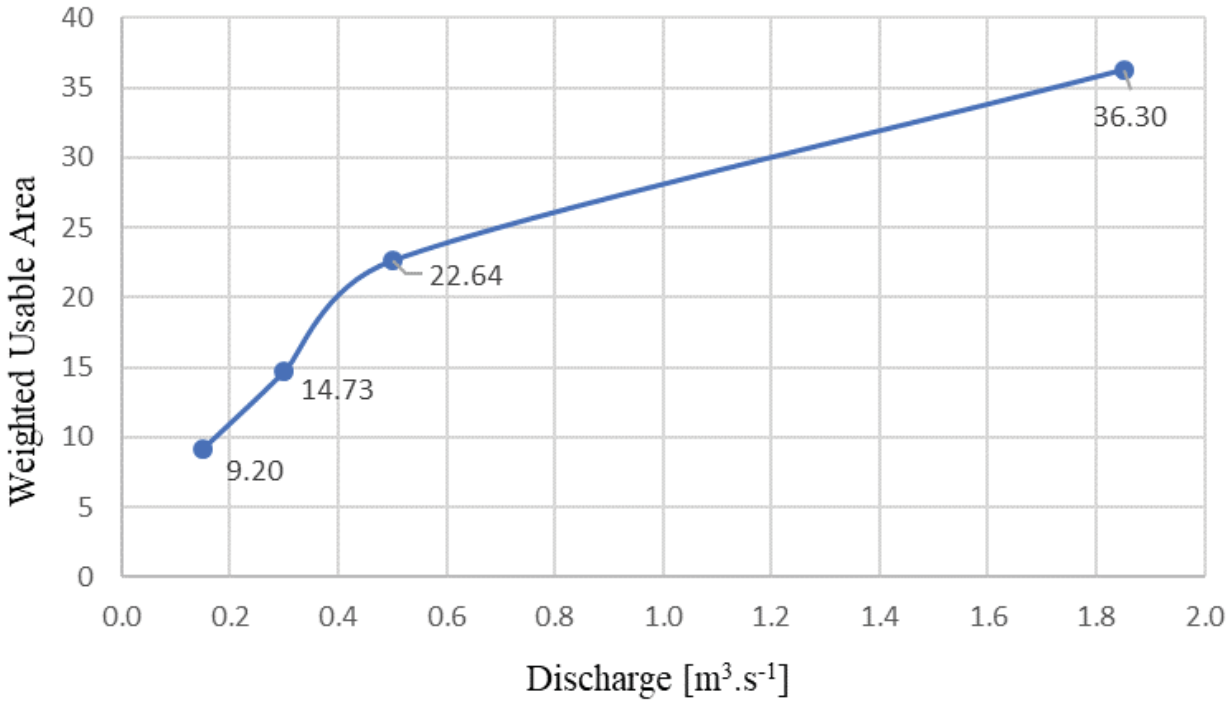

Fig. 6. *The weighed usable area (WUA) as a function of discharge [$m^3.s^{-1}$] in reference section for the brown trout*

Comparison of the results of the evaluation of the weighed usable area (WUA) by two methods

An evaluation of the quality of habitat assumes that the degree of accessibility of the physical habitat of targeted fish species may be characterized by a function that is defined as the weighted usable area (WUA). The quantification of the relation between the depth, velocity and water level area was used as the basis for an evaluation of the weighed usable area – WUA for the individual fish species.

WUA values obtained by both methods vary. It is necessary to remember that the WUA value represents the qualitative depiction of the biota development in a watercourse depending on the discharge, morphology or other parameters; therefore, the WUA development trend which is maintained is decisive. This is also documented by figure 7, which depicts the evaluation of the WUA curve by both methods, whereby the RHABSIM model values are corrected, i.e., reduced by the average difference between the results obtained by both methods. It may be anticipated that in the case of small watercourses with considerable differences in velocities and depths, more significant differences in the trend could occur; in this case, it is useful to verify or confirm the trend, even by the reference method.

Results and discussion

When applying the described method, it is necessary to bear in mind that fish are characterized by high variability, just as are all living organisms. Some limits determine their habitats and their behavior in these habitats, but these are quite extensive and do not enable the making of an unambiguous decision. This also leads to the conclusion that the parameter of channel should not be designed in a general manner but has to be determined individually for each river.

The following recommendations for the determination of the effect of the discharge and a riverbed's nature on the biological environment of a river may be formulated from the results obtained:

- The number of reference sections should be representative of the habitats existing in the section in question. We recommend that the reference sections and the percentage of represented habitats be selected based on the tachometric survey of the section of interest and be specified in the field together with ichthyologists.
- The collection of hydraulic and ichthyological data should be done simultaneously, and the hydrometric measurement of the velocity field for the verification of the hydraulic model should be performed as soon as possible; an ichthyological survey is not necessary for this measurement.
- The RHABSIM method objectively features the WUA development trend; the evaluation based on the methodology characterized in second method is appropriate only in controversial cases.
- We recommend evaluating WUA by the RHABSIM model, especially for the hydraulic module, which is optimized for modeling in the area of minimum discharges, but also for trouble-free communication of the individual modules.

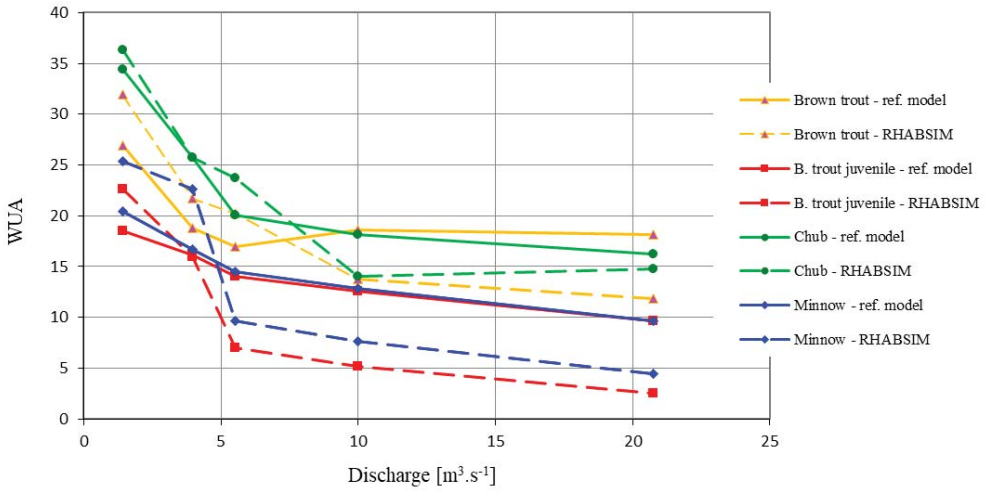

Fig. 7. *Comparison of WUA trends evaluated by both methods*

Based on the research results we may state that the method represents a new qualitative stage in determining the effect of the discharge and riverbed's nature (including technical work done within the river regulation) on biological alteration in an aquatic area despite the fact, that only a limited number of environmental factors (dissection of the riverbed, velocity field, river bed grain-size distribution, ichthyological survey) were evaluated.

Summary

The measurements made in the reference sections of the Teplá River demonstrated that the relation between the fish population and characteristics of the habitat gives a real picture of the changes induced by the topography of the riverbed (for instance by river regulations) and by discharge. The main advantage of the IFIM methodology is that it quantifies biological changes in the river as a function of the WUA and discharge through fish, which are bioindicators of environmental quality. In this way, quantitative data for experts on biotic and abiotic environments may be obtained. These experts can then establish an ecological flow or the parameter of flow restoration more objectively.

Acknowledgement

This study has been jointly supported by the by the Scientific Grant Agency under Contract No. VEGA 1/0068/19 and VEGA 1/0632/19.

References

[1] Bovee, K. D., Lamb, B. L., Bartholow, J. M., Stalnaker, C. B., Taylor, J. & Henriksen, J. Stream Habitat Analysis Using the Instream Flow Incremental Methodology. Information and Technology Report USGS/BRD/ITR-1998-0004. Fort Collins, CO: U.S. Geological Survey BRD, 1998.

[2] Hawkins, C.P., Kershner, J.L, Bisson, P.A., Bryant, M.D., Decker, L.M., Gregory, S.V., Mcculloch, D.A., Overton, C.K., Reeves, G.H., Steedman, R.J., Young, M.K. A hierarchical approach to classifying stream habitat features. *Fisheries,* 18 (6) (1993) 3–12.

[3] Annear, T., Chisholm, I., Beecher, H., Locke, A. Instream flows for riverine resources stewardship. Revised edition. Wyoming: Cheyenne, Instream Flow Council, 2004.

[4] Tharme, R. E. (2003) A Global Perspective on Environmental Flow Assessment: Emerging Trends in the Development abd Application of Environmental Flow Methodologies for rivers. River Research and Applications, 19 (2003) 397 – 441.

[5] Stalnaker, C., Lamb, B. L., Henriksen, J., Bovee, K., Bartholow, J. The Instream Flow Incremental Methodology. A primer for IFIM. U. S. National Biological Service. Biological Science Report 29, 1995.

[6] Mikautadze,D., Kvabziridze, M. Climate of Imereti in 2010 against a Background of Global Warming. Bulletin of the Georgian National Academy of Sciences, vol. 9, no. 2 (2015) 136-140.

[7] Surmava, A., Intskirveli, L., Buachidze, N. Numerical Simulation of Distribution of Contaminants Discharged to Kura River. Bulletin of the Georgian National Academy of Sciences, vol. 9, no. 1 (2015) 165-170.

[8] Ayllón, D., Almodóvar, A., Nicola, G.G., Elvira, B. Interactive effects of cover and hydraulics on brown trout habitat selection patterns. River Res. Appl. 25 (8) (2009) 35-43. http://dx.doi.org/10.1002/rra.1215.

[9] Ivan, P., Macura, V., Štefunková, Z., - Škrinár, A., Majorošová, M. Vojtková, J. Use of Bioindication for Design Parameters of River Training in Urbanized Areas. Procedia Engineering: World Multidisciplinary Civil Engineering-Architecture-Urban Planning Symposium 2016, WMCAUS 2016. Vol. 161, (2016) 36-41, Elsevier, DOI: 10.1016/j.proeng.2016.08.494, ISSN 1877-7058.

[10] Parasiewicz, P., Walker, J.D. Comparison of mesohabsim with two microhabitat models (PHABSIM and HARPHA). River Research and Applications, 23 (2007) 904–923.

[11] Schiemer, F. Fish as indicators for the assessment of the ecological integrity of large rivers. Hydrobiologia, 3 (2000) 271–278; 422–423.

[12] Wolter, C., Vilcinskas, A. Characterization of the typical fish community of inland waterways of the north-eastern lowlands in Germany. Regul. Rivers: Res. Mgmt. 13 (1997) 335- 343.

[13] Schmutz, S. – Jungwirth, M. Fish as indicators for large river connectivity: The Danube andits tributaries. Archiv für Hydrobiologie, 115 (1999) 329–348.

[14] Chovanec, A., Hofer, R., Schiemer, F. Fish as bioindicators. Trace metals and other

contaminants in the environment, Vol. 6, (2003) 639-676.
[15] Lasne, E., Bergerot, B., Lek, S., Laffaille, P. Fish zonation and indicator species for the evaluation of the ecological status of rivers: example of the Loire basin (France). River Research and Applications, 23 (2007) 877–890.
[16] Verneaux J. Les poissons et la qualite´ des cours d'eau. Annales Scientifiques de L'Universite´ de Franche-Comte´ 4 (1981) 33–41.
[17] Macura, V., Škrinár, A., Kalúz, K., Jalčovíková, M., Škrovinová, M. Influence of the morphological and hydraulic characteristics of mountain streams on fish habitat suitability curves. River Research and Applications, Vol. 28, No. 8 (2012) 1161-1178. ISSN 1535-1459.
[18] Macura, V., Škrinár, A., Štefunková, Z., Muchová, Z., Majorošová, M.Design of Restoration of Regulated Rivers Based on Bioindication. In Procedia Engineering: World Multidisciplinary Civil Engineering-Architecture-Urban Planning Symposium 2016, WMCAUS 2016. Vol. 161, (2016) Elsevier, s. 1025-1029. DOI: 10.1016/j.proeng.2016.08.843, ISSN 1877-7058.
[19] Macura, V., Štefunková, Z., Majorošová, M., Halaj, P. Škrinár, A. (2018) Influence of discharge on fish habitat suitability curves in mountain watercourses in IFIM methodology. J. Hydrol. Hydromech, Vol. 66, No. 1 (2018) 1 - 11, ISSN 0042-790X.

Annals of Agrarian Science

Journal homepage: http://journals.org.ge/index.php

Spatial and time dynamics of glaciers following the Little Ice Age on the southern slope of the Greater Caucasus

Davit Svanadze[a,b], Vazha Trapaidze[a], Giorgi Bregvadze[a], Irakli Megrelidze[a,b]

[a]Iv. Javakhishvili Tbilisi State University, 1, Chavhavadze Ave., Tbilisi, 0179, Georgia

[b]The Ministry of Environment Protection and Agriculture of Georgia, 50, David Agmashenebeli Ave., Tbilisi, 0012, Georgia

Received: 10 June 2018; accepted: 19 November 2018

A B S T R A C T

The article presents an analysis of the scale in space and time of degradation of some glaciers on the southern slope of Central CaucasusRidge following the Little Ice Age to modern times by the method of remote sensing of short distances. It also describes the opportunities and advantages of using this method as compared to the traditional methodology of Orthorectifying and mappingof aerial pictures. In the study, we used the historical and topographic maps of different periods, archived historical materials of aerial photographing, remote sensing and modern aerial imagestaken with an unmanned aerial vehicle (UAV) (Phantom 4pro) in 2017. The study, besides the traditional approach, is based on the new technique of UAV photography, creating a digital three-dimensional so called "point cloud" model and its use in calculations of various glacial-geomorphological parameters with photogrammetry software and geo-information systems (Pix4D, Global Mapper, ArcGIS). The article gives a detailed description of opportunities of the UAV survey in terms of high-mountainous relief and hampering factors. It was established that the glaciers were quantify following the Little Ice Age and the values of their retreat depend on the concrete types of glaciers and geographical factors.

The mentioned glaciers are typical for the soutern slope of the Caucasus Range and are located between mountain Elbrus and Mkinvartsveri arrays next to the watershed ranges. The analysis of dynamics evidences that in the study period, the retreat varies between 0.8 and 4.2 km.

Keywords: Little ice age, Glacier fluctuation, Moraine, Remote sensing, UAV unmanned aerial vehicle, GIS mapping.

*Corresponding author: Davit Svanadze; E-mail address: dato.svanadze@ens.tsu.edu.ge

Introduction

For the last half a billion years, the climate on the earth has been characterized by an alternation of warm and cold periods. The reasons for such an alternation have been active volcanism, cyclical alternation of the earth's orbital location in the Solar system, changing composition of the atmosphere, shape of continents and ratio between the land and the ocean and a set of many other factors. The XX and XXI centuries in the history of the earth's climate are marked by a global change, with the anthropogenic activities playing a significant role. The impact of global warming is confirmed by now and it is demonstrated by a recent increase in the average temperature on earth by 0.6ºC [1]. Time period from 1990 to 2000 was distinguished by the highest temperature background for the last 150 years, since the onset of the instrumental measurements. The trend in global temperature has increased sharply in recent years and as compared to 1961-1990, an increase in the average temperature of the land reached 0.24-0.44ºC [2].

The ongoing climate change has a decisive influence on such an important component of the geographical layer as cryosphere, which is

one of the forming elements of the earth climate and a good indicator of its changes both, in the global and regional aspects [3]. The basic impact taking place in parallel to the climate change is irreversible degradation of the glaciers in the mountainous systems for the last 200 years which is associated with the continuous increase ofglobal temperature since the LIA (Little Ice Age).It will lead to the reduction of the freshwater resources and hydropower potential of the rivers and supply of irrigation and drinking water systems and increase in the probability of periglacial risks associated with glaciers. The southern slope of Great Caucasus range and its adjacent ridges, has experienced a strong reduction in glaciation after the maximum glacier extent at the end of the LIA (≈1820-1850), like other mountainous regions, it have been marked by a significant abatement of glaciation [4].

The goal of the study is to provide a spatio-temporal analysis of the dynamics of the large valley glaciers of the central part of Great Caucasusand restoration of their geometrical changesof behavior from the Little Ice Age to modern times. This problem was solved by using a synthesis of traditional and modern methods and different techniques to observe the process, including an unmanned aerial vehicle, as well as different approaches to data processing, including 3D and Geographical Information Systems software, when combined with the glacial-geomorphological method, allows obtaining and swiftly processing much better qualitative and quantitative data. This methodology was used to calculate the morphometric properties of the glaciers, restore document the dynamics of their equilibrium line altitude and calculate a number of glaciological parameters.

It should be noted, that the method used by us to study the glaciers further provides important opportunities to calculate many such numerical values, cannot be calculated by using the traditional cartographic and geodetic methods or those of remote sensing.

Objectives and methods

Study Area

The study area covers the southern slope of Central Caucasus range. With its diversified climatic and relief conditions and compatibility between them and in respect of ongoing modern glaciation, Caucasus is an specific geographical situation on the Eurasian Continent, as a transient hearth of modern glaciation transient between the glaciations in the continental (the Pamirs, Tian Shan) and humid marine climate (the Alps). In addition, glaciers exist in different climate conditions, like humid (West Caucasus), moderately humid (Central Caucasus) and moderately dry continental (East Caucasus) climates with the diversity of the climatic-geographical conditions typical to Caucasus Ridge [5]. The main center of glaciation of them is in Central Caucasus, at 43.2^0-43.1^0; 42.7^0-44.4^0. Between mountains Elbrus and Mkinvartsveri, where the relief reaches the highest points (Mount Elbrus at 5642 m, Dikhtau at 5025 m, Shkhara 5203 m, Mkinvartsveri at 5047 m, with over 10 highest peaks over 5000 m altitude along the given section), its average height is 4100 m above sea level. The mean annual amount of precipitations is 3000 mm. In this region, while the amount of precipitations in the eastern part of the Ridge is 10 times less [6] The difference between the amount of precipitations on the southern and northern slopes of the Ridge is also large. Such a difference in climatic conditions results from the location of Caucasus Ridge on the border between the moderate and subtropical climatic zones [7]. In addition, Caucasus Ridge is under the influence of the warm and humid air masses of the Atlantic Ocean and Mediterranean sea on the one hand and of the continental air masses of Siberia, Central Asia and Iran mountainous regions. The most important role in the formation of the climate of Caucasus ranges played by the Black and Caspian Seas. In terms of such diversified climatic conditions, the character of the modern glaciation is also diverse both, on the northern slope of Caucasus Ridge and in the western, eastern and central parts of it. The principal regularities of the climatic conditions and modern glaciation are as follows: the amount of precipitations decreases from west to east and the influence of the continental air masses increases, and the equilibrium line altitude (ELA) of the glaciers increases to 2500-2700 m in West Caucasus, to 3200-3400 m in Central Caucasus and 3700-3950 m in East Caucasus.

Methods and materials

GIS and Areal Mapping methods

One of the most convenient means to gather, store, analyze and visualize the geo-spatial data of different themes and scales is – the geographical information systems (GIS) [8]. In combination with such methods, as remote sensing, unmanned

Table 1. *Coverage of the areas photographed during the UAV flight*

Glacier and adjacent periglacial zone	UAV flay date	No. of aerial photos	Coverage area of an orthophotom^2	No. of points, 10^6	Density of points per sq.m. X;Y;Z;	Orthophotoresolution, cm	≈ Scale
1. Adishi	25/08/2017	1143	5.86	110.1	38	8.3	1:300
2. Khalde	30/08/2017	989	4.8	98.8	36	9.1	1:350
3. Shkhara	27/08/2017	818	3.9	92.7	36	8.1	1:400
4. Zopkhito	08/09/2017	914	3.31	107.4	40	7.59	1:300

aerial vehicle, which has been extensively used in various fields recently and exploration of the study object. Unlike the traditional cartographic methods, it provides good opportunities to obtain highly accurate and thoroughly informative data, including 2D, 3D and 4D cartographic information. Data processing is fast and most of production processes can be automated [9-11]. At the first stage, a geo-database of the study glaciers was created and integrated in a single coordinate space (UTM WGS-84, Zone38).The digital data obtained from the observations of the glaciers and their periglacial zones with an aerial vehicle and electronic and paper versions of different periods and available archive material of remote sensing and cartography are included in this data base structure. For the sake of thorough data integration, digital elevation models were used: a) through the manual digitalization of contour lines of a 1:50000-scaled topographic map of the Soviet period and b) a detailed relief model acquired with the UAV. Modern information about the studied glaciers and other field observations were collected with an unmanned aerial vehicle (DJI Phantom4Pro) by using flight control and planning software (Pix4D) (See Tab.1).

The gained data were processed in theGlobal Mapperand Esri ArcGIS software. The aerial survey of the glacier tongues and periglacial zones referred in the table (see table 1)was done in August and September of 2017. The aerial survey needs a preliminary study of the study area and evaluation of its parameters. At the first stage of the flight planning, the relief of the territory was evaluated, the longitudinal and lateral profiles were drafted at the office by using topographic maps, digital relief models and other available internet sources (Google Earth, SRTM – Shuttle Radar Topography Mission 30m), what was necessary if considering the high degree of dissection of the relief of the area, short fields of vision and presence of barriers to avoid a collision of the drone with the surrounding slopes or other relief forms. The technical parameters of the UAV are limited: the maximum flight duration with one take-off is 30 minutes; in case of a slight wind, the duration of the battery operation reduces to ≈ 26-28 minutes. A drone also has some height limitations and it can operate at maximum 500 m from the takeoff point. It should also be noted, that a drone can be used maximum up to6000 m above sea level. By considering all the above-listed limitations, the survey area was divided into sections of ≈0.2km^2 (690×310 m) following the flight safety parameters (SFig. 1), and the coordinates of takeoff points and extreme points of the missions were identified for each zone to avoid the collision of the drone with the relief barriers.

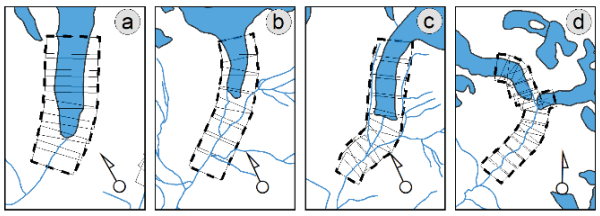

Fig. 1. *Plan of aerial survey of the glacial glacial zone of the glaciers and flight missions: a) Adishi, b) Shkhara, c) Khalde, d) Zopkhito*

The flight was done at 300 m flight level above take-off altitude from each takeoff point. In addition, it is important to ensure a continuous radio communication with the control panel. In order to gain highly accurate X;Y;Z coordinates of the study area (LAS Point Cloud Data), the coverage of the photographs is desirable to vary from 60 to 80%

during the flight. It is true that this will reduce the photographing area to ≈2,5 km^2, but it improves the data accuracy in a three-dimensional space. Coverage of even 0-10% is sufficient to generate an orthophotowith the image quality quite satisfactory for 2D GIS deciphering purposes.

Parametersof the glaciers and their calculation

A good indicator in the study of glaciers variation is the location of the glacier tongue above the sea level in altitude, time and space, variation of the glacier tongue and surface topography, formation of a moraine cover, its morphometry, etc. In the Little Ice Age period, the moraine extent of the same period was well preserved in the periglacial zone of some valley glaciers, and they can be used to restore the location of a glacier and various morphometric indicators of the relevant period. The advantage of the method lies in the possibility to swiftly obtain and calculate a number of accurate glacial-morphological parameters what is often impossible by using traditional deciphering of cartographic aerial photos or if possible, is a labor-consuming process. As for the study of the territory with the field geodetic apparatus, its use in the high mountains is quite limited and needs extensive labor. Two factors are important in this respect: a UAV is capable of producing maximum 1000 coordinate points (X;Y;Z) per square meter on the one hand and on the other hand, what is no less important, no matter how great the density of the survey of the territory and exploration of the topographic surface with the geodetic apparatus is, an aerial photo is impossible to produce. Following the processing of the data of UAV used by us during the field study (LAS point cloud data; X;Y;Z average density of 40 points/m^2) with high accuracy, many parameters of a glacier dynamics were made possible to decipher and calculate (Fig. 2). By manual digitalization and semi-automatic processing of the point cloud in Global Mapper software media, we restored the location of the glacier in the modern period and Little Ice Age period, calculated the location of the tongue above sea level in the Little Ice Age, indicators of the tongue retreat both, in length and height, designed a high-resolution and highly accurate relief model and its lateral and longitudinal profiles by using the modern methodology.

In the study of glaciers, alongside with the Geographical Information Systems, we used literary sources [4], [11], [12] and method of overlay of the cartographic maps (1890-1911. maps of the Russian Empire) and remote sensing archive materials. By comparing the old and modern data, we obtained numerical indicators, which thoroughly describe the glacier dynamics in the last 200 years.

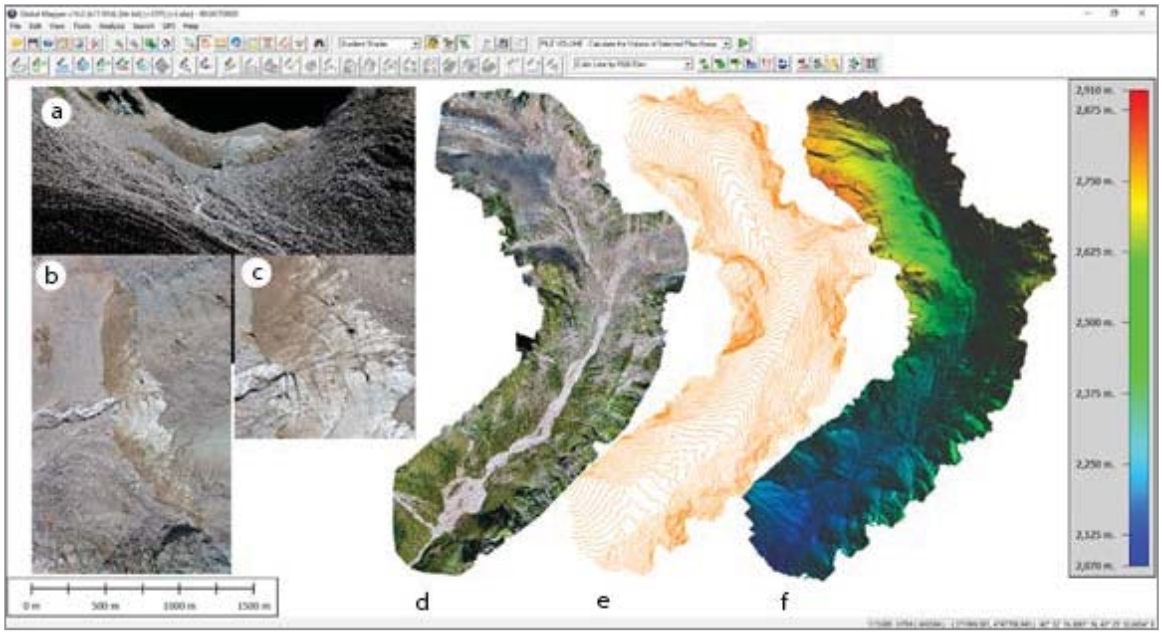

Fig. 2. *Glacier Zipkhito: a) LAS x; y; z point cloud data; b, c) glacier tongue, d) orthophoto, e) elevation contours with a 10 m spacing, f) digital relief model*

Results and analysis

The analysis of the gained results evidences that the glaciers on the southern slope of Caucasus rangeare in the phase of active diminution demonstrated by a significant tongue retreat, increased altitude above sea level and decreased thickness at the same time. The variation of the parameters is associated with the process of the glacier dynamics. As an example, we calculated the characteristic parameters and their variation forof 25 glaciers in the study from the Little Ice Age to modern times (Tab. 2).

Table 2. *Dynamics of the glacier tongues from LIA to modern period*

Glacier	Type of glacier	Tongue elevationin different periods, asl, m			Difference in the periods, m		Average annualelevation change, m/yr		Total elevation in 1820-2010-17	Retreat in 1820-2010-17
		I≈ 1820	II ≈ 1960	III ≈ 2010-2017	II ≈ 1960	III ≈ 2010-2017	II ≈ 1960	III ≈ 2010-2017		
Shkhara	Valley	2310.00	2490.00	2535.00	180.00	45.00	1.29	0.79	225.00	888.00
Guli	Valley	2580.00	2800.00	2920.00	220.00	120.00	1.57	2.11	340.00	1081.00
Ushba	Complex valley	2060.00	2380.00	2590.00	320.00	210.00	2.29	3.68	530.00	1243.00
Adishi	Valley	2270.00	2380.00	2415.00	110.00	35.00	0.79	0.61	145.00	1326.00
Kibisha	Cirque	3090.00	3190.00	3225.00	100.00	35.00	0.71	0.61	135.00	1359.00
Khalde	Valley	2330.00	2500.00	2525.00	170.00	25.00	1.21	0.44	195.00	1542.00
Boko	Valley	2285.00	2440.00	2637.00	155.00	197.00	1.11	3.46	352.00	1592.00
Nageba	Valley	2170.00	2413.00	2550.00	243.00	137.00	1.74	2.40	380.00	1600.00
Tbilisa	Valley	2540.00	2815.00	3010.00	275.00	195.00	1.96	3.42	470.00	1622.00
Marukhi	Valley	2340.00	2400.00	2561.00	60.00	161.00	0.43	2.82	221.00	1734.00
Buba	Valley	2400.00	2820.00	2950.00	420.00	130.00	3.00	2.28	550.00	1770.00
Kirtisho	Valley	2320.00	2425.00	2618.00	105.00	193.00	0.75	3.39	298.00	2007.00
Mna	Suspended valley	2660.00	2855.00	3050.00	195.00	195.00	1.39	3.42	390.00	2053.00
Shdavluri	Valley	2320.00	2640.00	2720.00	320.00	80.00	2.29	1.40	400.00	2178.00
Gergeti	Valley	2600.00	2930.00	3113.00	330.00	183.00	2.36	3.21	513.00	2187.00
Tsaneri	Complex valley	2060.00	2280.00	2376.00	220.00	96.00	1.57	1.68	316.00	2203.00
Koruldashi	Valley	2160.00	2480.00	2800.00	320.00	320.00	2.29	5.61	640.00	2249.00
Dolra	Valley	2370.00	2540.00	2932.00	170.00	392.00	1.21	6.88	562.00	2338.00
Namkvami	Valley	2460.00	2730.00	3023.00	270.00	293.00	1.93	5.14	563.00	2362.00
Laila	Complex valley	2100.00	2220.00	2620.00	120.00	400.00	0.86	7.02	520.00	2467.00
Zopkhito	Valley	2120.00	2480.00	2560.00	360.00	80.00	2.57	1.40	440.00	2603.00
Chalaati	Complex valley	1620.00	1800.00	1940.00	180.00	140.00	1.29	2.46	320.00	2646.00
Lekhziri	Complex valley	1780.00	1970.00	2224.00	190.00	254.00	1.36	4.46	444.00	3698.00
Tviberi	Complex valley	2031.00	2140.00	2428.00	109.00	288.00	0.78	5.05	397.00	4096.00
Kvishi	Complex valley	2300.00	2415.00	2780.00	115.00	365.00	0.82	6.40	480.00	4224.00
Average		**2291.0**	**2501.3**	**2684.1**	**210.3**	**182.8**	**1.5**	**3.2**	**393.0**	**2122.7**

One of the most important factors characterizing the variability of the glaciers is the variation of the altitude of the glacier tongues above sea level in time and space. We give the data about the tongue variations of 25 glaciers for three periods, starting the LIA (≈ 1820) to the middle of the XX century (≈1950-1960) and the most recent modern period. R. Gobejishvili [6] gives the altitudes of the tongues of the first and second periods above sea level. Aerospace photos and digital relief model (SRTM) of different periods (2010-2017) were used to obtain the contemporary data about the location of the glacier tongues and their altitudes.

The data analysis has made it clear that the glaciers continue active retreat in both most recent periods as compared to the first, LIA period. If during the LIA period, the location of the tongues of the considered glaciers above sea level was 2291 m on average, the similar data in the II period (1960s) were 2501 m and 2684 m in the III period (See Table 2). The total difference in elevation of the glacier tongues above sea level made 400 m.

The analysis of the table makes it clear that in the considered period, an average annual value of the glaciers elevation has increased from 1.5 to 3.2 m since 1960s caused by the current climate change and sustainable thermal balance variation established on earth. A larger retreat is seen with the complex types of valley glaciers. Most of the glaciers (88%) retreated within the range of 2-3 km (See Fig. 2). The response of complex valley glaciers and large glaciers to the current climate changes is particularly worthwhile. The value of their retreat is twice as much as an average value as a result of the glacier tongues descending to lower altitudes, their physical condition, mechanical destruction, water currents, exposition and influence of other factors. Average annual retreat of the considered glaciers is 10.7 m/yr, while this indicator for complex valley and large glaciers varies between 18 and 22 m/yr. There is no doubt that the degradation of the glaciers considered in the similar period did not take the same pace and included the periods of short pauses, but in the final run, the retreat of the glaciers took a high pace [13], [14]. It is true that there are certain differences fixed in the average values of retreat of glaciers, but in this case too, most of them (88%) retreated by 8-12 m on average (See Fig. 3).

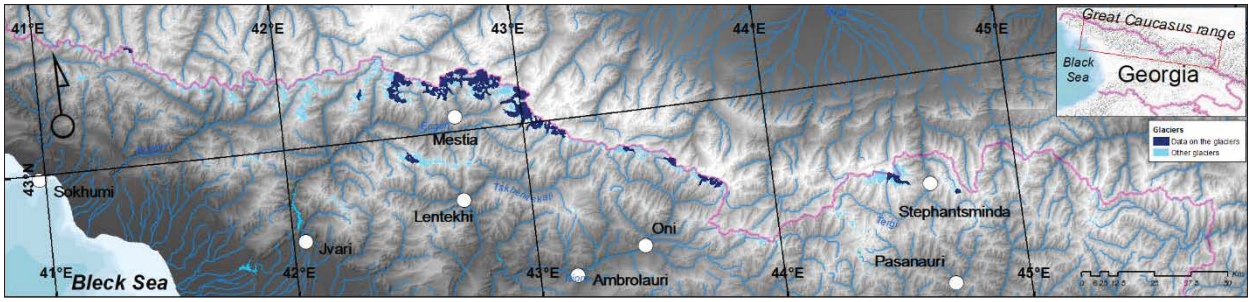

Fig. 3. *Plan of location of the glaciers*

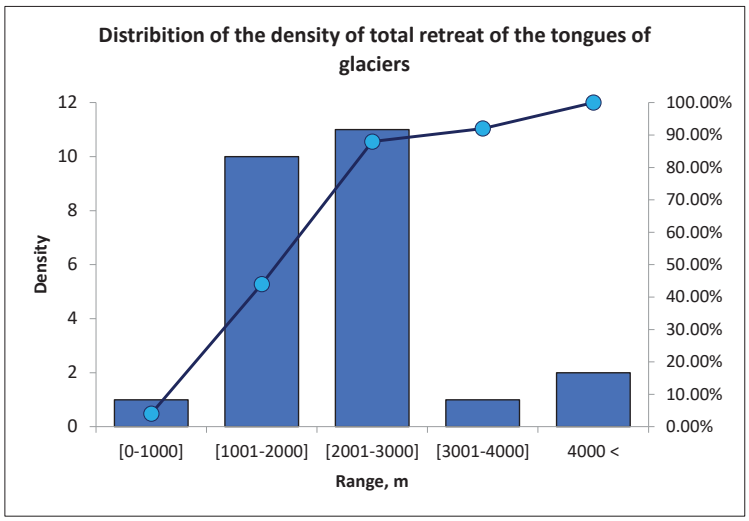

Fig. 4. *Distribution of the density of total retreat of the tongues of glaciers in ≈ 1820-2017*

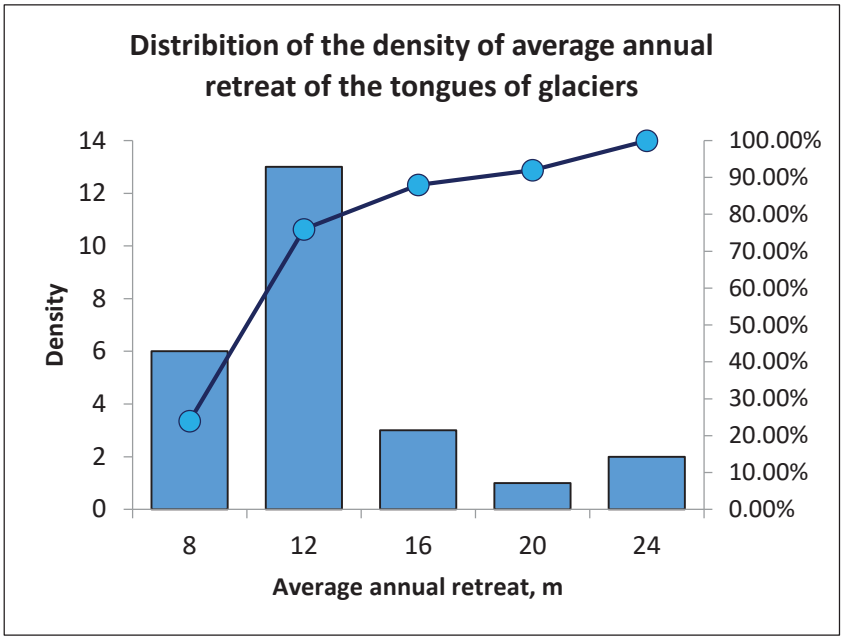

Fig. 5. . *Distribution of the density of average annual retreat of the tongues of glaciers in ≈ 1820-2017*

Conclusion

In the maximal phase of the Little Ice Age (≈1820), the glaciers were in the period of quite active irreversible degradation and melting evidenced by their gradual and swift retreat. Dynamics of melting of glaciers at southern slopes of the Greater Caucasus is in direct proportion with current climatic cycles, at that these processes are more noticeable at gorge-type glaciers. The reduction of the valley glaciers for the last 200years has exceeded 40% of the total area of the maximal phase and still takes an active course. If such trends continue without any changes, presumably the reduction of the large valley glaciers will reach 65% by 2100 what will presumably cause the disappearance of small karr glaciers. These processes lead to the increase inequality in the within-year distribution of a hydrological flow of the major rivers in the region and great amplitudes in different seasons. At that, increase in melting intensity predetermines the growth of intensity and frequency of glacial mudflow formation, since the glaciers with stable balance carry less risk of glacial mudflows and abrupt freshets.

Acknowledgment

The authors would like to thank to the Shota Rustaveli National Science Foundation (SRNSF) for the financial support (grant PhDF2016_77)

References

[1] Meladze M., Meladze G., A trend of increasingly frequent droughts in Kakheti Region, Annals of Agrarian Science, (2017) 96-102.

[2] Shahgedanova M., G. Nosenko G., Kutuzov S., O. Rototaeva O., Khromova T., Deglaciation of the Caucasus Mountains, Russia/Georgia, in the 21st century observed with ASTER satellite imagery and aerial photography. The Cryosphere, 2014.

[3] Beritashvili B. Climate and its change. Georgian Technical University, Tbilisi, 2011 (in Georgian).

[4] Gobejishvili R., Svanadze D., Lomidze N., Dvalashvili G.,Dynamics of valley glacier in the XIX-XXI-th centuries on the souther slope of the central Caucasus (In Georgian). Tbilisi : Institute of Geography, Proceedings I(80) (2006) 219-229.

[5] Maruashvili L. I., Phisical Geography of Georgia, Monograph. Publ. house "Metsniereba", Tbilisi, 1971 (in Georgian).

[6] Gobejishvili R., Lomidze N., Tielidze L. Late Pleistocene (Wurmian) glaciations of the Caucasus, in: Quaternary Glaciations: Extent and Chronology, edited by: Ehlers, J. Gibbard, P.L., and Hughes, P.D. Elsevier, Amsterdam, 141-147, doi:10.106/B978-0-444- 53447-7.00012-X, 2011.

[7] Tielidze Levan, Wheate Roger. The Greater Caucasus Glacier Inventory (Russia, Georgia

andAzerbaijan), The Cryosphere,12,81–94 (2018) 81-92.
[8] Eva Savina Malinverni, Claudia Croci and Fabrizio Sgroi laciers monitoring by remote sensing and GIS techniques in open source environment. Ancona: University Politecnica of Marche, Department DARDUS, Ancona, Italy, . EARSeL Proceedings 7. (2008) 120-132.
[9] Bernd Resch, Florian Hillen, Andreas Reimer, Wolfgang Spitzer Towards 4D Cartography - Four-dimensional Dynamic Maps for Understanding Spatio-temporal Correlations in Lightning Events. Bernd Resch, Florian Hillen, Andreas Reimer, Wolfgang Spitzer. The Cartographic Journal, 4 (2013) 266-275.
[10] Oliver Wigmore, Bryan Mark. Monitoring tropical debris-covered glacier dynamics from high-resolution unmanned aerial vehicle photogrammetry Cordillera Blanca, Peru., The Cryosphere, 3 (2017) 2463-2480.
[11] Podozerski K., Ledniki Kavkazskovo Khrebta, Tiflis : Zapiski Kavkaskovo tdela Imperatorsovo ruskovo geograpihcheskovo obshestvo, Knijka XXIX, 1911 (in Russian).
[12] Tielidze L.,Modern and Old Glaciers of Georgia, Samshoblo, Tbilisi, 2016.
[13] Radim Stuchlík, Zdeněk Stachoň, Petr Kubíček.Unmanned Aerial Vehicle – Efficient mapping tool available for recent research in polar regions. Brno : Department of Geography, Faculty of Science, Masaryk University, (2015), pp. 210-221.
[14] Lambrecht. A., Mayer C., Hagg. W., Popovnin.V,, Rezepkin. A., Lomidze. N., and Svanadze. D., .A comparison of glacier melt on debris-covered glaciers in the northern and southern Caucasus., The Cryosphere, 4 (2011) 525-538.

Annals of Agrarian Science

Journal homepage: http://journals.org.ge/index.php

Neonicotinoids against sucking pests on winter wheat stands in the Forest-Steppe Zone of Ukraine

Fedir Melnichuk[a], Larisa Melnichuk[b], Svetlana Alekseeva[a], Michailo Retman[b], Oleksandra Hordiienko[a]

[a]Institute of Water problems and Reclamation Academy of Agricultural Science, Nauky str., Gora, Boryspil district, Kyiv region, 08324, Ukraine

[b]Institute of Water Problems and Melioration of the National Academy of Sciences of Ukraine, 37, vul. Vasylkivska, Kyiv, 03022, Ukraine

Received: 25 June 2018; accepted: 29 November 2018

A B S T R A C T

Saturation of crop rotation with grain cereal crops (corn, winter wheat) leads to the creation of favorable conditions for the development of sucking pests and, consequently, increasing of their density of population and harmfulness on winter wheat crops. The comparative evaluation of the effectiveness of neonicotinoids against the group of sucking pests (Sun pest (Eurygaster integriceps), wheat aphids, thrips) on crops was done in 2016-2017. Insecticide Engeo 24.7% SC was the most effective against the Sunn pest. His maximum technical efficiency reached 100.0% and was obtained on 7th and 14th day after treatment. The most effective for spraying against aphids were Engeo 24.7% SC and Actara, 24% SC, that shown 99.7% and 98.3% reduction of aphids number on 7th day compared to the control respectively. The application of investigated insecticides significantly reduced the population of aphids, trips and Sun pest, that results in increasing in quantitative and qualitative indices of winter wheat yield.

Keywords: Wheat, Sucking pests, Aphids, Bugs, Insecticides, Crop.

*Corresponding author: Michailo Retman; E-mail address: retman_m.s@ukr.net

Introduction

In recent years, there has been a violation of the agricultural crops alternation in the crop rotation of most farms, when one crop is grown in the same field for two or more years in a row. In the Forest-Steppe Zone of Ukraine, a situation is characterized when 3-5 crops (corn, soybeans, sunflower, winter rape, winter wheat) prevail in the farm. In some cases, the area under the corn takes up 50-75% of the total area of the plowed land of the farm. Due to the excessive saturation of the crop rotation with one culture, the favorable conditions for the pest proliferation and the infection spread are created [1].

More than 360 species of insects and other animal organisms, including nematodes, rodents, birds and representatives of other fauna classes damage cereals in Ukraine [2]. Sucking pests are especially dangerous. In particular, mass outbreaks of the sunn pest (*Eurygaster integriceps*), wheat aphids, thrips, cicadas cause significant damage of winter wheat plants. This leads to a shortage or full loss of grain yield. Thus, according to the Institute of Plant Protection of the National Academy of Agrarian Sciences of Ukraine, damaging the stem of culture with a sunn pest can reduce yield by 50-54% [3].

New chemicals against pests appear every year in the State list of pesticides and agrochemicals authorized for use in Ukraine. With the implementation of modern agricultural technologies, there is a tendency to increase the use of highly effective insecticides with low application rates, that minimizes their influence on the environment. Preferably, these chemicals are from the group of

neonicotinoids that are highly effective against pests and, at the same time, are low toxic for the humans and animals [4].

Neonicotinoids are a relatively new class of insecticides. One of the success factors of these plant protection products is that their application is affecting pests with developed resistance to insecticides from other chemical groups. The prevalence of neonicotinoids is due to the variety of methods of their application (spraying, pre-sowing seed treatment, introduction into irrigation water in drip or irrigated systems). In addition, these chemicals have opened new opportunities in the development of products for protection of seeds and seedlings [4, 5].

The mechanism of action of neonicotinoids shows itself in disturbance of the central nervous system of insects. Active ingredients act as a competitor to acetylcholine of the postsynaptic membrane receptor. In this case, excessive excitation of the nerve cells occurs and thereby disturbs the normal conduction of the nerve impulse through the synapses, which is a consequence of a violation of the functional activity of the acetylcholine receptor. As a result, convulsions and paralysis developed in insects, which leads to their mortality [6, 7].

In the Ukrainian market, insecticides from the group of neonicotinoids are most widely represented on the basis of the following active ingredients: imidacloprid, thiamethoxam, thiacloprid and acetamiprid (Table 1). Their combinations with pyrethroids are also used in order to increase their effectiveness against crop pests: Engeo 24.7% SC (thiamethoxam, 141 g/l + lambda-cyhalothrin, 106 g/l); Borey 20% SC (imidacloprid, 150 g/l + lambda-cyhalothrin, 50 g/l); Connect 11,25% SC (imidacloprid, 100 g/l + beta-cyfluthrin, 12.5 g/l); Proteus 11% OD (thiacloprid, 100 g/l + deltamethrin, 10 g/l); Inasuma 13% WG (acetamiprid, 100 g/kg + lambda-cyhalothrin, 30 g/kg) and others.

Therefore in 2016-2017 to optimize winter wheat protection measures, a comparative assessment of the effectiveness of neonicotinoids against the group of sucking pests (sunn pest, wheat aphids, thrips) was made on stands of this crop.

Materials and methods

Field trials were carried out in 2016-2017 in the Kyiv region conditions. For investigations, the registered chemicals from the neonicotinoid group were used: Actara, 24% SC and Mospilan, 20% SP In addition, for the comparison of efficacy, the complex insecticides Engeo 24,7% SC, Connect 11,25% SC and Proteus 11% OD were used. In the experiments, the winter wheat sort Myronivska 65 was grown, the seed planting rate was 4,5 millions per hectare. The size of the experimental plots is 50 m^2 (10,4 x 4,8 m), replication – 4 times. Allocation of plots is randomized.

Scores of pests, sampling and analysis were carried out in accordance with generally accepted methods [8]. The number of larvae and adult insects of the sunn pest was counted for 1 m^2, while the insects were counted on 8 test sites of 50x50 cm (0.25 m^2) size. For the scores of the thrips, 5 spikelets were selected in 10 places of the plot. Samples were placed in paper bags. Then the number of thrips and their average number per spikelet was counted in the laboratory. The score of the wheat aphids was counted on each site for 100 stems (5 stems in 20 places), imago and larvae were observed on leaves, stalks and spikelets.

Table 1. *The main active ingredients of neonikotinoids in Ukraine*

Active ingredient	Name of insecticide	Manufacturer	Rate of application
Imidacloprid	Confidor, 20% SL	Bayer Ag, Germany	0,1-0,35 l/ha
Acetamiprid	Mospilan, 20% SP	NIPPON SODA CO., LTD, Japan	0,05-0,50 kg/ha
Thiacloprid	Calypso, 48 % SC	Bayer Ag, Germany	0,15-0,30 l/ha
	Biscaya, 24% OD		0,20-0,40 l/ha
Thiamethoxam	Actara, 24 % SC	Syngenta Crop Protection Ag, Switzerland	0,15-0,16 l/ha

Research results

The occupation of winter wheat crops by pests was determined from the tillering phase. In the species composition of the aphids, the Grain aphid (*Sitobion avenae* F.) was most common, the Sunn pest was dominated among the shield bugs (Scutelleridae), *Eurygaster austriaca* Schrank occurs sporadically, *Aelia acuminata* L. and other species of bugs were found. The number of larvae and imago of wheat aphids reached 50.0-80.5 / plant, thrips – 23.3-27.0 / spikelet, imago of the Sunn pest – 5,3-8.3 /m^2 during the observations before the application of insecticides in the early-medium milk stage of winter wheat.

The treatment of crops with insecticides contributed to a decrease of the occupancy of plants by pests (Table 2). The highest effectiveness against Sunn pest was provided by insecticide Engeo 24.7% SC. Thus, on average, on the 3rd day after its application, the death of this pest reached to 92.5%,

and 100.0% – on the 7th and 14th day.

On average, over two years, the effectiveness of the Actara, 24% SC was 88.6% and 95.8% on the 3rd and 7th day after spraying respectively. Somewhat lower was an efficiency of Proteus 11% OD, that on the 3rd day after spraying reached to 86.9%, on the 7th – 89.7%. With the application of insecticide Mospilan, 20% SP the mortality rate of these phytophages was lower and reached only 69.8% and 84.6%, respectively (Table 3).

Also, on the 3rd day after spraying in the variant with the insecticide Actara, 24% SC the population of larvae and imago thrips was decreased by 93,8%, and on the 7th day – by 99.1%. Application of the Mospilan, 20% SP ensured the mortality rate of these phytophages on the 3rd day at the level of 88.2%, on the 7th – 93.0%. Insecticide Engeo 24.7% SC showed the effectiveness against the thrips slightly higher, compared with the Actara, 24% SC. Thus, on the 3rd day after application of Engeo 24.7% SC the death of the thrips reached to 98.0%, on the 7th day – 99.0%. Somewhat lower was an efficiency of Proteus 11% OD, that on the 3rd day after spraying reached to 96.2%, on the 7th – 98.2%.

At the observations on 14th day after spraying, the increasing of the effectiveness of insecticides was noted. So, in variants with the use of Actara, 24% SC, Proteus 11% OD and Engeo 24.7% SC efficiency was almost the same and reached to 99.1-99.6%. In the variant with the application of Mospilan, 20% SP this indicator was only 94.4%.

During the research period it was found that the use of insecticides provided high effectiveness against wheat aphids. Their mortality rate on the 3rd day after application of the Mospilan, 20% SP was 85.4%, on other variants with insecticides it reached 89,3-92,6%. On the 7th and 14th days the preparations Actara, 24% SC, Proteus 11% OD, Connect 11,25% SC and Engeo 24.7% SC were most efficient, supply the mortality of wheat aphids at level – 95.4-99.7%.

At harvesting it was found that protection of winter wheat plants by spraying with insecticides contributed to the preservation of quality indicators of the yield. So, the mass of 1000 grains in the variant with Actara, 24% SC, Proteus 11% OD and Engeo 24.7% SC reached 46.3, 46.4 and 46.5 g, respectively, that was on 4.9-5.1 g higher than control. Application of the Mospilan, 20% SP and Connect 11,25% SC provided the increasing of the mass of 1000 grains up to 46.0 g, that was on 4.6 g higher than the control indicator (Table 4).

The higher yield of wheat grain was obtained on all variants of the experiment with application of insecticides, in comparison with the control. So, the yield on variants with the Actara, 24% SC, Proteus 11% OD and Engeo 24.7% SC exceeded the control by 0.49 and 0.51 mt / ha, and by 0.03-0.05 mt/ha in comparison with the variant with Mospilan, 20% SP and Connect 11,25% SC.

Table 2. *The number of winter wheat pests in the early-medium milk stage of winter wheat (Kyiv region, 2016-2017)*

Variant	Application rate, kg (l)/ha,	Year	Number of pests before treatment			Number of pests on … day after treatment								
						3rd			7th			14th		
			Sunn pest, exemplars/ m^2	thrips larvae, exemplars /spikelet	wheat aphids, exemplars /plant	Sunn pest, exemplars/ m^2	thrips larvae, exemplars /spikelet	wheat aphids, exemplars /plant	Sunn pest, exemplars/ m^2	thrips larvae, exemplars /spikelet	wheat aphids, exemplars /plant	Sunn pest, exemplars/ m^2	thrips larvae, exemplars /spikelet	wheat aphids, exemplars /plant
Control	-	2016	7,8	27,0	50,0	8,0	32,5	68,0	8,3	44,5	96,5	8,5	51,8	134,3
		2017	5,5	24,5	80,5	6,0	29,3	107,8	6,3	36,5	132,3	6,8	42,0	162,8
		average	**6,7**	**25,8**	**65,3**	**7,0**	**30,9**	**87,9**	**7,3**	**40,5**	**114,4**	**7,7**	**46,9**	**148,6**
Actara, 24% SC	0,15	2016	8,3	24,5	53,8	0,5	1,8	8,0	0,3	0,5	4,8	0,0	0,3	2,8
		2017	5,3	23,3	76,5	1,0	2,3	10,0	0,3	0,3	5,3	0,3	0,5	2,3
		average	**6,8**	**23,9**	**65,2**	**0,8**	**2,1**	**9,0**	**0,3**	**0,4**	**5,1**	**0,2**	**0,4**	**2,6**
Mospilan, 20% SP	0,12	2016	7,5	24,3	52,5	2,0	3,3	13,3	1,0	2,3	11,0	1,0	2,0	6,5
		2017	6,0	24,0	78,5	2,0	4,3	11,3	1,0	3,5	9,0	0,8	3,3	2,0
		average	**6,8**	**24,2**	**65,5**	**2,0**	**3,8**	**12,3**	**1,0**	**2,9**	**10,0**	**0,9**	**2,7**	**4,3**
Engeo 24.7% SC	0,18	2016	8,0	26,5	51,5	0,3	0,5	6,8	0,0	0,3	2,8	0,0	0,0	0,5
		2017	5,3	23,5	75,0	1,0	0,8	5,3	0,0	0,5	1,5	0,0	0,3	0,5
		average	**6,7**	**25,0**	**63,3**	**0,7**	**0,7**	**6,1**	**0,0**	**0,4**	**2,2**	**0,0**	**0,2**	**0,5**
Connect 11,25% SC	0,5	2016	8,0	27,0	53,0	0,8	1,5	7,4	0,5	1,2	3,9	0,3	2,0	2,0
		2017	7,0	24,4	81,0	1,2	1,4	9,0	1,0	1,7	3,5	0,8	2,4	1,5
		середнє	**7,5**	**25,7**	**67,0**	**1,0**	**1,5**	**8,2**	**0,8**	**1,5**	**3,7**	**0,6**	**2,2**	**1,8**
Proteus 11% OD	1,0	2016	7,0	28,0	54,4	0,5	0,8	7,8	1,0	0,9	3,0	0,5	0,5	1,0
		2017	6,8	25,4	79,5	1,0	1,4	6,5	0,5	0,5	2,1	0,0	0,3	0,8
		середнє	**6,9**	**26,7**	**67,0**	**0,8**	**1,1**	**7,2**	**0,8**	**0,7**	**2,6**	**0,3**	**0,4**	**0,9**

Table 3. *Efficiency of insecticides against winter wheat pests in the conditions of the Central Forest-Steppe of Ukraine (Kyiv region, 2016-2017)*

Variant	Application rate, kg (l)/ha,	Year	Efficacy on … day after treatment, %								
			3rd			7th			14th		
			Sunn pest	thrips larvae	wheat aphids	Sunn pest	thrips larvae	wheat aphids	Sunn pest	thrips larvae	wheat aphids
Actara, 24% SC	0,15	2016	93,3	95,0	87,3	96,2	99,0	94,6	100,0	99,5	97,8
		2017	83,9	92,5	91,2	95,4	99,2	96,2	95,7	98,9	98,7
		average	**88,6**	**93,8**	**89,3**	**95,8**	**99,1**	**95,4**	**97,9**	**99,2**	**98,2**
Mospilan, 20% SP	0,12	2016	76,0	90,9	79,5	88,4	95,3	88,0	88,7	96,5	94,9
		2017	63,6	85,6	89,8	82,7	90,6	93,4	87,2	92,3	98,8
		average	**69,8**	**88,2**	**84,6**	**85,5**	**93,0**	**90,7**	**87,9**	**94,4**	**96,9**
Engeo 24.7% SC	0,18	2016	96,2	98,5	89,7	100,0	99,3	97,0	100,0	100,0	99,6
		2017	83,9	97,4	95,4	100,0	98,7	98,9	100,0	99,3	99,7
		average	**90,0**	**97,9**	**92,6**	**100,0**	**99,0**	**98,0**	**100,0**	**99,7**	**99,7**
Connect 11,25% SC	0,5	2016	89,7	95,4	88,5	93,8	97,3	95,7	96,4	96,1	98,4
		2017	74,5	95,2	91,6	79,8	95,4	97,3	85,0	94,3	99,1
		average	**82,1**	**95,3**	**90,0**	**86,8**	**96,3**	**96,5**	**90,7**	**95,2**	**98,7**
Proteus 11% OD	1,0	2016	94,4	97,4	87,5	89,2	97,9	96,6	94,7	99,0	99,2
		2017	79,4	95,0	94,0	90,2	98,6	98,4	100,0	99,3	99,5
		average	**86,9**	**96,2**	**90,8**	**89,7**	**98,2**	**97,5**	**97,4**	**99,1**	**99,4**
SSD_{05}			**7,6**	**3,8**	**3,5**	**2,7**	**1,5**	**1,4**	**1,6**	**1,5**	**1,1**

Table 4. *Yield of winter wheat in dependence on application insecticides (Kyiv region, 2016-2017)*

Variant	Application rate, kg (l)/ha,	Year	Yield, t/ha	Mass of 1000 grains, g
Control	-	2016	5,08	41,8
		2017	4,46	41,0
		average	4,77	41,4
Actara, 24% SC	0,15	2016	5,65	47,3
		2017	4,81	45,3
		average	5,23	46,3
Mospilan, 20% SP	0,12	2016	5,61	47,0
		2017	4,79	45,0
		average	5,20	46,0
Engeo 24.7% SC	0,18	2016	5,68	47,5
		2017	4,82	45,5
		average	5,25	46,5
Connect 11,25% SC	0,5	2016	5,5	46,9
		2017	4,7	45,0
		average	5,1	46,0
Proteus 11% OD	1,0	2016	5,6	47,3
		2017	4,8	45,5
		average	5,2	46,4
SSD_{05}			0,38	3,9

Conclusions

1. Saturation of crop rotation with grain crops (corn, winter wheat, barley) leads to the creation of favorable conditions for the development of sucking phytophages and, accordingly, to increase their density of population (larvae and imago wheat aphids (50,0-162,8 / plant), trips (23.3-51.8 / spikelet), imago of the Sun pest (5.3-8.5 / m2) on winter wheat stands.
2. Preparations from the neonicotinoids group were highly effective against sucking wheat pests for 2 weeks. The maximum technical efficiency against them was noted in the variant using insecticide Engeo 24.7% SC and reached 99.6-100.0%. Somewhat lower efficiency was shown by Actara, 24% Cp (97.9-99.2%) and Proteus 11% OD (97.4-99.4%).
3. The application of insecticides significantly reduced the occupation of plants by aphids, thrips and Sun pest, resulting in increased wheat yield and a mass of 1000 grains.

References

[1] Petrukha O.I., Agrotechnics in the pests control, Sugar beets, 2 (1980) 29-31 (in Russian).
[2] Strategy and Tactics of Plant Protection, Vol. 2, Tactics, Alfa-Steviya, Kyiv, 2015 (in Ukraine).
[3] Sekun M.P. Hazardous sunn pest, Svit, Kyiv, 2002 (in Ukraine).
[4] L. V. Ermolova, I. V. Lep'oshkin, I. V. Mudryy, Modern problems of toxicology, food and chemical safety, 4 (2004) 5-7.
[5] Bazaka G. Ya., Dukhnytsky V., General characteristics of pesticides of the neonikotinoids group, Naukoviy Visnyk of LNUVMBT named after S. Z. Gzhytsky 15 # 1 (55) (2013) 3-9 (in Ukraine).
[6] Sekun M. P., Neonicotinoids in agrarian production, Protection and quarantine of plants, 58 (2012) 180-191 (in Ukraine).
[7] Sekun M.P. Zherebko V.M. et al., The Handbook of Pesticides, Kolobir, Kyiv, 2007 (in Ukraine).
[8] Methods of Testing and Application of Pesticides, Svit, Kyiv, 2001 (in Ukraine).

Annals of Agrarian Science

Journal homepage: http://journals.org.ge/index.php

Determination of the ratio hematite/goethite by soil color

Yu.N. Vodyanitskii

Lomonosov Moscow State University. Faculty of Soil Science, 1, Leninskie gory, Moscow, 119234, Russia

Received: 10 September 2018; accepted: 12 November 2018

A B S T R A C T

The content and composition of hematite and goethite can solve important tasks of genesis, as well as soil classification. It is proposed a new method of determining the index I_{Lab} = [Hematite/(Hematite+Goethite)] on color soil system CIE-L*a*b*. The method is based on calculating soils Redness (Red) and then calculating the I_{Lab}, based on reference Red of hematite and goethite. Replacement of Fe^{3+} to Al^{3+} is taken into account through amendments to the color of goethite, admitting that Al-hematite color does not differ from color pure hematite. The new technique was proven on Northern Italy andosols and was give results similar to results, received for converting optical spectrum on Kubelka-Munk theory. But the new technique has the advantage of ease of calculation and the ability to use the old color data obtained in the Munsell system. Validating new methods in luvisols is showed an agreement index values I_{Lab} with real [Hematite/(Hematite+Goethite)] in those parts where there are profile have pure hematite and goethite. In luvisols containing Al-goethite and Al-hematite, admixture Al generates an error in the calculation. To delete the error, it is proposed an amendment to the distorting effects of aluminum in lattice goethite, ewith high content: 8-12 mole Al %. Cambisols have a value index I_{Lab} also vary depending on the impurities Al in hematite and goethite. From samples with particles of pure goethite Red higher than cambisols containing Al-goethite. After adjustment for the Al-share in goethite the share of hematite becomes comparable to its share in the cambisols samples with pure goethite.

Keywords: Hematite, Goethite, Luvisoils, Cambisols, Genesis, Geochemistry

*Corresponding author: Yuri Vodyanitskii; E-mail address: yu.vodyan@mail.ru

Introduction

Hematite αFe_2O_3 and goethite αFeOOH as the most stable Fe-(hydr)oxides forms, are widely distributed in soils of different genesis and age. To the greatest extent Fe-(hydr)oxides are concentrated in the oxisols and cambisols [1-3], and also – in many loess soils [4, 5]. Content of hematite and goethite is useful to solve important tasks of genesis and classification: for example, to distinguish between oxisols and cambisols [1].

At the same time, genesis and geochemistry of these αFe-minerals are varies considerably. So, goethite is formed in acidic environment and in conditions of high humidity and moderate temperature, whereas hematite is formed in neutral conditions and with low humidity and high temperature [6]. This opens up opportunities to the ratio hematite/goethite to determine a soil evolution history. Huge significance for geochemistry has Fe substitution for Al in the lattice of these minerals, particular for goethite. For example, the degree of substitution of aluminum associated with age of alluvial soils (Victoria, Australia) [7]. In the more ancient soils with age 760 thousand years Al content was higher (8-12 mol %) than in young soils with age ~ 40 thousand years, where the Al contents was only 3.5-5 mol %. There are other important differences in the content of aluminum in soils with goethite of different genesis. Comparison of the proportion of Al in goethite of alfesols (Indiana, United States) and oxisols (Goya, Brazil) showed a statistically significant difference. Oxisols goethite is contain 11-14 mole Al %, whereas alfisols goethite – only 7-9 mole Al % [8].

Accurate information on soil goethite and hematite gives Mossbauer spectroscopy, especially in a strong cooling, to the temperature of liquid nitrogen – 4 k [6, 9]. In addition to the percentage of Fe in goethite and hematite Mossbauer spectroscopy is allows you to judge the degree of particles mess structure, that is associated with the destructive influence of Al or Ti impurities on the (hydr)oxides structure. With the development of spectrophotometers it is appeared able to exact number-definition of soil color and judge the correlation of main soil pigments. These include: humus as a black pigment, carbonates as a white pigment, Fe-(hydr)oxides as red and yellow pigments [10]. It is primarily red hematite αFe_2O_3 and yellow goethite αFeOOH. It is asked a few techniques using optical spectrum of soil to determine the hematite and goethite share. The end result of the analysis is usually expressed as the ratio [Hematite/(Hematite+Goethite)]. Let us name this ratio as index I.

Optical-mineralogical methods of an index I determination is based on the ratio of red and yellow parts of the soil spectrum. The most common technique is based on converting optical soil spectrum using equations of Kubelka-Munk [11, 12, 13]. Then a new spectrum is differentiated twice and compares the amplitudes of two reflexes: 530 nm for hematite and 413 nm for goethite. Attitude [Hematite/(Hematite+Goethite)], calculated by this method are denoted by index I_{K-M}. This method can serve as a benchmark in determining the ratio of hematite and goethite on optical spectra of soil. Disadvantage: the complicated procedure is requirement to use a computer programs.

At present, the color of the soil is characterized mainly by two optical systems: earlier Munsell system and more modern system of CIE-L*a*b* [10, 14-16]. Munsell color point is defined by three characteristics: Hue (H), Value (V) and Chroma (C). Because no equivalent perception of light and dark color tones all cylindrical color space is filled.

In the CIE-L*a*b* system: L* is coordinate set of lightness (varies from 0 to 100, from the darkest to the lightest), chromatic component is defined by two Cartesian coordinates a* and b*. The first coordinate is indicated the position of the colors range from green (-a*) to the red (+a*), and the second is ranged from blue (-b*) to yellow (+b*) [3, 14]. Coordinates a* and b* are distinguished clearly contribution of Fe-minerals to the soil color.

Since orthogonal CIE-L*a*b* system is much better then convenient cylindrical Munsell system [3, 10, 14], then the color of minerals and soils we express only in CIE-L*a*b* system. Data sources, expressed in Munsell, we were transferred to CIE-L*a*b* system, algorithms re-accounts is published in papers [17, 18]. Soil scientists have gathered information about the Munsell color of the soil, published in numerous articles. But learn from them hematite and goethite information using known approaches is impossible. Therefore, we are proposed a new approach that would use previously received information about Munsell color to extract information on the ratio in soils of hematite and goethite. Of course, the new technique is suitable for counting relations [Hematite/ (Hematite+Goethite)] in soil samples, with modern spectrophotometer issuing the result immediately in the CIE-L*a*b*. Ratio [Hematite/(Hematite+Goethite)] is calculated on new methods, let the index of I_{Lab}.

The objective of this study: to propose a new method for determining the ratio hematite/goethite by the soil color in the CIE-L*a*b* system.

Objects

We are analyzed Fe-(hydr)oxides using dashboards Sheinost and Schwertmann [19] on reference samples (hydr)oxides of iron (n = 277). Among them: hematite αFe_2O_3, maghemite γFe_2O_3, goethite αFeOOH, lepidocrocite γFeOOH, ferrihydrite $2Fe_2O_3 \cdot FeOOH \cdot 4H_2O$ and feroxyhite δFeOOH. Their colorimetric characteristics in the source were expressed in Munsell, we counted them in CIE-Lab system.

To compare two methods: 1) with the conversion of optical spectrum according to the Kubelka-Munk functions, and 2) new techniques we were used the color data of modern andosols and paleosols in Northern Italy [20].

Basic researches are devoted to the analysis of luvisols of southern Spain, the source data is published in [2]. In addition, researches are devoted our data on color of cambisols from Lithuania, and Arkhangelsk, Perm and Vologda regions (Russia).

Methods

The methodology of calculating the ratio of hematite/goethite by the soil color in the CIE-Lab System. First of all, the minerals color it is necessary to express one number.

As can be seen from the table 1, Fe-minerals is shown redness (a*) and yellowness (b*), although in different proportions. The ratio between the redness

(a*) and yellowness (b*) use as an indicator (Red) of each mineral and soil sample; let us express Red it in the form:

Red = [a*/(a* + b*] (1)

Value (hydr)oxide Red is reduced in this order: hematite (αFe_2O_3) > feroxyhite (δFeOOH) > ferrihydrite > (2Fe2O3·FeOOH·4H2O) > maghemite (γFe_2O_3) > lepidocrocite (γFeOOH) > goethite (αFeOOH). Red of hematite is maximal: Red = 0.51, and Red of goethite is: Red = 0.16. The degree of Red of hematite have expressed about 3 times stronger than the goethite. We emphasize that these values Red was obtained on a pure Fe-minerals.

Content of hematite and goethite was studied in soils enriched Fe-(hydr)oxides: oxisols, cambisols, etc. [2, 6]. Their ratio is usually expressed in the form: [Hematite/(Hematite+Goethite)].

This relationship you can count on soil color CIE-Lab system using index Red. In soils with two contrasting pigments: red hematite and yellow goethite Red index is range from 0.51 in the presence of single hematite to 0.16 - in the presence of single goethite. Intermediate index values Red will have samples with different fractions of hematite and goethite in the absence of other Fe-pigments in the soil. The second condition: minimum index value Red = 0.16 meets soils with pure goethite, but if there is only one Al-goethite Red value falls below 0.16.

Attitude [Hematite/(Hematite+Goethite)] defined by the new methodology is based on soil color CIE-Lab system will be denoted by I_{Lab}. The index of the I_{Lab} races-read from the formula:

$I_{Lab} = 1 – [(0.51 – Red)]/(0.51 – 0.16)$, (2)

where is 0.51 – averaged magnitude of hematite Red and 0.16 – averaged magnitude of goethite Red.

In soils, especially tropical ones, occur Fe-(hydr)oxides with a partial substitution of Fe^{3+} by Al^{3+}. Aluminum is reducing hue of ferruginous minerals. Amendments to the color of both minerals are difficult. Let us confine adjusted only one mineral, where the substitution of iron as much as possible, i.e. to take into account the effect of Al on the goethite color. We are assume that the color of Al-hematite is not different from the color of pure hematite (due to the low degree of substitution of iron in hematite), and for distorting effect on the color of the aluminum is meet Al-goethite.

Comparing the new technique with the methodology of calculating the ratio of hematite/goethite by Kubelka-Munk equation. For this comparison, we are used work [20], where counting relations [Hematite/(Hematite+Goethite)] based on spectral color information of modern soils and paleosoils (North Italy) using Kubelka-Munk function, as well as Munsell Color. We were changed the color in the CIE-Lab system, and then calculated the index of I_{Lab}. The results of the comparison of two methods of counting relations [Heme-Titus/(Hematite+Goethite)] are given in the table 2.

As can be seen, the mean values of relationship [Hematite/(Hematite+Goethite)] for n = 10 are differ not substantially: $I_{K-M} = 0.05 \pm 0.01$ and $I_{Lab} = 0.06 \pm 0.02$; difference is not authentically P 0.95. The correlation coefficient between the indices I_{K-M} and I_{Lab} is r = 0785.

Thus, the new technique is give results similar to results, received for converting optical spectrum on Kubelka-Munk theory, but has the advantage of ease of calculation and the ability to use the old color data obtained in the Munsell system.

Now let us consider the application of the new methodology for calculating the relationship [Hematite/(Hematite+Goethite)] in soils with pure Fe-minerals and mixed with aluminum for example luvisols and kambisols.

Table 1. *Fe-(hydr)oxides color, expressed in Munsell system and CIE-L*a*b* system. The original data in the paper [19]*

Минерал	Munsell	CIE-L*a*b*			
		L*	a*	b*	Red
Hematite	1.2 YR 3.6/5.2	36.6	20.9	20.4	0.51
Feroxyhite	4.2 YR 3.8/6.0	38.7	19.1	29.3	0.39
Ferrihydrite	6.6 YR 4.9/6.3	50.0	15.4	34.9	0.31
Maghemite	8.3 YR 3.1/3.2	31.4	7.4	18.0	0.29
Lepidocrocite	6.8 YR 5.5/8.2	56.1	18.5	46.4	0.28
Goethite	0.4 Y 6.0/6.9	61.0	8.2	44.1	0.16

Table 2. *Mansell color and CIE-L*a*b* system color of recent andosols (RS) and paleosols (I-IV) in Northern Italy. The values I = [Hematite/(Hematite+Goethite)], calculated based on the Kubelka-Munk equations (I_{K-M}) and based on CIE-L*a*b* system. The original data is in the paper [20].*

Sample (depth, cm)	Munsell	CIE-L*a*b*				I_{Lab}	I_{K-M}
		L*	a*	b*	Red_{Lab}		
RS-A (0-20)	9.6 YR 5.5/3.6	56.7	6.8	25.7	0.21	0.14	0.07
RS-Bw1 (20-40)	9.6 YR 5.4/3.5	56.7	4.6	18.7	0.20	0.11	0.10
RS-C1 (80-100)	9.3 YR 7.0/3.7	71.6	5.8	26.1	0.18	0.06	0.09
I-1 (280-300)	8.9 YR 5.6/4.0	56.7	6.8	24.4	0.22	0.17	0.08
II-1 (460-480)	0.3 Y 6.9/3.8	71.6	4.5	27.1	0.14	0.00	0.00
III-1 (840-860)	9.5 YR 6.5/4.0	66.6	5.4	25.1	0.18	0.06	0.04
III-3 (92-940)	9.8 YR 6.8/4.0	71.6	4.5	25.9	0.15	0.00	0.02
IV-1 (1000-1020)	0.1 Y 6.7/4.1	66.7	4.0	26.1	0.13	0.00	0.01
IV-3 (1040-1060)	9.6 YR 6.6/3.8	66.7	5.4	25.1	0.18	0.05	0.03
IV-4 (1060-1080)	9.4 YR 6.3/3.9	66.7	5.4	25.1	0.18	0.05	0.06
Average						0.06± 0.02	0.05± 0.01

Results and discussion

Relationship between Hematite and Goethite in luvisols

The main feature of luvisols is the texture profile differentiation; clay accumulates in the horizon argic, its color ranges from brown to red, depending on the composition of the Fe-(hydr). Luvisols are holded 500-600 million HA in the world, mainly in (sub)tropical regions [21]. We were analyzed two red-brown color luvisols (profiles RB and MO) in the province of Cordoba in southern Spain, described in [2]. Iron minerals are presented in two color: red hematite and (Al)-hematite and yellow goethite and (Al)-goethite. In the upper part of the both profiles in Fe-minerals part of Fe^{3+} is replaced by Al^{3+}. Replacing is extent lesser (to 7 mole Al % in the iron hematite) and twice stronger (up to 14 mole Al % replaces in goethite). It is obvious that the optical effect of the Al presence in the lattice of goethite is higher than from its iron replacement in hematite. The minerals iron impurities are not present at the profile bottom.

Let us compare the calculated value index I_{Lab} with real attitude [Hematite/ (Hematite+Goethite)]. As can be seen from table 3, at the profiles bottom where there are pure hematite and goethite, almost for all samples $I_{Lab} \approx$ [Hematite/(Hematite +Goethite)]. This means that the optical properties of goethite and hematite in luvisols are close to standard minerals on Sheinost and Schwertmann [19]. A notable deviation is observed only sample only MO-6 where I_{Lab} = 0.23, whereas [Hematite/ (Hematite +Goethite)] = 0.00. Empire share hematite (when calculating by color), obviously, is due to the increased redness real Fe-minerals in the sample MO-6 compared with reference minerals.

Table 3. *Color and Fe-minerals in luvisols of southern Spain. The original data is in the paper [2].*

Sample (depth, cm)	Al-goe-thite, %	Al-he-matite, %	I	Mansell	L*	a*	b*	Red	I_{Lab}	ΔRed
Profile RB										
RB-11(22-45)	1.65	2.80	0.63	7.5 YR 6/4	61.1	8.4	22.3	0.27	0.33	0.11
RB-12 (45-70)	2.25	3.10	0.58	8 YR 7/4	70.9	7.2	23.2	0.24	0.23	0.12
RB-13 (70-105)	2.80	2.80	0.50	7.5 YR 7/4	70.9	7.9	22.6	0.26	0.28	0.07
RB-14(105-130)	2.20	3.75	0.63	8 YR 7/5	70.9	9.0	29.0	0.24	0.23	0.14
RB-15*(130-155)	4.90	1.65	0.25	8 YR 7/5	70.9	9.0	29.0	0.24	0.23	
RB-16 (155-170)*	4.95	0.90	0.15	9 YR 8/3	80.5	3.8	18.6	0.17	0.03	
RB-17(170-190)*	4.35	-	0.00	1 Y 8/2	80.5	0.8	14.0	0.05	0.00	
RB-18(190-230)*	3.60	-	0.00	2 Y 8/1.5	80.5	0.0	10.9	0.00	0.00	
RB-19(230-260)*	4.40	-	0.00	2 Y 8/2	80.5	0.0	14.6	0.00	0.00	
RB-20(260-300)*	4.15	-	0.00	10 YR 8/2	80.5	1.6	13.4	0.11	0.00	
Profile MO										
MO-1 (0-8)	1.95	3.95	0.67	6 YR 6/5	61.0	12.2	26.3	0.32	0.46	0.07
MO-2 (8-50)	2.10	4.10	0.66	6 YR 7/6	70.9	13.8	32.0	0.30	0.40	0.09
MO-3 (50-65)	1.50	4.80	0.76	5 YR 6/6	61.0	15.8	30.6	0.34	0.52	0.09
MO-4 (65-75)	1.50	3.20	0.68	6 YR 7/5	70.9	11.6	26.4	0.31	0.43	0.09
MO-5 (75-100)	1.40	3.00	0.68	7 YR 7/4	70.9	8.4	22.1	0.27	0.31	0.13
MO-6 (100-145)*	3.10	-	0.00	7.5 YR 7/3	70.9	6.0	16.9	0.26	0.23	
MO-7(145-180)*	2.80	-	0.00	10 YR 8/2	80.5	1.6	13.4	0.11	0.00	

* – goethite and hematite without Al.

Characteristically, that luvisols without hematite in the lower parts of the two rips have a low Red = 0.00-0.26. The higher the goethite, the lower the redness: correlation coefficient dependency on Red from the contents of goethite is negative: r =-0. 58. Thus, in the lower layers, where the only Fe-pigment is goethite, increasing its number is lead to lower the already low Red soil.

At the luvisols top are contained hematite and goethite, both enriched with aluminum. This change of the chemical composition of Fe-minerals is lead to heavy distortion of the results of calculation of I_{Lab} index. In fact, in the samples profile RB share Al-hematite from its amount with Al-goethite is reaches 50-63 % while the index calculation based on sheer colors I_{LAB} goethite is show the proportion of hematite only 23-33%. It is clear that the error is obliged to impurities Al in Fe-minerals because the calculation is based on optical reference analysis, pure particles of hematite and goethite. To correct a mistake will make an amendment to the distorting effects of aluminum on the color of goethite with 8-12 Mole Al %. To a first approximation, the influence of aluminum on the color of hematite (2-5 mole Al %) negligible, let us limited to the influence of Al on the color of the goethite only.

Let us calculate the value soil reduction ΔRed due to the influence of Al on the color of goethite, proceeding from the real relationship between Al-hematite and Al-goethite. To do this, we are transform the equation (2) and make it real relation I = [Hematite/(Hematite+Goethite)]. Reduction of soil ΔRed will be calculated from the equation:

$$\Delta Red = 0.51 - 0.35x\{1 - [Hematite/(Hematite+Goethite)]\} - Red \quad (4)$$

The value of ΔRed for luvisols with Al-goethite are listed in table 3. To RB profile ΔRed values ranging from 0.07 to 0.14, on average ΔRed = 0.11, to MO profile ΔRed values ranging from 0.07 to 0.13, average ΔRed = 0.09. Generalized average ΔRed is 0.10. Thus, Al in goethite is understates the luvisols Red on average 0.10. This ΔRed can be used for correction of Al influence on goethite color in soils containing goethite with 8-12 mole Al %.

The ratio hematite/goethite in cambisols

Characteristics of cambisols are heavy texture and a reddish tone, with a low content of iron compounds [21]. Since usually cambisols is weathered weakly they often receive from legacy particles of hematite and goethite. Cambisols are took 1.5 billion HA in the world, they are the most common soils in the world [21].

We were studied four carbonate cambisols in European Russia: 1) in Pinega district, Arkhangelsk, 2) in Perm district, 3) in Zarasai district, Lithuania, 4) in Cherepovets district, Vologda. The results are shown in table 4. As can be seen, the index value of Red is vary in a wide range: from 0.18 to 0.40. Even wider range index values I_{Lab}: from 0.07 to 0.69. Such a large spread of optical indicators is indicated heterogeneity sampling.

A possible reason is the difference in the chemical composition of goethite in cambisols. Indeed, eight samples have pure goethite and four samples is composed goethite with part of Fe^{3+} substituted for Al^{3+}, these two groups are varying in their optical properties. As can be seen from the table 4, cambisols with pure goethite have high Red = 0.33 ± 0.02, and the I_{Lab} index = 0.50 ± 0.05, that is 50% of hematite. The indicators of soil containing Al-goethite significantly below: Red = 0.22 ± 0.02, and the proportion of 17% total hematite: I_{Lab} = 0.17 ± 0.06. Difference of both soil groups is authentically P 95.

Make amendments in color of cambisols with Al-goethite. To do this we will use the data about the average reduction Red previously received for luvisols: ΔRed = 0.10. If ΔRed = 0.10 to add the cambisols containing Al-goethite, the index value will increase significantly I_{Lab} (table 4). As a result, the average value of the I_{Lab} team cambisols with Al- goethite will increased: $I_{Lab(Corrected)}$ = 0.45 ± 0.06. Now the $I_{Lab(Corrected)}$ index of two samples is matched up and their difference becomes unreliable at P 95.

Thus, the amendment on Al in goethite gives more similar picture: 45% of hematite in the same series as that designs cambisols with pure flocking (50%).

Conclusion

Index I = [Hematite/(Hematite+Goethite)] is widely used in the study of the genesis and soil classification. In addition to the mineralogical it is known the optical method of obtaining I index using Kubelka-Munch equation. We are proposed a simpler method of determining I_{Lab} index on soil color using the optical CIE-L*a*b* system. The method is based on calculating soils Redness (Red) and then calculating the I_{Lab}, based on reference Red

Table 4. *Color and Fe-minerals in the cambisols of the Russian plain. The original data is in the book [10].*

Horizon (depth, cm)	Fe-minerals	Fe_{Tot} %	Fe_{DCB} %	L*	a*	b*	Red	I_{Lab}	$I_{Lab-corr}$
Pinega district, Arkhangelsk, Russia									
BM (7-16)	Hematite, goethite	2.41	1.29	60.3	14.5	26.3	0.35	0.55	
B (16-24)	Hematite, goethite	3.65	2.22	57.8	16.8	25.2	0.40	0.69	
D_{Ca} (44-62)	Hematite, goethite	1.00	0.48	71.9	12.0	30.4	0.28	0.35	
Perm district, Russia									
AY (7-12)	Hematite, goethite	4.18	1.57	58.9	11.1	24.7	0.31	0.43	
B1 (19-36)	Hematite, goethite	5.29	2.00	57.6	15.4	25.8	0.37	0.61	
B2 (36-56)	Hematite, goethite	5.34	2.20	56.6	15.8	24.9	0.39	0.65	
Zarasai district, Lithuania									
PYg (0-10)	Hematite, Al-goethite		1.42	66.2	8.0	29.3	0.21	0.16	0.43
$B1_{Ca}$ (40-50)	Hematite, goethite		1.09	67.9	11.3	29.0	0.28	0.35	
BC_{Ca} (80-100)	Hematite, goethite		0.49	68.8	11.9	30.0	0.28	0.35	
Cherepovez district, Vologda, Russia									
PY (0-20)	Hematite, Al-goethite		0.77	62.7	5.4	21.8	0.20	0.11	0.40
B (31-52)	Hematite, Al-goethite		0.48	75.3	6.7	29.8	0.18	0.07	0.34
C (66-85)	Hematite, Al-goethite		1.18	63.0	11.3	28.8	0.28	0.35	0.63

Fe_{Tot} – total content Fe in soil, Fe_{DCB} – Fe, extracted with DCB, $I_{Lab-corr}$ – I_{Lab} index after correction for Al in goethite.

of hematite and goethite. Replacement of Fe^{3+} to Al^{3+} is taken into account through amendments to the color of goethite, admitting that Al-hematite color does not differ from color pure hematite.

Thus, the new technique was proven on Northern Italy andosols and was give results similar to results, received for converting optical spectrum on Kubelka-Munk theory. But the new technique has the advantage of ease of calculation and the ability to use the old color data obtained in the Munsell system.

Validating new methods in luvisols is showed an agreement index values I_{Lab} with real [Hematite/(Hematite+Goethite)] in those parts where there are profile have pure hematite and goethite. In luvisols containing Al-goethite and Al-hematite, admixture Al generates an error in the calculation. To delete the error, it is proposed an amendment to the distorting effects of aluminum in lattice goethite, ewith high content: 8-12 mole Al %. Cambisols have a value index I_{Lab} also vary depending on the impurities Al in hematite and goethite. From samples with particles of pure goethite Red higher than cambisols containing Al-goethite. After adjustment for the Al-share in goethite the share of hematite becomes comparable to its share in the cambisols samples with pure goethite.

Acknowledgment

The author thanks N.P. Kirillova for help in the work.

References

[1] S.W. Buol, F.D.Hole, R.J. McCracken, Soil genesis and classification. Iowa State university Press, Ames., 1973.

[2] J. Torrent, A. Cabedo, Sources of iron oxides in reddish brown soil profiles from calcarenites in Southern Spain, Geoderma. 37 (1986) 57-66.

[3] R.A. Viscarra Rossel, B. Minasny, P. Roudier, A.B. McBratney, Colour space models for soil science, Geoderma. 133 (2006) 320–337.

[4] J. Ji, W. Balsam, J. Chen, L. Liu, Rapid and quantitative measurement of hematite and goethite in the Chinese loess-paleosol sequence by diffuse reflectance spectroscopy, Clays Clay Miner. 50 (2002). 208-216.

[5] X. Long, J. Ji, V. Barron, J. Torrent, Climatic thresholds for pedogenic iron oxides under aerobic conditions: Processes and their significance in paleoclimate reconstruction, Quater. Sc. Rev. 150 (2016) 264-277.

[6] U. Schwertmann, E. Murad, D.G. Schulze, Is there Holocene reddening (hematite formation) in soils of axeric temperate areas? Geoderma. 27 (1982) 209-223.

[7] I.P. Little, R.J. Gilkes, Aluminum substitution in goethites in soils from alluvium, Gippsland, Victoria, Austral. J. Soil Res. 20 (1982) 351-354.

[8] R.B. Bryant, N. Curi, C.B. Roth, D.P. Fransmeier, Use of an internal standard with differential X-ray diffraction analysis for iron oxides, Soil Sci. Soc. Amer. J. 47 (1983) 168-173.

[9] V.F. Babanin, V.I. Trukhin, L.O. Karpachevskiy, A.V. Ivanov, V.V. Morozov, Soil Magnetism. Moscow-Yuroslavl. 1995 (in Russian).

[10] Yu.N. Voduanitskii, L.L. Shishov, Study of some soil processes on soil color. Dokuchaev Soil Institute. Moscow. 2006.

[11] V. Barron, J. Torrent, Use of the Kubelka-Munk theory to study the influence of iron oxides on soil color, J. Soil Sci. 37 (1986) 499-510.

[12] A.C. Scheinost, A. Chavernas, V. Barron, J. Torrent. Use and limitation of second-derivative diffuse reflectance spectroscopy in visible to near-infrared range to identify and quantify Fe oxide minerals in soils, Clays Clay Miner. 46 (1998) 528-536.

[13] J. Torrent, V. Barron, Diffuse reflectance spectroscopy of iron oxides, Encyclop. Surface Colloid Sci. 2002.

[14] Yu.N. Voduanitskii, N.P. Kirillova, Application of the CIA-Lab system to characterize soil color, Eur. Soil. Sc. 49 (2016) 1259-1268.

[15] Yu.N. Voduanitskii, L.L. Shishov, A.A. Vasilev, E.F. Sataev, An analysis of the color of forest soils on the Russian Plain, Eur. Soil. Sc. 38 (2005) 11-22.

[16] J. Torrent, V. Barron, Laboratory measurement of soil color: theory and practice. SSSA. 31 (1993) 21-33.

[17] Yu.N. Voduanitskii, N.P. Kirillova, Conversion of Munsell color coordinates to CIA-L*a*b* system: Tables and calculation examples, Moccow University Soil Sc. Bull. 71 2016) 139-146.

[18] N.P. Kirillova, Yu.N. Voduanitskii, T.M. Sileva, Conversion of soil color parameters from the Munsell system to the CIE-L*a*b* system, Eur. Soil. Sc. 48 (2015) 468-475.

[19] A.C. Scheinost, U. Schwertmann, Color identification of iron oxides and hydroxysulfates: use and limitations, Soil Sci. Soc. Am. J. 63 (1999) 1463-1471.

[20] C. Colombo, G. Palumbo, E. Di Iorio, F. Russo, F. Terribile, Z. Jiang, Q. Liu, Soil development in a Quaternary fluvio-lacustrine paleosol sequence in Southern Italy, Quaternary Int. 418 (2016) 195-207.

[21] World reference base for soil resources. World Soil Resources Reports, No 103, FAO, Rome. 2006.

Annals of Agrarian Science

Journal homepage: http://journals.org.ge/index.php

Ecological Assessment of Pastures of Eastern Georgia (Kakheti)

Mariam Merabishvili

Agricultural University of Georgia, Kakha Bendukidze University Campus, 240, David Aghmashenebeli Alley., Tbilisi, 0131, Georgia

Received: 12 February 2019; accepted: 9 May 2019

A B S T R A C T

The article discusses a complex survey conducted in Kakheti pastures. Cinnamonic carbonate and raw carbonate soils are spread in the area of the inner Kakheti pastures. Studied soils with heavy metals (Cd, Cu, Pb, Zn) are not contaminated and do not exceed the maximum permissible concentration (MPC). In case of Arashenda village, the process of erosion and degradation is under the medium risk level. In Gombori and Shakhvetila villages the risk of degradation and erosion is relatively high.

Keywords: Pasture, Heavy Metals, Erosion, Degradation,Visual Research, Overgrazing

*Corresponding author: Mariam Merabishvili; E-mail address: mmera2008@agruni.edu.ge

Introduction

Pastures as a resource, has a great importance for the country, in terms of its use, so it is necessary to ensure their sustainable condition. One of the main conditions for the use of pasture is to determine the correct loading, which is defines the amount of livestock on a hectare of pasture, during the period of grazing without reducing its productivity and worsen the vegetation cover [1]. Results are correlated with environmental factors such as: (erosion, soil texture, temperature, evaporation, etc.) [2]. The research was conducted on the above mentioned issues [3].

Anthropogenic factor effects on pasture conditions a lot, pastures close to village populated areas are more eroded and degraded due to excessive grazing than distant pasturelands [4,5].

The study of the deterioration of pasture areas has been conducted in the southern part of Kazakhstan, where the worsen of soil structure is due to improper grazing [6].

Similar long-term surveys have been conducted in Armenia that, it is estimated that, on the pasture it is significantly reduced productivity and modified vegetation cover [7-9].

Several studies have been conducted in Azerbaijan, including for the protection of the grazing territories of pastures that threaten the ecological balance, which is a complex study of soil ecology (study of physical-chemical properties) [10-14].

Food production and their growth has a positive impact on pasture conditions [15]. In Georgia the situation on the pastures and related issues has been studied by many researchers. Among them reviewed the reduction of pasture productivity, their improvement and proper management [16,17].

During the years, the unsystematic, exploitation of natural food plots deterioration of the botanical composition of the vegetation cover, to worsen feed and hay quality also reduces herbage yield and their productivity, contributing to the spread of turf, diseases and erosion processes, and finally environmental pollution. In order to improve existing situation, it is necessary to have optimal loading of livestock and implementation of environmental protection measures on pastures [3].

The bioproductivity of fodder grasses of subalpine hayfields depends on the fertility of soil, the degree of erodibility and herbage thickness [18].

Nowadays, soils of pastures are not sufficiently enriched with mineral or organic fertilizers, soils are contaminated with weed grass, because of the failing of rotational grazing, it has been started the erosion process on pastures [19].

In the soils of Georgia, many studies have been carried out regarding heavy metals by various scientists [20-25].

Soil contamination by heavy metals (Cu, Zn, Pb) is one of the important problems on pastures, regarding the raised issue, the research was conducted in Georgia, in 9 km. radius from village Kazreti, Madneuli mining and processing enterprise, on the milk products of cows. It has been determined that the considerable increasing of Maximum Permissible Concentration (MPC) has been observed in soil, green grass, also in the blood of cows, on these pastures, as well as in milk products (cheese, matsoni) [26].

Erosion process is one of the reasons of degradation of soils of Georgia. Regarding erosion process many studies have been conducted in Georgia by many scientists [27-30].

For assessing the current situation, it is recommended to conduct visual assessment of the soil cover conditions (erosion), heavy metals and evaluation of pastures by visual appraisal.

Objectives and methods

Studies were conducted in Georgia, specified in Kakheti region. The research objects are located in three villages of Gurjaani and Akhmeta municipalities: Arashenda, Cheremi and Koghoto.

Village Arashenda located in the upper drain of the river "Lakbe" at 760 m. height altitude from the sea level. On Arashenda study territory, have been made 10 soil profiles.

Village Cheremi is located on the north-east slope of the Gombori Range, altitude from the sea level is 1000m. The left side of the river Chermiskhevi (Alazani right tributary). In study territory in Cheremi village have been made 10 soil profiles.

Village Koghoto is located on Alazani plain on the right side of the river Alazani at 460 m. from the sea level. In the study area of village Koghoto have been made 5 soil profiles.

According to the selected methodology and research components from 7 research objects have been taken (0-20) (20-40) cm. depth, 14 soil samples. In the raised article, it has been reviewed three objects. The soil samples have been conducted laboratory analyzes regarding the following heavy metals (Cd, Cu, Pb, Zn) content.

Laboratory analyzes of soil samples of pastures have been implemented in Michail Sabashvili Institute of Soil Science, Agrochemistry and Melioration and in the laboratory of ecological agriculture and nature protection;

Analysis of soil samples were performed by the following methods: Soil texture composition was determined by the pipe method; Reaction of soil solution (pH) – in the potential meteoric method in water sampling; hygroscopic water-drying method at 105ºC; Exchangeable bases –trilon B via titre [31]. Mobile N and P content (ISO/TS 14256-1:2003) determination of exchange calcium atomic-absorption spectrometer [32].

Study of common forms of (Cd; Cu; Pb; Zn) according to the Austrian standard (ISO 11466:1995), atomic-absorption methodology (Perkin Elmer 2100) and graphite tube (Perkin Elmer Aanalyst 700) by spectrometer [33].

Soil mapping was created using geoinformation systems (GIS).

For visual assessment of pasture, during the collecting of pasture plot samples, have been used “preferential sampling” and “random sampling” designs. The plots were selected based on the “preferential sampling design” which means, that you can choose the pasture place subjectively, according to certain criteria on the position of your plot. Other sampling methods are random designs; they are usually developed on the basis of satellite images and the selection of plots is done randomly by Geographic Information Systems (GIS) [34,35].

Visual assessment of the pasture, finds out on pasture places 10X10 (In total 100) which is the sample of the demonstration. According to many criteria, there have been created the questionnaire based on the world scientific experience, in the questionnaire it is evaluating existing pasture condition via percentage, such as: erosion tracks; vegetable cover and etc. [35].

Based on information which were collected on pastures, two indicators were created, the first index called susceptibility to erosion (SEI), and the second index is pasture degradation index (PDI).

Susceptibility to erosion (SEI), is clearly shown in the colours of the traffic lights according to the approved methodology [34] during the research, as needed, we have added orange colour, for observing medium risk level signs of degradation, taking into consideration colours above, the layout is following:

Index Range	Risk to Erosion Level	Light
76-100	Low Risk	Green
51-75	Medium Risk	Yellow
26-50	Medium Strong Risk	Orange
0-25	High Risk	Red

Based on calculation indices and by easily expressing, visual appraisal of pastures, evaluating the condition of pastures accordingly.

Results and Analysis

On research territories, in the collected soil profiles have been made soil texture and chemical analyzes (Tab. 1; 2).

Table 1. *Soil Texture*

Objects, profile, N	Horizon, depth (cm)	Fractions, %						
		1-0,25	0,25-0,05	0,05-0,01	0,01-0,005	0,005-0,001	<0,001	<0,01
Arashenda 2	A - 0-5	3	32	17	13	2	33	48
	AB - 5-20	6	24	17	15	6	32	53
	B - 20-40	6	21	25	4	8	36	48
	BC -40-60	8	34	7	8	13	30	51
Arashenda 7	A -0-20	4	42	19	7	12	16	35
	B -20-40	1	29	23	10	14	23	47
	BC -40-60	1	26	21	4	24	24	52
Arashenda 9	AB -0-35	6	23	9	17	18	27	62
	B -35-91	2	11	17	11	32	27	70
	BC_1-91-120	0	33	10	4	30	23	57
Cheremi 3	AB -0-28	0	15	5	17	44	19	80
	BC_1-40	0	16	12	10	24	38	72
	BC_2-40-58	3	27	23	7	18	22	47
	CD -58-80	2	40	10	13	18	17	48
Cheremi 6	AB- 0-20	1	31	12	12	15	20	56
	BC-20-70	1	23	23	5	12	36	53
Cheremi 10	AB- 0-30	10	26	23	9	8	24	41
	BC- 30-60	10	40	6	1	21	22	44
Koghoto 2	A- 0-20	1	16	30	9	15	29	53
	BC- 20-40	0	31	10	13	18	28	59
Koghoto 4	A- 0-20	0	30	12	18	22	18	58
	BC -20-40	0	29	20	18	16	17	51
Koghoto 5	A- 0-20	2	35	23	9	16	15	40
	BC- 20-40	4	38	18	8	22	10	40

Table 2. *Main characteristics*

Objects, profile, N	Horizon, depth (cm)	Hygr. H_2O,%	pH	$CaCO_3$, %	Humus %	Cation exchange capacity, mg/equivalent in 100g. soil			Sum,%	
						Ca^{2+}	Mg^{2+}	Sum. $Ca^{2+}+Mg^{2+}$	Ca	Mg
Arashenda 2	A - 0-5	3.52	8.4	8.18	7.4	20.27	6.76	27.03	75	25
	AB - 5-20	4.38	8.6	10.91	6.3	17.06	5.45	22.51	76	24
	B - 20-40	4.38	8.4	9.09	5.4	24.56	7.5	32.06	77	23
	BC -40-60	4.38	8.5	11.82	2.1	23.87	5.81	29.68	80	20
Arashenda 7	A -0-20	2.67	8.2	21.36	6.8	22.64	10.47	33.11	75	25
	B -20-40	3.73	8.3	23.18	4.5	10.42	7.17	25.59	72	28
	BC -40-60	1.21	8.4	21.36	2.7	16.89	5.64	22.53	75	25
Arashenda 9	AB -0-35	2.88	8.2	15.91	8.3	20.27	6.42	26.69	76	24
	B -35-91	5.71	8.4	22.27	6.8	19.12	5.22	24.34	78	22
	BC.91-120	4.38	8.3	22.73	4.6	17.06	6.14	23.20	73	27
Cheremi 3	AB -0-28	4.38	7.7	2.27	9.4	30.7	6.82	37.52	82	18
	BC_1-40	3.52	8.0	6.82	8.2	27.97	8.19	36.16	77	23
	BC_2-40-58	2.46	8.3	13.18	7.1	23.08	6.36	29.44	78	22
	CD -58-80	2.04	8.4	19.09	6.1	24.09	6.02	30.11	80	20
Cheremi 6	AB- 0-20	3.31	7.9	9.09	9.6	20.95	7.77	28.72	73	27
	BC-20-70	3.31	8.3	22.73	7.1	19.93	7.1	27.03	74	26
Cheremi 10	AB- 0-30	2.04	7.0	0.91	8.1	25.09	5.02	30.11	83	17
	BC- 30-60	2.25	8.3	4.09	6.1	19.4	5.69	25.09	77	23
Koghoto 2	A- 0-20	2.04	8.5	30.45	8.7	16.05	5.03	21.08	76	24
	BC- 20-40	0.81	8.4	29.54	7.4	14.76	4.92	19.68	75	25
Koghoto 4	A- 0-20	5.71	8.4	35.45	7.2	16.34	5.56	21.09	75	25
	BC -20-40	5.42	8.4	36.36	6.5	17.22	6.2	23.42	73	27
Koghoto 5	A- 0-20	12.1	8.3	36.36	8.2	16.39	5.36	21.75	75	25
	BC- 20-40	2.50	8.4	42.27	6.4	14.46	5.17	19.63	74	26

In Arashenda village study territory, for the illustration have been chosen three soil profiles, which belongs to cinnamonic carbonate (prof.2) and raw carbonate (prof.7; 9) soils.

The cinnamonic carbonate soil is characterized by the profile A-AB-B-BC (prof.2). The profile 2 is heavy loam, where the fraction 1-0.25 content is 3-8%, content of fine particles is 30-36%, content of physical clay fraction is between 48-53 % (Tab.1). Higroscopical water fluctuates 3,52-4,38%. The profile is characterised alkaline reactions 8,4-8,6, Ca content is 8,18-11,82%. The humus content in upper horizons is high and reaches 7,4%, but in the depth in lower horizon 2,1%. The soil is saturated exchangeable basis. The sum of exchangeable basis consists 22,51-32,06 mg/equivalent in 100g. Ca predominates 75-80% (Tab. 2)

Raw carbonate soils have the following structure: A-AB-BC (prof. 7; 9), prof. 7 heavy loam, prof.#9 is a light clay, where 1-0.05 mm fractions content 0-6%, the physical clay faction (<0.01 mm) is 35-70%, clay fraction (0,001) is 16-27% (Tab. 1). The higroscopic water varies between 1.21 and 5.71%, its highest rate is observed in the horizon -B.

The profile is characterized with alkaline reaction; pH indicator slightly varies between 8.2-8.4. Content of $CaCO_3$ varies between 15,92-23.18%. The soil is characterized with high and deep content of humus. In horizon A the humus content in consists 6.8-8,3% and in BC-horizon 2.7-4,6%. The soil is saturated with bases. The sum of the exchangeable cations is 22.53-33.11 mg. eqv. in 100g. soil. From exchangeable bases Ca is predominates 72-78% (Tab. 2).

In Cheremi village study territory, have been chosen three soil profiles, which belongs to cinnamonic carbonate (prof. 3; 10) and raw carbonate (prof. 6) soils.

Cinnamonic carbonate soil is characterized by a profile: AB-BC_1-BC_2-CD (prof. 3) and AB-BC (prof.10). Prof. 3 in upper horizons are medium loamy and in lower horizons are heavy clay texture prof. 10 medium loamy texture, where 1-0.25 mm fraction content is 0-10%, content of fine particles is

17-38%, content of physical clay fraction is between 47-80% (Tab.1) The content of higroscopical water is between 2.04-4.38%, pH-7.0-8.4 weakly alkaline and alkaline. Content of $CaCO_3$ varies between 0,91-19.09%. The humus content is high and in the upper horizons consists 8,1-9.4%, in lower horizons 6.1%. The soil is saturated with bases, from exchangeable bases Ca is predominates 77-82% (Tab. 2).

The soil profile 6 is raw carbonate, the profile is characterized: AB-BC, the profile has heavy loam texture, 20-36%, content of clay 20-36%, amount of physical clay fractions 53-56% (Tab.1). The content of higroscopical water is 3,31%, pH- 7.9-8.3 weakly alkaline. Content of $CaCO_3$ varies between 9,09-22,73%, the humus content is high and consists 7,1-9,6%. The soil is saturated with bases, the sum of the exchangeable cations varies 27,03-28,72 mg.eqv. in 100g. soil. from exchangeable bases Ca is more than 73% (Tab. 2).

In Koghoto Village study territory, have been chosen three soil profiles, which belongs to raw carbonate soils. Profiles 2; 4 and 5 characterized with profiles: A-BC.

Profiles 2 and 4, has heavy loam texture, profile 5 has a light loam texture, fine particles' content in three profiles varies between 10-29%, physical clay particles 40-59%. In total, in three soil profiles, the content of higroscopical water varies between 0,81-5.71%. pH-8.3-8.5 is alkaline. Content of $CaCO_3$ varies between29,45-42.27%. The humus content is high and in the upper horizons consists 7,2-8,2%, in lower horizons 6.4-7,4%. The soil is saturated with bases, from exchangeable bases Ca is predominates (73-76%).

These research objects are not contaminated by heavy metals and its contents, as well as the ratio, are absolutely acceptable for each sample in comparison to the limit of permissible concentrations (MPC).

At the same time, in soil samples noted minor changes in heavy metals content. The result of the survey is reflected in Table 3. The data received is comparable with the (MPC) indexes developed by E. Bakradze, Vodianiski, Urushadze and other authors [36].

On natural pasturelands there is no contamination by Pb and Cd in comparison to maximum permissible concentration (MPC) the result is below the critical edge.

In the research samples, the difference of Cu content in the soil layers is approximately 3-5 to 8-10 mg/kg.

Based on literature sources, it is possible to say, that existing difference is natural and therefore, it is defined by the "acceptable" criterion.

In case of Cu and Zn the difference between the depth of upper and lower layers (0-20), (20-40) is insignificant, that means that the content of heavy metals is almost equally distributed.

Supposedly, there is no source of pollution by heavy metals in this area. The concentration obtained is mainly derived from the deep layer of the soil, which can be conditioned by the biogenic factors and vegetation cover.

On the research territory of pastures, there is mentioned 9-10 mg. difference of the content of Zn and Cu, which can be due, to the abundance of natural substances, that come from the rock.

The survey was carried out to verify the condition of natural pastures in order to determine, whether the place is contaminated by heavy metals concentration on intensive grazing pasture territory.

Studied soils are not contaminated with heavy metals (Cd, Cu, Pb, Zn), their content in samples does not exceed so-called maximum permissible concentrations (MPC), accordingly, to this, it is impossible to move it into the food chain and polluted the product.

Based on visual research, in village Arashenda from 55 studied samples, it is visible, that erosion and degradation level of the risk is predominates, this is expressed by "yellow" colour this means medium risk of erosion. Plots of grazing territory of Arashenda village, which is located 700 m. above the sea level, they are more prone to erosion (Fig. 1)

Table 3. *The content of heavy metals (mg/kg).*

Objects	Soil depth, cm	Cu	Zn	Cd	Pb
Arashenda	0-20	39.48	58.94	<1	<5
	20-40	33.33	48.17	<1	<5
Koghoto	0-20	29.52	37.86	<1	<5
	20-40	57.09	53.07	<1	<5
Cheremi	0-20	56.45	53.61	<1	<5
	20-40	58.17	55.16	<1	<5

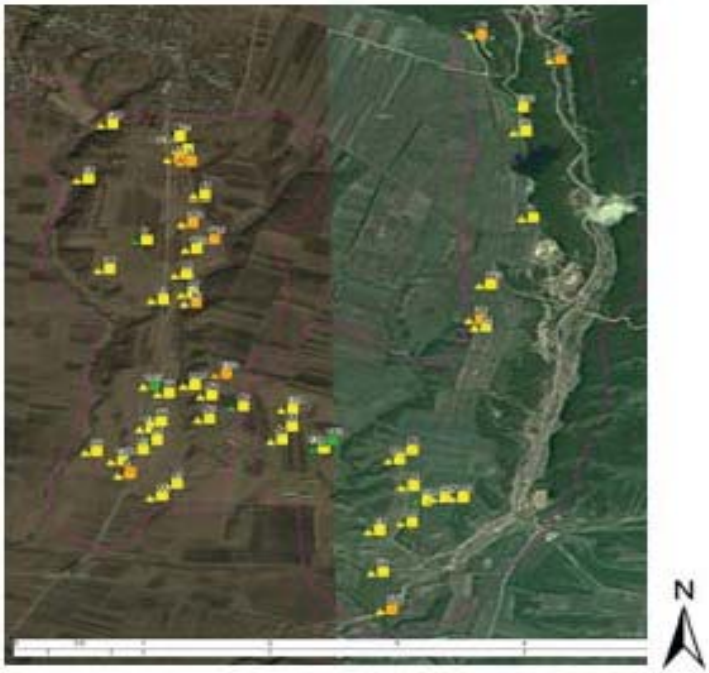

Fig.1 Village Arashenda, four colour map of pastures

Susceptibility to Erosion (SEI)
- Low
- Medium
- Medium strong
- High

Pasture Degradation Index (PDI)
- Low
- Medium
- Medium strong
- High

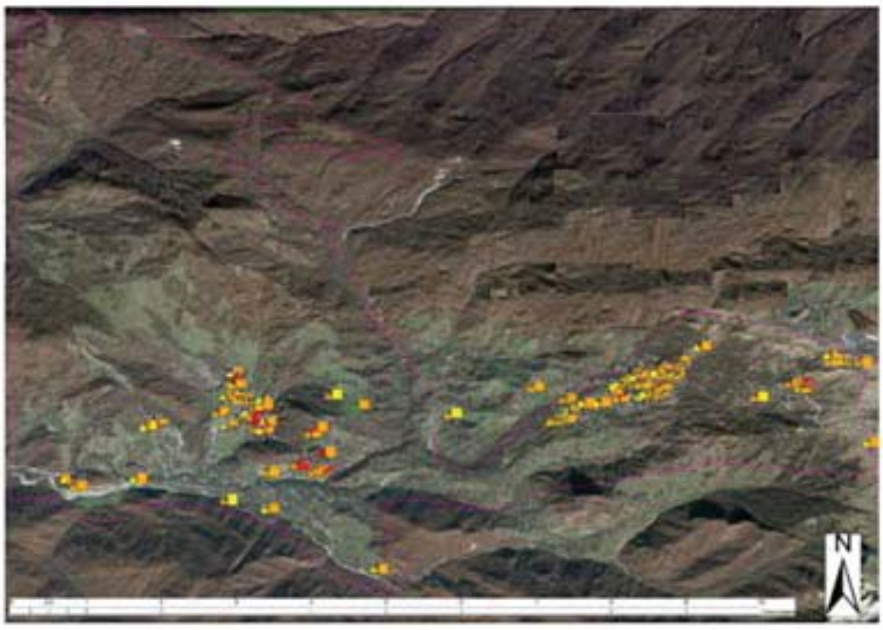

Fig.2 Village Gombori, four colour map of pasture

Susceptibility to Erosion (SEI)
- Low
- Medium
- Medium strong
- High

Pasture Degradation Index (PDI)
- Low
- Medium
- Medium strong
- High

Fig.3 Village Shakhvetila four colour map of pasture

Conclusion

The originality, of this research is that in the framework of the same research, several components have been studied at the same time, as follows: soil cover condition, erosion, contamination by heavy metals and visual assessment of pasture.

In the inner part of Kakheti region, there are distributed raw carbonate and cinnamonic carbonate soils on pastures.

According to soil texture cinnamonic carbonate soils have a heavy clay content. The reaction is alkaline and weakly alkaline, carbonated, high humus content, soils are saturated with bases; From exchangeable bases Ca is predominant.

According to soil texture, raw carbonate soils are mostly heavy and light clays. The reaction is alkaline, carbonated, the humus content is relatively high, deeply humifed, soils are saturated with bases, from exchangeable bases Ca is predominant.

Studied soils are not contaminated by heavy metals (Cd, Cu, Pb, Zn), by the existing concentration on the pastures with heavy metals, it is impossible to contaminate the food product.

In the object of Arashenda dominates, medium level of erosion and degradation processes, thus, increasing the quantity of livestock and pasture using proficiently is very fruitful.

On objects of Gombori and Shakhvetila village pastures erosion and degradation level is relatively high.

For better coordination of Gombori village pastures, it is necessary to determine the quantity of cattle, which are grazed in defined pasture territory, because of protecting rotational grazing rule, according to avoid overgrazing.

In case of Shakhvetila village pastures, the risk of high degradation maybe caused by climate conditions, strict and snowy winter and a frequent rain, which leads to unreachable ways to pastures, in addition, it is mentionable, that the process of reforestation in Shakhvetila and Gombori is a precondition for losing pastures.

References

[1] E. Klapp, Wiesen and Weiden, Berlin and Hamburg, 1966.

[2] G.Sh. Mammadov, S.A. Hajiyev, Rational use of soils under forage grass condition of Nakhchevan Autonomous Rebuplic, J. Annals of Agrarian Science 8 (1) (2010) 18-21 (in Russian).

[3] G. Agladze, Food production, Damani, Tbilisi 2010 (in Georgian).

[4] A.A. Torekhanov, Impact of rangeland use on livestock productivity, J. Annals of Agrarian Science 4 (2) (2006) 60-64 (in Russian).

[5] F.A. Guliyev, K.Y. Babayev, I.J. Karimov, R.I. Tahirov, R.T. Karimov, The influence of anthropogenic factors on the soil and vegetative cover in the south-east part of Azerbaijan on the basis of space images, J. Annals of Agrarian Science 13 (2) (2015) 39-43.

[6] A.A. Torekhanov, Soil conservation basics for rangeland use, J. Annals of Agrarian Science, 3 (4) (2005) 62-67 (in Russian).

[7] B.Kh. Mezhunts, The influence of mineral fertilizers and under-sowing on yield and fodder quality of trampled pastures, J. Annals of Agrarian Science 8 (2) (2010) 61-64 (in Russian).

[8] B.Kh. Mezhunts, M.A. Navasardyan, T.A. Sargsyan, The state of pastures of the dry steppe zone of Ararat valley of Armenia and the ways of their optimization, sustainable development of mountain territories, Vladikavkaz, 3 (5) (2010) 119-123 (in Russian).

[9] B.Kh. Mezhunts, The influence of two-year rest of heavily trampled pastures on bioproductivity of grass associations, J. Annals of Agrarian Science 11 (2) (2013) 61-64 (in Russian).

[10] I.I. Mardanov, Agroecological pecularities of mountain-meadow landscapes of Azerbaijan, J. Annals of Agrarian Science 6 (2) (2008) 34-36 (in Russian).

[11] G.Sh. Mammadov, S.A. Hajiyev, Ecological models of fertility management of soils under pastures in Nakhichevan Autonomous Republic, J. Annals of Agrarian Science 9 (4) (2011) 42-44 (in Russian).

[12] G. Sh. Mammadov, S.Z. Mammadova, Ecological assessment of Azerbaijan soils for their rational use, J. Annals of Agrarian Science 9 (1) (2011) 88-95 (in Russian).

[13] G. Sh. Mammadov. N.N. Sirajov, Soil-ecological characteristics of mountain-meadow soils of the north-eastern slope of the Great Caucasus of Azerbaijan, J. Annals of Agrarian Science 10 (2) (2012) 111-114 (in Russian).

[14] A.F. Gasanova, The comparative evaluation of winter pasture soils of Azerbaijan, J. Annals of Agrarian Science 8 (1) (2010) 50-53 (in Russian).

[15] G.D. Agladze, Forage production as the most important branch of agriculture in Georgia, J. Annals of Agrarian Science 7 (1) (2009) 19-21 (in Russian).

[16] G.D. Agladze, Animal breeding and fodder production in Georgia: analysis of current situation and perspectives of its development information 1. Animal breeding, J. Annals of Agrarian Science 4 (2) (2006) 54-59 (in Russian).

[17] G.D. Agladze, Animal breeding and food production in Georgia: analysis of the current situation and perspectives of its development information 2. Food production, J. Annals of Agrarian Science 4 (3) (2006) 32-37 (in Russian).

[18] R.T. Lolishvili, T.M. Subeliani, The bioproductivity of fodder grasses of subalpine hayfields of Central Caucasus, J. Annals of Agrarian Science 8 (4) (2010) 26-30 (in Russian).

[19] T. Urushadze, A. Bajelidze, Sh. Lominadze, Soil science, Batumi, 2011.

[20] T. F. Urushadze, G.O. Ghambashidze, W.H. Blum, A. Mentler, Soil contamination with heavy metals in Imereti region (Georgia), Bulletin of the Georgian National Academy of Sciences 175 (1) (2007).

[21] G.O. Ghambashidze, W.H. Blum, T.F. Urushadze, A. Mentler, Heavy metals in soils, J. Annals of Agrarian Science 4 (3) (2006) 7-11.

[22] G. Ghambashidze, T. Urushadze, W. Blum, A. Mengler, Heavy metals in some soils of the West Georgia, Pochvovedenie 8 (2014) 1014-1024 (in Russian).

[23] G.D. Agladze, G.V. Basiladze, E.G. Kalandia, The influence of the environment polluted from the heavy metals on the quality of milk production, J. Annals of Agrarian Science 7 (3) (2009) 29-32 (in Russian).

[24] P. Felix-Henningsen, M.A.H.A. Sayed, E. Narimanidze-King, D. Steffens, T. Urushadze, Bound forms and plant availability of heavy metals in irrigated, highly polluted kastanozems in the Mashavera valley, SE Georgia, J. Annals of Agrarian Science 9 (1) (2011) 111-119.

[24] T.T. Urushadze, D. R. Khomasuridze, Practice

in agroecology, Mtsignobari, Tbilisi, 2010 (in Georgian).
[25] G.D. Agladze, G.V. Basiladze, E.G. Kalandia, The influence of the environment polluted from The heavy metals on quality of milk products, J. Annals of Agrarian Science 7 (3) (2009) 29-32 (in Russian).
[26] G. P. Gogichaishvili, T. F. Urushadze, T. T. Urushadze, The forecast of the intensity of soil erosion for main soils of Georgia, J. Annals of Agrarian Science 6 (1) (2008) 22-30.
[27] O. Ghorjomeladze, G. Gogichaishvili & N. Turmanidze, Evaluating of erosion processes of soil with different factors (sediments, relieff, soill, vegetation cover), J. Georgian Academy of Agricultural Sciences, Moambe 26 (2009)175-179 (in Georgian).
[28] G. Gogichaishvili, O. Ghorjomeladze & N. Turmanidze, Evaluating of erosion of soils of Georgia and its sustainability, Georgian Academy of Agricultural Sciences, Moambe 29, (2011) 188-192 (in Georgian).
[29] G. Gogichaishvili, O. Ghorjomeladze & N. Turmanidze, The dynamic of erosivity during the whole year, J. Georgian Academy of Agricultural Sciences, 30 (2012)189-199 (in Georgian).
[30] G. Talakhadze, L.Nakashidze, R.Kirvalidze, Lab-Practical Study Book of Soil Science, Ganatleba, Tbilisi, 1973 (in Georgian).
[31] K. Mindeli, L. Guntaishvili, N. Machavariani, D. Kirvalidze, Kh. Mindeli, L. Gamsakhurdia, Lab-practical study book of soil science, Universali, Tbilisi, 2011.
[32] A. J. Parker, The topographic relative moisture index: an approach to soil-moisture assessment in mountain terrain: Physical Geography, Variables used are inclination, aspect, topographic position and slope configuration, 3(2), 9 (1982).
[33] J. Etzold & R. Neudert, Monitoring manual for summer pastures in the Greater Caucasus in Azerbaijan, sustainable management of biodiversity, south Caucasus, working paper, GIZ, 2013.
[34] E. Bakradze, Y. Vodyanitskii, T. Urushadze, Z. Chankseliani, M. Arabidze, About rationing of the heavy metals in soils of Georgia, J. Annals of Agrarian Science 16 (1) (2018) 1-6.

Annals of Agrarian Science

Journal homepage: http://journals.org.ge/index.php

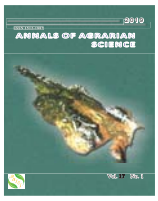

Investigation of Simultaneous Occurrence Probabilities of Some Dangerous and Spontaneous Meteorological Phenomena for Various Physical and Geographical Conditions of Georgia Using Multiplication and Addition Theorems of Probabilities

Elizbar Elizbarashvili[a], Mariam Elizbarashvili[b*], Marika Tatishvili[c], Shalva Elizbarashvili[a], Nana Chelidze [a]

[a]Climatology and Agrometeorology Division, Institute of Hydrometeorology, Georgian Technical University,150, Agmashenebeli Ave., Tbilisi, 0112, Georgia

[b]Department of Geography, Faculty of Exact and Natural Sciences, Ivane Javakhishvili Tbilisi State University, 1, Chavchavdze Ave., Tbilisi, 0179, Georgia, Email:

[c]Weather Forecasting, Natural and Technogenic Disaster Modeling Division, Institute of Hydrometeorology, Georgian Technical University, 150, Agmashenebeli Ave., Tbilisi, 0112, Georgia

Received: 5 November 2018; accepted: 5 January 2019

A B S T R A C T

The occurrence probabilities of some independent dangerous and spontaneous meteorological phenomena complexes for different physical and geographical conditions of Georgia have been estimated using multiplication and addition probability theorems. The complex of precipitation -strong wind events occurs on the Colchis Lowland on average every 20 days in December and January, on the Eastern Georgia plains once per year in May, on the Likhi ridge every 5-7 days during whole year.The occurrence of intensive precipitation-strong wind complex is possible in Western Georgia 1 time per decade, in Eastern Georgia - 1 time in 25 years and in the highland zone of the Greater Caucasus approximately 9-10 times in every 25years and on Likhi Ridge once per month. The occurrence of the hail-strong wind complex is possible on average every 50 and 20 years (warm period of year) in the South Georgian Highlands and in Eastern Georgia respectively. The fog-strong wind complex in Greater Caucasus high-mountain zone in May can be realized on average every decade and on the Likhi Ridge every 3-5 days.

Keywords: Probability, Meteorological phenomena, Complex of events, Climatic conditions, Dangerous weather, Precipitations.

*Corresponding author: Mariam Elizbarashvili: E-mail address: mariam.elizbarashvili@tsu.ge

Introduction

Dangerous and spontaneous meteorological phenomena, such as extreme temperature, rainfall, hail, blizzard, fog, strong and hurricane winds, etc., create emergency situations, causing damages and even human victims.

Natural weather phenomena, as the result of modern anthropogenic impact have been significantly intensified and often have catastrophic character. The intensification of natural meteorological phenomena has affected ecosystems and economy of Georgia, as it is evidenced by the impact of global warming on the regional climate, and even on the landscape structure [1-3].

Investigations of some dangerous and spontaneous weather phenomena over Georgian territory were initiated by one of the author of this article in the late 70th- at the beginning of 80th of last century. In the result of these studies the main features of the statistical structure of cloudiness, thunderstorm processes, abundant and intense rainfall, strong surface winds, the probabilistic

characteristics of fogs, including hazardous fogs [4, 5], extreme anomalies of mean monthly air temperature [6], frosts [7], hurricane winds [8] and other spontaneous meteorological phenomena [1, 9] were revealed [10-14].

Thus, for present a rather rich literature has been collected that characterize geography, structure and dynamics of individual spontaneous meteorological phenomena on the territory of Georgia. However, sometimes some events attack simultaneously, overlapping each other and thereby aggravate situation. For example, increased wind during shower, fog with snow, hurricane with hail, etc. To reduce the negative consequences of complex of these phenomena, one must know their probabilistic characteristics for the given locality.

These phenomena are independent from each other; therefore the probabilities of their joint occurrence can be determined using the multiplication and addition theorems of probabilities [15].

In this paper, the occurrence probability of some independent dangerous and spontaneous meteorological phenomena complexes for various physical and geographical conditions of Georgia has been estimated using multiplication and addition theorems.

2. Study Area

Georgia is characterized by exceptional variety of physical-geographical and climatic conditions [1, 16]. Its territory combines high-mountain, middle-mountain, hilly, low-flat, flat and plateau-like reliefs. The location of some lowlands don't exceed sea level, and individual mountain peaks ranges exceed 5000 m height.

In the northern part of the territory in the direction from the north-west to the south-east there extends the Main Caucasian Ridge. In the southern part, almost parallel to the Main Caucasus Ridge, there extends the South Georgian Highlands, which is part of the Lesser Caucasus. The main Caucasian ridge is connected to the South Georgian mountain range by the Likhi Ridge, which divides Georgia into two climatic regions: the West, with humid subtropical climate and the East, with moderately dry continental climate. Between the Great Caucasus and the South Georgian upland there is a tectonic depression, which is represented by lowlands, river valleys, plains and plateaus: the Black Sea coast, the Colchis Lowland, the Imereti highlands, East Georgia plains, the Alazani Valley.

3. Data and methods

According to the basic provisions of the probability theory [15], the probability of the set of independent events A and B, can be calculated using multiplication theorem of probabilities:

$$P(AB)=P(A)P(B), \quad (1)$$

and the probability of realization of one of the events is determined by the addition theorem of probabilities

$$P(A+B)=P(A)+P(B)- P(AB), \quad (2)$$

where P(A) –probability of A event, P(B) – probability of B event, if we consider the complete system of events A_i, where i = 1,2,3, ... n.

If it is known that there has been occurred event B, then the probability of event A is calculated in accordance with the Byes theorem:

$$P(A/B)=[P(Ai)P(B)]/ P(Ai)P(B). \quad (3)$$

P(A/B) – is called conditional probability.

In our case, two opposite events are considered: A_1 - the existence of specific meteorological phenomenon (precipitation, hail, fog, strong and hurricane winds, etc.) and A_2 - the absence of the same phenomenon. The sum of the probabilities of these phenomena equals to 1, so they form a complete system of events.

To study pattern of precipitation-strong wind complex probabilities based on the mean annual data and construct corresponding map, the observation materials of 16 meteorological stations were used and for complex probabilities of phenomena characteristic for the regions monthly data were used. Also the resources of scientific- application handbook were used as initial data [17].

In presented research 7 posts were chosen considering Georgian physical-geographical conditions: seaside resort Batumi (2m) characterizing Georgian Black Sea coastline, Samtredia (28m) located in central part of Colchis Lowland, Tbilisi (403m) typical for eastern lowland part of Georgia, Telavi (550-900m) located at north-eastern slope of Gombori Ridge characterizing foothill and low mountain zone of eastern Georgia, Akhalkalaki (1716m) characterizing the climatic conditions of the South Georgian Highland and Kazbegi (3600m) characterizing high mountain zone of Great Caucasus and Mta-Sabueti (1242m) located on climate separating Likhi Ridge.

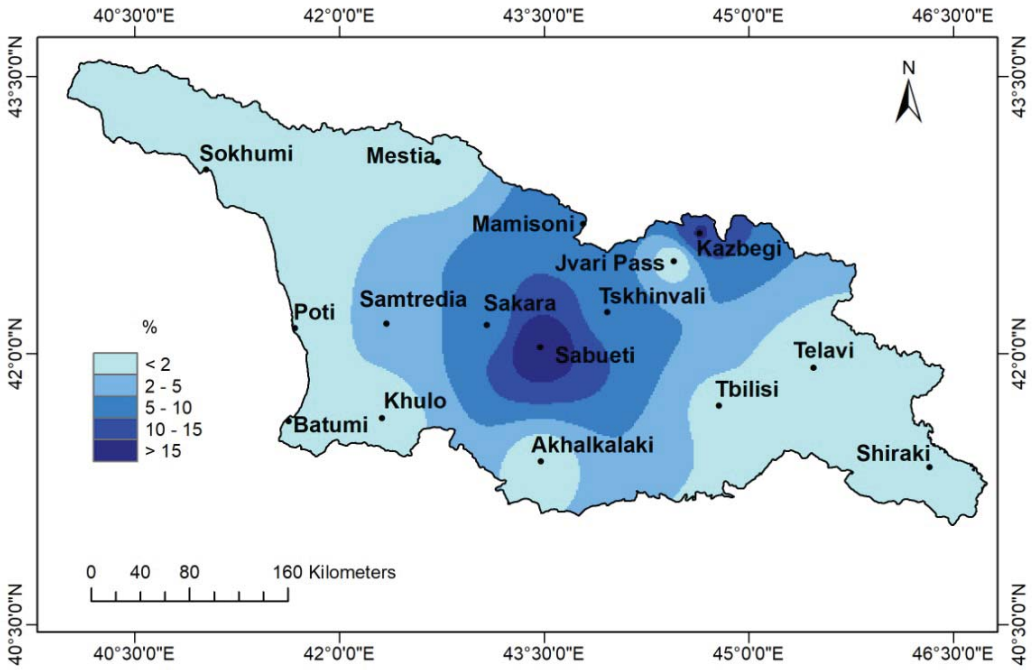

Fig. 1. *The distribution probability (%) of precipitation-strong wind complex mean annual probability*

4. Discussion

The map of precipitation-strong wind complex mean annual distribution probability, calculated according to the equation (1) has been presented on Fig.1.

From the map it follows that the greatest probability of the complex as a whole (15-20%) per year is recorded on the Likhi Ridge (about 70 days per year). On the eastern part of the southern slope of the Greater Caucasus, the probability of the same complex is 10-15% (35-50 days). At the Black Sea coastline the occurrence probability of the complex is 2%, and in most of the Southern Georgia Highland and the plains of Eastern Georgia it does not exceed 1%, which corresponds to 7 and 4 days. Obviously during year the occurrence of both individual meteorological phenomena, as well as their complexes, changes significantly.

For example in the Table 1 there are presented values of empirical occurrence probabilities of some typical and dangerous meteorological phenomena for Telavi: hail, fog, strong wind, precipitation and intense precipitation. The wind is strong when its speed exceeds 15 m / sec, and precipitation is considered to be intense when their daily amount exceeds 20 mm.

From Table 1 it follows that for Telavi the most presumable phenomena are fog and precipitation, including intense precipitation. The probability of fog in winter months increases to 17-23%, which amounts 5-7 days, and the probability of precipitation month dependence varies between 7-10%. The occurrence probability of other dangerous meteorological phenomena is low, even if they cause significant damages.

Table 1. *Empirical occurrence probabilities of some dangerous meteorological phenomena (%) Telavi*

Event	Month											
	1	2	3	4	5	6	7	8	9	10	11	12
Hail	0	0	0.07	1.3	2.7	2	0.3	0.7	0.3	0.3	0.07	0
Fog	20	17	20	10	3	3	2	2	3	10	13	23
Strong wind	3	4	5	3	2	2	0.7	1	2.3	5	2.3	2.7
Precipitation	10	7	10	10	10	10	10	10	7	7	10	7
Intense precipitation	0.3	1.3	1.3	3	7	7	3	3	3	3	3	1.3

Table 2. *Probabilities of the most dangerous meteorological phenomena (%) combinations (Telavi)*

Months	Precipitation-fog			Intense precipitation-strong wind			Hail-strong wind		
	P(AB)	P(A+B)	P(A/B)	P(AB)	P(A+B)	P(A/B)	P(AB)	P(A+B)	P(A/B)
1	2	28	10	0.009	3	0.3	0	3	0
2	1	12	6	0.052	5	1	0	4	0
3	2	28	10	0.065	6	1	0.0035	5	0.12
4	1	19	9	0.09	6	3	0.039	4	2
5	0.3	13	10	0.14	9	7	0.054	5	3
6	0.3	13	10	0.14	9	7	0.04	4	2
7	0.2	12	10	0.021	4	0.3	0.002	4	0.2
8	0.2	12	10	0.04	4	0.4	0.007	1	0.7
9	0.2	9	7	0.069	3	0.3	0.0069	2	0.3
10	0.6	16	6	0.15	8	3	0.015	3	0.3
11	1	22	8	0.069	5	0.3	0.0161	5	0.8
12	2	28	10	0.025	4	1	0	2	0

In Table 2 there are presented the probabilities of the most dangerous phenomena combinations: precipitation-fog, intense precipitation-strong wind, and hail-strong wind by months, calculated by equations (1, 2, 3) based on table 1 data.

From Table 2 it follows that the occurrence probability of the precipitation-fog event complex P (AB) in winter months, as well as in the beginning of spring and at the end of autumn is 1-2%, and in summer months decreases to 0.2%. The occurrence probability of one of the events P (A + B) (precipitation or fog) is much bigger and amounts to 9-28%, the maximum in December, January and March and the minimum in September. While considering fog, the probability of precipitation P (A/B) increases, making 6-8% in fall and at the end of winter, and 9-10% for all rest months.

It also follows from Table 2 that the occurrence probabilities of complex precipitation-strong wind and hail-strong P (AB) are very low. The probability of one of the events of the complexes P (A + B) is 3-9% in the first case and 1-5% in the second one. During strong winds period the probability of intense precipitation and hail P (A/B) increases and amounts to 0.3% in May.

Figure 2 shows the annual course of the most dangerous probability combinations of meteorological phenomena for different physical-geographical conditions of Georgia.

Locations and phenomena combinations: 1-Telavi (hail-strong wind); 2-Batumi (heavy precipitation-strong wind); 3- Samtredia (precipitation - strong wind); 4- Tbilisi (precipitation - strong wind); 5- Akhalkalaki (hail-strong wind); 6- Kazbegi (fog-strong wind); 7-Mta-Sabueti (precipitation-strong wind); 8-Mta-Sabueti (heavy precipitation-strong wind); 9-Mta-Sabueti (precipitation-fog); 10-Mta-Sabueti (fog-strong wind). On Fig. 1a) curves 1 and 5 coincide.

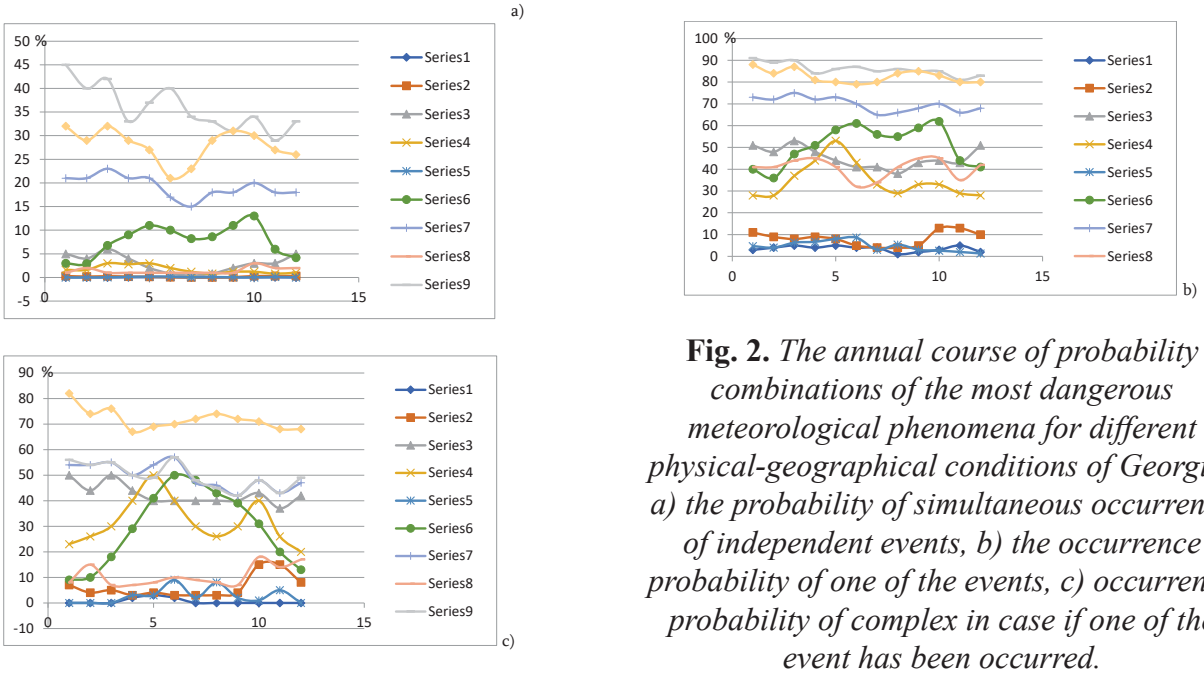

Fig. 2. *The annual course of probability combinations of the most dangerous meteorological phenomena for different physical-geographical conditions of Georgia: a) the probability of simultaneous occurrence of independent events, b) the occurrence probability of one of the events, c) occurrence probability of complex in case if one of the event has been occurred.*

As follows from Fig. 2 the annual course of occurrence probability of various variants of meteorological phenomena complexes depends essentially on the physical and geographical conditions of the location. For example, the probability of simultaneous occurrence of strong wind and precipitation on the Colchis Lowland (Samtredia) fluctuates on average from 0.4 to 5% during the year, the minimum in May and maximum in December and January, while on East Georgia plains (Tbilisi) probability of the same complex is 1-3%, the minimum in August and November, and maximum in May. The occurrence probability of precipitation-strong wind complex on the Likhi Ridge (Mta-Sabueti) makes 15-23%, the minimum in July and the maximum in March. Consequently, precipitation-strong wind complex occurs on the Colchis Lowland on average every 20 days on December-January, on Eastern Georgia plains in May per year only once, and on the Likhi Ridge every 5-7 days. The occurrence probability of one of the phenomena from the precipitation- strong wind complex in the Colchis Lowland during the year fluctuates between 38-51%, the minimum in August, and the maximum in December-January, and on the Eastern Georgia plains is 28-53%, the minimum in January -February, and the maximum in May, and at Likhi Ridge ranges between 65-75%. When one of the events from the precipitation-strong wind complex occurs, the probability of its second component occurrence during the year on the Colchis Lowland ranges from 37 to 50%, the minimum in November and July, and the maximum in December-January and March, and on the East Georgia plains the probability of the corresponding event is 20-40%, the minimum in December, August and November, and the maximum in March and May, and on the Likhi Ridge ranges between 42-55% minimum in September, the maximum in March.

Precipitation-strong wind complex is characterized by a small probability on the Black Sea coast (Batumi), which frequently is the most dangerously coincided with a storm. The probability of this complex during year ranges from 0.03% (July-August), - 0.3% (January), the probability of this complex in Eastern Georgia is even less, and on the Likhi Ridge it ranges between 1-3%, the maximum in October . Thus, this complex can be realized on the Black Sea coast on average 1 time per decade, and on the Likhi ridge - 1 time per month. The occurrence probability of one of the phenomena complex is 4-13% on the Black Sea coast, a minimum in July-August and maximum in October-November, and the occurrence probability of the complex, with the onset of one of the events, ranges from 3% (summer July-September) up to 15% (October-November January); For the Likhi Ridge, respectively 32-45%, the minimum in June and the maximum in April, September-October, and 7-18%, the minimum in March-April, September and the maximum in December.

Very rarely there is hail-strong winds complex, which on 19.07.2017 in Telavi has catastrophic nature and caused significant material damages. The maximum probability of this complex at foothill and lowland zones of East Georgia (Telavi) is 0.04-0.06% (April-June), and at the South Georgia Highlands (Akhalkalaki) - 0.16-0.17% (May June). This means that the complex hail-strong wind for the indicated months occurs on average 1 time in 50 years and for 20 years, respectively for Eastern Georgia and the South Georgian Highlands. The occurrence probability of one of the complex's events throughout the year varies from 1% in August to 5% in March and May and in the South Georgian Highlands from 1% in December to 8-9% in May-June. The probability of the complex significantly increases when one of the events has been already occurred and reaches 3-9% (May-June) respectively.

Unlike the considered meteorological phenomena complex, the fog-strong wind complex has been characterized by significant probability in mountains. The occurrence probability of this complex of phenomena on the Likhi Ridge (Mta-Sabueti) varies within the limits of 21% (June) - 32% (January, March), and on the Caucasus (Kazbegi) - within 3% (January-February) - 11% (May). Thus, this complex can be realized, respectively, on average 3-5 days and every ten days. The likelihood of realizing one of the phenomena of the same complex is 79-88% at Likhi Ridge, and on Caucasus -36-62%, and the occurring probability of the complex upon realizing one of the events varies, respectively, from 67% (April) to 82% (January) and from 9% (January) to 50% (June).

On the climate separating Likhi Ridge there is also high probability of precipitation-fog complex -29-45%, the minimum on November and maximum on January. This complex is happening every 2-3 days. The probability of one of the phenomena of the complex during the year fluctuates within 81-91%, the minimum also in November and the maximum in January, and occurrence probability of

the complex at the onset of one of the events varies within 42% (September, October) - 56% (January).

5. Conclusion

The simultaneous occurrence probability of strong wind and precipitation on the Colchis Lowland varies from 0.4 to 5% during the year, and on Eastern Georgia plains it is 1-3%, and on the Likhi Ridge it is 15-23%. The occurrence probability of one of these phenomena is 38-51% in the Colchis Lowland, and in Eastern Georgia it is 28-53%, and in the Likhi Ridge ranges between 65-75%. In case of one of the events, the occurrence probability of the second component of the complex is 37-50% in the Colchis Lowland, while in East Georgia it is 20-40%, and in the Likhi Ridge ranges between 42-55%.

The occurrence probability of the complex of intense precipitation-strong wind fluctuates throughout the year on the Black Sea coast and the Colchis Lowland within 0.03% -0.3%, and on the Likhi Ridge it is 1-3%. The occurrence probability of one of the phenomena of the complex is 4-13% on the Black Sea coast, a minimum in July-August and maximum in October-November, and the occurrence probability of the complex, with the onset of one of the events, ranges from 3% (summer July-September) , up to 15% (October-November January). For the Likhi Ridge it is respectively, 32-45%, the minimum in June and the maximum in April, September-October, and 7-18%, the minimum in March-April, September and the maximum in December.

The maximum occurrence probability of complex hail-strong wind in the foothill and lowland zone of Eastern Georgia is 0.04-0.06% (April-June), and in the South Georgian Highlands - 0.16-0.17% (May June). The occurrence probability of one of the complex's events throughout the year varies from 1% in August to 5% in March and May in the South Georgian Highlands from 1% in December to 8-9% in (May, June). The occurrence probability of the same complex, when one of the events has been happened, reaches 3-9% (May-June).

The complex fog-strong wind is characterized by significant probability in the mountains. The occurrence probability of this phenomena complex on the Likhi Ridge ranges from 21% to 32%, while for the Caucasus (Kazbegi) ranges from 3% to 11%. The likelihood of happening one of the phenomena of the same complex is 79-88% in the Likhi Ridge, and in the Caucasus -36-62%, and the probability of happening the complex in the case when one of the event has been already occurred varied respectively from 67% (April) to 82% (January) and from 9% (January) to 50% (June).

References

[1] E. Elizbarashvili. Climate of Georgia. Tbilisi, 2017 (in Georgian) .

[2] E. Sh. Elizbarashvili, M. E. Elizbarashvili. Possible Transformation of the Caucasus Natural Landscapes in Connection with Global Warming. Meteorology end hydrology, 10 (2005) 53-57 (in Russian) .

[3] E. Sh. Elizbarashvili, M. E. Elizbarashvili. The Main Problems of Landscape Climatology. Tbilisi, 2006 (in Russian)

[4] E. Sh. Elizbarashvili, O. Sh. Varaza nashvili, N. S. Tsereteli, M. E. Elizba rashvili, and Sh. E. Elizbarashvili. Dangerous Fogs on the Territory of Georgia. Russian Meteorology and Hydrology, Vol. 37, Issue 2, February (2012) 106-11.

[5] E.Sh.Elizbarashvili, T.K.Zubitashvili, Mists in Eastern Georgia. Proceedings of the Russian Academy of Sciences, a series of geographic,5,(2007) 112-115.

[6] E. Sh. Elizbarashvili, R. Sh. Meskhia, M. E. Elizbarashvili. Dynamics of occurrence frequency of extreme anomalies of monthly mean air temperature in Georgia in the 20th century and its effect on precipitation and on the river water discharge. Russian Meteorology and Hydrology, January Vol. 32,Issue1 (2007) 71-74.

[7] E. Sh. Elizbarashvili, O. Sh. Varazanashvili, M. E. Elizbarashvili, N. S. Tsereteli. Light frosts in the freeze-free period in Georgia. Russian Meteorology and Hydrology , Volume 36, Issue 6, June (2011), 339-402.

[8] E. Sh. Elizbarashvili, O. Sh. Varazanashvili, N. S. Tsereteli, and M. E. Elizbarashvili. Hurricane Winds on the Territory of Georgia. Russian Meteorology and Hydrology, March, Volume 38, Issue 3 (2013) 168–170.

[9] E. Sh.Ellizbarashvili, M.E. Elizbarashvili. Extreme Weather Events over the Territory of Georgia, Tbilisi, 2012 (in Russian).

[10] J. D. Alibegova, E. Sh. Ellizbarashvili. Statistical Structure of Atmospheric Precipitation in

Mountain areas. Gidrometeoizdat, Leningrad, 1980 (in Russian).
[11] J. D. Alibegova, E. Sh. Elizbarashvili. On the statistical structure of the cloud field over Transcaucasia. Meteorology and hydrology, 4 (1977), 57-62 (in Russian).
[12] J. D. Alibegova, E. Sh. Ellizbarashvili. Statistical structure of surface wind in Transcaucasia. Tr. GGO named after A.I Voeikov, vol. 396, 1977. (in Russian).
[13] K.A.Sapitski, E.Sh.Elizbarashvili. On the alignment of the number of days with 20mm rainfall according to Poisson for some points in Georgia. Communications of the Academy of Sciences of the Georgian SSR 68, №2 (1972) 110-118 (in Russian).
[14] E.Sh. Elizbarashvili, N.Sh. Gongladze, S.R. Vlasova, B.Galborova, A.A. Popov. About thunderstorm activity in Eastern Georgia. Izvestiya AN SSSR., Series geography, 1 (1983) 130-139 (in Russian).
[15] T.A.Agekian, Bases of the Theory of Errors, Nauka, Moscow, 1972 (in Russian)
[16] E. Sh.Ellizbarashvili. Vertical zoning of the climates of Transcaucasia. Izvestiya of the USSR, Academy of Sciences, a series of geographic, №4 (1978) .97-103 (in Russian).
[17] Scientific and Applied Handbook on the Climate of the USSR. Series 3. Perennial data. Parts 1-6, issue.14, Gidrometeoizdat, Leningrad, 1979 (in Russian).

Annals of Agrarian Science

Journal homepage: http://journals.org.ge/index.php

Issue of organization of material logistics of work of agricultural machinery in complex mountain-level land conditions

B.B. Basilashvili , I.M. Lagvilava, Z.K. Makharoblidze, R.M. Khazhomia

Agricultural University of Georgia, Kakha Bendukidze University Campus, 240, David Aghmashenebeli All., Tbilisi, 0131, Georgia

Received: 19 March 2018; accepted: 09 May 2018

A B S T R A C T

At any stage of the development of society, scientific-technical progress represents the main conditioning factor for this development. As far as scientific-technical progress represents the process of guaranteed development of any field of engineering. Therefore, some unconscious, unprofessional and interfering dependence with this process is accompanied by sufficiently multilateral negative results. The complex natural and industrial conditions of Georgia, especially in mountainous and complex-relief conditions, necessitate the introduction and development of special scientific directions, in particular the need to develop issues of mechanization of mountain agriculture at the level of modern scientific-technical progress in this field.

Keywords: Energy means, Assembly units, Exchange fund, Consumption of spare parts, Fuel consumption, Agrotechnical.

*Corresponding author: Bejan Basilashvili, E-mail address: bejan.basilashvili@mail.ru

Introduction

The natural and climatic as well as production conditions of agriculture in Georgia are quite diverse and this diversity is particularly sensitive on the performance of agricultural processes in mountainous and having complex relief areas, when such factors as the size and contouring of the processed area, the inclination and general state of the relief, climatic and soil conditions etc., significantly affect on the individual operational indicators of the performed processes (agrotechnical, energy, technical-economical etc.). This circumstance necessitates the development of a special directions of agriculture in Georgia, in particular, the development of issues of mountain agriculture and the corresponding means.

The development of mountain agriculture in Georgia requires the upgrading of relevant research, design, technological, engineering, and experimental works at the modern level, since they are a significant reserve for the perfect development of the country's agriculture [1, 2].

It is determined that in Georgia more than 60% of the land area, profitable for the production of agricultural products, is located on the slopes. It is also determined that the tasteless properties and nutritional value of the products produced on the slopes of the high-mountainous zones are quite high and they are exceeding the analogous indices of production produced on plain conditions. At the same time, it has been calculated and determined that development of the slopes, with steepness up to 8 ... 10°, would additionally produce more than 10 ... 15% of production (fruit, grapes, tea, etc.), and the development of slopes with value more than 20°, makes additional income in production – it is doubled [2,3].

Just like the general development of agriculture, the perfect development of slopes and mountain lands primarily depends on the level of mechanization of production processes. The issue of the rational selection of energy means and technological machines, as well as the implementation of complex

mechanization for plain conditions, is relatively easy to solve. Mechanization of agriculture in having complex relief and mountain lands, as well as in other similar conditions, is a problematic issue.

First of all, the mechanization of production processes of agriculture depends on the providing and proper selection of the corresponding mobile energy means and technological machines. Significant is, also determined due the according calculation of parameters the correct compilation and completion of the corresponding machine and tractor units, based on the theoretic calculations, determination of their technological parameters and operating modes, the improvement of methods of application of technology, the structural optimization of all links in engineering service. For modern agriculture, the uninterrupted, consistent and effective implementation of researches and development in this direction represents a significant problem [4, 5].

To ensure a high level of mechanization of field husbandry works in the agricultural enterprise and the implementation of complex mechanization of crop production, as well as for the full value realization of the operational properties and capabilities of machinery, the available power of work should be in range of 22...25 kW/man, and the energy supply of agriculture should be 4...6 kW/ha. As significant parameter is also the complex parameter-the density of mechanized works (conditional standard ha/ha) [6, 7].

In order to achieve and maintain of mentioned parameters in a specific region or in an agricultural enterprise, it is necessary to select and operate agricultural machinery on the basis of proper engineering calculation with taking into account the corresponding natural-production conditions.

At the present stage, in the conditions of management polymorphism, the selection and distribution of agricultural machinery by region is not obey the full value engineering calculations or control checks and the nomenclature-quantitative selection is mainly made by an individual approach. For this reason, incomplete application of their capabilities or cases of their work with overload is frequent.

In addition, the general organization of material logistics for the operation of agricultural machinery that is the main task of the logistics and oil products supply, provides a reliable modern supply of agricultural enterprises by the necessary machinery, equipment and spares for them, as well as materials for the operation of these machines and equipment, as well as for all branches of the economy.

The required number of exchange stock of unit assemblies for the whole economy would be determined from the simplified formula:

$$n_{O.\Phi} = m\rho T_B K_H / T_{CP} \cdot \qquad (1)$$

where m - is the number of machines on that these assembly units are installed;

ρ – is the number of assembly units for one machine;

T_B – is the time of complete restoration of the assembly unit, including the time on transportation;

K_H – is the coefficient taking into account deviations from the established terms of restoration and other normative (K_H= 1,2 ... 1,8);

T_{CP} - is the average life of the assembly unit before replacement.

The smaller values of K_H are assumed for large farms and vice versa.

The value of the coefficient K_H at operation of agricultural machinery in complex mountain-plain conditions undergoes a change in the direction of increase that also leads to an increase in the number of required assembly units.

The number of replaceable working bodies of machines and recoverable spares would also be calculated using the following simplified formula

$$n_{з.ч} = m_м \rho_м \left[\frac{\Omega_C}{T_P \left(1 + n_{рем}\right)} + A_{CTP} \right], \qquad (2)$$

where m_M - is the number of the same type machines;

ρ_M – is the number of parts or work tools per machine;

Ω_C, T_p - are respectively, the seasonal load per machine and the average periodicity of parts replacement, ha,h;

n_{pem} – is the number of parts repairs for the period of its service;

A_{CTP} – is the number of insurance fund sets per machine.

At existing reasonable norms for the consumption of spares, their required quantity would be determined by the formula

$$n_{з.ч} = m_м M_н / 100, \qquad (3)$$

where M_Y – is the rate of consumption of this part for 100 vehicles per year.

The required amount of materials for the repair, maintenance and storage of machines would be determined in accordance with the available regulations according to the following formula

$$Q_{м} = \Pi_{р} M_{н.м}, \qquad (4)$$

where Q_M – is the required quantity of materials, kg, pcs., etc.;

Π_p – is an annual program of this type work;

$M_{H.M}$ – is the rate of consumption of this type of material per machine.

The annual requirement of the economy in the each type fuel is determined from the statistical data of past years or by a simplified calculation by formula [3, 6]

$$Q_{т.г} = \frac{Э_{т.д}}{1000}\left(\Sigma F_i Q_{Ti}\right), \qquad (5)$$

where $Q_{TГ}$ – is the annual fuel consumption, t;

$Э_{T.D}$ – is a correction factor that takes into account the additional fuel consumption, connected with the inclination and roughness of the surface of the plots, passages, preparation

F_i – is the volume of *i* work, ha, t, etc.;

Q_{Ti} – is the fuel consumption per unit of performed work, kg/ha, kg/t, etc.

In the absence of more reliable data, the value $Э_{T.D}$ would be approximately accept as $Э_{T.D}$= 1,05 ... 1,08. The values of F_i and Q_{Ti} are accepted accordingly of the flow charts and the norms of production and consumption of fuel for mechanized work.

According to the Q_{Ti} is determined required capacity of fuel storage tanks, m³

$$V_{х} = Q_{т.г} Э / \rho, \qquad (6)$$

where Э – is the coefficient, taking into account the necessary production stock of oil products;

ρ – is the density of fuel.

For diesel fuel and petrol, respectively, we can accept the average values ρ=825 kg/m³ and ρ=700 kg/m³.

The numerical value of Э depends on the conditions for the delivery of oil products to the farm and would vary from 0.1 up to 0.5. Averaging for common farms would be accepted as Э= 0.15 ... 0.20.

The need for fuel for the month, season, etc. would be calculated by the formula (5).

The general principles of the organization of the engineering and technical service described are also valid for the newly created machine and technological stations (MTS), the number of which is continuously growing throughout all Georgia, and whose main tasks are: rendering services in the production of mechanized works; processing of agricultural products; provision of equipment for rent and hire; rendering of services in the field of maintenance, including maintenance and repair of equipment; manufacture of spares; material logistics of agricultural enterprises in the service area; execution of construction works, etc. With consideration of these areas of activity, the structure of the engineering and technical service of modern MTS is formed on the basis of general principles of specialization and division of labor [8,9].

In the field of engineering and technical services of large farms and MTS, with consent of farmers would also be included the farm enterprises. On the orders of farmers, they can be provided with the following types of services, either on a permanent or temporary basis or on a one-time basis: implementation of mechanized activities for the production and realization of agricultural products; rent of equipment; on effective application and maintenance of equipment; sale and pre-sale service of machinery, etc. All these services are possible only on a voluntary mutually beneficial basis that represents the fundamental principle of a market economy.

Conclusion

The calculated accordingly of enterprise's production directions rational supply of its functioning by material and technical means, in particular the appropriate machinery, replacement working bodies of machines and spares, materials for repair, maintenance and storage of machines, annual fuel requirements, as well as a qualified engineering and technical management of all production processes, represents the determinative factor of the whole activity and functioning of the economy, not depending on its production scale.

Rational organization and professional management of the process of material logistics of agricultural technological processes represent a necessary condition for achieving of optimal final results.

References

[1] B.B. Basilashvili, Z.Sh. Makharoblidze, I.M. Lagvilava, Calculation of scale factors in the modeling of the processes under study. Proceedings of Agrarian Science, Vol. 11, No. 1 (2013) 56-58.
[2] R.M. Makharoblidze, Methods of impact theory and rheology in agricultural mechanics. Ganatleba. Tbilisi, 2008 (in Russian).
[3] B.B. Basilashvili, I.M. Lagvilava, Z.Sh. Makharoblidze, R.M. Khazhomia, Criterial modeling of field-husbandry technological processes service baskur. Annals of Agrarian Sciense. Vol. 16, No. 1, 2018.
[4] V.A. Aliluev et al., Technical operation of the machine and tractor fleet. Agropromidat, Moscow, 1991. (in Russian).
[5] J.V. Katsitadze et al. Technical service of machines, Ganatleba, Tbilisi, 2008. (in Russian).
[6] A.A. Zangiev, A.V. Shpilko, A.G. Levshin, Operation of the machine-tractor fleet, Kolos, Moscow, 2008 (in Russian).
[7] A.P. Karabanitsky, E.A. Kochkin, Theoretical basics of production operation of machine-tractor fleet. Kolos, Moscow, 2009 (in Russian).
[8] B.B. Basilashvili, I.M. Lagvilava, O.A. Asatiani, A.B. Kobakhidze, Modeling of running ability indicators of tandem wheeled self-propelled chassis. Annals of Agrarian Sciense. Vol. 11, No. 2 (2013) 52-56.
[9] A.V. Kuznetsov, Fuel and lubricants. Kolos, Moscow, 2010 (in Russian).

Annals of Agrarian Science

Journal homepage: http://journals.org.ge/index.php

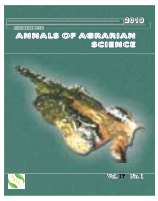

Modeling of Technological Process In Rotary Tiller

D.R. Khazhakyan

National Agrarian University of Armenia, 74, Teryan Str., Yerevan, 0009, Armenia

Received: 15 May 2018; accepted: 5 September 2018

A B S T R A C T

To identify the specifics of the interaction of the soil and the rotary working equipment, the issues of modeling the technological process of the rotary tiller and its interaction with the soil has been investigated. Comparison of soil strain and deformation values through the application of the ANSYS WORKBENCH software enabled to conclude that the highest strain value in the soil is observed during the soil cutting. The issues of modeling the technological processes of the rotary tiller and its interaction with the soil has been investigated throughout the research. From this perspective it is important to measure the sizes of the slices cut from the soil and to identify the cutting form. The latter are related to both the structure of the rotary tiller and the moving velocity/forward speed/ of the soil cultivating machine, as well as to the rotating numbers of the operating equipment. At the same time during the planning of the working equipment it is possible to get functional relations between various parameters studying the specifics of these relations and improving the structure of the working equipment.

Keywords: Rotary tiller, Rotary hoe, Modeling, Soil, Strain, Deformation.

*Corresponding author: D. Khazhakyan; E-mail address: khazhakyan@gmail.com

Introduction

Soil cultivating machine with rotating equipment like rotary tiller (or rotary hoe) cuts the soil slices, turns over the soil and enables to mix the soil proportionally or to mix the fertilizer with the soil [1,2] The soil cultivation with rotary hoe enables to provide the sufficient soil looseness, which creates favorable conditions for the growth and development dynamics of the ferments vital for plants growth at the 10-12 cm depth of the soil plowing horizons. Thus, the soil reclamation with the rotary hoe has a significantly positive influence on the biological conditions of the crops growth and development process. With this regard a number of researchers [3, 4] have mentioned that the soil cultivation with the rotary hoe has a positive effect on the soil physical properties and on the improvement of water and nutritional regime conditions in crops.

Application of rotary tillers promotes the reduction of traction resistance. That is why these tillers are used in such conditions, where no other alternative is left. When cultivating the soil with rotary hoes the soil looseness holds well for a long time. Sometimes the depth of rotary tillage amounts to 15-20 cm, then the soil density decreases at the depth of 30 cm. This is accounted for the vibration impact [5] of the rotary tiller's blades.

In order to study the work of the rotary tiller it is recommended to design it through software and to model its process.

It is relevant to implement the design works of the rotary tiller by means of SOILDWORKS software development kit, which has an opportunity of making diverse geometrical modifications and the finished design is possible to further integrate in the ANSYS Workbench software package, which creates a vast platform for automated design and analyses with finite elements [6][7].

The design of the rotary tiller is a stage process and it should be implemented through the design of its individual parts. First, it is necessary to design its

disc and axis planning the latter's sizes according to the fastening device of the power unit. Two types of blades were designed: straight and staple, which were installed on the disc of the rotary tiller by two items intermittently.

The soil is also designed separately as a solid substance, so as it would be further possible to get the characteristics of working equipment-soil interactions/ratio through its modeling and attributing elastic properties to the soil [8]. Later on, in order to model the soil inhomogeneity it will be possible to design several parts of the unit modeling the soil structure and to observe the characteristics of the rotary tiller and soil interaction when the latter passes along the connecting junctures of those parts.

As it is known the rotary tiller implements two types of movements: forward/linear and rotating. During the modeling process forward/linear movement velocity is conveyed to the soil cultivating machine, while the working equipment is provided with rotational movement velocity. During the study of this stage it is possible to carry out numerous measurements, which can serve as a base for the further improvement of the working equipment.

By applying the method of finite elements analysis the solid unit conventionally is divided into finite elements, which come forth as finite-constituent particles of the solid unit to which the parameters of the unit is attributed. Thus, the interaction of the solid units is observed via finite particles. During the analysis of the problem, depending on the tasks and the required precision it is possible to decrease or increase the divisibility rate of the finite elements, whereupon receiving the needed precision rate of calculations.

The aim of research

The aim of the current research is to simulate the interaction of the rotary tiller with soil.

The object of research

The object of the current research is the interaction of soil – working equipment in the simulation environment.

For this purpose rotary tiller designed through the software of Solidworks has been introduced into the software environment of ANSYS Workbench, the sizes of which have got an experimental nature. Cutting of the soil through rotary tiller is introduced in Fig. 1.

When studying the simulation results we notice that as a result of cutting with the rotary tiller the soil deformation is higher than the geometrical sizes of the blade sticking. This phenomenon is accounted for soil adhesion/coherence and the vibratory character of the rotary tiller. The longitudinal deformation is higher than the sum of the longitudinal sizes of oppositely arranged longitudinal blades, while the vertical deformation is higher than the length of blade.

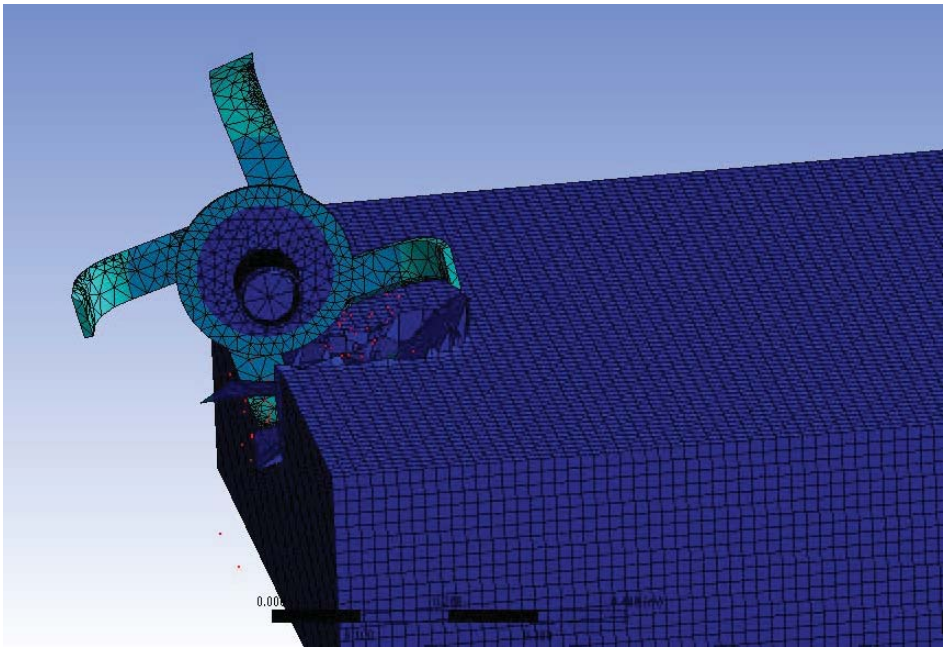

Fig. 1. *Soil cutting scheme through rotary tiller*

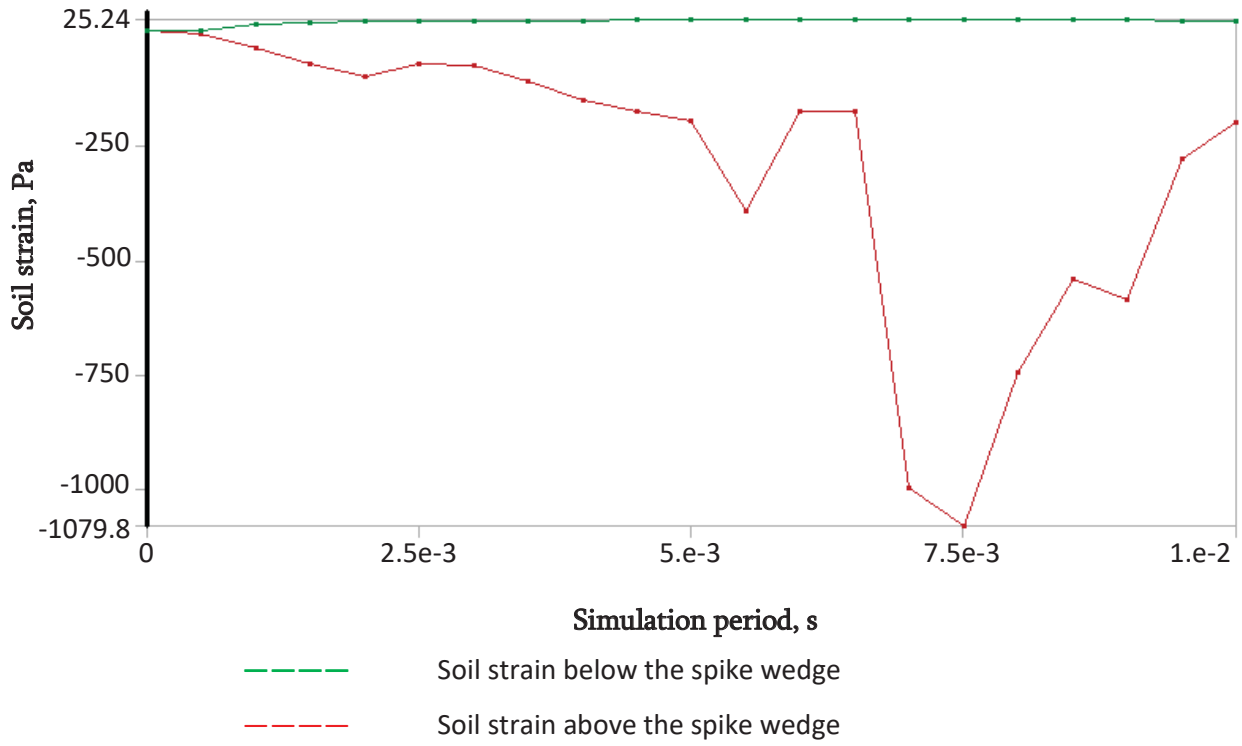

Fig. 2. *Soil strain values during the cutting with rotary tiller*

While considering the soil– working equipment interrelation the soil strain was investigated as well, the diagram of which is introduced below Fig. 2

Strain is the relation/ratio of deformation with the initial length of the unit or it is the relation of the unit affecting power (with regular direction) with the affected surface [9,10].

The diagram shows that at the moment when the blade of the rotary tiller is stuck into the soil the strain increases abruptly, later during the cutting it is getting lower. This means that at the accessing moment of the working equipment the soil demonstrates maximum resistance, after which the resistance decreases until the access of the next blade. So the diagram of the regular strain indicates that in order to improve the structure of working equipment in the rotary tiller it is vital to pay attention to such factors, which influence the decrease of resistance at the cutting moment. They are, for instance, the attack angle, blade sharpness, sharpening angle, the blade form, etc.

Conclusion

1. During the design of the working equipment it is possible to obtain functional relations between various parameters and through disclosing their nature to improve the structure of the working equipment.
2. The simulation results show that the maximum strain of the soil is manifested at the sticking moment of the blade, which should serve as the main indicator for the improvement of the structure in rotary tiller.

References

[1] M. Keshuan, D. Lieyun, Finite element analysis of tunnel-soil-building interaction using displacement controlled model, 7 th WSEAS Int. Conf. on Applied Computer & Applied Computational Science (ACACOS '08), Hangzhou, China, April 6-8, 2008, pp. 306-311.

[2] M.R. Azadi, S. Nordal, M. Sadein, Nonlinear behavior of pile-soil subjected to torsion due to environmental loads on jacket type platforms, WSEAS Transactions on Fluid Mechanics, issue 4, volume 3 (2008) 390-400.

[3] P.M. Vasilenko, Cultivators (Construction, Theory and Calculation), Publishing House of the Academy of Sciences of the Ukrainian SSR, Kiev, 1961 (in Russian).

[4] G.N. Sineokov, Theory and Calculation of

the Rotary Tillers, Machinery Construction, Moscow, 1977 (in Russian).
[5] G.G. Ramzanova, Analysis of the Working Bodies of Tillage Cutters, Electronic Bulletin RSEAU, Part 1, Moscow, 2015 (in Russian).
[6] Magd Abdel Wahab, The Mechanics of Adhesives in Composite and Metal Joints: Finite Element Analysis with ANSYS, 2014.
[7] Daryl L. Logan, A First Course in the Finite Element Method, Fifth edition, Cengage Learning, 2011.
[8] A. Heath, A strain-based non-linear elastic model for geomaterials, WSEAS transactions on applied and theoretical mechanics, issue 6, volume 3 (2008) 197-206.
[9] J. Lubliner, Plasicity Theory, Revised Edition, University of California at Berkeley, 2006.
[10] S. J. Poulos, The Stress-Strain Curve of Soils, GEI Internal Report, 1971.

Annals of Agrarian Science

Journal homepage: http://journals.org.ge/index.php

Introduced Holstein Breed Livestock in Georgia

T. Qachashvili[a], L. Tortladze, A. Chkuaseli

Agricultural University of Georgia, 240, David Aghmashenebeli Ave., Tbilisi, 0159 Georgia

Received: 15 May 2018; accepted: 5 September 2018

A B S T R A C T

The current work represents the adaptation perspective of Holstein Breed Livestock introduction in Kakheti intensive agricultural zone of Georgia and the phenotypical, exterior and interior peculiarities of the milk/cash cows researched by us. Besides the above we conducted the analysis of the scientific research on important factors which will contribute to successful breeding of Holstein Livestock in local natural and climate conditions. The study of acclimatization process of Holstein Livestock demonstrated that the heat resistence index in newly born cows is 2,2-3,3 units lower than in non-parturient cows. Following the recommended quality and amount of nutriment ration ensured the normal health condition and maiantained the level of reproductivity ability. As a result we have 2-3% of livestock type standard live weight retardation and withers height. It should be mentioned that the received data can be considered acceptable dynamic in the conditions of Georgia. As for bringing arterial pulse and breathing rate to norm – it became possible after installing recirculating fans in cow stolls. Thus, the clinical analysis as well as live weight growth and development dynamic of the tested Holstein type heifers demonstrated that the tested indices are within the physiological norms.

Keywords: Holstein, adaptation, heat resistance, productivity, nutriment ration, growth and development

*Corresponding author:T. Qachashvili; E-mail address: t.qachashvili@caucasusgenetics.ge

Introduction

Natural milk production has been the most urgent problem in Georgia for a long time which in the conditions of existing extensive systems in stock breeding requires immediate intensification, implementation of various necessarry activities in line with breeding and adaptation of intensive breeds of livestock.

Today in most of the countries where the natural milk production problem is solved there is Holstein stock bred. It is not occasional that the Holstein breed cattle is in the center of attention, it is the most popular breed in milk production sector which is also distinguished for its live weight, distinct milking forms, with the special form and location of udders which despite the capacity is located higher and spreads in width when filled up. Besides the above, the Holstein breed of cattle has peculiar quality of its intensive growth and development as well as big capacity of milking which is achieved through healthy and balanced food [1-2].

In the USA more than 80% of livestock is Holstein breed and the milking capacity of each is more than 9000 kg. The Holstein Association has registered 19 million of cattle in the country [3-5]. In Germany the Holstein share in the population is 60% in 28500 livestock famrs; more than 1,7 million of cattle of high capacity. In Europe the improvement of the breed is implemented according to the plan and the process is managed by EAAP (European Federation of Animal Science)[4]. If we review East and, in particular, Israeli experience today there is approximately one hundred thousand cattle which produces around 1 billion kg of milk annually which fully meets the needs of local population on milk and milk products and a part of the products is exported [5].

Over the last years farmers import European breed cattle in Georgia. Due to the peculiarities

of homeostatic capacities the set of physiological disorders causing negative results is revealed. It is identified that apart from other breeds, the Holstein breed more easily adopts to environmental conditions and to achieve the maximum of its genetic capacity it is necessary to create conditions which best correspond to its genotype. Consequent from the above breeding of Holstein cattle in untypical natural environment is very important. In general the genetically predetermined norm of reaction of animals defines its environment adaptation capacity limits. It is noteworthy that in some cases the ignorance of adaptation peculiarities impeded the adjustment to extreme environmental conditions [6-10].

Today there are 4250 cows (industrial breeds) imported in our country. Out of this number 2170 is Hosltein breed and the most of them (1570) are in Kakheti region. It should be mentioned that the breeding of Hosltein cattle in Kakheti intensive agrarian zone has not been scientifically studied and there are no corresponding recommendations developed. It is urgent to study the peculiarities of Holstein cow productivity potential realization as well as to study the economic and biological peculiarities of it in the new environmental conditions which is of significant national economic importance (development of intensive farming and increase of raw milk production), while on the other hand, in order to reveal the high genetic qualities of this breed, it is necessary to create such conditions which fully correspond to its genotype.

Goal and Methodology of the Research

The goal of our research was scientific justification of Holstein cattle breeding in the conditions of Kakheti region. To accomplish the research we observed 25 breeds of 5-6 months pregnant nonparous Holstein cattle imported from Estonia by Norshi Ltd. on March 15, 2016. Consequent from the research goal the observation was conducted over the whole herd as well as over the breeding and development of locally reproducted calves (studied 12 heifers from their birth till the age of copulation). In parallel with the above we accomplished zoo technical analysis of the food.

Consequent from the mentioned goals the following results were obtained in the period of the research:

- Description of the clinical status indicator of the cattle in different periods of procreation;
- Register of the received nutriments;
- Study of the nutritiousness of the nutriments;
- Dynamics and calculation of average daily weight gain of heifers;

Results and Analysis

Development of peculiarities of an organism depends on heredity (genotype) and environmental conditions. When we are talking about the adaptation of animals to these or those extreme conditions we agree to take into consideration the fact that any dislocation of animals is accompanied by negative results. Environment is the basic limiting factor of revealing genetic capacities of an organism. In the condition of extremely high air temperature influence European milk cow breeds are characterized by limited homeostatic capacity which results in the whole set of physiological disorders causing decrease in reproductivity, growth intensity, milking productivity, period of agricultural exploitation and other undesirable results. It is obvious that considering the existing natural and economic conditions and biological peculiarities of cattle predefines the selection of relevant technological methods in cattle farming [11-15].

On the first stage of cattle farming of the nulliparous and primaparous cows the whole set of problems related to feeding and breeding arose. Though the revealed mistakes were eliminated and the technological process was improved.

It is particularly important to define clinical indicators (changes in the indicators according to various factors) of cattle in the process of adaptation to new environmental conditions which enables to define its health condition. Therewithal the important criteria which characterize the quality of adaptation and its maintenance in the given environment are growth and development, productivity and reproductivity [16-17].

Visual observation of the animals demonstrated that the imported animals are less adapted to the summer heat. We studied the resistence to the high temperatures by nonporous speices by calculating the heat-resistence index according to I.A.Rauschenbach [18]. The first test was done in the morning (8-9 o'clock) when air temperature was 16-20^{o}C; the second test was done during the hot daytime period at 15-16 o'clock when the temperature was 28-32^{o}C. The heat resistance

index of nonporous cows was lower than of prim parous cows. The body temperature of nonporous cows in the morning under the condition of 20^{0}C air temperature was 38,8^{0}C, while the body temperature of prim parous cows varied from 38,2 to 38,4^{0}C; under the condition of 30^{0}C air temperature the body temperature of nonporous cows increased by 0,8^{0}C and in prim parous cows it increased by 0,2 -0,3^{0}C. Correspondingly the index of heat-resistance of prim parous cows was 2,2-3,3 units less than that in nonporous cows.

In line with it we revealed the number of visually observed problems such as saliva foam formation during the chewing process, inflammation of joints and cloven hoofs, liquid stool and in some cases loss of the cattle The conducted zoological analysis of the feed and its ingredients revealed:

- The protein content is low;
- The portion of nutritiousness in the feed is 30-40%
- The concentrated feed content in corn silage is 60-70% consequent from its nutritiousness though it should not exceed 38-40%;
- The ration contains big number of carbohydrates (sugar+starch) while according to the norm the ration of a milking cow must contain 62-108 gr. of sugar per 1 FU (290 gr. DM. per kilo) and 93-100 gr. of starch;
- The use of 0,7 kg of soda as a buffer reduces the energy content in the ration which in turn causes the reduction of the milking;
- The corn grains in silage is not powdered which hinders its digestion;
- The nutrient mixture is over-grinded (Fig.).

Unbalanced feed of cows, the use of concentrates including carbohydrates in big amount demonstrated negative effect on PH of first stomach on generation of evaporating fatty acids and their correlation. As a result of it the ethanoic acid decreases to 40%, propionic acid is increased by 40%. The decrease of ethanoic acid in its turn causes the following: decrease of milk and fat formation, toughening of active champing, decrease in saliva formation. Insufficiency of buffer substance (neutralizer) results in increase of acidity which, in its turn, is a precondition of decrease of cellulose digestion [19]. As it was already mentioned in case that such process lasts it may cause fat reduction in milk, inflammation of joints and cloven hoofs, liquid stool. All the above caused disproportion of sugar-protein correlation (the norm is 0.8=1.0 which means that 100 gr. m/protein must contain 80 gr of sugar). It is known that the quality and volume of the feed component substances as well as their correlation defines the effectiveness of the feed which ensures the productivity, health and reproductive capacity of animals [20,21].

In parallel we observed the breeding of the calves. We selected 12 units of the same age based on the analogy. It is known that the correct breeding of the calves defines the health and reproductivity of the mature cows at the same time the live weight of an animal at certain age and its exterior represents the indicator of the growth quality.

We used the breed standard for comparison [22]. Based on the capacity of the farm we tried to use the rational system of breeding which supports the normal growth and development, and ensures formation of high capacity and strong constitution. The feed ration was composed of the available feed components with the consideration of feeding norms which gave us the guarantee that we receive such desirable weight of the animals which will meet the requirements of the first class and higher standards during the first mating. All the above ensures that we get desirable live weight of cows in future.

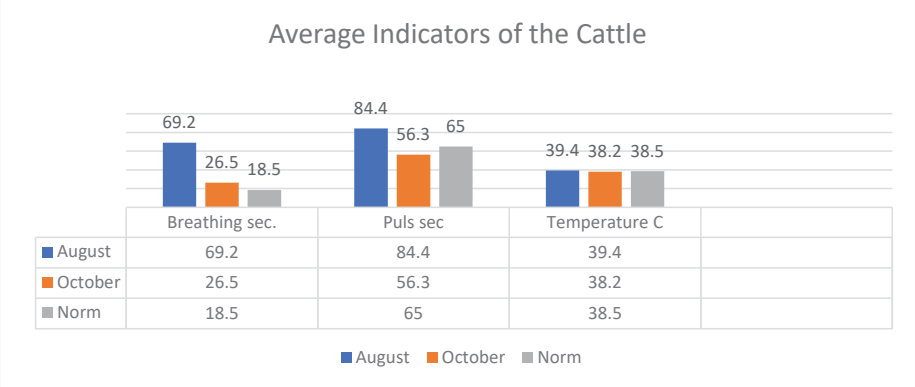

Fig. *The Average Clinical Indicators of the Cows*

Table 1. *Feed consumption from birth to the age of 15 months per one animal*

Feed	kg	Dry substance. kg	mgj	Feed unit	Digestable protein, kg
milk	410	32,0	1,11	123	13,5
concentrate	650	578,5	7,67	650	72,15
hay	720	597,6	5,04	324	36,7
Oat straw	430	356,9	2,45	94,6	5,59
Silage	2070	517,5	4,76	476,1	28,98
Green mass	3400	697,0	88,4	680	88,4
Total	7750	2779,5	109,4	2347,7	245,32

Table 2. *Growth and development dynamic of heifers, n = 12*

Age/months	Standard/mass/kg	Result in correlation with the standard, kg	Standard/height, cm	Result in correlation with the standard, cm
2	75	71	83	82
8	235-240 (237)	237	112	110
15	390-400 (395)	386	128	125
22	550-560 (555)	520	137	134

Holsteiner breed standard considers: live mass of 75 kg in 2 months of age, by the end of milk feed period [23]. The indicators of the tested heifers was 5% less than the standard. At the age of 8 months the standard is 237 kg [23], which is 3% more than the tested heifer mass; and at the age of 15 months the standard is 395 kg while the locally bred heifers achieved 386 kg. This indicator is considered a good result in Georgian reality but it lagged behind compared to the European standard. The tested heifer also showed retardation by 3-4% in height growth compared to standard. The listed disadvantages need to be taken into consideration when planning the growth of heifers though usually these are ignored.

The observation over the dunamic of the growth and development of the animals demonstrated 2-3% of retardation from the breed standard – live mass and whithers height. Despite the above these indicators may be considered applicable in local conditions.

Breathing is an unintegrated sign of life. The volume of oxygen in the organism of cattle is limited thus it requires to get oxygen from the environment. The dynamic of respiratory movements demonstrated that the respiration frequency is directly related to the age. It is similar to puls frequency variability – the highest indicator is registered at birth and it dicreases with the age which varies within the norm.

According to the literature data the body temperature of animals is almost permanent and does not suffer significant changes (except sick animals). Apart to the temperature the puls of animals and especially the breathing frequency significantly changes.

Table 3. *Clinical Status of the Heifers*

Age, month	Temperature ^{0}C	Pulse (minute)	Respiration frequency
At birth	39,02	81,0	34,20
6 months	38,40	70,40	31,20
12 months	38,14	59,7	20,60
18 months	38,6	57,50	18,40
24 months	30,17	54,8	18,30

Table 4. *Clinical Status of Animals*

Test period	Frequency of Arterial Pulse	Breathing Frequency
Pregnancy 5-6 months.	66	26,0
Pregnancy 8-9 months.	79	29,0
First parturition	85	33

The puls frequency of the tested six to nine months pregnant nulliparous cows showed the puls frequency increase by 13 beats (11.9%). The puls increase to 85 beats per minute during the first parturation. Hence the pulse frequency was several times less in the first half of the pregnancy period than in the second half and especially compared to the parturition. The results of the respiration frequency data analysis are similar which can be justified by the hot summer days.

The summer heat became injurious for the newly imported animals. Due to the bad ventilation of the building the first symptoms of thermal stress were revealed (frequent breathing, concetration of animals at water places, saliva formation, foam at the mouth and etc.). In instant response to the mentioned the recirculation fans were montaged in the right and left sides of the farm in 12-14 m distance from the feed table.

The body temperature of an animal is the complex indicators of its thermal condition which gives clear picture of its organism condition. In hot weather the evening temperature of the cattle is 0.5-0.6 C higher compared to the norm which must not be considered a pathology [24]. 1-2 degrees increase of the body temperature is the sign of pathology. The body temperature during the parturition is particularly worthy attention. High temperature may be caused by the influence of thte environment on the body of a newborn calf, later the temperature may slightly change though it varies within the physiological norm limits. As for the heart contraction frequency, i.e. puls – it is periodic rythmal blood vessels widening which is connected to the dynamic of vessels filling during the one cycle of the heart. Particularly high puls was detected in claves during the parturition which later was decreased and in the age of six months it reaches 70, 20 beats a minute. Later it decreases more to 20 beats and changes significantly until the copulation. At the same time all variations of the indicators were within the physiological limits of the breed.

Conclusion

- Index of heat-resistence of primaparous cows was 2,2-3,3 units less than that in nonporous cows.
- The quality and volume as well as the correlation of nutriments in the animal feed daily ration defined the stabilization of the feed consumption ration for animals to maintain

production and normal health and reproduction capacity.

- 2-3% of retardation from the breed standard in live mass and whithers height can be considered an applicable dynamic in Georgian conditions.
- The clinical analysis and the live weight growth and development dynamic of the tested Holstein breed hifers demonstrated that the studied indicators are within the physiological norms which justifies good adaptation capacity of the animals in the hot climate conditions of Kakheti region.

References

[1] N. K Gotsiridze, G. A. Dalakishvili – Effectiveness of cross-breeding of field red Holstein-Friesian and angler breeds in Georgian conditions. Scientific works of Georgian Zootechnical Veterinary Study and Reseach Institute. Vol. 1,1986, pp. 128-132 (in Georgian).

[2] Miglior F., Muir B.L., and Doormaal. B.J. Van. Selection Indices in Holstein Cattle of Various Countries. American Dairy Science Association, J. Dairy Sci. 88 (2005) 1255-1263.

[3] J.R.Campbell; R.T. Marshall, Dairy Production and Processing, Long Grove, Illinois, US, 2016.

[4] Bonny, Holstein Breed. 2004.

[5] B. Benechis, Change of the Base Year of Cows and Ox Evaluation in Israel, Guidebook for Milking Cows Selection Genetic Basis, Tel-Avi, 2002 .

[6] H.S. Thomas, Storey's Guide to Raising Beef Cattle, Health, Handling, Breeding, Therde Edition; SF207.T47, 2009.

[7] The Internet Archive, Dr. Larry W. Specht, Penn State University, 10 Apr 2008 https://web.archive.org/web/20080410084659/http://www.das.psu.edu/pdf/red-and-white-20070514.pdf accessed 3 September 2018.

[8] Ansell R.H. Observations on the reaction of British Friesian cattle to the lugnt ambient temperatures of the United Arab Emirates, University of the Bern. Thesis. 1974 pp.30-38.

[9] A.L. Tumanian, Peculiarities of Holstein Breed Black-and-White Cows Adaptation Subtropical Climate, PhD Authors Thesis, Krasnodar, 2003.

[10] G.M. Tunikov, Rational Methods of Feeding Holstein Cows in Yard Housing Conditions, Zootechnology, 4 (2011) 16-17.

[11] G. Gogoli, Environment and Animals; Ecological Problems of Productivity in Cattle Breeding, Metzniereba, Tbilisi, 1999 (in Georgian).

[12] G. Gogol, R. Barkalaya, Heat influence on milking cow productivity and the ways of its balancing. Scientific works of PhD, G. Peradze University, 2017, 56-59 (in Georgian).

[13] J. Gugushvili, G. Gogoli, Z. Lashkhi, Interspecies and Interbreed Hybridization, Tbilisi, 2016 (in Georgian).

[14] Roche JR, Berry DP, Kolver ES. Holstein-Friesian strain and feed e ects on milk production, body weight, and body condition score pro les in grazing dairy cows. J Dairy Sci., 89 (2006) 3532-3543.

[15] K. Mikadze, Livestock Behavior, Tbilisi, 2014 (in Georgian).

[16] Tillard E, Humblot P, Faye B, Lecomte P, Dohoo I, Bocquier F. Post calving factors ecting conception risk in Holstein dairy cows in tropical and sub-tropical conditions, Eriogenology, 69 (2008) 443-457.

[17] Trevisi E, Amadori M, Cogrossi S, Razzuoli E, Bertoni G. Metabolic stress and in amatory response in high-yielding, periparturient dairy cows. Res Vet Sci., 93 (2012) 695-704.

[18] G. Gogoli, Environment and Animals, Ecological Problems of Productivity in Livestock Breeding, Tbilisi, 1999.

[19] A. Chkuaseli, A. Chubinidze, A. Chagelishvili, M.Khutsishvili, Anumal Feed, II Part, Guidebook – Edition Global-Print, Tbilisi, 2011, pp.107-108. (in Georgian).

[20] G.Gogoli, L. Tortladze, Livestock Breeding, Tbilisi, 2010 (in Georgian).

[21] The Internet Archive, DeLaval, Dairy knowledge, 07 Oct. 2008 https://web.archive.org/web/20061007153430/http://www.delaval.co.uk/Dairy_Knowledge/EfficientDairyHerdMgmt/Management_Of_The_Dairy_Cow.htm accessed 01 Sep. 2018

[22] A. Chkuaseli, A. Chubinidze, A. Chagelishvili, Livestock Feed Part I, Guidebook, Edition Global-Print+, Tbilisi, 2011, pp. 261-267.

[23] Meelis Ots, Feeding of calvs and heifers, VL. 0191, University of Tartu, 2017

[24] T. Kurashvili, M. Kereselidze, Veterinary, Tbilisi, 2013 (in Georgan).

Annals of Agrarian Science

Journal homepage: http://journals.org.ge/index.php

Heavy metals specific proteomic responses of a highly resistant Arthrobacter globiformis 151B

O. Rcheulishvili[a,c,f*], L. Tsverava[b], A. Rcheulishvili[a], M. Gurielidze[d], R. Solomonia[b], N. Metreveli[c], N. Jojua[f], H-Y Holman[e]

[a]Department of Physics of Biological Systems of Andronikashvili Institute of Physics of Iv. Javakhishvili Tbilisi State University, 6, Tamarashvili Str., Tbilisi, 0177, Georgia

[b]Centre for Pathogen Research, Ilia State University, 3/5 Kakutsa Cholokashvili Ave., Tbilisi, 0162, Georgia

[c]Institute of Biophysics, Ilia State University, 3/5 Kakutsa Cholokashvili Ave., Tbilisi, 0162, Georgia

[d]S.Durmishidze Institute of Biochemistry and Biotechnology of the Agricultural University of Georgia, 240, David Aghmashenebeli All., Tbilisi 0159, Georgia

[e]Lawrence Berkeley National Laboratory, One Cyclotron Road, Berkeley, CA 94720, USA

[f]European University, 17, Sarajishvili Ave., Tbilisi, 0189, Georgia

Received: 21 September 2018; accepted: 12 December 2018

A B S T R A C T

The gram positive aerobic bacteria Arthrobacter globiformis 151B is a promising candidate for bioremediation of Cr(VI) and other metals ions because it exhibits resistance against high concentrations of Cr(VI) and other metallic ions. This bacterial species could reduce highly toxic and carcinogenic Cr(VI) into Cr(III). In this study, we investigated tolerance and accumulation of Cr(VI) and Zn(II) on protein level by proteomic approach. Arthrobacter globiformis 151B was grown at 3 following conditions: 1. with Cr (VI); 2. with Zn(II); 3. without Cr(VI) and Zn(II). Bacterial cells were harvested in a time dependent fashion (36, 60 and 120h after the starting of cultivation) and changes in proteome expression was analyzed using two-dimensional gel electrophoresis and liquid chromatography and mass spectrometry (LC-MS/MS) coupled with bioinformatics to identify proteins. Significant changes in protein expression included both up- and downregulation of different groups of proteins. Most remarkable changes were associated with metal-binding proteins and proteins involved in active transport. Parallel experiments with Atomic Absorption Spectroscopy revealed that reduced chromium appears mostly soluble and mainly associated with organics: especially with bacterial proteins. Our results signify that Arthrobacter globiformis 151 B is naturally equipped at the proteomic level correspondingly with the relevant genes, to survive extreme toxic conditions, thus has great potential for bioremediation.

Keywords: Heavy metals, Parallel experiments, Bioinformatics, Bacterial protein, Bacterial cells, Arthrobacter.

*Corresponding author: Olia Rcheulishvili: E-mail address: olia.rcheulishvili@iliauni.edu.ge

Introduction

Arthrobacter and many other members of the actinobacteria group are common residents of soil and have high tolerance to stressful conditions encountered in the soil environment, including the ability to degrade para-substituted phenolic compounds and humic substances [1]. The particular strain of this family, *Arthrobacter globiformis* 151B is Gram-positive, aerobic bacteria, which can survive in heavy- metal contaminated territory and has high potential for environment remediation [2]. This strain was isolated out of basalt samples from heavy metal contaminated site of Georgia –Kazreti [2]. Our previous studies by ESR spectroscopy has shown that bacteria posses the ability to reduce Cr(VI) into Cr(III), which is less soluble and less

toxic compound [3, 4]. FTIR absorption spectroscopy showed that Arthrobacter oxydans is capable to reduce Cr(VI) and complete uptake of 35 µg/mL of Cr(VI) concentration was achieved in about 10 days after Chromium addition into the medium [5]. We have also shown that Cr(VI) reduction process is very fast, and occurs on bacterial cell wall [2]. This reduction is not influenced by the presence of Zn(II) at concentration of 40 mg/L, but the higher concentrations (200 mg/L) inhibits the reduction of Cr(VI), by preventing the contact of Cr(VI) with bacterial cell wall [3]. The Cr(VI) reduction mechanisms, and the fate of reduced Cr(III) are under study. Some of studies provide evidence that Cr(VI) reduction is an enzymatically catalyzed reaction attributed to soluble proteins for some bacteria [6] and cell membranes for others [7, 8].

Further study of the mechanisms Cr(VI) reduction by *Arthrobacter globiformis* 151B is an important topic, because such bacteria could be effectively used for bioremediation processes. In the present study we have inquired (1) if heavy metal exposure Cr(VI), Zn(II) induces changes in the proteome of *Arthrobacter globiformis* 151B and (2) what is the fate of reduced Cr(III). Experiments were conducted in a time dependent fashion and 2-D electrophoresis/MS and Atomic Absorption Spectroscopy (AAS) approaches were used. As far as we know no such studies were conducted before.

Materials and methods

Bacterial Growth Conditions

Bacterial cells of *Arthrobacter globiformis* 151B were grown aerobically in 250-mL Erlenmeyer flasks as a 100-ml suspension in TSB broth (Sigma) at 21˚C. The cells were grown with a constant shaking (at a speed of 100rpm). The experiments were carried out on the following groups of bacteria: 1. Cells without any salt addition; 2. Cells with addition of only Cr(VI); 3. Cells with addition of only Zn(II); Experiments were started at the early stationery phase of bacterial cell growth. Cr(VI) and Zn(II) were added simultaneously to the bacterial cell cultures at this stage as K_2CrO_4 and $ZnSO_4$ respectively. Their (metals) concentration made up 40 mg/l in a nutrient liquid medium. The experimental samples from these groups were taken in a time dependent fashion: 36, 60 and 120 hours after the start of cultivation. Experimental design is provided in figure 1. Bacterial culture growth without or with Cr(VI) and Zn(II) proceeded without medium renewal.

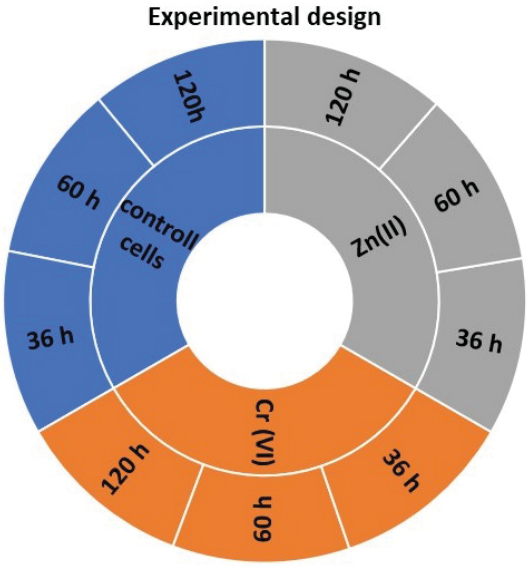

Fig. 1. *The scheme of experimental design*

Evaluation of Cr(VI) and Zn(II) resistance

Culture growth was monitored by measuring optical density at 490 and 590nm. The viability was detected by cell growth on agar plates with a cell suspension dilution. Bacterial resistance against Zn(II) and Cr(VI) was detected by counting of the Colony Forming Units on metal containing agar plates. Cell viability was observed on high (>1000 mg/l) metal concentration conditions.

After growing, bacterial cells were harvested from the nutrient medium by centrifugation (3,000g, 15 min, 4˚C), rinsed twice in a Phosphate buffered saline (PBS) and samples prepared either for 2 - D electrophoresis/MS or Atomic absorption spectroscopy analysis.

For determination the metal accumulation capacity by bacteria itself, wet biomass of bacterial pellet (after centrifugation and washing procedures) was placed in an adsorption-condensation lyophilizer and dried following the procedure reported in [9], dried cells were ashed in nitric acid, diluted with bidistilled water and analyzed by atomic absorption spectrometry (aas). Analyst 800 was used.

2-D electrophoresis and MS

Sample preparation

Bacterial cell wall lyses and protein extraction- The samples for 2-D electrophoresis and MS analysis

were carried out essentially as described in [10] Bacterial pellets were resuspended in buffer (20 mM Tris-acetate, pH 7.8, 20 mM NaCl, 2 mM EDTA, 100µg/mL lysozyme). Samples were incubated for 30 min at 37°C with intermittent vortexing. 9M Urea, 4% Tween 40, 2% Pharmalyte, 2% Mercaptoethanol, 2% protease inhibitor (bacterial) were added and lysates were centrifuged at 15,000 × *g* for 30 min at 4°C.

Metal accumulation ability by bacterial proteins was determined by atomic absorption spectroscopy, on the portion of extracted proteins.

Protein Quantification. Protein concentration is supernatants was quantified by a micro-BCA kit (Pierce, Thermo Scientific) in quadruplicate. Appropriate buffer controls were used.

Isoelectric focusing

Isoelectric focusing (IEF) strips (linear pH 3–10 and pH 4-7) were rehydrated in 8M urea, 0.5% Triton X-100, 0.5% Pharmalyte 3–10, and 30 mM Destreack reagent overnight. Protein samples (40 µg) were loaded onto rehydrated strips in buffer containing 7M urea, 2M thiourea, 2% Triton X-100, 0.1% ASB-14, 2-mercaptoethanol, 2% Pharmalyte 3–10, bromophenol blue and 2% protease inhibitor. IEF was carried out at 500 V for 3 h and 3,500 V approximately for 18 h.

Equilibration

IEF strips were equilibrated for 15 min in a buffer containing 0.05M Tris-HCl (pH 6.8), 6M urea, 30% glycerol, 3% SDS, and 1% DTT, followed by equilibration in the same buffer with 2.5% DTT iodoacetamide instead of 1% DTT for 15 min.

SDS Electrophoresis

SDS electrophoresis was run on a 1-mm thick, 12.5% polyacrylamide gel at 25°C. For the first 1 hour 10 mA per gel at 80 V was applied and then for 17 h 12 mA per gel at 150 V.

Staining, Scanning, and Analysis

The gels were stained with a silver stain kit (GE-Healthcare), omitting the glutaraldehyde step. Silver-stained gels were scanned with an image scanner (Labscan 6.0. GE Healthcare). Images were digitalized and processed using Image Master 2D platinum 7.0 software. In each series of experiments, the three type of *A. globiformis* 151B samples were analyzed concurrently for each time point. Proteins that exhibited at least 1.5-fold difference between the conditions were selected. The relative intensities of protein spots coinciding by location (isoelectric point and molecular weight) from different experiments were compared by *t*-test. The significantly differentially expressed protein spots ($p < 0.05$) were excised, destained, and stored at −20°C until MS analysis.

In-gel Digestion

Excised proteins were reduced with TCEP and alkylated with iodoacetamide. Samples were then treated with acetonitrile, dried, and rehydrated in activated trypsin (Thermo Scientific, Pierce) to begin digestion; proteins were digested at 37°C overnight. After digestion, the supernatant was pipetted into a sample vial and loaded into an autosampler for automated LC-MS/MS analysis.

MS analysis

Mass spectrometry experiments were performed using LTQ Fleet ion trap fitted with nanospray ion sources (ThermoFisher). The separation of peptides was performed by reverse-phase chromatography using EASY-nLC™ 1000 Integrated Ultra High Pressure Nano-HPLC system at a flow rate of 300nL/min and an LC-Packings (Dionex, Sunnyvale, CA) PepMap 100 column (C18, 75µM i.d. × 150mm, 3µM particle size). Peptides were loaded onto an LC-Packings precolumn (Acclaim PepMap 100 C18, 5µM particle size, 100A, 300µM i.d × 5mm) from the autosampler using 0.1% formic acid for 5min at a flow rate of 5µL/min to desalt samples and focus peptides prior to analytical separation. After this period, the six port valve was switched to allow elution of peptides from the precolumn onto the analytical column. Solvent A was water + 0.1% formic acid in water and solvent B was 100% acetonitrile + 0.1% formic acid. The LTQ instrument was operated in a data-dependent manner, in which a survey scan was performed to analyse the m/z values of ions which were eluted from a reverse-phase HPLC column. MS/MS spectra data were analyzed using SEQUEST (Proteome Discoverer 1.4), searching against UniProt UniRef100 Arthrobacter species protein databases.

AAS measurements

The total chromium and total zinc contents in bacterial proteome were measured using an atomic absorption spectrometer (Analyst 800) with an acetylene-air flame. The detection was carried out at 357.9 nm (for chromium) and at 213.8 nm (for zinc). The instrumentation detection limit for Cr measurement was 0.02 µg/ml and for Zn was 0.01 µg/ml.

Results and discussion

2-D gel electrophoresis

We examined the behavior of bacterial proteome under the influence of Zinc(II) and Cr(VI) to compare to control cells, using 2-D gel electrophoresis and mass spectrometry analyses. MS analysis was used to determine the identity of the excised proteins.

The 2-D gel electrophoresis of *Arthrobacter globiformis* 151B protein extracts was carried out initially with two pH gradients: 3.0 – 11.0 and 4.0 – 7.0. The majority of the proteins on the 3.0 – 11.0 pH gradient gels were concentrated between pH 4.0 and 7.0 (Figure 2-A.). Thus, for the better resolution and identification of differentially expressed bands 2-D gel electrophoresis was continued using strips with a pH gradient from 4.0 to 7.0. (Figure 2 - **B. C. D)**. Most significant stable differences were observed at 60h of cultivation and all results provided below represent the differences at this time point.

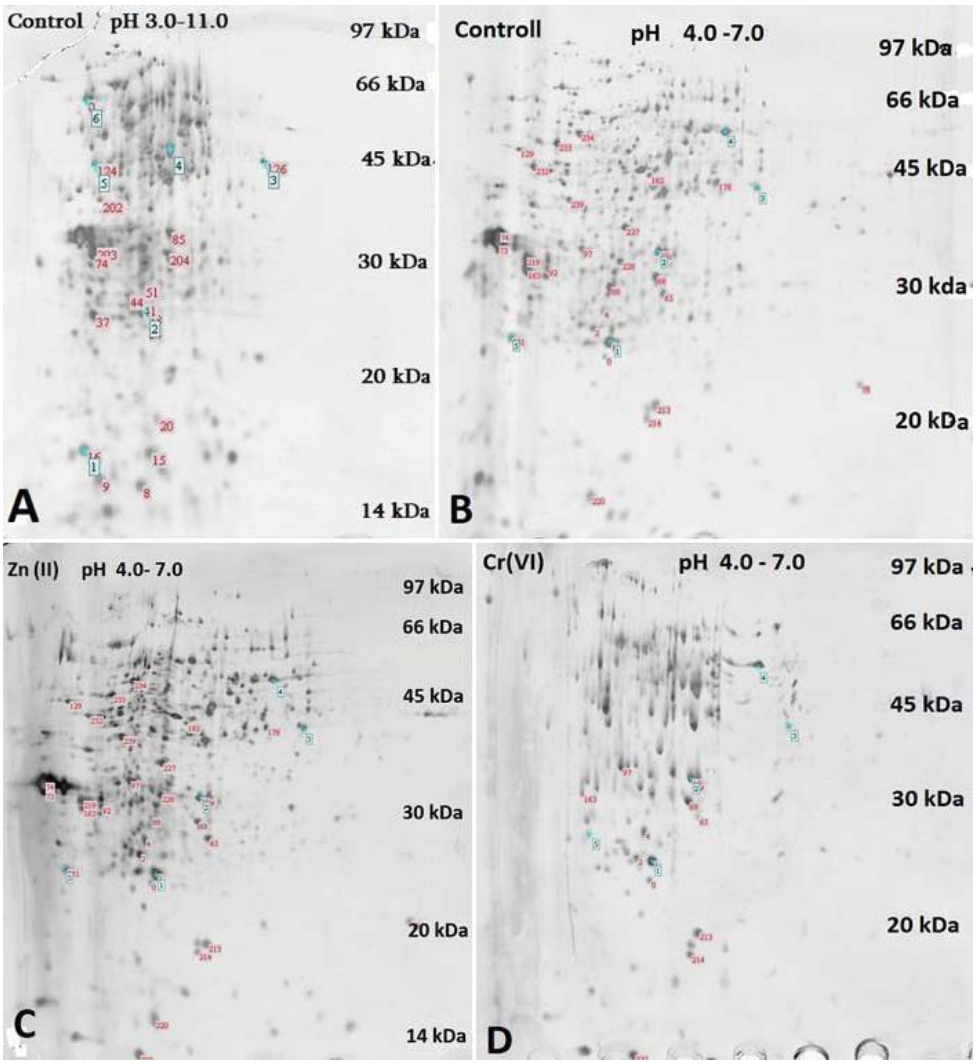

Fig. 2. *Represantitive images of silver stained 2-D gel electrophoresis gels of Arthrobacter globiformis 151 B, protein extracts 60 hour of growth. 2A: protein extract from control cells from 2-D strips with pH linear gradient 3.0 - 11.0; 2 B, C, D representative images of 2-D electrophoresis gels on strips with pH linear gradient 4.0 - 7.0; B - protein extract from control cells; C - protein extract from Zn(II) treated cells; D - protein extract from Cr(VI) treated cells.*

The cultivation of *Arthrobacter globiformis* 151 B with Cr(VI) results in statistically significant differential expression of 41 proteins as compared to untreated, control cells, whereas addition of Zn (II) induces the differential expression of 24 proteins (Table 1A-B).

Differently expressed proteins are involved in a variety of activities and functions. Function of 1st group proteins, expression of which is increased with metal treated cells, mostly relate to stress response reactions and maintenance of the cellular ion homeostasis. It is widely accepted that, these proteins also participate in protein translation processes, activate transcriptional factors and phosphorylate components of signal transduction systems. They can also participate in Zinc and Ferric ion binding processes and act as chaperones. (Table 1 A, B). Function of 2nd group proteins, expression of which decrease in Zn(II) and Cr(VI) treated cells, are mostly related to cellular energetic processes. These energetic processes are associated with cellular active transport. Functions of proteins from 2nd group mostly relate to the trans-membrane transport activity, ATP binding and ATP-ase activity, GTP-ase activity, NADP binding activities. (Table 1. A-B). Availability of Zn to biomolecules is tightly regulated by binding proteins, metallothioneins (MTs) and Zn transporters [19]. Cysteine synthase is increasing in Zn treated cells (see table 1B second row). It is interesting to note that, MTs are cysteine rich proteins that bind up to seven Zn ions with picomolar affinity and carry the labile Zn fraction to cellular compartments. MTs are induced during oxidative stress, scavenge reactive oxygen species (ROS) and reduce heavy metal intoxication [12, 11]. Thus the increase in Cystein synthase could stabilize the necessary conditions for MTs homeostasis. Chromium and Zinc concomitant action causes the strongest oxidative stress in the case of A. globiformis that is demonstrated by the increased activity of superoxide dismutase (SOD) and catalase [13].

Table 1 A. *The list of statistically significantly differentially expressed proteins between Cr(VI) treated bacteria and control groups (all changes are more than 1.5 fold). Proteins 27-41 are virtually absent in Cr(VI) treated cells. * -indicates for those proteins which are also significantly differentially expressed in Zn(II) vs Control comparisons (see also Table 1B)*

##	Proteins	Direction of changes	Molecular/biological functions
1	Succinate--CoA ligase	↑	ATP binding, metal ion binding, succinate-CoA ligase (ADP-forming) activity
2	Peptidyl-prolyl cis-trans isomerase	↑	peptide binding, peptidyl-prolyl cis-trans isomerase activity, unfolded protein binding (chaperone function)
3	2'-5' RNA ligase	↑	Ligase activity
4	Phage shock protein A (PspA) family protein	↑	Not given
5	Alanine dehydrogenase	↑	alanine dehydrogenase activity
6	Probable xylitol oxidase	↑	D-arabinono-1,4-lactone oxidase activity, flavin adenine dinucleotide binding
7	UncharacterizedN-acetyltransferase BWQ92_22005	↑	Proton donor and acceptor
8	50S ribosomal protein L25-	↑ *	Structural constituent of ribosome, 5s rna binding-participates In translation

9	Cysteine synthase	↑ *	Cysteine synthase activity
10	DNAstarvation/stationary phase protection protein	↑ *	Ferric ion binding, oxidoreductase activity, oxidizing metal ions, cellular ion homeostasis, response to stress
11	Chorismate mutase OS=Arthrobacter sp	↑ *	Prephenate dehydratase (pheA) L-phenylalanine biosynthetic process
12	GntR family transcriptional regulator	↑ *	catalytic activity, DNA binding, DNA binding transcription factor activity, pyridoxal phosphate binding
13	Response regulator receiver protein	↑ *	phosphorelay signal transduction system, regulation of transcription, DNA-templated, protein-glutamate methylesterase activity, chemotaxis
14	Putative periplasmic membrane protein	↑ *	metalloendopeptidase activity, zinc ion binding, chaperone-mediated protein folding
15	LSU ribosomal protein L25P	↑ *	Ribonucleoprotein, Ribosomal protein
16	Uncharacterized protein	↑ *	ATP-ase activity, transmembrane transport, Lipase activity, lipid metabolic process, outer membrane component,
17	Avirulence D protein (AvrD)	↑ *	Non predicted
18	Chlorite dismutase	↓	Non predicted
19	Oxidoreductase(electrons transfer from donors to acceptors)	↓	choline: oxygen 1-oxidoreductase activity
20	ABC transporter substrate-binding protein	↓	ATP-ase activity, ATP binding, trans-membrane transporter activity
21	Ketol-acid reductoisomerase (NADP(+))	↓	Ketol-acid reductoisomerase activity, metal ion binding, NADP binding, isoleucine biosynthetic process, valine biosynthetic process, Branched-Chain Amino acid biosynthesis, Mg-binding
22	Sugar ABC transporter substrate-binding protein	↓	ATP-binding cassette (ABC) transporter complex
23	Amino acid ABC transporter substrate-binding protein, PAAT family	↓	Ionotropic glutamate receptor activity, nitrogen compound transport,
24	Nicotinate phosphoribosyltransferase	↓	Transferase activity, transferring glycosyl groups, nucleoside metabolic process

23	Amino acid ABC transporter substrate-binding protein, PAAT family	↓	Ionotropic glutamate receptor activity, nitrogen compound transport,
24	Nicotinate phosphoribosyltransferase	↓	Transferase activity, transferring glycosyl groups, nucleoside metabolic process
25	MarR family transcriptional regulator	↓	DNA-binding, DNA- binding transcription factor activity, transcription DNA templated
26	Elongation factor G	↓	GTP-ase activity, GTP binding
27	Putative tricarboxylic transport membrane protein	↓	Integral component of membrane, outer membrane- bounded periplasmic space
28	SPG23_c14, whole genome shotgun sequence	↓	DNA binding, phosphoreley signal transduction system, regulation of transcription, DNA-templated,
29	tRNA pseudouridine synthase A	↓	tRNA processing, Isomerase, RNA binding, tRNA pseudouridine synthase activity,
30	Putative tricarboxylic transport membrane protein	↓	Integral component of membrane, outer membrane-bounded periplasmic space
31	C4-dicarboxylate ABC transporter substrate-binding protein	↓	ATP-binding, sequence specific DNA binding, transcription factor binding, phosphoreley signal transduction system, regulation of transcription, DNA-templated,
32	Citrate synthase	↓	Citrate (Si)-synthase activity, tricarboxilic acid cycle
33	Carbohydrate ABC transporter substrate-binding protein, CUT1 family	↓	Integral component of membrane
34	Transaldolase	↓	Sedoheptulose-7-phosphate: D-glyceraldehyde-3-phosphate glyceronetransferaze activity, carbohydrate metabolic process, penthose phosphate shunt
35	ATP synthase subunit beta	↓	ATP binding, proton-transporting ATP synthase activity, rotational mechanism, ATP synthesis coupled proton transport
36	ATP-binding transport protein NatA	↓	ATP ase activity, ATP binding
37	Type I restriction-modification enzyme subunit S	↓	Not given

38	Methionine aminopeptidase	↓	DNA binding, metal ion (divalent metal cations) binding, metalloaminopeptidase activity, positive regulation of transcription, DNA template, protein initiator methionine removal, regulation of DNA replication,
39	ATP synthase gamma chain	↓	ATP binding, proton transporting ATP synthase activity,
40	Signal transduction protein	↓	ATP binding, hydrolase activity, phosphorelay sensor kinase activity, integral component of plasma membrane
41	Nitroimidazol reductase NimA,	↓	cofactor binding

Table 1 B. *The list of statistically significantly expressed proteins between Zn(II) treated bacteria and control group (all changes are more than 1.5 fold)*

##	Proteins	Direction of changes	Molecular/biological functions
1	50S ribosomal protein L25-	↑*	Structural constituent of ribosome, 5s rna binding-participates In translation
2	Cysteine synthase	↑*	Cysteine synthase activity
3	DNAstarvation/stationary phase protection protein	↑*	Ferric ion binding, oxidoreductase activity, oxidizing metal ions, cellular ion homeostasis, response to stress
4	Chorismate mutase OS=Arthrobacter sp	↑*	Prephenate dehydratase (pheA) L-phenylalanine biosynthetic process
5	GntR family transcriptional regulator	↑*	catalytic activity, DNA binding, DNA binding transcription factor activity, pyridoxal phosphate binding
6	Response regulator receiver protein	↑*	phosphorelay signal transduction system, regulation of transcription, DNA-templated, protein-glutamate methylesterase activity, chemotaxis
7	Putative periplasmic membrane protein	↑*	metalloendopeptidase activity, zinc ion binding, chaperone-mediated protein folding
8	LSU ribosomal protein L25P	↑*	Ribonucleoprotein, Ribosomal protein
9	Uncharacterized protein	↑*	ATP-ase activity, transmembrane tranbsport, Lipase activity, lipid metabolic process, outer membrane component,
10	Avirulence D protein (AvrD)	↑*	Non predicted

11	Ribonucleoside-diphosphate reductase subunit beta	↑	metal ion binding, ribonucleoside-diphosphate reductase activity, thioredoxin disulfide as acceptor, Binds 2 iron ions per subunit
12	Acylpyruvate hydrolase	↑	hydrolase activity
13	Zn-dependent hydrolase	↑	metal ion binding, metalloendopeptidase activity, ribonuclease P activity
14	Succinyl-CoA ligase [ADP-forming] subunit alpha	↓	ATP binding,metal ion binding, succinate-CoA ligase (ADP-forming) activity, ATP + succinate + CoA = ADP + phosphate + succinyl-CoA. Binds 1 Mg^{2+} ion per subunit
15	Short-chain dehydrogenase/reductase SDR	↓	oxidoreductase activity aspartic-type endopeptidase activity
16	Superoxide dismutase	↓	metal ion binding, superoxide dismutase activity,Binds 1 Fe cation per subunit, 2 superoxide + 2 H^+ = O_2 + H_2O_2
17	ABC transporter permease	↓	antibiotic transmembrane transporter activity, ATPase activity,ATP binding, efflux transmembrane transporter activity, Confers resistance against macrolides
18	Ribosome-recycling factor	↓	translation, translational termination, Responsible for the release of ribosomes from messenger RNA at the termination of protein biosynthesis
19	LacI family transcriptional regulator	↓	alanine racemase activity, DNA binding, regulation of transcription, DNA-templated, transcription, DNA-template
20	ATP-dependent DNA helicase RecG	↓	ATP binding, ATP-dependent DNA helicase activity, nucleic acid binding, DNA recombination, DNA repair
21	D-isomer specific 2-hydroxyacid dehydrogenase, NAD-binding protein	↓	4-phosphoerythronate dehydrogenase activity, NAD binding, protein dimerization activity
22	LysR family transcriptional regulator	↓	DNA binding, DNA binding transcription factor activity
23	Alpha-hydroxy-acid oxidizing enzyme	↓	(R-pantolactone dehydrogenase (flavin) activity, FMN binding, oxydoreductase, Flavoprotein, FMN,
24	Uncharacterized lipoprotein YufN	↓	Component of cellular membrane,

Bacterial defensive mechanisms against high Cr(VI) concentrations, are shown in different ways: a) Chromate efflux by the ChrA transporter, which is the membrane potential driven energy-dependent process; b) Chromate reduction to Cr(III) carried out by chromate reductases, enzymes belonging to the widespread NAD(P)H-dependent flavoprotein family; c) Other mechanisms of bacterial resistance to chromate involve the expression of components of the machinery for repair of DNA damage, and systems related to the homeostasis of iron and sulfur [14].

Zinc is an essential trace element for most organisms; Zn^{2+} ion performs numerous structural, regulatory, and catalytic roles in a range of proteins. However, this nutrient can neither be synthesized nor degraded and individual cells need to be able to maintain steady levels of Zinc in the face of near-zero or excessively high environmental concentrations [15]. It is becoming increasingly apparent that the ability of commensal organisms to adapt to the host environment depends upon the ability to withstand large fluxes in Zinc availability that are produced by the host [15, 11]. Zn in bacteria is primarily used as a metalloenzyme cofactor with a total concentration in the 0.1–1.0 mM range [16, 17, 18]. Zn is incorporated into about 10% of all human proteins, and well over 300 enzymes are known to require Zn(II) for catalytic or structural functions [19, 20]. Metallic homeostasis of the cell, should be defended according the special metal sensors, which should correctly distinguish between the inorganic elements [21]. These metal sensor proteins transcriptionally regulate the expression of genes that encode metal transporters and other resistance proteins [22, 23, 24]. Almost half of all enzymes must associate with a particular metal to function [21]. Zinc fluxes are involved in regulating a wide variety of cellular functions, including host immune activation [25]. In most bacteria, the zinc uptake repressor (Zur) controls the expression of a small number of genes required to adapt to conditions of severe zinc depletion [20]. When the intracellular Zinc concentration is far below a critical threshold, $[metal]_{free} < 1/K_{metal}$, the zinc-free form of Zur has low affinity for the DNA operator, which overlaps the promoter, thus allowing unfettered access by RNA polymerase to transcribe the genes encoding a high affinity Zn uptake system(s) [20]. In addition, genes encoding the efflux system are transcriptionally repressed by the apo form of the Zn efflux repressor, ZntR in Escherichia coli, under these conditions. As levels of bioavailable Zn rise to $[metal]_{free} > 1/K_{metal}$ (Zinc-replete conditions), the Zinc-bound form of Zur binds tightly to the operator site, preventing transcription [15].

AAS Analyses

AAS measurements have revealed that portion of Zinc and Chromium, which are accumulated by *A.globiformis* 151B cells, are bound to bacterial proteins. These experiments indicated two different behavior tendency between Chromium and Zinc in the proteome of *Arthrobacter globiformis 151 B.* Concentration of Zinc in bacterial proteins is increasing after time and reaches maximal level after 120 hour growth, when bacterial medium contains 40 mg/l Zn(II). (Fig. 3 A). But behavior of Chromium in proteome quite differs from Zinc's: Chromium content in proteins is decreasing after time. If it was maximal at 35 hour of bacterial growth phase, after 120 hour, Chromium content in proteome is decreased significantly (Fig 3 B).

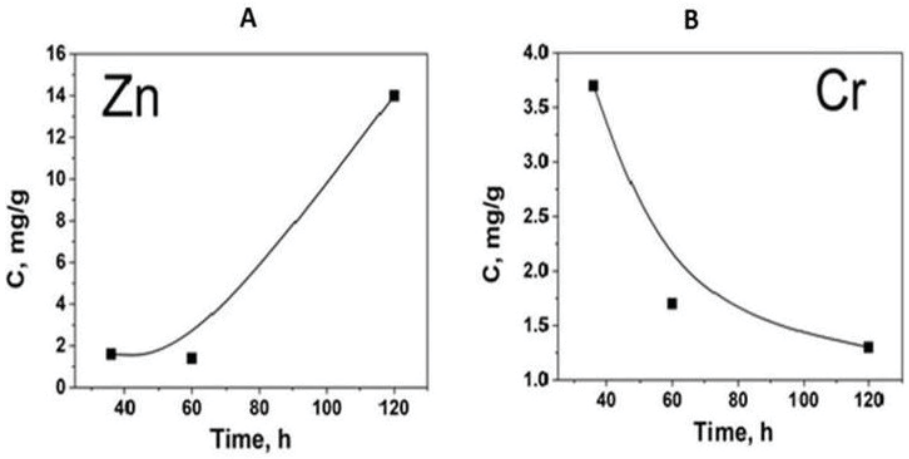

Fig. 3. *The dependence of the concentration of Zn(II) and Cr (mg/g) in proteins from the time T (h) of cultivation of bacteria Arthrobacter globiformis 151 B.*

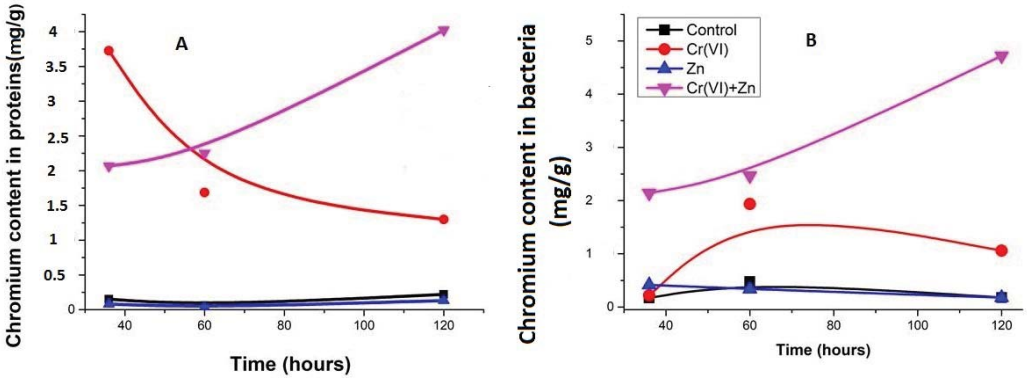

Fig. 4. *Chromium accumulation capacity in proteins (A) and in the whole bacteria itself (B). Influence of Zinc(II) ions on Chromium accumulation capacity in bacterial proteins (A) and in bacteria (B).*

In this experiment we examined Zn(II) and Cr(VI) joint action on the chromium accumulation capacity, on both: protein or bacterial levels. Samples were made according to abovementioned design: same concentration of Cr(VI) and Zn(II) were added, but together (joint). Experiment reveal, that Zinc(II) ions, on given concentration (40 mg/l), enhances bacterial ability for Chromium accumulation Fig. 4 B. Zinc also increases Chromium content in bacterial proteins (reduced Chromium-protein binding) Fig. 3A. and the concentration of proteins with bound chromium-increased after time (for 120 hour). Zinc action enhances Chromium accumulation in bacteria by two metals simultaneous presence. Without Zinc, chromium content in proteome tends to decrease after time. And maximal content is observed at early stage of cultivation-36 hour. For 120 hour Cr content in proteins is significantly decreased.

Conclusion

Remarkable changes in bacterial proteome were associated with metal-binding proteins and proteins involved in active transport. Experiments with atomic absorption spectroscopy revealed that reduced chromium appears mostly associated with organics: especially with bacterial proteins. Zinc(II) ions enhances bacterial ability for Chromium accumulation. Zinc(II) also increases reduced Chromium-protein connections and their content increases after time (for 120 hour).

Acknowledgements

This work was funded by Grant #FR/218 018/16 from Shota Rustaveli National Science Foundation (SRNSF).

Conflicts of Interest

None declared.

References

[1] M. Unell, P.E. Abraham, M. Shah, B. Zhang, C. Rückert, N.C. VerBerkmoes, K. Jansson, Impact of Phenoloc Substrate and Growth Temperature on the Arthrobacter chlorophenolicus Proteome, Journal of Proteome research. *8* (4), (2009) 1953–1964 DOI: 10.1021/pr800897c.

[2] N.Y. Tsibakhashvili, T.L. Kalabegishvili, A.N. Rcheulishvili, I.G. Murusidze, S.M. Kerkenjia, O.A. Rcheulishvili, H.Y. Holman, Decomposition of Cr(V)-diols to Cr(III) complexes by *Arthrobacter oxydans,* Microb Ecol., 57 (2009) 360-365.

[3] N.Y. Tsibakhashvili, T.L. Kalabegishvili, A.N. Rcheulishvili, E.N. Ginturi, L.G. Lomidze, O.A. Rcheulishvili, D.N. Gvarjaladze, H.Y. Holman, Effect of Zn(II) on the reduction and accumulation of Cr(VI) by *Arthrobacter* species. J Ind Microbiol Biotechnol, 38 (2011) 1803-1808.

[4] N.Y. Tsibakhashvili, L.M. Mosulishvili, T.L. Kalabegishvili, E.I. Kirkesali, I.G. Murusidze, S.M. Kerkenjia, M.V. Frontasieva, H.Y. Holman, Biotechnology of Cr(VI) transformation into Cr(III) complexes. J radioanal Nucl Chem 278 (2008) 565-569.

[5] N. Asatiani, M. abuladze, T. Kartvelishvili, N. Bakradze, N. Sapojnikova, N. Tsibakhashvili, L. Tabatadze, L. Lejava, L. Asanishvili, H.Y. Holman, Effect of Cr(VI) action on Arthrobacter oxydans. Curr Microbiol 49 (2004) 321-326.

[6] Y. Ishibashi, C. Cervantes, S. Silver, Chromium

reduction in Pseudomonas putida. App Environ Microbiol 56 (1990) 2268–2270.

[7] T.L. Daulton, B.J. Little, J.J. Meehan, D.A. Blom, L.F. Allard, Microbial reduction of chromium from the hexavalent to divalent state. Geochim Cosmochim Acta 71 (2007) 556–565.

[8] C.R. Myers, B.P. Carstens, W.E. Antholine, J. M. Myers, Chromium (VI) reductase activity is associated with the cytoplasmic membrane of anaerobically grown Shewanella putrefaciens MR-1. J Appl Microbiol 88 (2000) 98–106.

[9] L.M. Mosulishvili, E.I. Kirkesali, A.L. Belokobilsky, A.L. Khizanishvili, M.V. Frontasyeva, S.F. Gundorina, C.D. Oprea, Epithermal neutron activation analysis of blue-green algae Sp. Platensis as a matrix for selenium-containing pharmaceuticals. J. Radioanal Nucl Chem 252 (2002) 15-20.

[10] M. Nozadze, E. Zhgenti, M. Meparishvili, L. Tsverava, T. Kiguradze, G. Chanturia, G. Babuadze, M. Kekelidze, L. Bakanidze, T. Shutkova, P. Imnadze, S.C. Francesconi, R. Obiso, R. Solomonia, Comparative proteomic studies of *Yersinia pestis* strains isolated from natural foci in the Republic of Georgia; Front. Public Health, 16 October (2015) https://doi.org/10.3389/fpubh.2015.00239.

[11] V.K. Subramanian, L.J.A. Figueroa, A. Porollo, J.A. Caruso, S.G. Deepe, Granulocyte macrophage-colony stimulating factor induced Zn sequestration enhances macrophage superoxide and limits intracellular pathogen survival. Immunity 39 (2013) 697–710.

[12] P. Coyle, J.C. Philcox, L.C. Carey, A.M. Rofe, Metallothionein: the multipurpose protein.Cell Mol Life Sci.59 (2002) 627–647.

[13] N. Asatiani, T. Kartvelishvili, N. Sapojnikova, M. Abuladze, L. Asanishvili, M. Osepashvili, Effect of the Simultaneous Action of Zinc and Chromium on Arthrobacter spp, An International J. of Environmental Pollution Water Air and Soil Pollution, DOI:10.1007/s11270-018-4046-0 229 (2018) 12.

[14] M.I. Ramírez-Díaz, C. Díaz-Pérez, E. Vargas, H. Riveros-Rosas, J. Campos-García, C. Cervantes, Mechanisms of bacterial resistance to chromium compounds, Biometals, Vol. 21, Issue 3, (2008) 321–332.

[15] B.A. Gilston, S. Wang, M.D. Marcus, M.A. Canalizo-Hernández, E.P. Swindell, Y. Xue, A. Mondragón, T.V. O'Halloran, Structural and mechanistic basis of zinc regulation across the E. coli Zur regulon, PLoS Biol. (2014) 12, e1001987.

[16] S.L. Begg, B.A. Eijkelkamp, Z. Luo, R.M. Couñago, J.R. Morey, M.J. Maher, C.L. Ong, A.G. McEwan, B. Kobe, M.L. O'Mara, J.C. Paton, C.A. McDevitt, Dysregulation of transition metal ion homeostasis is the molecular basis for cadmium toxicity in Streptococcus pneumoniae. Nat. Commun. 6 (2015) 6418.

[17] F.E. Jacobsen, K.M. Kazmierczak, J.P. Lisher, M.E. Winkler, D.P. Giedroc, Interplay between manganese and zinc homeostasis in the human pathogen Streptococcus pneumoniae. Metallomics, 3 (2011) 38–41.

[18] C.E. Outten, T.V. O'Halloran Femtomolar sensitivity of metalloregulatory proteins controlling zinc homeostasis. Science 292 (2001) 2488–2492.

[19] C. Andreini, L. Banci, I. Bertini, A. Rosato, Counting the zinc-proteins encoded in the human genome. J. Proteome Res. 5 (2006) 196–2011.

[20] D.A. Capdevila, J. Wang , D.P. Giedroc, Bacterial Strategies to Maintain Zinc Metallostasis at the Host-Pathogen Interface, J Biol Chem. 291(40) (2016) 20858–20868 doi:[10.1074/jbc.R116.742023]

[21] K.J Waldron, J.C. Rutherford, D. Ford, N.J. Robinson, Metalloproteins and metal sensing; *Nature,* vol 460 (2009) 823–830.

[22] A.W. Foster, D. Osman, N.J. Robinson, Metal preferences and metallation. J. Biol. Chem. 289 (2014)28095–28103.

[23] A.W. Foster, C.J. Patterson, R. Pernil, C.R. Hess, N.J. Robinson, Cytosolic Ni(II) sensor in cyanobacterium: nickel detection follows nickel affinity across four families of metal sensors, J. Biol. Chem. 287 (2012) 12142–12151.

[24] H. Reyes-Caballero, G.C. Campanello, D.P. Giedroc, Metalloregulatory proteins: metal selectivity and allosteric switching. Biophys. Chem. 156 (2011) 103–114.

[25] L. Rink, H. Haase, Zinc homeostasis and immunity, Trends Immunol 28 (2007) 1-4.

Annals of Agrarian Science

Journal homepage: http://journals.org.ge/index.php

Application of potassium-rich processed dactte tuff as a fertilizer of slow and long-lasting effect

S.K. Yeritsyan, M.V. Gevorgyan

National Agrarian University of Armenia, 74, Teryan Str., Yerevan, 0009, Republic of Armenia

Received: 22 December 2018; accepted: 12 February 2019

A B S T R A C T

Together with the Institute of General and Inorganic Chemistry of NAS RA, the researchers of National Agrarian University of Armenia have developed the method of deriving a complex fertilizer of slow and long lasting effect from potassium-rich alumino-silicates (processed dacite tuff, PDT) containing potassium, calcium, magnesium, phosphorus and silicium, from which the nutrients pass into the soil solution gradually. Upon the field and vegetation experiments it has been stated that in case of using PDT with the amount equivalent to potassium, it provides higher yield in 10,0-15,3 % than it is in case of using potassium chloride.

It has been proved that PDT prevents the leaching of ammonium and nitrate ions from the soil, which is very important for the reduction of the nitrogen loss from the nitrogenous fertilizers and for the environmental protection; it also promotes the increase of phosphorus and potassium in the yield and enhances the crops drought-resistance.

Keywords: Dacite tuff, Efficiency, Nitrogen loss, Active phosphorus, Potassium, Yield capacity.

*Corresponding author: S. Yertisyan; E-mail address: s_eritsyan@yahoo.com

Introduction

Among the mineral fertilizers used in the agricultural production the potassium fertilizers also make a certain amount. Potassium chloride is mainly used which is derived from Sylvinite. But the mentioned mineral variety is not found in many countries, also in the republic of Armenia.

Potassium chloride also contains 47 % chlorine, which has an adverse effect on the soil properties and also on the yield quality of some crops (potato, tobacco, grape vine, etc.)[1,2].

Alumino-silicates rich in potassium [3-6], as well as nano-modified natural zeolites [7] are of industrial importance for the enlargement of the varieties of potash fertilizers and the base of production raw material [1,4,5,8-10].

The researchers of the institute of general and inorganic chemistry at NAS, RA and those of ANAU have disclosed that it is possible to obtain potassium fertilizer out of the alumino-silicates which are rich in potassium, such as, for example, the dacite tuff, moreover, they have revealed that it is possible to realize this process through ecologically safe methods. The derived fertilizer is allowed to be used in organic agriculture as well. The fertilizer contains plants available potassium, as well as calcium, magnesium, phosphorus, silicium, which penetrate into the soil solution gradually and that is why they are considered to be fertilizers of slow and long-lasting effect [8]. It is also endowed with indirect positive influences, for example, it can absorb up to 500 %water and due to this property it temporarily absorbs the humidity from the environment, which the plants use gradually. It is obvious that it is particularly prioritized for the agriculture in dry conditions [9].The fertilizer is also able to absorb NH_4^+ and NO_3^- ions (up to 45-50 mg/eq), due to which the loss of nitrogen and other nutrients introduced into the soil is prevented [10]. Being endowed with the ability of absorbing the heavy metals in non-exchangeable way, the mentioned

fertilizer can be used for the re-cultivation of the soils contaminated with heavy metals [11].The fertilizer promotes the strengthening of the plants root system resulting in the better/more efficient use of soil humidity and nutrients by the plants, it also contributes to the increase of plants available phosphorus and potassium, which takes place at the expense of the solubility increase of hardly soluble compounds and the opportunity to reduce the application dosages[12]of phosphorous and potassium fertilizers or to improve the plants nutrition with phosphorus, particularly in the soils poorly provided with phosphorus [13-15], appears.

The impact of the fertilizer maintains in the soil for several years, thus it is possible to apply it in the same place once in 3-5 years [16].

Objectives and methods

The objective of the research is to find out the agro-chemical characteristics of the fertilizer (dacite tuff) of slow and long-lasing influence containing potassium, calcium, magnesium, Silicium and phosphorus extracted from the potassium-rich alumino-silicates and its efficiency on the example of spring barley experiments comparing it with potassium chloride.

The field experiments have been conducted in dry steppe and steppe zones (non-irrigated) of RA in three repetitions, the size of an experimental bed is 50 m^2, they were implemented by the following scheme:

1. Without fertilization (control)
2. $N_{90}P_{90}$ (background)
3. background+K_{90}(KCl)
4. background +K_{90}(PDT)

NH_4NO_3, Ca $(H_2PO_4)_2 \cdot H_2O$, KCl and the processed dacite tuff have been used.

The vegetation experiments have been conducted in the ANAU greenhouse in four repetitions by the following scheme /the holding capacity of a vessel was 6,5 kg air-dry soil/:

1. Without fertilization (control)
2. N_2P_2 (background)
3. background+K_2(KCl)
4. background+K_1(PDT)
5. background+K_2(PDT)

In the experiments N_2 is equal to 0,2 g N per 1 kg soil, P_2 –is equal to 0,2 g P_2O_5, K_1-is 0.1 g K_2O,K_2-is 0,2 g K_2Oper 1 kg soil. Ammonium saltpeter, double superphosphate, processed dacite tuff (PDT) and potassium chloride have been used. The processed dacite tuff has the following composition: K_2O-9,9 %, CaO-13,0 %, MgO-7,5 %, P_2O_5-0,18 %, Al_2O_3-7,5 %, SiO_2-47,1%, H_2O-9,4%.

Results and analyses

The field experiments were conducted in Arzakan community of Kotayk region in the forest brown and carbonated soils with almost neutral reaction and low humus content, which is weakly provided with nitrogen and phosphorus and well provided with potassium (table 1).The field experiments in Hatsashen community of Aragatsotn region were carried out in the brown carbonated soils which are poor in humus and poorly provided with nitrogen and averagely provided with phosphorus and potassium and in Artik province the experiments were implemented in the carbonated black soils, where the humus content makes 4,45 %, pH-7,1 and these soils are weakly provided with plants available nitrogen, phosphorus and potassium (Table 1).

In the field experiments the impact of the application of KCl and PDT on $N_{90}P_{90}$background is remarkable on the growth, yield capacity and chemical composition of the grain of the spring barley in all three sites; anyhow the influence rate depends on the variant of the fertilization.

Table 1. *Agro-chemical indicators of the experimental plots(plowing layer)*

Sampling site	Humus, %	pH	EC	$CaCO_3$ %	Physical clay, %	Available nutrients, mgin100 g soil		
						N	P_2O_5	K_20
Kotayk region Arzakan community	3,11	7,1	0,12	3,5	52,1	3,5	1,5	40,7
Aragatsotn regionHatsashen community	2,85	7,3	0,20	8,6	54,8	2,6	3,1	33,1
Shirak region Artik province	4,45	7,1	0,29	1,4	63,6	4,1	1,6	17,5

Table 2. *The impact of PDT and KCl on NPK content in the spring barley grain, % (2017)*

Variants	Arzakan community			Hatsashen community			Artik community		
	N	P_2O_5	K_2O	N	P_2O_5	K_2O	N	P_2O_5	K_2O
1.	1,42	0,56	0,44	1,53	0,47	0,43	1,38	0,39	0,41
2.	1,73	0,72	0,40	1,79	0,58	0,41	1,80	0,59	0,37
3.	1,75	0,70	0,55	1,76	0,53	0,54	1,85	0,74	0,48
4.	1,81	0,87	0,67	1,79	0,87	0,70	1,87	0,90	0,67

Variants 1. without fertilization (control), 2. N90P90(background), 3. background +K90(KCl), 4. background+K90(PDT)

So, we can see that the plants growth, weight of the grains in an ear and the yield capacity is lower in control variant. Only in case of nitrogen and phosphorus application the yield has increased by 5,7-10,9 c/ha as compared to that of control variant, which is rather high in Artik province making10,9 c/ha (table 2), which is related to the relatively high precipitation rate and low soil fertility in the steppe zones, in conditions of which the fertilizers demonstrated rather high efficiency.

In case of using potassium chloride or PDT on the nitrogen-phosphorus background the highest grain yield/24,9-41,3 c/ha/ was obtained in the variant of $N_{90}P_{90}K_{90}$ (PDT), moreover this regularity stays stable independent of the soil provision with potassium. Thus, in the experimental variant of $N_{90}P_{90}K_{90}$ (PDT) the yield surplus against the variant of$N_{90}P_{90}$ (background) has made 4,5-7,8c/ha, and against the variant of background + K_{90} (KCl) it is3,3-4,1c/ha. We think that this regularity is related to the positive side effects of PDT: it promotes the strengthening of the plants root system, reduction of the water amount spent for getting a yield unit, more efficient accumulation of the moisture resulted from the precipitations, as well as it promotes the increase of the available phosphorus and potassium quantities in the soil [17].

The use of the fertilizer has also promoted the increase of the amounts of the main nutrients (NPK), which is more noticeable in case of using PDT (table 3).We think that it is connected with the improvement of plants nutrition particularly with phosphorus and potassium.

Table 3. *The impact of PDT and KCl on the growth and yield capacity of spring barley (average data for 2016-2017)*

Variants	Arzakan community			Hatsashen community			Artik community		
	Plants height, cm	Weight of grains in an ear, g.	Grain yield, c/ha	Plants height, cm	Weight of grains in an ear, g.	Grain yield, c/ha	Plants height, cm	Weight of grains in an ear, g.	Grain yield, c/ha
1.	43	0,65	15,2	37	0,51	14,5	49	0,81	22,6
2.	48	0,81	23,1	44	0,66	20,2	56	1,10	33,5
3.	49	0,83	24,0	43	0,70	21,6	58	1,18	37,2
4.	51	0,92	27,6	45	0,78	24,9	61	1,27	41,3

Variants: 1. Without fertilization (control), 2. N90P90(background), 3. background +K90(KCl), 4. background+K90(PDT)

The comparative efficiency of the processed dacite tuff (PDT) and potassium chloride has been studied also in the vegetation experiments. The soil (brown) was selected from Hatsashen community of Talin region. The mechanical composition of the soil was clay and sandy heavy, pH-was 7,3, carbonates made 8,6 %, the plants available nitrogen made 2,6 mg N, phosphorus content was 3,1 mg P_2O_5, potassium was 33,1 mg K_2O, in 100 g soil. According to these data the soil is poor in nitrogen and is averagely provided with phosphorus and potassium. The goal of the vegetation experiments has been to investigate the comparative impact of the processed dacite tuff (PDT) and potassium chloride on the mitigation of the loss of nitrogen forms (NH_4^+ and NO_3^-) from the soil and from the nitrogenous fertilizers inserted into the soil, as well as the comparative impact on the growth and yield capacity of spring barley (Table 4,5). It should be mentioned that in the production due to the reduction of nitrogen loss from nitrogenous fertilizers their application dates get restricted or nitrogenous fertilizers of long-lasting effect are used [18].In order to study the issue the vegetation vessels were periodically provided with excessive water amounts, so as the outflow in the filtrate occurred and where the content of NH_4^+ and NO_3^- (table 4) was determined. The results show, that up on the application of PDT, the loss of NH_4^+ and NO_3^- ions from the soil is considerably mitigated. So, in the non-fertilized variant (control) the loss of nitrogen is minimal and this is related to the low content of NH_4^+ և NO_3^- ions in the soil. While in N_2P_2 variant, where NH_4NO_3 was used as a nitrogenous fertilizer the nitrogen loss was rather high. Almost similar loss rate was observed when potassium chloride on the background of N_2P_2 was used [variant $N_2P_2K_2$ (KCl)]. While in case of the use of PDT on the background of N_2P_2 the nitrogen loss considerably decreased in all calculating periods (Table 4).As a result the plants growth and yield capacity have also changed (Table 5).According to the data of that table in the variant of $N_2P_2K_2$ (PDT) the grain yield has made 16,5 g, which is higher than the control one by 7,6 g (85,4 %), against the N_2P_2 variant it is higher by 3,0 g (22,2 %), and comparing to $N_2P_2K_2$ (KCl) variant by 1,9 g (13,0 %).Thus the highest yield was resulted in the variant where PDT was used on the background of N_2P_2.

Table 4. *The impact of the processed dacite tuff (PDT) and KCl on the leaching mitigation of NH_4^+ (numerator) and NO_3^- (denominator) from the soil, mg/l (vegetation experiment, the crop is spring barley)*

Variant	Periods of Analyses				
	3-leaves-growth stage	5-6-leaves growth stage	Ear-formation stage of the growth	Milk maturation stage	The total during vegetation
1.	0,11 0,17	0,07 0,04	0,02 0,01	n/a n/a	0,20 0,22
2.	2,45 5,76	1,02 2,84	0,13 0,31	0,07 n/a	3,67 8,91
3.	2,40 5,79	1,16 2,67	0,10 0,28	0,08 n/a	3,74 8,74
4.	0,35 2,13	0,13 0,76	0,02 0,18	n/a n/a	0,50 3,07
5.	0,21 0,76	0,07 0,58	0,02 0,10	n/a n/a	0,30 1,44

Variants: 1.Without fertilization (control), 2. N_2P_2(background), 3background +K_2 (KCl), 4.background+K_1(PDT), 5. background+K_2(PDT)

Table 5. *The impact of the processed dacite tuff (PDT) and KCl on the plants growth and grain yield of spring barley (vegetation experiments, 2017)*

Variants	Plants height cm	The number of grains in an ear, n	The weight of grains in an ear, g	yield, g./ vessel	The weight of thousand grains, g.
1.	39	15,0	0,60	8,9	39,6
2.	47	21,4	0,90	13,5	42,0
3.	47	23,1	0,97	14,6	42,1
4.	48	22,9	0,97	14,5	42,3
5.	48	25,9	1,10	16,5	42,4

Variants: 1. Without fertilization (control), 2. N2P2(background), 3. background +K2 (KCl), 4. background+K1(PDT), 5. background+K2(PDT)

Conclusion

1. The fertilizer of slow and long-lasting effect (PDT) is recommended for the agricultural production, which is resulted through the physical-chemical treatment of potassium-rich alumino-silicates, by means of which the potassium, calcium, magnesium and phosphorus of the mineral turn into the plants available forms and penetrate into the soil solution gradually.
2. In dry steppe and steppe (non-irrigated) conditions of RA PDT provides grain yield surplus of spring barley equal to 3,3-(11,0-15,3%) c/ha as compared to that of potassium chloride in case when PDT is used on the nitrogen-phosphorus background.
3. Having a high absorption capacity (45-50 mg/eq)the fertilizer (PDT) considerably prevents nitrogen leaching from the nitrogenous fertilizers introduced into the soil, which, in vegetation experiments, has made 7,34-7,48 for NH_4^+ and for NO_3^- it has made 2,84-6,03against the variants of $N_2P_2$and $N_2P_2K_2$ (KCl).
4. In vegetation experiments when using PDT on the background of N_2P_2 the surplus of the grain yield ofspring barley makes 3.0 g. (22,2 %) against the N_2P_2variant and 1,9 g (13,0 %) against the $N_2P_2K_2$ (KCl) variant.

References

[1] A. Yagodin, Agro-chemistry. Manual for the students of higher education institution. Publishing house VO "Agro industry publishing house", Moscow, 1989 (in Russian).

[2] N.E. Vlasenko, Potato Fertilizer. M. “Agro industry publishing house”, 1987 (in Russian

[3] Ya.M. Ammosova, Silica in the agronomy system. Agrochemistry, 10 (1990) 103-108 (in Russian).

[4] Belyaev G. N., Khorenyan E. G., Bartikyan P. M. Efficiency of potassium fertilizers extracted from rhyolite-dacite tuffs of Armenia on sod-podzolic soils, Pochvovedenie, 8 (1994) 97-103 (in Russian).

[5] Loboda B. P, Application of Natural Fertilizers on the Basis of Free Silica of Khotynenskoye Zeolite Deposit in Agriculture, Moscow, 2009 (in Russian).

[6] A. N. Nurlybaev, Alkaline Rocks of Kazakhstan and Their Minerals, AN Kaz. SSR, Institute of Geological Sciences. 1973 (in Russian).

[7] G. Tsintskaladzea, L. Eprikashvilia, T. Urushadzeb, T. Kordzakhiaa, T. Sharashenidzea, M. Zautashvilia, M. Burjanadzea, Nanomodified natural zeolite as a fertilizer of prolonged activity, J. Annals of Agrarian Science, Vol.14, No.3 (2016) 163-168.

[8] Grigoryan G. O., Grigoryan K. G, Muradyan A. B, Kostanyan A. K, Bartikyan P. M. Methods

of obtaining hardly soluble fertilizers. Patent № 402 (RA) upon the request №000371 of Arm. ind. property, №2, 2006 (in Armenian).

[9] H.G. Ghazaryan, A.L. Mkrtchyan, G.G. Petrosyan, Climate changes and soil degradation process in Armenia, J. Annals of Agrarian Science, Vol.13 No.2 (2015) 34-38 (in Russian).

[10] S.K. Yeritsyan, R.R. Manukyan, L.S. Yeritsyan, A. Nelian, "Agro-Chemical Characteristics of Potassium-Rich Processed Dacite Tuff and Its Application as Potash Fertilizer" G.S. Davtyan Institute of Hydroponics problems NAS RA. Yerevan 2017 Proceedings of the 6-™ International Conference on "Modern Problems of Plants Soilless (Hydroponics) and Tissue in Vitro Cultures", Dedicated to the 70th Anniversary of the Institute, 2017, 38-45 (in Armenian).

[11] M.A. Galstyan, A.V. Shirinyan, S.S. Harutyunyan, S.J. Tamoyan, K.Sh. Sargsyan, Assessment and remediation of soils previously buried under mine tailings and contaminated with heavy metals, J. Annals of Agrarian Science, Vol.13 No.1 (2015) 46-53 (in Russian).

[12] K.F. Gladkova, The role of silicon in the plants phosphorous nutrition. Agro-chemistry, 3 (1982) 133-140 (in Russian).

[13] R.E.Yeleshev, A.L. Ivanov, S.K. Sadvakasov, Study of the influence of joint application of phosphorus silicon-containing fertilizers on the phosphate regime of the main soil types in Kazakhstan, Agro-chemistry, 1 (1990) 78-85 (in Russian).

[14] T.F. Urushadze, A.T. Tkhelidze, T.T. Urushadze, Agrochemical characterization of the main soil types of Georgia, J. Annals of Agrarian Science, Vol.12 No.4 (2014) 14-31

[15] T.F. Urushadze, T.O. Kvrivishvili, R.G. Kakhadze, Field school in soil science: Results and prospects, J. Annals of Agrarian Science, Vol.13 No.3 (2015) 51-54.

[16] S.K. Yeritsyan, N.V. Farsiyan, Influence of the consequences of fertilizers and ameliorants on winter wheat in conditions of the Askeran region of NKR / Bulletin of the Samara State Agricultural Academy, (2016) 28-32 (in Russian).

[17] A.V. Baranov, The influence of silicon on the growth, development and productivity of spring wheat under various conditions of mineral nutrition and water supply. Author's abstract. diss. Cand. Biol. Sciences. M., 2006 (in Russian).

[18] E. Gugava, A. Korokhashvili, Technologies for obtaining nitrogen fertilizers prolonged effect in wheat, J. Annals of Agrarian Science, Vol.16 No.1 (2018) 22-26.

Annals of Agrarian Science

Journal homepage: http://journals.org.ge/index.php

Analysis of the impact of the main factors affecting the pattern of tire depreciation

P.A. Tonapetyan, A.G. Avagyan

National Agrarian University of Armenia, 74, Teryan str., Yerevan, 0009, Republic of Armenia

Received: 15 August 2018; accepted: 04 October. 2018

A B S T R A C T

This study investigates the optimal internal tire pressure affecting the maximum tire usageof a particular minibus operating on a particular route in Armenia.Regression equations were developed that show the dependence of the tire usage on the internal tire pressure and wear.The results of operational and stand tests reveal the nature of the impact of the tread sipe density on tire usage. The analysis of the study shows that among the most influential factors affecting automobile tire usage are the density of tire tread sipes and the internal tire-pressure.

Keywords: Tires, Mileage, Weight, Internal tire pressure, Depreciation pattern, Tread height.

*Corresponding author: Pargev Tonapetyan; E-mail address: tonapetyan.pargev@mail.ru

Introduction

It is important to understand that the tires used in Armenia are imported from Russian manufacturers in Russia and the recommended maintenance values for optimal usage may be different for road, climate, and usage conditions in Armenia. Our study provides recommendations as to the optimal tire pressure and usage conditions required for maximum usage of tires in Armenia for important long arterial routes between major cities. This study shows most influential factors affecting automobile tire usagewere the density of tire tread sipes and the internal tirepressure [1-9].

Experiments were carried out for 215/75R16C radial model tires include tire tread pattern wear, both with the application of relevant stands and in real operating conditions.

Objectives and Methods

During stand testing, tire weight and tread height were measured for different mileage values; while during actual operation, the weight of the front and rear tires were measured for the same mileage values.The stand tests were carried out using “CTWIST” stands.The results of the stand tests are summarised (Tables 1 and 2).

Table 1. *The tread height of 215/75R16C Radial model tires depending on the mileage for different air pressure values*

Number of tests	Mileage, L	Tread height, h,mm		
		P=2.8	P=3.0	P=3.2
1	12000	8.984	8.671	8.898
2		8.880	8.800	8.740
3		8.778	8.930	8.584
average		8.881	8.800	8.741
1	36000	5.997	5.003	4.998
2		5.212	5.477	4.864
3		5.600	5.200	4.930
average		5.603	5.227	4.931
1	60000	2.263	1.739	1.693
2		2.090	1.870	1.810
3		1.920	1.999	1.925
average		2.091	1.869	1.809

Table 2. *The weight of 215/75R16C Radial model tires depending on the mileage for different air pressure values*

Number of tests	Mileage, L	Weight, m,kg		
		P=2.8	P=3.0	P=3.2
1	12000	23.420	23.352	23.062
2		23.324	23.241	23.159
3		23.230	23.130	23.258
average		23.325	23.241	23.160
1	36000	21.842	21.368	21.430
2		21.550	21.611	21.210
3		21.700	21.486	21.322
average		21.697	21.488	21.321
1	60000	20.401	20.121	20.168
2		20.280	20.170	20.088
3		20.155	20.220	20.006
average		20.279	20.170	20.087

The tests were carried out using the experimental planning method. Bк-type composite plans were used to process experimental data.

In statistical approach, the mathematical model of an object or a process is presented in the form of a two-dimensional second-order polynomial equation which has the following appearance [3,4,10-15].

$$Y = b_0 + \sum_{i=1}^{k} b_i x_i + \sum_{i,j=1}^{k} b_{ij}\ x_i x_j + \sum_{i=1}^{k} b_{ii} x_i^2, \quad (1)$$

where` b_0 is the free term, b_i is the linear impact coefficient, is b_{ij} double (pair) interaction coefficient, b_{ij} is the coefficient of the square term, k is the number of factors.

The vehicle mileage (L) and air pressure in tires (P) were chosen as free factors (x).Tire tread height(h)and weight (m) were chosen as optimizing factors (Y).

Factor levels and transformationintervals are given in Table 3.

Experiment planning matrix was developed to determine actual tread height and weight of215/75R16C Radial model tiredepending on vehicle mileage (L) and air pressure in tires (P) (Tables 4 and 5).

Table 3. *Factor levels and transformationintervals*

Factor level and transformationinterval	Factors studied	
	Pressure, P	Mileage, L
Code naming	X_1	X_2
Zero level, $x_i = 0$	3	36000
Transformation interval, Δx_i	0.2	24000
Lower level, $x_{\min} = -1$	2.8	12000
Upper level, $x_{\max} = +1$	3.2	60000

Table 4. *Experiment planning matrix determining actual tread height of 215/75R16C Radial model tires depending on vehicle mileage (L) and air pressure in tires*

N°	True value of factors		Coded value of factors		Tread height, h, mm
	P	L, km	X_1	X_2	$\bar{h}_i$
1	2	3	4	5	6
1	3.2	60000	1	1	1.809
2	2.8	60000	-1	1	2.091
3	3.2	12000	1	-1	8.741
4	2.8	12000	-1	-1	8.881
5	3.2	36000	1	0	4.931
6	2.8	36000	-1	0	5.603
7	3	60000	0	1	1.869
8	3	12000	0	-1	8.800
9	3	36000	0	0	5.227

Table 5. *Experiment planning matrix determining actual weight of 215/75R16C Radial model tires depending on vehicle mileage (L) and air pressure in tires*

N°	True value of factors		Coded value of factors		Weight, kg
	P	L	X_1	X_2	$\overline{m}$
1	2	3	4	5	6
1	3.2	60000	1	1	20.087
2	2.8	60000	-1	1	20.279
3	3.2	12000	1	-1	23.160
4	2.8	12000	-1	-1	23.325
5	3.2	36000	1	0	21.321
6	2.8	36000	-1	0	21.697
7	3	60000	0	1	20.170
8	3	12000	0	-1	23.241
9	3	36000	0	0	21.488

Results and analysis

As a result of mathematical processing of experimental data results, regression equation coefficients were determined and the following equations were developed:

- for determining tread height of 215/75R16C Radial model tire

$$m(X) = 21.641 - 0.122X_1 - 1.532X_2 + 0.208X_2^2 \quad (2)$$

- for determining weight of 215/75R16C Radial model tire

$$h(X) = 5.328 - 0.182X_1 - 3.442X_2 + 0.112X_2^2 \quad (3)$$

The adequacy of regression equation was verified by Fischer criteria[3,4,10-15].

Usingthe equations (2) and (3), a group of graphs showing the change of tread height and weight of 215/75R16C Radial model tires weremade depending on vehicle mileage and air pressure in tires (Figure1 and 2).

Under real operating conditions the vehicle tire interacts with the road pavement, and is subjected to surface irregularities including cutting and sharp objects found on the road.As a result of this interaction, as well as tire gyration, braking and acceleration; the tire tread sipes are worn unevenly. Therefore, the measurement error of the sipe height may exceed the permissible limit during road tests. By taking the circumstance into account, instead of using the tread height, it is advisable to weigh the tire and determine the weight loss caused by tire wear. Internal tire air pressure was measured on a daily basis maintain the stability of the internal air pressure. Tire pressures were measured and it was measured on a daily basis after the minibus was retired at the end of the day and was brought to the recommended pressure less 4%.In addition, the impact of the temperature increase on the internal pressure due to tire operation was not considered during the tests.

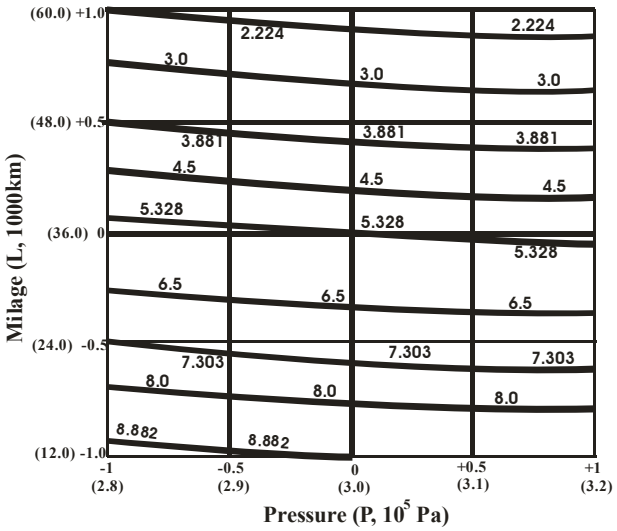

Fig. 1. *A group of graphs showing the change of tread height of 215/75R16C Radial model tiredepending on vehicle mileage (X_1)and air pressure in tires (X_2)*

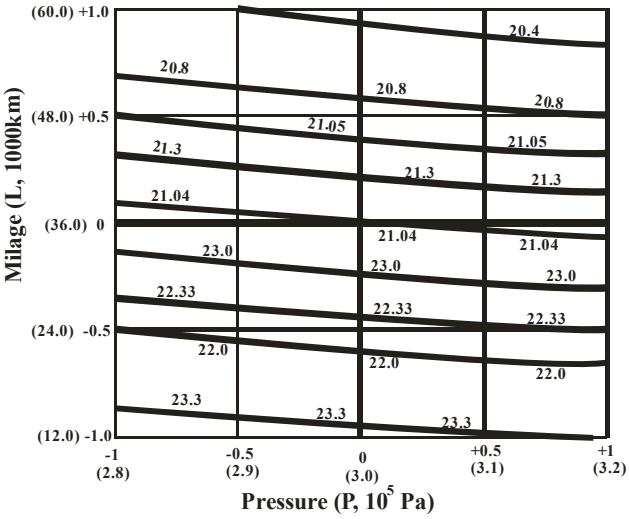

Fig. 2. *A group of graphs showing the weight change of 215/75R16C Radial model tiredepending on vehicle mileage(X_1)and air pressure in tires(X_2)*

The following regression equations (4 and 5) were developed as a result of the mathematical processing of the results obtained from measurements taken during mini bus operation:

- For measuring weight of rear tire

$$m(x) = 21.446 - 0.114X_1 - 1.418X_2 + 0.589X_2^2 \quad (4)$$

- For measuring weight of front tire

$$m(x) = 21.286 - 0.168X_1 - 1.579X_2 + 0.529X_2^2 \quad (5)$$

Usingequations (4) and (5), a group of graphs showing the weight change of front and rear tireswas made depending on vehicle mileage and air pressure in tires (Fig. 3 and 4).

Conclusion

Operational testing of minibus tires shows that the vehicleswill have maximum mileage under optimal pressure conditions.For example, when the tire inner pressure is within recommended limits, the weight of rear tire is 21.872 kg in case of 36000 km, while in case of 48000 km, the weight is 21.496 kg (the height of the tread is within limits of 5.2 mm, hence the tire tread wear is 2.8 mm), so tire tread wear tends to be minimal under optimal pressure conditions.The comparison of stand and operational testing results shows that the difference in tire weight loss is 3 to 7%, while the average tire tread wear in comparison is within 5%.

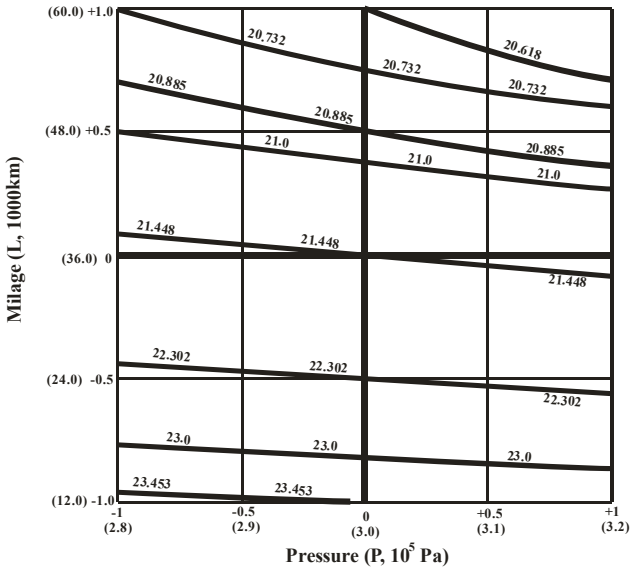

Fig. 3. *A group of graphs showing the weight change of rear tiredepending on vehicle mileage (X_1)and air pressure in tires (X_2)*

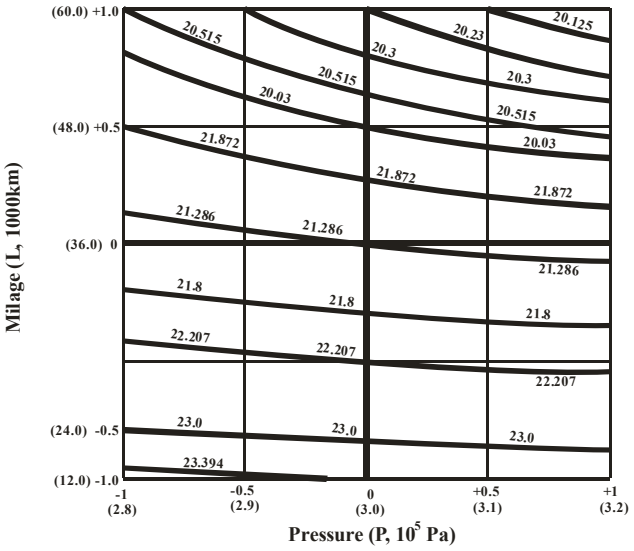

Fig. 4. *A group of graphs showing the weight change of front tiredepending on vehicle mileage (X_1)and air pressure in tires(X_2)*

The analysis of regression equations, developed by this study in both stand accelerated and real operating conditions visualised with the graphs indicates that the tire tread wear is more intense in the middle of the tire compared to the rims, and more pronounced when measuring between 24000 to 36000km of travel. The maintenance internal pressure of the tire (optimal value) maximizes the tire usage.

References

[1] Avagyan A.G., Factors affacting automobile tire resource and the evaluation of their Impact, NUACA,Collection of Scientific Works, Vol. III (46), Yerevan, 2012, pp. 69-74 (in Armenian).

[2] Avagyan A.G., Development of The method of evaluation of minibus tire resource based on the results of accelerated yests, Dissertation, Yerevan, 2016 (in Armenian).

[3] Grigoryan Sh.M., Tarverdyan A.P., Khachatryan A.Ts.,Petrosyan D.P.,Elements of Mathematical Statistics and Theory of Experimental Planning, Asoghik, Yerevan, 2001 (in Armenian).

[4] Spirin N. A., Lavrov V. V., Planning Methods and Processing of Engineering Experiment Results. Yekaterinburg, 2004 (in Russian).

[5] Shokouhfar, Shahram Moustafa, Development of a rolling truck tyre model using an automatic model regeneration algorithm. International J. of Vehicle Systems Modelling and Testing, (2016) 52-62.

[6] Hamad Sarhan Aldhufairi, Oluremi Ayotunde Olatunbosun Developments in type design for lower rolling resistance: a state of the art review. Proceedings of the Institution of Mechanical Engineers, Part D: J. of Automobile Engineering (2017) 96-104.

[7] Y.Nakajima, Application of computational mechanics to tire design -yesterday, today, and tomorrow. Tire Science and Technology: December, vol. 39, no 4 2011, pp. 223-244.

[8] Jinn-Tong Chiu and Chau-Rung Shui Analysis of the Wet Grip Characteristics of Tire Tread Patterns. Tire Science and Technology: January-Marchvol. 46, no 1, 2018, pp.2-15.

[9] Dmytro A. Mansura, Nicholas H. Thom, and Hartmut J. Beckedahl A.Novel Multiscale Numerical Model for Prediction of Texture-Related Impacts on Fuel Consumption. Tire Science and Technology: January-March, vol. 45, no. 1, 2017, pp. 55-70.

[10] Barabashyuk V.I., Kredentser B.P., Miroshnichenko V.I., Planning an Experiment in Engineering, Kiev, 1984 (in Russian).

[11] 11.Ermakov S.M., Zhiglyavsky A.A., Mathematical Theory of Optimal Experiment. Nauka, Moscow, 1987 (in Russian)

[12] Zazhigaev L.S., Kishyan A.A., Romanikov Yu.I., Methods of Planning and Processing the Results of a Physical Experiment, Atomizda, Moscow, 1978 (in Russian).

[13] Montgomery D.K. Experiment Planning and Data Analysis, Shipbuilding, Lion, 1980.

[14] Statistical Methods of Empirical Data Processing. Recommendations, Publishing House of Standards, Moscow, 1976 (In Russian).

[15] Kovel A.A., Pokidko S.V., Mathematical planning of an experiment when developing electronic devices, Izv. Universities Instrument making, 51, № 8 (2008) 13 -18. (in Russian).

Annals of Agrarian Science

Journal homepage: http://journals.org.ge/index.php

Structural and Magnetic Properties of Silver Oleic Acid Multifunctional Nanohybrids

S. Khutsishvili[a], P. Toidze[b], M. Donadze[b], M. Gabrichidze[b*], T. Agladze[b], N. Makhaldiani[b]

[a]A.E. Favorsky Irkutsk Institute of Chemistry of the Siberian Branch of the Russian Academy of Sciences, 1, Favorskogo Str., Irkutsk, 664033, Russia

[b]Technical University of Georgia, Department of Chemical and Biological Technologies 69, M. Kostava Str., Tbilisi, 0175, Georgia

Received: 15 May 2018; accepted: 19 September 2018

ABSTRACT

Sols of core-shell silver NPs are synthesized by electrochemical method. The method provides the ability to adjust the particle size by changing both the concentration of oleic acid and the residence time τ_0 in the organic phase. We synthesized silver nanoparticles with oleic acid concentration of 0.25% (Ag&0.25%OA) and 0.75% (Ag&0.75%OA). These silver nanoparticles have been studied using modern physical–chemical methods: Transmission Electron Microscopy (TEM); Fourier Transform Infrared Spectroscopy (FT-IR); Dynamic Light Scattering (DLS); Thermogravimetric and Differential Thermal Analysis (TGA and DTA); Electron Paramagnetic Resonance (EPR). DTA curves indicate the chemical nature of bond ligand in the secondary shell.This conclusion supported by quantum chemical simulation by using quantum-chemical software HyperChem-8 and semi-empirical calculation method ZINDO. In the EPR spectra of silver-containing sols Ag&0.25%OA and Ag&0.75%OA a complex wide asymmetric signal with several resonant lines is recorded, which is consistent with a wide size distribution of nanoparticles. It is important to note that a change in the oleic acid layers of the nanoparticles seems to affect the dimension of the nanocrystallites that are being formed. The presence of the FMR resonance line in Ag&0.75%OA may indicates the presence of Ag-cubic cells in nanoparticles with internal magnetic fields significantly larger than the Zeeman field, the available EPR in the X-band range.

Keywords: Core-shell, Nanoparticles, Oleic acid, Ligand, Charge, Activation energy.

*Corresponding author: Maia Gabrichidze: E-mail address: gabrichidze.maia@gmail.com

Introduction

Silver nanoparticles is one of the important and interesting nanomaterials, the use of which is promising in the environment (water and air purification, catalysis), in the field of biomedicine (diagnosis and treatment of cancer), food industry (packaging materials), in the manufacture of medical instruments (antibacterial coatings), in optical devices, cosmetics, in the pharmaceutical industry.

Due to their nano-size, metallic silver particles have unique physicochemical, biological properties that are associated with an increased ratio of surface area to volume. In this regard, it is necessary to determine the physicochemical properties of nanoparticles in order to establish the expected chemical, physical and catalytic activity.

Effective application of nanoparticles as building blocks in bottom-up design of multicomponent nano-composites requires monitoring of fundamental properties, such as size, charge, chemical reactivity and ability of nanoparticles to disperse in various media. Owing to high aspect ratio, metal nanoparticles tend to agglomeration, aggregation and corrosion processes finally leading to loss of valuable properties inherent to building of blocks. Chemisorption of organic ligand shell

provides steric stabilization of nanoparticle core preventing its degradation. The present study is focused on characterization of metal core-ligand shell interactions as well as on ligands molecules interaction in primary and secondary layers of the shell - phenomena largely determining bottom-up strategy for synthesis of multifunctional hybrid nanoparticles [1].

Experimental

Chemicals and instruments. The reagents used in this study are purchased from Sigma-Aldrich unless otherwise specified and used without purification. Chemical interactions of surfactant with NPs studied by FT-IR spectroscopy in a range of 400–4000 cm^{-1} with the resolution of 0.5 cm^{-1} (Thermo Nicolet, Avatar 370) use the KBr technique. Size, shape and chemical composition of isolated NPs are estimated from TEM (Tesla BS 500) and SEM (JSM-6510LV) images. The samples are prepared by placing small drops of a sol onto the carbon-coated copper grid. The size distribution of NPs in a sole is evaluated from laser beam dynamic light scattering data (Zetasizer-Nano, Malvern). Prior to sample placing into a cuvette, the as-prepared sols are diluted with hexane 1:8. The structural and thermal stability properties of nanoparticles are characterized by thermo-gravimetric analysis (TGA) and differential thermal analysis (DTA) technique (NETZSCH, STA-2500, Regulus). In both cases characterized by activation energies calculated from OA transformation during the thermal decomposition, using Ozawa -Flynn-Wall method derived from the integral iso-conversional method [2, 3].

EPR spectra were recorded on a FT X-band Brüker ELEXSYS E-580 spectrometer (X-wave range 9.7 GHz). Precision of the measurement of *g*-factor was ±0.00018. CW EPR-spectra were recorded of the 1 and 3 samples (0.025 g) at the following conditions: amplitude modulation 10.0 G, modulation frequency 100 kHz, averaged scans 35, field range 3000 G / centre field 3100 G, time constant 0.04 s, conversion time 0.12 s, microwave power 0.6325 mW. CW EPR-spectra were recorded of the 4 and 5 samples (0.025 g) at the following conditions: amplitude modulation 10.0 G, modulation frequency 100 kHz, averaged scans 1, field range 6800 G / centre field 3500 G, time constant 0.04 s, conversion time 0.12 s, microwave power 0.6325 mW.

The metals percentage of the studied nanocomposites was evaluated by atomic absorption analysis using a HITACHI TM 3000, detector SDD XFlash 430-H (Table 1).

Preparation of sols of AgNPs. Sols of silver NPs in a hexane are synthesized by electrochemical method in a reactor consisting of sacrificial silver anode (99.9% purity), and aluminum (99.9%) cathode, which upon rotation crosses immiscible layers of aqueous (0.05 M $AgNO_3$, doubled distilled water) and organic (hexane, 0. 25% and 0. 75% OA) solvents [1, 4]. The experimental set-up allows silver ions formed at the anode to discharge at the cathode surface poisoned by surfactant (OA), which adsorbs at sites favorable for silver adatoms and inhibits the growth of silver nanoclusters. The latter is weakly adsorbed at the surface and strongly bonded to amphiphile OA molecules which are easily washed out from cathode upon rotation forming stable sols of Ag–OA core–shell NPs in hexane. The method provides the ability to adjust the particle size by changing both the concentration of oleic acid and the residence time τ_0 during which the metal cluster formed at the border of the cathode-water electrolyte allows the amphiphile surfactants to adsorb from the organic phase. The results of measuring the size of silver nanoparticles using the DLS method are shown (Table 2).

Table 1. *The elemental analysis of the samples*

Sample	Mass content, %		
	C	O	Ag
Ag&0.25%OA	11.8	3.6	84.6
Ag&0.75%OA	12.8	3.9	83.3

Table.2. *Size of silver nanoparticles coverage by oleic acid*

Concentration OA(%)	Z-Average (d.nm)	PdI	τ_o (sec)
0.25	15.62	0.15	45
0.50	14.95	0.14	42
0.75	15.74	0.14	39
1.00	16.96	0.24	36

In the present study, electrosynthesis has been carried out at experimental conditions yielding assembles of spherical silver NPs Ag&0.25%OA by TEM (Fig. 1a). The histogram (Fig. 1b) of the size distribution shows the average diameter of the NPs is 14.4±4.2nm. ΔQ – number of particles in %. Size distribution of Ag&0.25%OA and Ag&0.75%OA determined from DLS method is Z_{ave}=15.62 nm, PdI= 0.15 and Z_{ave}=15.74 nm, PdI= 0.14 (Table 2).

FT-IR spectroscopy. The chemical bonding of OA molecules to silver nanoclusters in diluted OA solutions are characterized by appearance of two new bounds at 1639 and 1509 cm^{-1} (Fig. 2a) which are typical for the asymmetric and symmetric carboxylate stretch. These effects are interpreted as the evidence of OA bidentate bonding to silver via two symmetrically coordinate oxygen atoms of the carboxylate head [5]. The effect of increase in oleic acid concentration on FT-IR spectra characteristics (Fig.2b). According to these data the major effect is appearance of a new peak at 1708.6cm^{-1} that is characteristic for C=O bond stretch.

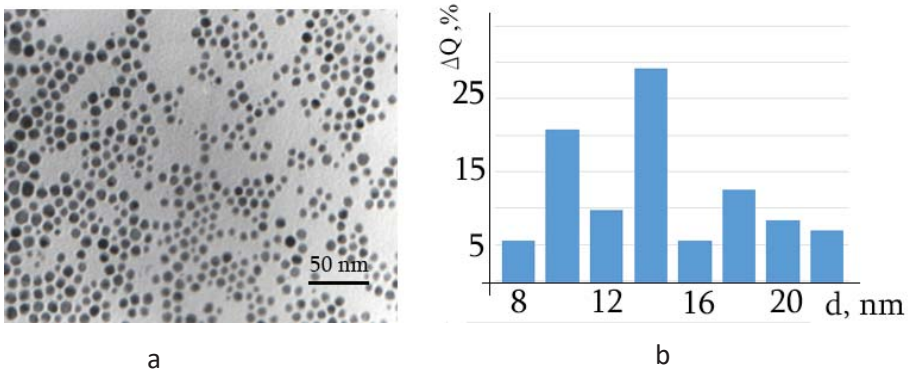

Fig. 1. *TEM image (a) and histogram of the size distribution (b) of silver NPs capped of 0.25%OA*

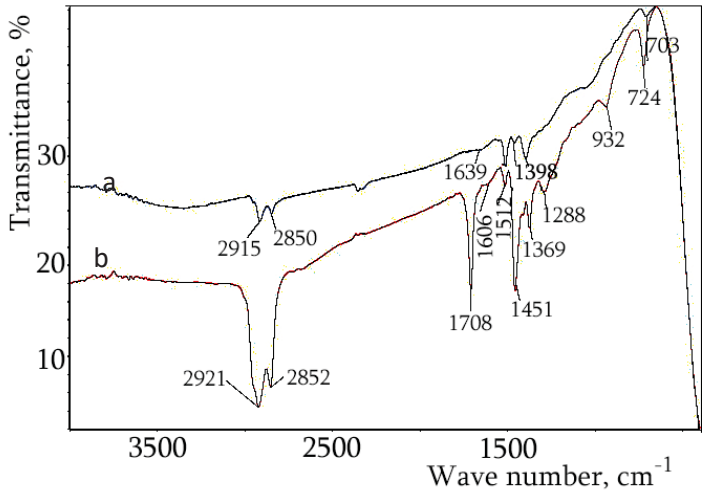

Fig. 2. *FT-IR spectra silver nanoparticles capped by monolayer (a) and bilayer (b)*

TGA and DTA measurements data. The application of dynamic TG methods holds great promise as a tool for unraveling the mechanisms of physical and chemical processes occurred during the decomposition of solids. In this investigation, Ozaw -Flynn-Wall- (OFW) methods have been used to analyze the non-isothermal desorption kinetics of silver nanoparticles capped with oleic acid ligand. TGA and DTA curves of Ag&0.25%OA and Ag&0.75%OA samples are measured at heating rate (β) 5 K/min (Fig. 3 a, b).

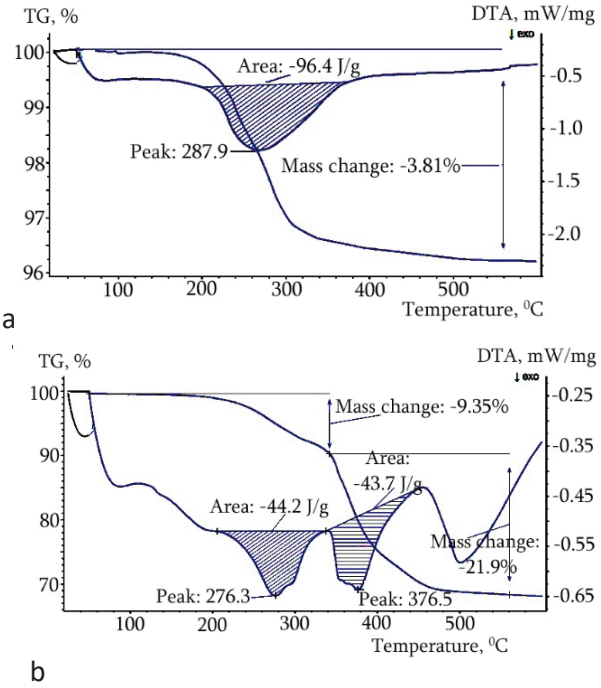

Fig. 3. *TGA and DTA curves of Ag&0.25% OA (a) and Ag&0.75% OA (b) samples*

TGA patterns in diluted OA solutions are characterized by one step mass loss (3.81%) curve. DTA curve measured under the same conditions displays exothermic peak at 287.9 °C. Corresponding enthalpy is 96.4 J/g. Contrary to these data, TGA curves measured in OA rich solutions display two step mass loss 9.35 % (50 – 340 °C) and 21.89 % (340-600 °C). Corresponding DTA curve displays two exothermic peaks at 276.3 and 376.5 °C. Calculated enthalpies are 44.22 J/g and 43.77 J/g. Thermodesorption E_a values have been calculated by Ozawa-Flynn-Wall (OFW) method derived from the integral iso-conversional method using Doyle's approximation (Equation 1) [6].

$$f(a) \approx 7.03 \cdot 10^{-3} \cdot \frac{AE_a}{\beta R} \exp(-1.052 E_a / RT) \quad (1)$$

According to this method:

$$\ln \beta = \ln \frac{AE_a}{Rg(x)} - 5.331 - 1.052 \cdot \frac{E_a}{RT} \quad (2)$$

where A is frequency factor and g (x) is function depends on the rate of conversion, β – heating rate, T – temperature, R = 8.31J/mol·K. Thermodesorption activation energies calculated by OFW method (Equation 1) as a function of the conversion degree (Fig. 4). Sharp increase in E_a observed at low mass losses in concentrated solution indicates the change of desorption mechanism in bilayer system.

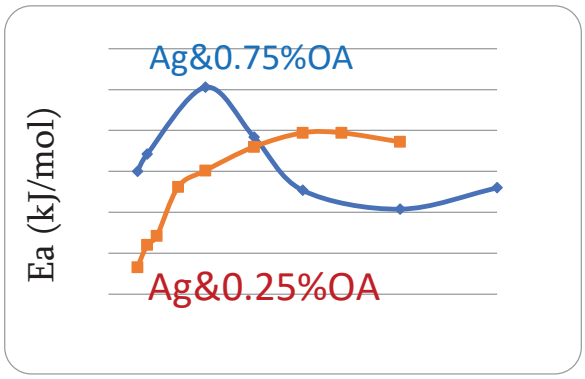

Fig. 4. *Thermodesorption activation energies calculated by OFW method as a function of the conversion degree.*

The calculation of the coating of nanoparticles with OA was calculated according to equation 3.

$$N = \frac{4\rho r^3 \pi \omega N_A}{3(100-\omega)M_{OA}} \quad (3)$$

where N is the number of oleic acid ligands per particle, ρ = 10.49g/cm^3 is the density of the silver, r= 7.2nm is the average radius of the Ag&0.25%OA (based on the TEM results, Fig.1), ω=3.81% is the weight loss (in %), N_A = 6.022 × 10^{23} mol^{-1}, is Avogadro's constant, and M_{OA} = 282.47 g/mol is the molecular weight of oleic acid.

The number of ligands was calculated for Ag&0.25%OA N=1385. Assuming that the surface of the NPs is covered with a close packed monolayer of the surfactant, the surface area S occupied by the oleic acid ligand A indicates the ratio of the total surface area of the particle to the number of oleic acid ligands A=0.46nm^2. Considering the fact that the area of one molecule of oleic acid S=0.21nm^2, percentage of silver nanoparticle surface coating

with oleic acid molecules is 45%.

Quantum-chemical simulation. Molecular models of free and adsorbed oleic acid at silver NPs are created by using quantum-chemical software HyperChem-8 and semi-empirical calculation method ZINDO1[7]. Electrostatic potentials significantly vary from chemisorbed OA molecules (Fig.5 a,b). Ligand interaction with Ag NPs results in increase of effective charge and electrostatic potential at silver surface indicating charge transfer from ligand carboxyl group to nanoparticle atoms.

Formation of a secondary layer in solutions rich in OA is accompanied by increase electrostatic potential at silver.

According to quantum, chemical calculations of chemisorbed OA silver ligand interaction resulted in redistribution of electron density at OA molecule. The electrostatic potential at carboxyl group of monolayer and bilayer OA are U_1=-1.173e/Å and U_2=-1.217e/Å correspondingly (Fig.5a,b).

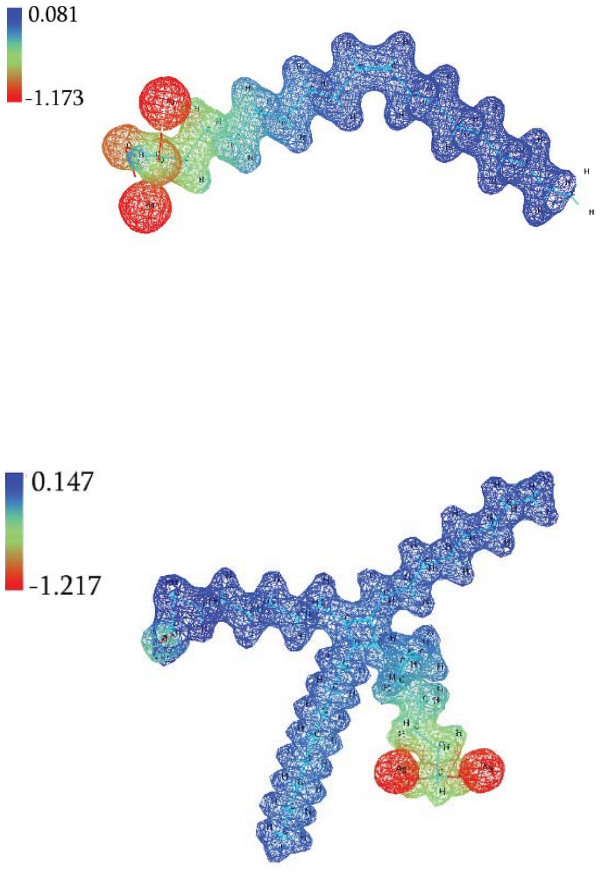

Fig. 5. *Electrostatic potentials maps for chemisorbed mono (a) and bilayer (b) OA molecules.*

Discussion

An increasing volume of studies aimed at examination of the mechanism of unsaturated fatty acid ligands interaction with metals and metal oxide cores have been conducted by means of TEM, DLS, FT-IR, TGA, DTA and EPR methods [8-16]. The bidentate covalent bonding of oxygen atoms of polar carboxylic groups with core NPs assumed to be the driving force formation of chemisorbed ligand monolayer. Appearance of a new FT-IR peak at 1708cm^{-1} characteristic for C=O bond stretch (Fig. 2b), as well as two step mass loss TGA curves and appearance two exothermic peaks at DTA curves (Fig.3b) shown in present study clearly demonstrate that at high OA concentration Ag NPs are capped by adsorbed ligand bilayers. Contrary to widely accepted concept on physical nature of ligands, bonding in the secondary shell [8, 9, 16] significant enthalpies calculated from DTA curves indicates the chemical nature of bonding. This conclusion supported by quantum chemical simulation leads to the model of formation C=C double bonds as a result of coupling of delocalized p-electrons of primary and secondary layers. Inversion of the secondary OA layer apparently originated from repulsion of polar carboxylic groups in a secondary shell owes to increase in negative charge at oxygen atoms. Finally, this leads to formation of branching ligand network. The other important conclusion on the mechanism of ligand chemisorption is followed from variation of thermodesorption activation energies with conversion degree (Fig.4). It is widely accepted that formation of ligand primary adsorbed layer follows Langmuir low, which assumes adsorption at homogenous substrate and predicts independence of adsorption energy from surface coverage. Our experimental data are in sharp disagreement with these assumptions. In contradiction to Langmuir adsorption model the data shown at Fig.4 testify a significant change in thermodesorption activation energy with variation in a number of adsorbed OA molecules in a primary shell. To interpret activation energy patterns we have to account for the fact that nanoparticles surface formed under highly nonequilibrium conditions due to artificial termination of crystal grow and freezing irregular structure by capping agent. These leads to more realistic model accounting for effect of surface inhomogeneity resulting in increase of adsorption energy with surface coverage. Complex variation of $E_{a.}$ with mass loss in presence of OA excess apparently

reflects contribution of several factors: increase in E_a as OA molecules desorbed from sites with higher adsorption energy and simultaneous variation in chemical bond strength in a secondary layer.

EPR. In the EPR spectra of silver-containing sols Ag&0.25%OA and AG&0.75%OA, a complex wide asymmetric signal with several resonant lines is recorded (Fig.6), which is consistent with a wide size distribution of nanoparticles [10-12]. In similar metal-containing nanosystems, like other disordered or partially ordered systems, have a spread in the symmetries of the nearest environment of individual paramagnetic centers, so in the EPR spectra we observe not one line, but the envelope of a set of lines with close, but different from each other parameters. The presence of nanoparticles of different diameters and different supramolecular organization of the system as a whole, including.

The inevitable absence of a regular periodic structure and the uneven distribution of nanoparticles in a stabilizing medium, affects the symmetry of the signal. The lines with a peak-to-peak width ΔH_{pp} of several hundred Gauss are caused by collective electronic spin phenomena for a metal-containing nanomaterial [13], which are explained as RKKY interactions, exchange interactions of magnetic ions with conduction electrons [14-17], significant line broadening can be attributed to Korringa interaction [16], ferromagnetism [13, 17] and other exchange interactions [18].

The EPR signal (1), the so-called superpara-magnetic, consists of several overlapping components with an average *g*-factor of 2.09-2.13 and a line width (ΔH) of about 500-800 G. This line is due to the conduction electrons of CESR nanoparticles [12, 13, 19, 20], while the spin-orbit interaction for bulk Ag is so significant that the resonant signal can be observed only at very low temperatures [21]. Such a broad signal can also be associated with some localized EPR active (paramagnetic) surface states. Note in the case Ag&0.25%OA sols with the one layer of oleic acid (Fig. 6a) in comparison with Ag&0.75%OA, the broad line becomes more intense with a changing environment due to decrease in the "shielding" of the nanoparticles between themselves. In addition, the nanoscale particles are closely located to each other, as a result of which dipole-dipole interactions between them intensify, which also could be leads to an additional line broadening.

In the EPR spectra of silver-containing sols, the anisotropic signal (2), which belongs to divalent silver. The appearance of such highly oxidized silver states on the surface of nanoparticles occurs through the disproportionation of Ag(I), which leads to the formation of Ag(II) ions and metal Ag^0 silver [22, 23]. EPR characteristics of the complexes accord with the available literature data for analogous two-valence silver [24, 25].

It is important to note that a change in the oleic acid layers of the nanoparticles seems to affect the dimension of the nanocrystallites that are being formed. Thus, in the sols, when passing from the mono- to the bilayer of oleic acid, both small particles and larger multidomain agglomerates are found. So, the narrow weak signal (3) in the region of the *g*-factor 2.005 also refers to the spin resonance of conduction electrons from zero-valent silver [24, 26-28]. This line is usually characteristic of small nanoparticles, usually around 2 nm [29-30]. The presence of the FMR resonance line (4) in Ag&0.75%OA may indicates the presence of Ag-cubic cells in nanoparticles with internal magnetic fields significantly larger than the Zeeman field, the available EPR in the X-band range (Fig. 6b) [10, 13, 17]. At low temperature of 77 K the FMR signal is broadened several times. This resonance line arises from silver nanocrystallites with the properties of a bulk material representing a multi-domain system, where spins are oriented along the direction of the field.

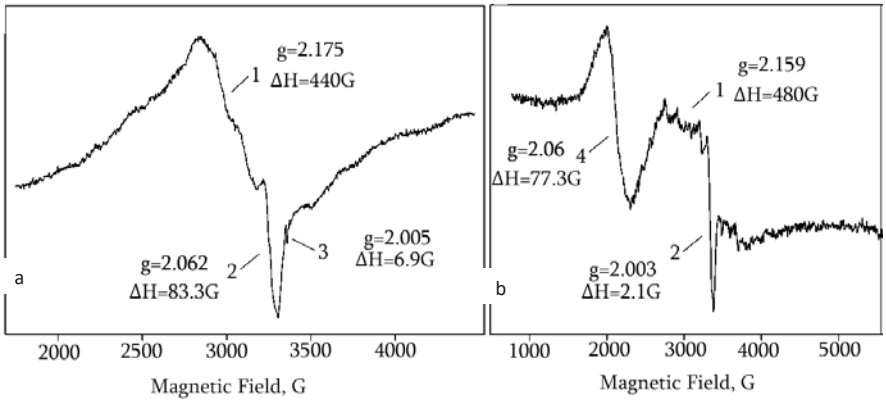

Fig. 6. *Ag&0.25% OA (a) and Ag&0.75% OA (b)*

The inevitable absence of a regular periodic structure and the uneven distribution of nanoparticles in a stabilizing medium, affects the symmetry of the signal. The lines with a peak-to-peak width ΔH_{pp} of several hundred Gauss are caused by collective electronic spin phenomena for a metal-containing nanomaterial [13], which are explained as RKKY interactions, exchange interactions of magnetic ions with conduction electrons [14-17], significant line broadening can be attributed to Korringa interaction [16], ferromagnetism [13, 17] and other exchange interactions [18].

The EPR signal (1), the so-called superparamagnetic, consists of several overlapping components with an average *g*-factor of 2.09-2.13 and a line width (ΔH) of about 500-800 G. This line is due to the conduction electrons of CESR nanoparticles [12, 13, 19, 20], while the spin-orbit interaction for bulk Ag is so significant that the resonant signal can be observed only at very low temperatures [21]. Such a broad signal can also be associated with some localized EPR active (paramagnetic) surface states. Note in the case Ag&0.25%OA sols with the one layer of oleic acid (Fig. 6a) in comparison with Ag&0.75%OA, the broad line becomes more intense with a changing environment due to decrease in the "shielding" of the nanoparticles between themselves. In addition, the nanoscale particles are closely located to each other, as a result of which dipole-dipole interactions between them intensify, which also could be leads to an additional line broadening.

In the EPR spectra of silver-containing sols, the anisotropic signal (2), which belongs to divalent silver. The appearance of such highly oxidized silver states on the surface of nanoparticles occurs through the disproportionation of Ag(I), which leads to the formation of Ag(II) ions and metal Ag^0 silver [22, 23]. EPR characteristics of the complexes accord with the available literature data for analogous two-valence silver [24, 25].

It is important to note that a change in the oleic acid layers of the nanoparticles seems to affect the dimension of the nanocrystallites that are being formed. Thus, in the sols, when passing from the mono- to the bilayer of oleic acid, both small particles and larger multidomain agglomerates are found. So, the narrow weak signal (3) in the region of the *g*-factor 2.005 also refers to the spin resonance of conduction electrons from zero-valent silver [24, 26-28]. This line is usually characteristic of small nanoparticles, usually around 2 nm [29-30]. The presence of the FMR resonance line (4) in Ag&0.75%OA may indicates the presence of Ag-cubic cells in nanoparticles with internal magnetic fields significantly larger than the Zeeman field, the available EPR in the X-band range (Fig. 6b) [10, 13, 17]. At low temperature of 77 K the FMR signal is broadened several times. This resonance line arises from silver nanocrystallites with the properties of a bulk material representing a multi-domain system, where spins are oriented along the direction of the field.

Conclusion

In the present study we claimed, that secondary ligand layer of the shell forms branching structure of chemically bonded ligand molecules. This conclusion supported by quantum chemical simulation which leads to the model of formation C=C double bonds resulting from coupling of delocalized p- electrons of primary and secondary layers. Desorption activation energy patterns displayed significant variation in activation energies with ligand surface coverage testifying inconsistence with widely accepted Langmuir adsorption model. More realistic model of ligand chemisorption accounting for energetic inhomogeneity of metal nanoparticle surface is proposed. In the EPR spectra of silver-containing sols Ag&0.25%OA and Ag&0.75%OA a complex wide asymmetric signal with several resonant lines is recorded, which is consistent with a wide size distribution of nanoparticles. It is important to note that a change in the oleic acid layers of the nanoparticles seems to affect the dimension of the nanocrystallites that are being formed. The presence of the FMR resonance line in Ag&0.75%OA may indicates the presence of Ag-cubic cells in nanoparticles with internal magnetic fields significantly larger than the Zeeman field, the available EPR in the X-band range.

Acknowledgments

The above project has been fulfilled with financial support of Shota Rustaveli National Science Foundation of Georgia (GrantNo.217020). Any idea in this publication is possessed by the author and may not represent the opinion of Shota Rustaveli National Science Foundation of Georgia.

The authors are grateful to the Baikal Analytical Center for the special measurements. Research completed by Khutsishvili Spartak in the framework

of the scientific project V.44.1.2. of the program of fundamental research of SB RAS.

References

[1] M. Donadze, M. Gabrichidze, S. Calvache, T. Agladze, Novel method of preparation of the hybrid metal (I) – metal (II) oxide nanoparticles, Int. J. Transactions of the IMF 94 (1) (2016)16-23.

[2] J.H. Flynn, The Isoconversional method for determination energy of activation at constant heating rate, J. Therm. Anal. 27 (1) (1983) 95-102.

[3] T. A. Ozawa New method of analyzing thermogravimetric data, Bull. Chem. Soc. Japan 38 (1965) 1881-1886.

[4] T. Agladze, M. Donadze, P. Toidze et al. Synthesis and Size Tuning of Metal Nanoparticles, Z.Phys. Chem. 227 (2013) 1187-1198.

[5] D.H. Lee FTIR spectral characterization of thin film coatings of oleic acid on glasses, J. Mat. Sci. 34 (1999) 139-146.

[6] C. Doyle, Kinetic analysis of thermogravimetric data, J. Appl. Polym. Sci. 5 (15) (1961) 285–292.

[7] K.Yang, H.Peng, Y.Wen, N. Li, Re-examination of characteristic FTIR spectrum of secondary layer in bilayer oleic acid-coated Fe_3O_4 nanoparticles, Appl. Surf. Sci. 256 (2010) 3093–3097.

[8] Q. Lan, C. Liu, F. Yang et al., Synthesis of bilayer oleic acid-coated Fe_3O_4 and interface nanoparticles and their application in pH-responsive Pickering emulsions, J. Coll. Sci. 310 (2007) 260–269.

[9] L. Shen, P.E. Laibinis and T.A. Hatton, Bilayer surfactant stabilized magnetic fluids: synthesis and interactions at interfaces, Langmuir 15 (1999) 447-453.

[10] S. Nellutla, S. Nori, S.R. Singamaneni, J.T. Prater, J. Narayan, A.I. Smirnov, Multi-frequency ferromagnetic resonance investigation of nickel nanocubes encapsulated in diamagnetic magnesium oxide matrix, J. Appl. Phys. 120 (22) (2016) 1-9.

[11] V. Angelov, H. Velichkova, E. Ivanov, R. Kotsilkova, M.H. Delville, M. Cangiotti, A. Fattori, M.F. Ottaviani, EPR and rheological study of hybrid interfaces in gold-clay- epoxy nanocomposites, Langmuir 30 (44) (2014) 13411-13421.

[12] M.V. Lesnichaya, B.G. Sukhov, E. Gasilova, G. Aleksandrova, T. Vakul'skaya, S. Khutsishvili, A. Sapozhnikov, I. Klimenkov, B. Trofimov, Chiroplasmonic magnetic gold nanocomposites produced by one-step aqueousmethod using κ-carrageenan, Carbohydrate Polymers 175 (2017) 18-26.

[13] A. Smirnov, EPR studies of nanomaterials. In: (Ed.) S. Misra, Multifrequency Willey-VCH, Verlag (2011) 825-843.

[14] M. Schlott , H. Schaeffer, B. Elschner, Gd^{3+}-ESR in the intermediate valent cerium compounds $Ce_xLa_{1-x}Os_2$, Zeitschrift für Physik B Condensed Matter 63 (4) (1986) 427- 436.

[15] J. Stöhr, H. Siegmann, Magnetism: From Fundamentals to Nanoscale Dynamics, Springer-Verlag, Berlin Heidelberg, 2006.

[16] P. Venegas, P. Netto, Exchange narrowing effects in the EPR linewidth of Gd diluted in Ce compounds, J. Appl. Phys. 83 (11) (1998) 6958-6968.

[17] P. Shin, S. Wu, Magnetic anisotropic energy gap and strain effect in Au nanoparticles, Nanoscale Research Letters 5 (2010) 25-30.

[18] M. Kakazey, N. Ivanova, G. Sokolsky, J. Gonzalez-Rodriguez, Electron paramagnetic resonance of MnO_2 powders, Electrochemical and Solid-State Letters 4 (5) (2001) 1-4.

[19] F. Blatter, K. Blazey, Conduction electron spin resonance of silver in zeolite AgY, Z. Phys. D - Atoms, Molecules and Clusters 18 (1991) 427-429.

[20] S. Sako Kimura, K. Size, Effect in CESR of magnesium and calcium small particles, Surface Sci. 156 (1985) 511-515.

[21] X. Li, A.Vannice, ESR studies of well-dispersed Ag crystallites on SiO_2, J. Catalysis 151 (1995) 87-95.

[22] M. Ali, A. Shames, S. Gangopadhyay, B. Saha, D. Meyerstein, Silver(II) complexes of tetrazamacrocycles: studies on e.p.r. and electron transfer kinetics with thiosulfate ion, Transition Metal Chemistry (Dordrecht, Neth.) 29 (2004) 463-470.

[23] M. Kester, A. Allred, Ligand-induced disproportionation of silver (I), J. American Chemical Society 94 (1972) 7189-7189.

[24] S. Khutsishvili, T. Vakul'skaya, N. Kuznetsova, T. Ermakova, A. Pozdnyakov, G. Prozorova, Formation of stable paramagnetic nano-compositescontaining zero-valence silver and copper in a polymeric matrix, J. Phys. Chem. C

118 (33) (2014) 19338–19344.
[25] J. McMilan, B. Smaler, Paramagnetic resonance of some silver(II) compounds. J. Chem. Phys. 35 (1961) 1698-1701.
[26] H. Moon, J. Kim, M. Suh, Redox-active porousorganic framework Chemie producing silver nanoparticles from AgI ions at room temperature, Angew.Chem. Int. Ed. 44 (2005) 1261-1265.
[27] G. Deligiannakis, Y. Trapalis, C. Boukos, N. Kordas, CW and pulsed EPR study of silver nanoparticles in SiO_2 matrix, J. Sol-Gel Science Technology 13 (1998) 503–508.
[28] S. Khutsishvili, T. Vakul'skaya, G. Aleksandrova, B. Sukhov, Stabilized silver nanoparticles and clusters Ag_n of humic-based bioactive nanocomposites, J. Cluster Sci. 28 (2017) 3067-3074.
[29] V. Timoshenko, T. Shabatina, Yu. Morozov, G. Sergeev, Complexation and chemical transformations in the ternary system silver-carbon tetrachloride- mesogenic cyanobiphenyl at low temperatures, J. Struc. Chem. 47 (1) (2006) 145-150.
[30] J. Michalik, H. Yamada, D. Brown, L. Kevan, Small silver clusters in smective clay interlayers, J. Phys. Chem. 100 (1996) 4213-4218.

Annals of Agrarian Science

Journal homepage: http://journals.org.ge/index.php

Prevalence of Bovine Tuberculosis and Its Risk Factors in Georgia

Levan Tsitskishvili[ab]*, Tengiz Kurashvili[c], Levan Makaradze[c], Iuri Baratashvili[c], Guram Samadashvili[ab], Gabriel Glunchadze[ab], Laura Bartaia[ab], Zaza Samadashvili[ab]

[a]Ivane Beritashvili Center of Experimental Biomedicine, 14, Levan Gotua Str., Tbilisi, 0160, Georgia

[b]International Association "Veterinarians Sans Frontiers – Caucasus",10, Ivane Javakhishvili, Str., Tbilisi, 0102, Georgia

[c]Agricultural University of Georgia, 240, David Agmashenebeli Ave., Tbilisi, 0159, Georgia

Received: 14 September 2018; accepted: 12 November 2018

A B S T R A C T

The main goal of this study was twofold: 1) to assess regional distribution of bovine tuberculosis (bTB) in domestic cattle in Georgia; and 2) to describe the disease risk factors in the country. Study sample and methods: Randomly selected cattle carcasses were examined in all operational slaughterhouses. The information on cattle age, sex, breed, and origin were obtained from the national registry. Post-mortem sanitary inspection of carcasses was done for all randomly selected cases. In case of macroscopic changes, samples from internal organs and lymphatic nodes were collected for further histopathological and microbiological examination. Geographical coordinates for all participating slaughterhouses and farms were measured and integrated into GIS system. Descriptive statistical analysis was performed to describe bTB regional distribution in Georgia and stratified risk analysis was done to identify high risk strata for bTB in the country. In total, 2286 carcasses were examined in 36 slaughterhouses nationwide. Out of these, 552 cases were further investigated by histopathological and microbiological methods. Using this hybrid approach (histopathological and microbiological testing), an estimated bovine TB rate is 0.44% (0.36-0.54%) in slaughtered cattle in Georgia. Out of ten regions, only three had bTB cases. The estimated rates were 0.98% (0.27-2.49%), 1.36% (0.28-3.92%), and 1.84% (0.50-4.65%) for Kvemo Kartli, Shida Kartli, and Samstkhe-Javakheti regions respectively. The study revealed that the disease antecedents in the region, cattle female gender and older age (>2years old), are bTB risk-factors in Georgia. Stratified analysis shows that the stratum with the highest composite risk (>2 years old female cattle slaughtered in the region with bTB antecedents) has estimated bTB prevalence - 1.61%.

Keywords: Cattle, Zoonosis, Bovine Tuberculosis, Risk factors, Pathology Assessment, Cross-sectional study.

*Corresponding author: Levan Tsitskishvili; E-mail address: tsitskishvili.l@gmail.com

Introduction

Natural milk production has been the most urGeorgia has one of the highest rates of human tuberculosis (TB) (156 per 100,000 WHO) in Eastern Europe. This rate is nearly three times higher than the regional average. Although TB is one of the major health priorities in Georgia, a rate of newly identified cases a year (88 per 100,000) remains unacceptably high. For comparison, the rate of all TB cases in industrialized countries is 23 per 100,000.

It is estimated that about 2 % of all TB cases and 10 % of all non-respiratory TB cases in humans have bTB origin in developing countries. The routes of bovine TB transmission from cattle to humans include direct exposure to infected cattle or consumption of contaminated animal products.

First cases of bTB have been recorded officially in two regions of Georgia (Samstkhe-Javakheti and Kvemo Kartli) around the mid-twentieth century. The following nationwide epidemiological assessment was conducted in 1953-1965 and revealed bTB cases in 73 farms of the country. As

a result of bTB eradication measures by 1972, the number was reduced to 15 farms in five districts of the country. Then, the number of affected areas increased again, and bTB cases were recorded in 19 districts of the country in 1980-1985 (See Figure 1). The last known bTB study in Georgia showed multi-drug resistance of bovine mycobacteria strains isolated from carcasses of infected animals [1].

Materials and Methods

Study Design: This was exploratory cross-sectional study in which randomly selected cattle carcasses were examined in all concurrently operational slaughterhouses. The information on cattle age, sex, breed, and origin were obtained from the national registry. Post-mortem sanitary inspection of carcasses was performed for all randomly selected cases. In case of macroscopic changes, samples of select internal organs and lymphatic nodes were collected for further histopathological and microbiological examination. Geographical coordinates of all participating slaughterhouses and farms were measured and integrated into GIS system.

Bovine TB Diagnosis: Pathology Assessment was done in accordance of Parlane, et al., 2014: I) lung lesion score was calculated by counting the total number of lesions as follows: 0 - no lesions, 1 - 1–9 lesions, 2- 10–29 lesions, 3 - 30–99 lesions, 4 - 100–199 lesions, 5 >200 lesions;II) A total lymph node lesion score per animal was calculated by pooling scores for four pulmonary lymph nodes (left and right bronchial and anterior and posterior mediastinal). Scores for individual lymph nodes was estimated as follows: 0 - no lesions, 1 - 1–19 small lesions (1–4 mm diameter), 2 ->20 small lesions (1–4 mm diameter) or medium size lesion(s) (5–9 mm diameter), 3 - large lesion(s) (>10 mm diameter) [2-4].

For histological examination sections were hematoxylin and eosin stained. Scoring of histopathological lesions in the lymph nodes was based on the scale described by Wangoo, et. al., 2005: Stage 0 - no granulomas are observed; Stage I - granulomas are composed of accumulations of epithelioid macrophages with low numbers of lymphocytes,neutrophils and Langerhans multinucleated giant cells and an absence of necrosis; Stage II - granulomas are similar to Stage I granulomas but also have central infiltrates of neutrophils and lymphocytes and necrosis could be present, Stage III granulomas exhibit complete fibrous encapsulation and significant necrosis and mineralization can be present; Stage IV - granulomas are characterized by multiple coalescing caseo-necrotic granulomas with multi-centric necrosis and mineralization. The histopathological score was based on the most severe lesion observed in each pulmonary lymph node section with scores ranging from 0 to 4, corresponding to Stages 0 to IV, respectively. A total histopathological score was compiled by pooling scores for each of the four pulmonary lymph nodes. Scoring of gross and histopathological lesions was assigned without knowledge of the slaughterhouse source [5].

Tissue and lymph node samples (mostly head and cervical lymph nodes) from every bTB suspected animal was subjected to bacterial isolation. Samples from all tissues were pooled, homogenized with sterile distilled water and decontaminated with 0.35% hexadecylpyridinium chloride for 30 minutes [2], centrifuged at 1,300 X g for 30 minutes and cultured onto Coletsos and 0.2% (w/v) pyruvate-enriched Lowenstein-Jensen media (Bio-Rad, Carlsbad, CA, USA) at 37^0C. [3] Isolates wasassessed by determining traditional cultural and biochemical properties for Bovine Mycobacteria.

The primary outcome measure – positive bTB case - was defined as bovine TB characteristic changes by both histopathological and microbiological assessments.

Statistical Analysis: Proportions (%) of the randomly selected carcasses and of cases that were selected for further histopathological and bacteriological examination were computed for each region. Bovine TB mean rates and its 90% confidence intervals were estimated for each region by using Clopper-Pearson (exact) and Wilson tests. Bivariate relationship between bovine TB and select risk factors (age, gender, breed, and origin) as well as variation of the disease rates across regions for each risk factor were examined by chi-squire tests. All risk factors that were potentially associated ($p<0.20$) with primary outcome were used in stratified analysis. The later was performed to determine high risk strata of bTB in Georgia.

Statistical analyses were done in SAS 9.2 and all reported results are two-sided at 5% significance level.

Results

During the study period, 322,074 cattle were slaughtered in ten regions of Georgia (more than 70% of these in four regions of the country: Imereti, Kakheti, Kvemo Kartli, and Shida Kartli). Although the rates were proportional to overall domestic cattle population in the regions, the numbers of the slaughtered animals varied from 1873 (Racha) to 70494 (Imereti) across the regions (see Table 1). 2286 animal carcasses (0.7% of all slaughtered cattle) were randomly selected from all slaughterhouses that were operational in all ten regions of the country during the study period. Animal ID number, age, gender, breed, and geographic origin information were obtained from the National Registry. The carcasses of all randomly selected animals were then inspected by a trained veterinarian and in the case of macromorphological changes (every 4th or 5th case), internal organ and lymph node samples were further examined by histopathologic and microbiologic methods. The number of the carcasses investigated varied from 41 (Racha) to 467 (Imereti) and exceeded 140 cases for seven regions (Table 1).

Table 1. *Frequencies and proportions of investigated animals by region during study period (02/2017-08/2018)*

Region	Total number of slaughtered animals	Proportion of Cases (Percent of total number of animals slaughtered in the country)	Number of randomly selected carcasses	Proportion of inspected carcasses (Percent of animals slaughtered in the region)
Achara	12574	3.9	141	1.1
Guria	7766	2.4	80	1.0
Imereti	70494	21.9	467	0.7
Kakheti	46643	14.5	381	0.8
KvemoKartli	52001	16.1	408	0.8
Mtskheta-Mtianeti	28489	8.8	102	0.4
Racha-Lechkhumi	1873	0.6	41	2.2
Samtskhe-Javakheti	6413	2.0	217	3.4
Samegrelo-ZemoSvaneti	29074	9.0	228	0.8
ShidaKartli	66747	20.7	221	0.3
Total	322074	100.0	2286	0.7

By applying hybrid histopathologic and microbiological diagnostic approach, out of the 552 examined cases 11 cases were identified to be bTB positive. Therefore, the estimated prevalence and its 95% confidence interval for bovine TB prevalence in cattle slaughtered in Georgia is 0.44% (0.36-0.54%). The rates vary across the regions: no bovine TB case was detected in seven regions of the country and bTB prevalences are 0.98% (0.27-2.49%), 1.36% (0.28-3.92%), and 1.84% (0.50-4.65%) for Kvemo Kartli, Shida Kartli, and Samtskhe-Javakheti, respectively (Table 2).

The distribution of bTB risk factors by region is shown in Table 3. Although most of the slaughtered cattle (79%) were female animals, the rate varied substantially across the regions. The lowest rate, 43.5%, was recorded in Imereti and highest rate, 91.7%, in Samegrelo. The gender difference among regions was statistically significant (P<0.001). One explanation of the previous fact might be the import of male cattle from some regions of Georgia to the neighboring countries.

Table 2. *Bovine TB prevalence in slaughtered animals by region*

Region	Number of researched animals	Positive cases (%)	95% CI*
Achara	141	0.00	0.00 -2.58
Guria	80	0.00	0.00 -4.51
Imereti	467	0.00	0.00 -0.79
Kakheti	381	0.00	0.00 -0.96
KvemoKartli	408	0.98	0.27 -2.49
Mtskheta-Tianeti	102	0.00	0.00 -3.55
Racha-Lechkhumi	41	0.00	0.00 -8.60
Samtskhe-Javakheti	217	1.84	0.50 -4.65
Samegrelo-ZemoSvaneti	228	0.00	0.00 -1.60
ShidaKartli	221	1.36	0.28 -3.92
Total	2286	0.44	0.36-0.54**

** Clopper-Pearson (Exact) test was used to compute 95% confidence intervals*
*** Wilson test with weight statement was used to compute 95% confidence intervals (weights were assigned based on ratio of the number of investigated cases in a region to the total number of slaughtered animals nationwide during the study period)*

Table 3. *Bovine TB prevalence in slaughtered animals by region*

Risk factor	For all regions	Achara	Guria	Imereti	Samegrelo-ZemoSvaneti	Racha	Mtskheta-Mtianeti	ShidaKartli	Kakheti	Kvemo-Kartli	Samtskhe-Javakheti	P-value
Total	2286 (100)	141 (6.2)	80 (3.5)	467 (20.4)	228 (10.0)	41 (1.8)	102 (4.5)	221 (9.7)	381 (16.7)	408 (17.8)	217 (9.5)	
Sex												<0.001
Male	480 (21.0)	43 (30.5)	11 (13.8)	203 (43.5)	19 (8.3)	9 (22.0)	4 (3.9)	77 (34.8)	33 (8.7)	62 (15.2)	19 (8.8)	
Female	1806 (79.0)	98 (69.5)	69 (86.3)	264 (56.5)	209 (91.7)	32 (78.0)	98 (96.1)	144 (65.2)	348 (91.3)	346 (84.8)	198 (91.2)	
Age												<0.001*
<2 years	332 (14.5)	57 (40.4)	16 (20.0)	83 (17.8)	4 (1.8)	5 (12.2)	11 (10.8)	50 (22.6)	35 (9.2)	48 (11.8)	23 (10.6)	
2-4 years	1145 (50.1)	68 (48.2)	17 (21.3)	287 (61.5)	98 (43.0)	18 (43.9)	55 (53.9)	146 (66.1)	68 (17.8)	242 (59.3)	146 (67.3)	
>4 years	419 (18.3)	13 (9.2)	4 (5.0)	97 (20.8)	36 (15.8)	18 (43.9)	36 (35.3)	25 (11.3)	51 (13.4)	91 (22.3)	48 (22.1)	
Unknown	390 (17.1)	3 (2.1)	43 (53.8)	0 (0.0)	90 (39.5)	0 (0.0)	0 (0.0)	0 (0.0)	227 (59.6)	27 (6.6)	0 (0.0)	
Breed												
Local	1378 (60.3)	85 (60.3)	54 (67.5)	394 (84.4)	82 (36.0)	41 (100)	91 (89.2)	188 (85.1)	131 (34.4)	162 (39.7)	150 (69.1)	<0.001*
Other	86 (3.8)	22 (15.6)	0 (0.0)	0 (0.0)	0 (0.0)	0 (0.0)	11 (10.8)	24 (10.9)	11 (2.9)	9 (2.2)	9 (4.1)	
Unknown	822 (36.0)	34 (24.1)	26 (32.5)	73 (15.6)	146 (64.0)	0 (0.0)	0 (0.0)	9 (4.1)	239 (62.7)	237 (58.1)	58 (26.7)	

** Only the cases without Miss/Unknown information was used in testing statistical significance*

In seventeen percent of randomly selected animals, information of the animal age was missing. In the group with no missing age information vast majority (82%) were adult animals (>2 Years old). Across the regions rate of young adult animals (2-4 years old) varied from 44% (Racha and Kakheti) to 71% (Samegrelo), and the range rates of adult animals (>4years old) were 9% (Ajara) and 43% (Racha). Age variation across the regions was statistically significant (P<0.001).

More than one third of the investigated cases had missing/unknown animal breed information. As 94% of all cases without missing breed information were local breed, all other breeds were combined into one group – non-local breed. Also as the exclusion of cases with missing breed information might reduce the analytic sample significantly, the risk factor was used only in univariate and bivariate analysis, and was disregarded in stratified analysis. The overall proportion of local breed animals varied between 79% and 100% across the regions.

Table 4 reports the results of bivariate analysis. Bovine TB antecedents in a region is the most important risk factor for the disease (P=0.002). Additionally, cattle female gender (P<0.10) and adult age (P=0.17) are also associated with the disease. As the disease prevalence is very low and the rates for young adult and adult groups are similar, these two were combined in one adult group (>2 years old) for further analysis.

Table 4. *Bovine TB prevalence in slaughtered animals by region*

Risk Factor	Number of researched animals	positive cases %	P-value
Total	2286	11 (0.48)	
Sex			0.09
Male	480	0 (0.0)	
Female	1806	11 (0.61)	
Age			0.17**
<2 years	332	0 (0.0)	
2-4 years	1145	9 (0.79)	
>4 years	419	2 (0.48)	
Breed			
Local	1378	10 (0.73)	0.65*
Other	86	1 (1.16)	
bTB (Region)			0.002
Yes	1059	11 (0.90)	
No	1227	0 (0.0)	

** Only the cases without missing/Unknown information was used for testing statistical significance*
***P-value derived from test that compares <2 and ≥2 years old animals*

As the low number of the primary outcome did not allow to do a multivariate examination of independent risk factors, stratified risk analysis was performed to identify high risk strata for bTB in the country. Animal gender, age, and bTBhistory of the region were used in the stratified analysis. The reason behind not using animal breed information is explained in a previous paragraph. The study showed that the stratum with the highest composite risk (>2 years old female cattle slaughtered in the region with bTB antecedents) has estimated bTB prevalence - 1.61%.

Discussion

This study examined bTB regional distribution along with its animal (age, gender, breed) and region (bTB history) level risk-factors in Georgia.

In this study, we found that all bTB cases were diagnosed in adult animals. This agrees to the existing evidence that older animal age is one of the important risk factors of bTB. Studies that were conducted in both developing and developed countries showed that the disease rate is significantly higher in adult animals compared to young ones [6-7]. There are two possible explanations of this association: 1) older animals have high probability to get in contact with the infectious agent source; and 2) bovine TB has long latent period [8].

There is contradictory information of animal gender role in bovine TB infection. While a study found that male gender is a significant risk factor of bTB [9], another study showed that female gender was associated with the disease development [10]. Our study showed that all diseased cases were diagnosed in female cattle. This might be explained by the fact that, in Georgia, female cattle are kept for longer time because of milk production and reproductive purposes. Therefore, the relationship found in our study might be confounded by animal age.

There is evidence that non-local breed cattle have high bTB risk compared to local ones [11]. Due to a high rate of missing breed information and a very low number of animals categorized as non-local breed, we were not able to examine the relationship between cattle breed and bTB infection. However, this should not significantly affect the study findings as the vast majority of the cattle in Georgia belong to the local breed.

This study found that bTB antecedents in the region is the most important risk factor of the infection. Previous studies also showed that the regions with bTB history has a significantly higher risk of the disease outbreak [12,13].

Based on Stratified analysis, this study showed that bTB risk in the highest risk stratum (>2 years old female cattle slaughtered in the region with bTB antecedents) is about 4 times higher than nationwide rate of the disease.

Future Studies

One of the main limitations of our study was that we were not able to confirm bacterial isolates by using molecular methods. Additionally, limited number of positive bTB cases did not allowed to perform multivariate analysis to examine independent relationship between the disease and its risk factors. This emphasizes the need of using more sensitive and accurate (e.g. PCR) molecular methods in future studies.

Recommendation

Bovine TB remains a public health problem in Georgia and requires measures to minimize the risk of the disease transmission to humans.

Funding: This work was supported by Shota Rustaveli National Science Foundation of Georgia (SRNSFG) [grant number FR 217822].

References

[1] I. Frangishvili, Doctoral Thesis "Mycobacterial testing of intestinal lymph nodes for bTB eradication in Georgia" .Tbilisi State Veterinary University, 2003, 48 (in Georgian).

[2] Corner LA, Trajstman AC, An evaluation of 1-hexadecylpyridinium chloride as a decontaminant in the primary isolation of Mycobacterium bovis from bovine lesions. Vet Microbiol., 18 (1988) 127–134.

[3] Santos N, Geraldes M, Afonso A, Almeida V, Correia-Neves M, Diagnosis of tuberculosis in the wild boar (Susscrofa): A comparison of methods applicable to hunter-harvested animals. PLoS One 5: 10.1371/journal.pone.0012663, 2010.

[4] Parlane NA, Shu D, Subharat S, Wedlock DN, Rehm BH, de Lisle GW, Buddle BM,Revaccination of cattle with bacilli Calmette-Guérintwoyearsafterfirstvaccination when immunity has waned, boosted protection against challenge with *Mycobacterium bovis*.

PLoS One. 9(9):e106519. doi: 10.1371/ journal.pone.0106519, 2014.

[5] Wangoo A, Johnson L, Gough J, Ackbar R, Inglut S, et al., Advanced granulomatous lesions in *Mycobacterium* bovis - infected cattle are associated with increased expression of type I procollagen gamma delta(WC1+) T cells and CD68+cells. J Comp Pathol 133 (2005) 223–234.

[6] Cleaveland C et al. *Mycobacterium bovis* in rural Tanzania: Risk factors for infection in human 87(1) (2007) 30-43

[7] Griffin JM, et al. A case-control study on the association of selected risk factors with the occurrence of bovine tuberculosis in the Republic of Ireland. Preventive Veterinary Medicine,27(3-4) (1996) 217-229

[8] Pollock, JM et al. Mycobacterium bovis infection and tuberculosis in cattle. Veterinary journal, 163(2),(1997) 115-127

[9] Kazwala RR et al. Risk factors associated with the occurrence of bovine tuberculosis in cattle in the Southern Highlands of Tanzania. Veterinary research communications, 25(8) (2001) 609-614

[10] Inangolet FO et al. A cross-sectional study of bovine tuberculosis in the transhumant and agro-pastoral cattle herds in the border areas of Katakwi and Moroto districts, Uganda. Tropical animal health and production. 40(7) (2008) 501-508.

[11] Omer MK et al. cross-sectional study of bovine tuberculosis in dairy farms in Asmara, Eritrea. Tropical animal health and production, 33(4) (2001) 295-303

[12] Rodwell TC et al. Evaluation of Population Effects of Bovine Tuberculosis in free ranging African Buffalo. J. Mammal, 82 (2001) 258-264.

[13] White P et al. Factors influencing the incidence and scale of bovine tuberculosis in cattle in southwest England, Preventive veterinary medicine. 63 (1-2) (2004) 1-7.

Annals of Agrarian Science

Journal homepage: http://journals.org.ge/index.php

Peculiarities of soils of high mountain (on Khevi example – on the Central Great Caucasus)

Ketevan Gogidze

Agricultural University of Georgia, Mikheil Sabashvili Institute of Soil Science, Agrichemistry and Melioration, 240, David Aghmashenebeli Alley, Tbilisi, 0159, Georgia

Received: 21 January 2019; accepted 12 March 2019

A B S T R A C T

The article includes the research in Khevi region of Central Caucasus. Study area was divided by expositions (north and south), inclination (0-10^0, 10-30^0, >30^0) and altitude (1700-2000 m – subalpine forests, 2000-2200 m – subalpine meadows, 2200-2500 m – alpine meadows). The number of soil profiles as a result of division was consisted of 18. By comparing the profiles of high mountain soils to each other, they do not stand out by genetic individuality.

Keywords: Soil, Pasture, Meadow-forest-mountain soils, Meadow-mountain soils, Subalpine, Alpine.

*Corresponding author: Ketevan Gogidze; E-mail address: qetusi86@gmail.com

Introduction

The studying of the soils of High Mountain of the Caucasus was started with great intensity from the beginning of the 20th century. The first researcher was S. Zakharov [1], who investigated the soils of high mountain of Georgia nearby the Lesser (Tskhratskaro) and Main Caucasus (Jvari passes). Subsequently, A. Voznesensky [2] studied mountain-forest soils in Zakatala district, but O. Mikhailovskay [3] investigated soils of subalpine forests in Samachablo. Subalpine soils of Klukhori district was studied by G. Akhvlediani and S. Tsintsadze [4]. There is a great contribution to study the soils of High Mountain of next researchers, G. Tarasashvili [5], A. Gogatishvili [6] and G. Talakhadze [7]. With using of modern research these soils has been studied by T. Urushadze [8-10]. The aim of his research was the peculiarities of genesis, legislation of geographical distribution and studying of classification of soils. The soils of the highmountains of Georgia also was studied by M. Sabashvili [11, 12], M. Sabashvili and M. Jikaeva [13], Sh. Shubladze [14] T. Urushadze, T. Kvrivishvili [15], T. F. Urushadze, W. E. H. Blum [16] and others. The high mountain soils were studied quite well, but in their investigations there are given less about comparative characterization of soils in subalpine and alpine belts.

In summer in the Central Caucasus (Khevi region) the pastures are used very intensively by population. Meanwhile, there are some problems of their care and improvement. The biggest problem is overgrazing of the pastures. It is important to study the soils on pasture for their further using and improvement. It is often overgrazing of pastures, it causes worsening of botanic and chemical composition of grass, decreasing of productivity and dismantling of sod [17]. Without studying of ecological conditions (subalpine and alpine belts, exposition, inclination), It is impossible the protection of soils of high mountain and Rational using.

Physical-geographical description of the region

For creating the relief of the Central Caucasus with tectonics, erosion, glacier activity and other widespread factors are karstic processes. Young

volcanism is presented in the Central Great Caucasus. The Central Great Caucasus is built by Mesozoic and Previous Mesozoic tiles.

Khevi region is built by quaternary fluvial and glacial sediments, Tertiary and Quaternary volcanic rocks and Jurassic sedimentary rocks. Kazbegi district is characterized by high tectonic and geomorphologic activities. The neovolcanic center of Kazbek was still active in late Quaternary. Three small apparatuses are localized in area: near Pkhelshe, downward Sioni and mouth of the river Chkheri [18].

Andesite flow of Pkhelshe has a submeridional direction, with endings it covered the old valley of river Tergi on the territory of villages Khurtisi and Pkhelshe and has changed the direction of Tergi to right by character of canyon. Next to flow of Pkhelshe by two rivers (Khurtisistskali and Pkhelshistskali) are made valleys of semicanyon and canyons. The center of flow of Pkhelshe is a volcanic massive Tkarshetismta (3417 m). Next geographical succession is flow of Arsha (andesite), which pouring out on the place of ruins Kazbegi crater and reached to the left bank of river Tergi, village Arsha. Its length is 8 km. Flow of Chkheri starts on the left slope of Kazbegi and reaches 9 km by length, comes down to the west on the left bank of river Tergi, between the villages Gergeti and Saketseti. Middle and upper sides of Arsha, the flows of Chkheri and to the north of Tsdo, together present a massive of lava, and is cutting by valleys of rivers Chkheri and Tsdostskali. The flow of Tsdo has poured out in region of glacier Abano. Its length is 8 km. It has finished on the left bank of river Tergi near village Tsdo. Flow of Gveleti starts near Archkhoti pass and finishes with two tongues, till Dariali valley. Its length is more than 3-4 km [19].

All described lavas are belonged to andesites and andesitedacites. The lateral center of Kazbegi massive N. I. Skhirtladze recognizes mountain Kichugzeri (3500 m a. s. l.), is located on the west slope of cone. The area of modern ice age on Kazbegi massive is 29, 44 km^2.

In study area mudflows are natural hazard and hot points are in Tergi river basin. So this location is in a zone of medium landslide hazard [20,21].

The gorge of river Snostskali by morphology is erosive and deeply fragmented (Khorkhi, Kvenamtistskali, Chaukhistskali, Shinostskali), on their mouth and slopes are too much hearths of avalanche and downpour, because of it, village Juta is torn off from Stepantsminda about four months. The gorge of Dariali near estuary of river Chkheri is presented by avalanche and rockfall. One of the main reason of retention of Dariali was river Chkheri downpour. In this process role had carried out snowy material of glaciers Ortsveri and Abano. In retention of Tergi participated Kuros Khevi, and from right side it united Tergi gorge in this place and has brought demolished material of Kuro massive, which is built with unsustainable schist for erosion [23].

Subalpine zone is characterized by short cool summers and severe long winters. The winter is cold with much snow. The duration of the vegetative season is from three to four months. The period without frost is from one to two months. The precipitation maximum occurs in spring and summer. The average annual relative air humidity reaches 70 to 79%. In the area of the subalpine forest dominates a high-mountain erosive-denudative relief with additional influence of former glaciation. Some relief forms were created by quaternary volcanism. Erosive gorges are located on steep slopes. Clay-shales, sandstones, limestones and moraine sediments are mainly met in East Georgia. Due to unfavorable ecological conditions subalpine forests are presented by specific species, structure and forms of the vegetation [24].

On the steep slopes in some places are a wide teritorries of alluvial plains. In the high mountains is forming the following kind of relief: 1) old peneplain-level (“cut”) ranges; 2) glacial relief – care, circus, terrace areas; 3) volcanic relief – plateaus (south mountains) and 4) erosion relief. Rock fragments and stones mainly cover Glacial and erosion high mountain reliefs, but the turf covers elements of the old peneplain and volcanic relief.

In the Main Caucasus above of the forest belt we have business with high mountain, where in the main part is spread out mountain-meadow soils. Among them is more important subalpine forest zone (with bound or woodland forests), which is transitional between forest and high mountain. Here are spread mountain-forest-meadow soils.

The subalpine forest is characterized by a limited growth, and as rule low productivity. These forests protect tall forests and agricultural land, in lower positions against mountain torrents, landslides, winds and snowfall and regulate the water regime.

The mountain-forest-meadow soils are formed under extreme climatic conditions, which are characterized by long winters and cool summers.

The period without frost lasts 3-5 months. The period of vegetation growth is 3-4 months. The cold climate of the high mountains supports an intensive weathering of the rocks and because of it an accumulation of a great number of rock fragments are on the soil surface [25].

There are several examples of dividing of high mountain. For example, M. Sakhokia marked out next zones:

1. Forests of middle zone of mountain (1000-1500 m a. s. l.)
2. Forests of upper zone of mountain (1500-1750 m a. s. l.)
3. Subalpine zone (1750-2300, 2500 m a. s. l.)
4. Alpine zone (2300-3000, 3100 m a. s. l.)
5. Two sub zones: lower alpine (2300-2700 m a. s. l.) and upper alpine (2700-3000 m a. s. l.); subnival (3000-3600 m a. s. l.)
6. Nival zone (above 3600 m a. s. l.) [26].

Objects and methods

The study area, Kazbegi municipality was divided by expositions (north and south), inclination ($0\text{-}10^0$, $10\text{-}30^0$, $>30^0$) and altitude for next zones:

1. 1700-2000 m – subalpine forests
2. 2000-2200 m – subalpine meadows
3. 2200-2500 m – alpine meadows

The number of soil profiles as a result of division was consisted of 18 [27-30]. The soils were studied by the World Reference Base for Soil (WRB). Among them, soil was described by the using of the Munsell Color Scale. During laboratorian examination was made following analysis: mechanic analysis by the pipe method; hygroscopic water, (pH) potential, calcium carbonates with calcimetry, common humus by the volumetric method, calcium and magnum definition via trilon B titre, Soil absorbed hydrogen (Exchange Acidity) [31].

Results and discussions

In the subalpine forests zone on the south, exposition soils have following build: A′-A″-AB-B-BC (Pr. 15), A-AB-B1-B2-BC (Pr. 5^I, 6). The first type of build is characterized for inclination $0\text{-}10^0$, the second type of build – $10\text{-}30^0$ and $>30^0$. The soil has light loam texture, vegetation – birch and pine forest, the quantity of roots growing together with the increasing of the inclination. On the south exposition the soils is characterizing with acid and neutral reaction (pH 5,5-7,3), in 100 g soil the sum of absorbed cation capacity is 3,67-13,86 mg. eqv., from absorbed bases Ca predominates Mg, unsaturated with basis, content of humus is 10,63-0,55%.

On the north exposition, soils have following build: A-AB-BC1-BC2 (Pr. 5), A-B-BC (Pr. 42), A′-A″-BC-CD (Pr. 4). The first type of build is characterized for inclination $0\text{-}10^0$, the second type of build – $10\text{-}30^0$ and - $>30^0$. The soil has light and medium loam texture, vegetation – steppe grass, the quantity of roots growing together with the increasing of the inclination. On the north exposition the soils are characterizing with acid and weak acid reaction (pH 5,2-6,18), in 100g soil the sum of absorbed cation capacity is 25,3-11,43 mg. eqv., from absorbed bases Ca predominates Mg, is unsaturated with basis, content of humus is 10,9-15,09%.

In subalpine forest zone south and north expositions have differences: soil build, vegetative cover, where the south exposition is presented by birch and pine forest, but the north – by steppe grass, is with reaction, mechanic content, humus content, in 100g soil with the sum of absorbed cation capacity.

Subalpine meadows are located at 2000-2200 m above sea level. Vegetative cover is presented by steppe grass on the south and north expositions.

In the subalpine meadow zone on the south exposition, soils have following build: A-AB-BC (Pr. 4^I, 3^I), A-AB-B-BC (Pr. 2^I). The first and second type of build are characterized for inclination $0\text{-}10^0$ and $10\text{-}30^0$, but the third type - $>30^0$. The soil has light loam texture, well developed sod, glacier stones are on the surface. On the south exposition the soils are characterizing with weak acid reaction (pH 5,5-6,3), in 100g soil the sum of absorbed cation capacity is 4,56-12,78 mg. eqv., from absorbed bases Ca predominates Mg, is unsaturated with basis, content of humus is 9,17-0,55 %.

In the subalpine meadow zone on the north exposition, soils have following build: A-BC (Pr. 29), A′-A″- BC (Pr. 2), A′-A″-AB – BC (Pr. 3). The first type of build is characterized for inclination $0\text{-}10^0$, the second – $10\text{-}30^0$ and the third - $>30^0$. The soil has medium loam texture, many roots and skeleton, it is observed biological activity; volcanic stones, steppe grass are on the surface. On the north exposition the soils are characterizing with weak acid reaction (pH 5,5-6,3), in 100g soil the sum of absorbed cation capacity is 7,45-15,7 mg. eqv., from

absorbed bases Ca predominates Mg, is unsaturated with basis, content of humus is 9,91-1,06 %.

In subalpine meadow zone, the south and north expositions have differences: texture, humus content, in 100g soil the sum of absorbed cation capacity, in the north are much roots skeletons, biological activity, volcanic stones and in the south – glacier stones on the surface.

Alpine meadows are located at 2200-2500 m above sea level. Vegetative cover is presented by steppe grass on the south exposition.

In the alpine meadow zone on the south exposition, soils have following build: A′-A″- BC (Pr. 37), A-AB-B-BC (Pr. 9), A′-A″-AB – BC (Pr. 1[I]). The first type of build is characterized for inclination 0-10^0, the second – 10-30^0 and the third - >30^0. The soil has light loam texture, number of roots and moisture become more with increasing of the slope, much roots, and vegetative cover is presented by steppe grass. On the south exposition the soils are characterizing with acid and weak acid reaction (pH 4,5-6,1), in 100g soil the sum of absorbed cation capacity is 19,23-7,29 mg. eqv., from absorbed bases Ca predominates Mg, is unsaturated with basis, content of humus is 11,18-0,95 %.

In the alpine meadow zone on the north exposition, soils have following build: A-BC (Pr. 1, 32), A′-A″-AB- BC (Pr. 33). The first and second type of build are characterized for inclination 0-10^0 and 10-30^0, the third - >30^0. The soil has medium and heavy loam texture, skeleton increases to the depth, much roots, rocks on the surface. On the north exposition the soils are characterizing with acid reaction (pH 4,7-5,5), in 100 g soil the sum of absorbed cation capacity is 35,45-10,71 mg. eqv., from absorbed bases Ca predominates Mg, is unsaturated with basis, content of humus is 11,23-3,11 %.

Thus, by considering of the main indicators of research objects, high mountain soils in various zones, different expositions and inclination, does not give a clear difference which may have had a genetic meaning. Soils are characterized by general signs - more or less the same capacity, a good expression of the humus horizon, high content of humus, texture and diversity of general properties, this is due to the general ecological resemblance (e.g. severity of climate) and the difference is local nature, it does not related to the peculiarities of genesis.

Table 1. *Main characteristics*

Objects, Profile №	Horizon, depth (cm)	pH	Humus, %	Hygr. H_2O %	Cation exchange capacity, mg/equivalent in 100g. soil				Sum %		
					Ca^{++}	Mg^{++}	H^+	ჯამი	Ca	Mg	H
Subalpine forests zone 1700-2000 m a. s. l.											
15 Tsdo S	A′ 0-10	6,5	9,22	1,02	10,02	3,67	1	14,69	68	25	7
	A″ 10-40	6,5	5,32	1,02	10,68	6,68	0,6	15,96	67	29	4
	AB 40-55	7,0	3,62	1,03	9,46	4,05	0	13,48	70	30	0
	B 55-95	7,1	2,79	1,02	11,35	5,35	0	16,7	68	32	0
	BC 95-150	7,3	2,02	1,02	10,11	4,04	0	14,15	71	29	0
5[I] Gergeti S	A 0 - 15	5,5	10,63	1,06	14,15	8,09	0	22,24	64	36	0
	AB 15 –30	5,5	3,37	1,02	12,13	7,41	1,8	21,34	57	35	8
	B1 30 – 50	5,8	0,75	1,04	11,69	5,01	1,8	18,5	64	27	9
	B2 50-70	5,9	0,75	1,02	13,15	6,74	1,8	21,69	49	43	8
	BC 70-90	6,1	0,55	1,02	12,45	6,36	1,8	20,61	50	41	9
6 Gergeti S	A 0-10	5,0	4,96	1,02	14,32	4,1	1	19,42	74	21	5
	AB 10-25	5,2	1,86	1,06	7,69	4,35	5	14,04	55	31	14
	B1 25-40	5,7	1	1,04	4,01	2,68	1,2	7,89	51	34	15
	B2 40-60	6,5	0,75	1,02	4,01	3,35	1,4	8,76	46	38	16
	BC 60-80	6,5	0,75	1,02	4,34	1,01	1,8	7,15	61	14	25
5 Stepantsminda N	A 0—10	7,1	7,88	1,02	8,18	2,15	1	11,33	73	19	8
	AB 10—22	5,8	5,42	1,04	4,43	2,73	2,6	9,76	45	28	27
	BC1 22—40	5,0	5,42	1,04	6,35	2,01	1	9,36	68	21	11
	BC2 40—60	5,8	3,93	1,06	10,03	5,02	2	17,05	59	29	12

42 Akhaltsikhe N	A 0--12	6,4	10,91	1,04	17,05	7,85	0,4	25,3	67	31	2
	B 12--30	5,0	9,43	1,02	6,02	4,01	1,4	11,43	53	35	12
	BC 30--65	5,2	3,37	1,02	6,69	3,68	1,8	12,17	55	30	15
4 Stepantsminda N	A′ 0-10	6,2	7,9	1,02	10,01	4,35	0,4	14,78	66	33	1
	A″ 10-20	5,7	8,9	1,04	9,21	5,11	0,8	15,12	61	34	5
	BC 20-40	5,5	1,73	1,02	10,57	6,82	1,2	18,59	57	37	6
	CD >40	-	-	-					-	-	-
Subalpine meadows zone 2000-2200 m a. s. l.											
4[I] Gergeti S	A 0-14	5,6	8,43	1,06	4,01	5,35	0,8	10,16	39	53	8
	AB 14-35	6,0	2,85	1,02	5,25	7,68	0,7	13,63	53	29	18
	BC 35-50	6,3	0,85	1,02	8,23	4,05	0,8	13,08	49	48	3
3[I] Gergeti S	A 0-13	5,8	9,17	1,02	9,36	5,32	0,4	15,08	58	35	7
	AB 13-30	5,4	5,94	1,04	11,86	4,45	2	18,31	47	35	18
	BC 30-55	6,0	1,77	1,04	9,35	5,04	2	16,39	65	25	10
2[I] Gergeti S	A 0-20	5,9	8,39	1,02	11,56	8,32	0,4	20,28	48	34	18
	AB 20-35	5,8	3,78	1,02	15,26	8,27	2,3	25,83	65	20	15
	B 35-50	6,2	0,75	1,04	12,35	9,03	0,6	21,98	47	45	8
	BC 50-80	5,7	0,55	1,02	10,68	6,68	0,6	15,96	50	38	12
29 Pansheti N	A 0--10	5,8	9,91	1,02	8,02	3,68	0,4	12,1	66	33	1
	BC 10--30	6,3	2,47	1,02	9,36	3,35	0	12,71	74	26	0
2 Stepantsminda N	A′ 0-20	4,7	8,6	1,02	27,27	6,38	1,8	35,45	65	20	15
	A″ 20-35	5,1	4,5	1,02	6,48	3,75	8,8	19,03	53	42	5
	BC 35-50	5,3	4,6	1,04	3,41	1,7	5,6	10,71	45	52	3
3 Stepantsminda N	A′ 0-20	5,5	9,4	1,02	14,32	4,1	1	19,42	74	21	5
	A″ 20-40	5,7	6,5	1,04	4,01	2,68	1,2	7,89	51	34	15
	AB 40-60	5,9	3,13	1,06	4,34	1,01	1,8	7,15	61	14	25
	BC 60-80	5,9	1,06	1,02	4,01	5,35	0,8	10,16	39	53	8
Alpine meadows zone 2200-2500 m a. s. l.											
37 Sno S	A ′0--25	4,5	11,18	1,04	5,45	4,78	2,8	13,03	42	37	21
	A″ 25--65	5,4	8,27	1,02	6,69	4,65	5,35	16,69	44	36	20
	BC 65--100	5,6	0,94	1,02	4,01	2,68	0,6	7,29	55	37	8
9 Pkhelshe S	A 0--12	5,9	8,85	1,02	12,69	5,34	1,2	19,23	66	28	6
	AB 12--30	5,5	5,11	1,03	10,11	5,39	1,6	17,1	59	31	10
	B 30--58	6,0	1,21	1,03	8,76	4,38	1,4	14,54	60	30	10
	BC 58--100	6,1	0,95	1,03	10,11	4,71	1,4	16,22	62	29	9
1[I] Gergeti S	A′ 0-5	5,6	8,90	1,02	17,05	7,85	0,4	25,3	67	31	2
	A″ 5-20	5,5	8,03	1,04	8,86	4,78	0,2	13,84	45	21	34
	AB 20-30	5,7	6,46	1,04	9,03	2,34	0,6	11,97	75	20	5
	BC 30-55	6,4	1,77	1,04	6,02	4,01	1,4	11,43	53	35	12
1 Stepantsminda N	A 0-18	5,1	8,12	1,02	8,02	3,68	0,4	12,1	66	33	1
	BC 18-40	5,4	3,12	1,06	9,36	3,35	0	12,71	74	26	0
33 Achkhoti N	A′ 0--10	5,5	10,77	1,08	27,27	6,38	1,8	35,45	80	18	2
	A″ 10--25	4,6	8,97	1,04	6,48	3,75	8,8	19,03	34	20	46
	AB 25--40	4,8	5,32	1,04	3,41	1,7	5,6	10,71	32	16	52
	BC 40--60	5,2	3,11	1,04	6,14	2,44	4,4	12,98	47	19	34
32 Achkhoti N	A 0--15	5,4	11,23	1,04	15,69	5,8	2,2	23,69	66	24	10
	BC 15--30	4,7	3,37	1,02	14,05	6,02	6,6	26,67	53	23	24

Table 2. *Soil Texture*

Profile №	Location, exposition, altitude	Horizon, depth (cm)	Fractions, %						
			1-0,25	0,25-0,05	0,05-0,01	0,01-0,005	0,005-0,001	<0,001	<0,01
Subalpine forest zone 1700-2000 m a. s. l.									
15	Tsdo, S	A′ 0-10	9	47	19	5	8	12	25
		A″ 10-40	17	39	15	11	8	10	29
		AB 40-55	12	37	29	5	12	5	22
		B 55-95	15	47	13	9	7	9	25
		BC 95-150	10	44	25	2	14	5	21
42	Akhaltsikhe, N	A 0--12	18	24	13	18	24	3	45
		B 12--30	10	23	22	14	28	3	45
		BC 30--65	12	26	25	10	10	17	37
Subalpine meadows zone 2000-2200 m a. s. l.									
4[1]	Gergeti, S	A 0-14	4	45	18	9	15	9	33
		AB 14-35	8	29	29	13	13	8	34
		BC 35-50	5	46	4	11	20	14	45
29	Pansheti, N	A 0--10	34	43	4	6	6	7	19
		BC 10--30	61	20	2	7	7	3	17
Alpine meadows zone 2200-2500 m a. s. l.									
37	Sno, S	A ′0--25	5	38	13	20	13	11	44
		A″ 25--65	0.6	53.4	26	7	5	8	20
		BC 65--100	29	45	4	6	2	14	22
33	Achkhoti, N	A′ 0--10	17	33	1	36	9	4	49
		A″ 10--25	5	17	22	16	34	6	56
		AB 25--40	4	26	18	3	11	38	52
		BC 40--60	4	27	31	13	18	7	38

Conclusion

1. Subalpine forests zone on different exposition and inclination are characterized by well-expressed humus horizon (A′-A″-AB or A-AB). These soils are characterized by acid and neutral reaction (pH 5,2-7,3), high content of humus (0,55-10,91 %), loam texture. In various ecological conditions, soils do not differ by nature of genesis.
2. Subalpine meadows zone on different exposition and inclination are characterized by well-expressed humus horizon (A-AB or A′- A″). These soils are characterized by acid and neutral reaction (pH 5,5-6,3), high content of humus (0,55-9,91 %), loam texture. In various ecological conditions, soils do not differ by nature of genesis.
3. Alpine meadows zone on different exposition and inclination are characterized by well-expressed humus horizon (A-AB or A′- A″). These soils are characterized by weak acid reaction (pH 4,5-6,1), very high content of humus (0,94-11,23 %), loam texture. In various ecological conditions, soils do not differ by nature of genesis.
4. Thus, comparing the high mountain soils to each other, they do not stand out by genetic individuality, which can be explained by general similarities of ecological conditions, which is not expressed in the genetic identity of individual objects.

Acknowledgments

This work was supported by Shota Rustaveli National Science Foundation (SRNSF) [grant # PhD_F_17_117, Studying of genetic peculiarities of soil in Kazbegi Municipality].

References

[1] S. A. Zakharov, To the Characteristics of the Soils of Mountainous Countries, fifth ed., Institute of Separation of Konstantinovsky, Moscow, 1914 (in Russian).

[2] A. Voznesensky, The soils of 1 and 11 divisions of steppe of Karaysky, Scientific Research Institute of Water Management. 11 (1935) 65-72 (in Russian).

[3] O. N. Mikhailovskay, On the Question of the Genesis of Soils of Highmountains, Academy of Sciences of the USSR, Moscow, 1936 (in Russian).

[4] G. D. Akhvlediani, S. I. Tsintsadze, The Soils of Klukhori District, Works of Institute of Soil Science and Agrochemistry GSSR, Tbilisi, 1949 (in Russian).

[5] G. M. Tarasashvili, The Soils of Mountain-Forest and Mountain-Meadows of East Georgia, Academy of Science of Georgia, Tbilisi, 1956 (in Georgian).

[6] A. D. Gogatishvili, To the question of studying of cenosis of soils of transitive subalpine zone, Institute of Soil Science. 9 (1958) 85-98 (in Russian).

[7] G. R. Talakhadze, The Main Types of Soils of Georgia, "Tsodna", Tbilisi, 1964 (in Georgian).

[8] T. Urushadze, The Soils of Forest of Georgia, "Soviet Georgia", Tbilisi, 1972 (in Georgian).

[9] T. F. Urushadze, The Soils of Some Pine Forests of Georgia, "Lesovedenie", Tbilisi, 1974 (in Russian).

[10] T. F. Urushadze, The Mountainous Soils of the USSR, "Agropromizdat", Moscow, 1989 (in Russian).

[11] M. N. Sabashvili, The Soils of Georgia, Institute of Soil Science of GSSR, Tbilisi, 1948 (in Russian).

[12] M. N. Sabashvili, M. A. Jikaeva, About of mountain-meadow soils of Kazbegi district, Academy of Science of GSSR. 11 (1950) (in Russian).

[13] M. N. Sabashvili, M. A. Jikaeva, About of mountain-meadow soils of Kazbegi district, Academy of Science of GSSR. 11 (1950) (in Russian).

[14] Sh. K. Shubladze, The Genetic Characteristics of the Soil of highmountains of the Central Caucasus, The Thesis of Agriculture, Tbilisi, 1987 (in Russian).

[15] T. Urushadze, T. Kvrivishvili, The Guideline of Soils of Georgia, "Mtsignobari", Tbilisi, 2014 (in Georgian).

[16] T. F. Urushadze, W. E. H. Blum, Soils of Georgia, Nova Publishers, New York, 2014.

[17] T. Urushadze, A. Korakhashvili, O. Kvirikashvili, L. Ninua, Some Aspects of Interdependence Between Soils and Pastures in the Central Caucasus, M. Sabashvili Institute of Soil Science, Aagrochemistry and Reclamation, Tbilisi, 1984 (in Georgian).

[18] L. I. Maruashvili, The Geomorphology of Georgia, Academy of Science of GSSR, Tbilisi, 1971 (in Russian).

[19] B. Goishvili, Khevi, National Academy of Science of Georgia, Tbilisi, 1981 (in Georgian)

[20] T. Hanauer, C. Pohlenz, B. Kalandadze, T. Urushadze, P. Felix-Henningsen, Soil distribution and soil properties in the subalpine region of Kazbegi; Greater Caucasus; Georgia: Soil quality rating of agricultural soils, Annals of Agrarian Science. 15 (2017) 1-10.

[21] I. V. Bondyrev, Geodynamical processes, in: I. V. Bondyrev, Z. V. Davitashvili, V. P. Sinngh (Eds.), The Geography of Georgia, World Regional Geography Book Series, Springer International Publishing, Switzerland, 2015, pp. 67-80.

[22] I. V. Bondyrev, Geodynamical processes, in: I. V. Bondyrev, Z. V. Davitashvili, V. P. Sinngh (Eds.), The Geography of Georgia, World Regional Geography Book Series, Springer International Publishing, Switzerland, 2015, pp. 87-95

[23] R. Khazaradze, K. Kharadze, Geographical Environment and Ongoing Geodynamic Processes in Kazbegi Municipality, National Academy of Science of Georgia, Tbilisi, 2012 (in Georgian).

[24] L. B. Makhatadze, T. F. Urushadze, The

Subalpine Forests of Caucasus, Academy of Sciences of the USSR, Moscow, 1972 (in Russian).
[25] M. Kordzakhia, Climate of Georgia, Geography Institute of Vakhushti, Tbilisi, 1961 (in Georgian).
[26] G. Agladze, P. Chkheidze, Natural Mowing and Pastures of Mtkheta-Mtianeti Region, Their Meaning in Resolve Problems of Livestock, National Academy of Science of Georgia, Tbilisi, 2012 (in Georgian).
[27] K38-54-A, Ministry of Geology of USSR, Geological Map M 1:50 000, 1983 (in Russian).
[28] K38-54-B, Ministry of Geology of USSR, Geological Map M 1:50 000, 1983 (in Russian).
[29] K38-54-G, Ministry of Geology of USSR, Geological Map M 1:50 000, 1962 (in Russian).
[30] K38-54-V, Ministry of Geology of USSR, Geological Map M 1:50 000, 1983 (in Russian).
[31] K. Mindeli, L. Guntaishvili, N. Macha-variani, D. Kirvalidze, Kh. Mindeli, L. Gamsakhurdia, Practical-Laboratory Manual of Soil Science, Tbilisi, 2011 (in Georgian).

Annals of Agrarian Science

Journal homepage: http://journals.org.ge/index.php

Sustaining paddy production through improved agronomic practices in the Gangetic alluvial zone of West Bengal

Pallabendu Haldar[a], Arindam Sarkar[*b], Manabendra Roy[a], Kabita Chowdhury[c]

[a] AICRP on Integrated Farming System, Directorate of Research, Bidhan Chandra Krishi Viswavidyalaya, Kalyani, Nadia, West Bengal-741235

[b] Regional Research Station (R & L Zone), Bidhan Chandra Krishi Viswavidyalaya, Jhargram, West Bengal-721507

[c] Department of Agricultural Chemistry and Soil Science, Bidhan Chandra Krishi Viswavidyalaya, Mohanpur, Nadia, West Bengal-741252

Received: 26 March 2019; accepted 1 May 2019

ABSTRACT

The article includes the research in Khevi region of Central Great Caucasus. Study area was divided by expositions (north and south), Excessive and imbalanced use of chemical fertilizer in modern agriculture has downgraded soil health. Farmers very often avoid organic fertilizer in crop production due to its unavailability. Stubble removal and other unscientific cultural practices are more likely to enhance soil degradation process and crop production in longer term. Here we undertook an experiment to identify suitable agronomic management practices for paddy cultivation in the Gangetic alluvial zone of West Bengal, India. Interactions between different cropping systems (Rice - Rapeseed - Fodder cowpea, Rice - Field pea - Fodder cowpea and Rice - Wheat - Fodder cowpea) and available nutrient sources through chemical fertilizer alone or in combination with organic fertilizers were studied. Crop uptake of nitrogen, phosphorous and potassium vis-a-vis different yield components as affected by management practices were investigated. Incorporation of leguminous crop (field pea) in the cropping sequence resulted in enhanced nutrient uptake and paddy production than other cropping systems. Application of organic manures mixed with chemical fertilizer has resulted into higher nutrient uptake and crop yield than chemical fertilizers alone. However, there was a significant difference with type of organic manure used. Application of farm yard manure and bio-gas slurry has resulted in maximum nutrient uptake and yield. Farm yard manure and bio-gas slurry being nitrogen poor, have the ability to supply nutrient for a longer time before exhaustion than nitrogen rich vermicompost and azolla. Our findings will be helpful to farmers for better use of their resources in agricultural management.

Keywords: Integrated nutrient management, Paddy cultivation, Cropping sequence, Crop nutrient uptake, Organic manure, Chemical fertilizer.

*Corresponding author: A. Sarkar, E-mail address: arin.psb@gmail.com

Introduction

Paddy is the most important staple crop among cereals in south-west Asia. In India, paddy is cultivated throughout the country, except few dry areas, the Indo-Gangetic plain being most important among them. Muddy soils, which are capable of holding enough water, have advantage of cultivating paddy here over other areas. The use of chemical fertilizer for nitrogen, phosphorous and potassium (NPK) in Indian agriculture is increasing progressively since its introduction to agriculture. It has reached to about 26.5 million tons in 2009-10 from only 78 thousand tons during 1965-66 [1-4]. For a profitable return, farmers are applying chemical fertilizers at the rate higher than recommended dose causing soil health deterioration. Decreasing soil health and crop production in long run resulting from excessive use of imbalanced inorganic fertilizer has been reported elsewhere [5, and references therein]. Leaching and run-off loss of inorganic nutrients pose acute problem of water-body eutrophication [6-9].

Thus society faces both environmental and economic threat. However the farmers are unable to understand the negative impact these type of malpractice.

The integrated nutrient management (INM) aims to find a suitable management practice which should be profitable as well as sustainable for the environment [10-13]. It combines all possible sources of nutrient viz. organic, inorganic and bio-fertilizer and helps us to achieve our goal without environmental degradation [10, 13, 14,]. Organic source of nutrients such as farm yard manures (FYM), vermicomposts, azolla etc. are rich in carbon, nitrogen and other essential compounds [15]. They not only provide the crop nutrient, but also help in improving soil health [10, 16]. However their field requirement is quite high due to lesser concentration of nutrients as compared to inorganic fertilizers [17, 18]. The ability of organic fertilizers to supply nutrient is dependent on nature and composition of material, soil microbial diversity and climatic condition. Sources such as FYM, vermicompost, green manure, bio-gas slurry are all made up of different chemical composition [19]. Thus degradability and crop suitability of these materials are different. The inorganic fertilizers, on the other hand being very concentrated in nutrients are required in lesser quantity [20]. Though their requirement is less, they are found to aggravate soil health degradation [21,22]. Never the less, fertile soils are prerequisite for higher crop yield. Thus we have to find a possible proportion of organic as well as inorganic fertilizers which not only gives profitable return, but protects our soil form further degradation.

Legume crops are essentially beneficial to agriculture. They fix atmospheric inorganic nitrogen and release them in soil, cutting a significant proportion of inorganic nitrogenous fertilizer requirement [23,24]. However their cultivation in Gangetic alluvium belt has declined considerably [25-28]. Farmers prefer cereals and oil seeds over legumes for their daily requirement. Legumes, if incorporated in the cropping sequence increases the chance of further cut down on cost of cultivation, which is also environmentally sound and viable [23, 24].

There are several reports available on influence of organic fertilizer on plant nutrition and crop yield. Applications of farm yard manure, vermicompost, azolla, bio-gas slurry were found to have positive effect on nutrient uptake as well as soil health [10, 14, 20, 21, 29, 30]. However, only few reports [13, 31-33] are available on combined influence of various sources of nutrients (various chemical and organic fertilizers) and different cropping sequence in our study area. We tried to combine various possible nutrient sources and prevalent cropping pattern of the area and investigated interaction effect existed within them. This study will identify the best possible combination of nutrient source and cropping sequence for the whole Indo-Gangetic plain.

We hypothesized that agronomic cropping system and the source of nutrient applied would affect the nutrient supplying capacity of soil, hence crop yield. We considered Rice–Rapeseed–Fodder cowpea, Rice–Field pea–Fodder cowpea and Rice–Wheat–Fodder cowpea cropping sequence for alternative cropping system and FYM, vermicompost, biogas slurry and azolla as possible organic nutrient source besides chemical fertilizer suitable for this region. Our objective was to find out the effect of organic and inorganic sources of nutrients on crop nutrient uptake and productivity of paddy. We also tried to find out the suitability of organic fertilizers in rice cultivation and farming system which aims for sustainable paddy cultivation in the area.

2. Materials and methods

2.1 Site description and experimental design:

The field experiment was conducted during the period of July 2013 to June 2015 at Central Research Farm, Gayeshpur, Nadia, West Bengal (23°8'N and 88°E, 15 MSL), under new alluvial Zone. The field was medium in slope having well irrigation facility. The site receives an average annual rainfall of 1460 mm and the annual temperature varies from 10°C (in January) to 37°C (in April). The initial soil characteristics were reported in Table 1. The experiment was laid out in strip plot design. All the nutritional management treatments were applied to rice, rapeseed, field pea and wheat, whereas fodder cowpea was grown in the residual fertility of the soil. The details of the treatments were listed in Table 2. Recommended cultural practices were followed for all the crops. The rice crop was harvested at 80 % physiological maturity and air dried for 3 days. After drying, the total plant was weighed, threshed and the grain yield was calculated. The straw yield was calculated by deducting grain yield from the total yield. The yield determining parameters of rice viz. number of panicle m^{-2}, number of filled grain panicle^{-1}, panicle weight (g), panicle length (cm) and test weight (g) were recorded after harvesting of the crop.

2.2 Nutrient analysis of soil and plant

The composite surface soil samples (top 15 cm) were collected from 25 different random locations of the experimental field and were mixed thoroughly. Total nitrogen (N) concentration was determined by modified Kjeldahl method [34], whereas hot alkaline $KMnO_4$ method [35] was followed for available N determination. Soil and plant phosphorus (P) concentration was determined by Olsen's method [36] and vanadomloybdo-phosphoric acid yellow color method by [37] respectively. Potassium (K) was determined flame photometry [34]. Crop nutrient uptake (kg ha^{-1}) was calculated by multiplying the concentration (%) of nutrients to the crop yield (kg ha^{-1}) using the following formula,

Nutrient uptake (kg ha^{-1}) = Nutrient concentration (%) × yield (kg ha^{-1}).

2.3 Statistical analysis

All the variables were subjected to ANOVA analysis meant for strip plot design [38] using SPSS (v21.0) software. The standard error of mean (S.Em±) and the value of critical difference (CD) at 5% level of significance were indicated in the tables to compare the difference between the mean values. Pearson correlations were calculated in Microsoft Excel (v2007). Figures were prepared using Sigmaplot (v10).

3. Results and discussion

3.1 Crop nutrient uptake as influenced by management practices:

We studied the changes in crop uptake of nitrogen, phosphorous and potassium (N, P and K) with different nutrient sources and management practice. There was significant variation in nutrient uptake by rice crop within different cropping sequence (C) and nutrient management (M). Generally C_2 cropping sequence reported higher nutrient uptake for N, P and K followed by C_1 and C_3. Though lesser amount of nutrient uptake was found for C_1 cropping sequence, the effect was statistically at par with C_2. The nutrient uptake in C_3 sequence was lowest and significantly differs from the rest. Paddy grain was enriched in N and P (53 and 68 % respectively) than straw (47 and 32 % respectively) except K, where straw retained higher K (77 %) against grain (27 %). Better nutrient uptake with combined application of inorganic and organic fertilizer was reported elsewhere [13, 18, 29, 32, 39]. Higher grain and straw yield was obtained from those plots where higher nutrient uptake was found, since minerals uptake by rice is associated with biomass production [40, 41].

The variation in N uptake with different treatments is reported in Table 3. The pooled data showed total N uptake (grain + straw) varied from 121.95 to 205.21 kg ha^{-1} among treatments. The grain nitrogen uptake (avg. 89.51 kg ha^{-1}) was more than straw (avg. 78.72 kg ha^{-1}). Higher grain and straw N uptake (avg. 93.86 and 82.75 kg ha^{-1} respectively) was found when legume crop, field pea was introduced in the cropping sequence (C_2) as compared to conventional rapeseed (C_1; avg. 90.16 and 79.98 kg ha^{-1}) and wheat (C_3; 84.52 and 79.98 kg ha^{-1}) cultivation practice. However, effect of C_1 and C_2 cropping sequence was statistically at par. Nitrogen uptake in terms of nutrient management practice (M) was different when organic and chemical fertilizer was applied in different combination. Higher grain and straw uptake was found in case of M_1 (avg. 96.21 and 85.11 kg ha^{-1} respectively), M_2 (avg. 99.05 and 86.33 kg ha^{-1} respectively) and M_3 (avg. 98.72 and 88.13 kg ha^{-1} respectively) followed by M_4 (avg. 80.00 and 68.99 kg ha^{-1} respectively) and M_5 (avg. 73.59 and 65.05 kg ha^{-1} respectively). Farm yard manure (FYM) incorporation (M_2) had resulted highest grain uptake (avg. 99.05 kg ha^{-1}), whereas straw uptake was highest when biogas slurry (M_3; avg. 88.13 kg ha^{-1}) was applied. However the difference between M_1, M_2 and M_3 was statistically insignificant.

Significant variation in P uptake was observed (Table 3) in rice grain and straw due to the variation in nutritional management treatments during both the years of investigation. Phosphorous uptake closely followed N uptake trend. Highest grain P uptake was recorded in C_2 cropping sequence (19.78 kg ha^{-1}) followed by C_1 (18.11 kg ha^{-1}) and C_3 (16.72 kg ha^{-1}). Though C_1 and C_2 produced similar effect, it was significantly low in C_1. Similar variation was found for straw P uptake. Highest concentration was found in C_2 (9.81 kg ha^{-1}) followed by C_3 (8.02 kg ha^{-1}) and C_1 (7.95 kg ha^{-1}). Among different management practices, higher grain and straw P uptake was found in M_2 (22.72 and 11.20 kg ha^{-1} respectively) followed by M_3 (21.09 and 10.52 kg ha^{-1}) and M_1 (19.62 and 9.83 kg ha^{-1}). Lowest amount of grain and straw P uptake was found in M_4 (14.70 and 6.61 kg ha^{-1}) and M_5 (12.89 and 4.80

kg ha^{-1}). Statistical analysis revealed M_1, M_2 and M_3 yielded statistically similar P uptake, whereas M_4 and M_5 produced poor results.

Highest grain K uptake was found in C_2 (25.59 kg ha^{-1}) followed by C_1 (24.32 kg ha^{-1}), however there was no significant variation (Table 3). Least uptake was recorded in C_3 (23.03 kg ha^{-1}) where Rice - Wheat - Fodder cowpea sequence was followed. Higher straw uptake was found in C_2 (72.22 kg ha^{-1}) followed by C_3 (67.58 kg ha^{-1}) and C_1 (67.13 kg ha^{-1}). However their effect was statistically at per. When it comes to nutrient management, grain K uptake in M_2 (29.12 kg ha^{-1}) and M_3 (28.08 kg ha^{-1}) was higher than the rest M_1, M_4 and M_5 (25.33, 20.41 and 18.62 kg ha^{-1} respectively). Straw K uptake was found to be higher in M_3 (99.37 kg ha^{-1}) followed by M_2 (96.91 kg ha^{-1}) and M_1 (90.93 kg ha^{-1}). Straw K uptake in M_4 and M_5 (75.13 and 70.30 kg ha^{-1} respectively) was significantly lower than others.

Figure 1 shows the interaction effect between cropping sequence (C) and nutrient management (M) for N, P and K uptake. There was significant variation between treatments. Cropping sequence C_2 along with M_2 nutrient management yielded best result in nutrient uptake (205.21, 39.31 and 109.56 kg ha^{-1} respectively for N, P and K). Field pea and cowpea being a leguminous crop in cropping sequence helps in fixing atmospheric N, improving soil nutrient status. The effect was further amplified when FYM was incorporated in the nutrient management system (M_2). Farm yard manure being rich in carbonaceous and lignin compound helps in restoring soil health and better nutrient uptake [42 and references therein]. Application of both organic and inorganic fertilizer together helps in slow release of nutrient, thus enhanced nutrient use efficiency [16, 43]. They also stimulate soil microbial activity, crop root growth and reduced nutrient loss resulting better uptake of water and nutrient [44]. However the effect was statistically insignificant when compared to other nutrient management line except M_4 and M_5 (against C_2). Similarly, C_1 and C_3 yielded comparable results with M_1, M_2 and M_3. Several reports [30,45] were available showing positive influence of vermicompost (M_4) and azolla (M_5) on crop nutrient uptake and yield. However, we didn't find any significant impact of them on nutrient uptake. Azolla and vermicompost being N rich is preferentially decomposed and have quicker turnover rate relative to FYM [46]. Thus, vermicompost and azolla may act as source of nutrients, but it might not be able to supply nutrients during entire crop duration or would have to apply in higher amount to achieve desired crop production.

3.2 Influence of cultural management on paddy yield and yield components:

Our data revealed significant variation in panicle no m^{-2} with different treatments. Highest no (315 panicle m^{-2}) was found under legume cropping sequence, where as other cropping sequence resulted similar panicle initiation (249 panicle m^{-2}). However, when compared within different nutrient sources, no significant difference was found within M_1, M_2 and M_3 (264, 265 and 267 respectively; see Table 4). However, M_4 and M_5 reported lowest no of panicle m^{-2} (247 and 231 respectively). The Fig. 2a shows the interaction effect between cropping sequence and nutrient sources. Best result was found in C_2M_2, followed by C_2M_3 and C_2M_1 (283, 278 and 275 panicle m^{-2} respectively). Adequate and sustained nutrient supply during vegetative growth stage might have resulted higher panicle no m^{-2} in these treatments [40, 41]. Among the nutrient sources M_4 and M_5 yielded poor result with cropping sequence (C).

The no of filled grain panicle^{-1} varied significantly among treatments. Best result was found in C_2 (163 grain panicle^{-1}; Table 4), i.e. when legume crop was incorporated in the cropping sequence. This was significantly higher than C_1 and C_3 (155 and 147 grain panicle^{-1} respectively). Similar range of result was found when different sources of nutrients (168, 163 and 163 grain panicle^{-1} for M_1, M_2 and M_3 respectively) were considered. However M_4 and M_5 yielded significantly lower no of filled grain panicle^{-1} (145 and 134 grain panicle^{-1} respectively). Figure 2b shows the interaction effect between cropping sequence and nutrient sources. The C_2M_2, like other parameter produced best result (189 grain panicle^{-1}), followed by C_2M_3 (175 grain panicle^{-1}). Legume crop incorporation and addition of organic fertilizer ensured sufficient nutrient supply during flowering to physiological maturity stage [41]. Reduced amount of N supply in M_4 and M_5 during this stage might have reduced no of filled grain panicle^{-1}.

Table 4 shows the variation in Panicle weight (g), panicle length (cm) and test weight. Highest panicle weight, panicle length and test weight was found in C_2 (2.65 g, 27.2 cm and 21.99 g respectively), followed by C_1 (2.55 g, 26.8 cm and

21.39 g respectively) and C_3 (2.47 g, 26.9 cm and 20.93 g respectively). Though the effect of C_1 was statistically at per C_2; C_3 produced significantly lower values. Among nutrient management, M_2 (2.66 g, 27.4 cm and 22.71gm respectively) proved to be superior to others. However there were no significant difference in terms of panicle weight, panicle length and test weight among various nutrient sources. The interaction effect between the cropping sequence and nutrient sources were presented in Fig. 3. Except for panicle weight, C_2M_2 reported maximum values. However we didn't find any significant difference between treatment combinations for these components.

The grain yield, straw yield and harvest index were presented in Table 9. Highest grain yield of 4.74 t ha^{-1} was obtained in cropping sequence C_2 to which leguminous crop was incorporated, followed by C_1 (4.66 t ha^{-1}). The yield was significantly lower when wheat crop was grown after rice (C_3; 4.42 t ha^{-1}). Similarly higher yield was obtained from M_2 (5.08 t ha^{-1}) where FYM was a significant source component followed by M_3 and M_1 (5.01 and 4.84 t ha^{-1} respectively). However the yield was significantly lower when either vermicompost (M_4; 4.18 t ha^{-1}) or azolla (M_5; 3.91 t ha^{-1}) was used as organic source of nutrient besides inorganic sources. Similar results were recorded for straw yield. Cropping sequence C_2 resulted better straw yield followed by C_1 and C_3. Though M_2 was better in case of grain yield than M_3, latter performed better when straw yield was considered. However, the effect of M_3, M_2 and M_1 was statistically insignificant. Straw yield from M_4 and M_5 was significantly lower than the others. Grain harvest index of rice did not change significantly in different treatments. However, incorporation of leguminous crop (C_2) and use of FYM as nutrient source (M_2) yielded better results than others.

Figure 4 shows the interaction effect of cropping sequence and nutrient sources on paddy yield parameters. The treatment combination of C_1M_3 yielded highest grain and straw, followed by C_2M_2 and C_2M_3. Though C_1N_3 was found best, interaction effect between line C_1, C_2 and M_1, M_2, M_3 was statistically similar. However, the treatment combination between line M_4, M_5 and C_1, C_2, C_3 produced lowest grain and straw yield and was statistically significant compared to others.

We found strong to very strong correlation ($p<0.001$) between the nutrient uptake and paddy yield parameters (Table 5). Very strong correlation between N, P and K indicates co-adsorption of nutrients by plants. Though all the nutrients (N, P and K) were strongly correlated with other yield parameters, the association of N was strongest ($r=0.98$, $p<0.001$). This suggests primary role of N on growth and yield of crops. Researchers have found N in adequate account accounted 75 to 90% variation in yield component [41]. Association of number of panicle m^{-2}, number of filled grain $panicle^{-1}$ and panicle wt with N, P and K were mostly very strong ($r > 0.8$, $p< 0.001$). Though panicle length is known to be influenced by nutrient uptake [41], we found only moderate correlation ($r=0.62$ to 0.75, $p<0.001$). Very strong correlation ($r > 0.9$, $p<0.001$) between grain and straw yield and NPK indicates influence of nutrient uptake on dry matter accumulation and subsequent crop yield [39, 40, 44]. Researchers have found positive associations of harvest index with grain yield and nutrient uptake. However, we found weak correlation between them. Climatology, location, and ecology of the study area might be responsible for rendering their association. The plots where nutrient uptake was higher were found to produce higher yield. Improved soil health from balanced use of organic and inorganic fertilizers has resulted in enhanced and sustained nutrient uptake from soils during entire crop growth period, increased biomass production and crop yield [41].

4. Conclusion

We studied the influence of cropping system and nutrient sources on crop nutrient uptake and paddy yield. Few treatment combination produced better results in terms of nutrient uptake and yield and were statistically significant than others. Nutrients uptake and yield was highest when leguminous crop field pea was incorporated in the cropping system (C_2). Leguminous crops fixed atmospheric nitrogen to soil as plant available form, which in turn helped in better nutrient uptake and therefore crop yield. However, C_1 and C_3 produced statistically similar result to C_2. However their (C line) interaction with external nutrient source (M line) varied significantly in terms of nutrient uptake and crop yield. Though their effect was similar on nutrient uptake and yield, their effect on soil environment might be different. Among different external nutrient sources, use of farm yard manure (FYM) alongside chemical fertilizer was found to be superior. Organic carbon rich FYM was able to sustain the crop nutrient supply during the entire crop duration. Higher nutrient uptake due to FYM application (in M_2)

was able to produce highest grain and straw yield in our study area. However, influence of chemical fertilizer alone or with biogas slurry (treatment M_1 and M_3 respectively) were statistically at par with M_2 in respect of nutrient uptake and yield. Though reports are available on positive influence of vermicompost and azolla (treatment M_4 and M_5 respectively), we found significantly less nutrient uptake and crop yield with their application. Azolla and vermicompost are nitrogen rich are preferentially degraded over carbon rich organic fertilizer such as FYM. Slow release of nutrient for longer time with FYM application might have out-performed nitrogen rich materials. Integration of these locally available fertilizer sources with dominant cropping system helped us to identify the best suitable cropping pattern and fertilizers to be applied for sustainable agriculture and net return. This study will also help policy makers to make certain to sustain agricultural production of India.

However, further study is required to understand possible nutrient dynamics and their uptake. Microbial diversity study and isotope tracing technique can help us to understand the changes going on in soil upon application of these fertilizers. These studies also make understand why some are out-performing others in terms of nutrient uptake and crop production. Studies may also be conducted with other available nutrient sources, such as sewage-sludge, fly ash from thermal power plant and their influence on crop production.

5. Acknowledgement

We thank Honorable Vice Chancellor and Directorate of Research, BCKV for their encouragement and necessary permission for carrying out the research. Authors are also grateful to ICAR for providing fund.

Reference

[1] V.P. Sharma, H. Thaker, Demand for Fertiliser in India: Determinants and Outlook for 2020. Indian Institute of Management, 2011.

[2] W. Hopper, Indian Griculture and Fertilizer: An Outsider's Observations. In Keynote address to the FAI Seminar on Emerging Scenario in Fertilizer and Agriculture: Global Dimensions. New Delhi: FAI, 1993.

[3] P.K. Jaga, Y. Patel, An overview of fertilizers consumption in India: determinants and outlook for 2020-a review. International J. of Scientific Engineering and Technology, 1(6) (2012) 285-291.

[4] Fertiliser Association of India, Fertiliser Statistics 2009-10 and Earlier Issues. The Fertiliser Association of India, New Delhi, 2010.

[5] S. Savci, Investigation of effect of chemical fertilizers on environment. APCBEE Procedia, 1 (2012) 287-292.

[6] D.O. Hessen, A. Hindar, G. Holtan, The significance of nitrogen runoff for eutrophication of freshwater and marine recipients. Ambio (1997) 312-320.

[7] R. Bhateria, D. Jain, Water quality assessment of lake water: a review. Sustainable Water Resources Management, 2(2) (2016) 161-173.

[8] B. Moss, Water pollution by agriculture. Philosophical Transactions of the Royal Society B: Biological Sciences, 363(1491) (2007) 659-666.

[9] G.D. Agrawal, Diffuse agricultural water pollution in India. Water science and technology, 39(3) (1999) 33-47.

[10] S.K. Zaman, M. Jahiruddin, G.M. Panaullahi, M.H. Mian, M.R. Islam, Integrated nutrient management for sustainable yield in rice-rice cropping system. In 17th World Congress of Soil Science, Bangkok (Thailand) (2002) 14-21 Aug.

[11] M. Arif, M. Tasneem, F. Bashir, G. Yaseen, R.M. Iqbal, Effect of integrated use of organic manures and inorganic fertilizers on yield and yield components of rice. J. of Agricultural Research, 52(2) (2014) 197-208.

[12] M.S. Aulakh, C. A. Grant, Integrated Nutrient Management for Sustainable Crop Production. The Haworth Press, Taylor and Francis Group: New York 2008.

[13] A.K. Patra, B. C. Nayak, M. M. Mishra, Integrated nutrient management in rice (Oryza sativa)-wheat (Triticum aestivum) cropping system. Indian J. of Agronomy, 45 (2000) 453-457.

[14] M.M. Islam, A. J. M. S. Karim, M., Jahiruddin, N. M. Majid, M. G. Miah, M. M. Ahmed, M. A. Hakim, Effects of organic manure and chemical fertilizers on crops in the Radish-Stem Amaranth-Indian spinach cropping pattern in homestead area. Australian J. of Crop Science, 5 (2011) 1370-1378.

[15] B. Gagnon, R. Lalande, S.H. Fahmy, Organic matter and aggregation in a degraded potato soil as affected by raw and composted pulp residue. Biology and fertility of soils, 34 (2001) 441-447.

[16] W. Mojeremane, M. Motladi, T. Mathowa, G.M. Legwaila, Effect of different application rates of organic fertilizer on growth, development and yield of rape (Brassica napus L.). International Journal of Innovative Research in Science, Engineering and Technology, 4(12) (2015) 11680-8.

[17] D. Alexander, S. Rajan, L. Rajamony, K. Ushakumari, S. Kurien, The adhoc Package of Practices recommendations for organic farming. Organic Farming, (2009).

[18] A.A. Ahmad, T.J. Radovich, H.V. Nguyen, J. Uyeda, A. Arakaki, J. Cadby, R. Paull, J. Sugano, G. Teves, Use of organic fertilizers to enhance soil fertility, plant growth, and yield in a tropical environment. In Organic Fertilizers-From Basic Concepts to Applied Outcomes. InTech, (2016).

[19] H.K. Murwira, P. Mutuo, N. Nhamo, A.E. Marandu, R. Rabeson, M. Mwale, C.A. Palm, Fertilizer equivalency value of organic materials of different quality. In B. D. Vanlauwe, Integrated plant nutrient management in Sub-Saharan Africa: From concept to practice. Trowbridge, UK: CAB International, (2002) 113 – 122.

[20] J.H. Chen, The combined use of chemical and organic fertilizers and/or biofertilizer for crop growth and soil fertility. In International workshop on sustained management of the soil-rhizosphere system for efficient crop production and fertilizer use. Land Development Department Bangkok Thailand, 16 (2006) 20.

[21] M.S. Khan, N.C. Shil, S. Noor, Integrated Nutrient Management for sustainable yield of major vegetable crops in Bangladesh. Bangladesh J. of Agriculture and Environment, 4 (2008) 81-94.

[22] S. Savci, An agricultural pollutant: chemical fertilizer. International J. of Environmental Science and Development, 3(1) (2012) 77-80.

[23] W.R. Stern, Nitrogen fixation and transfer in intercrop systems. Field crops research, 34 (1993) 335-356.

[24] P. Singh, B. Shahi, K.M. Singh, Enhancing Pulses Production in India for Improved Livelihood and Nutritional Security: An Analysis of Constraints and Strategies, (2016) DOI: http://dx. doi. org/10.13140/RG, 2(30789.24805).

[25] C. Johansen, J.M. Duxbury, S.M. Virmani, C.L.L. Gowda, S. Pande, P.K. Joshi, Legumes in rice and wheat cropping systems of the Indo-Gangetic Plain-Constraints and opportunities. International Crops Research Institute for the Semi-Arid Tropics, 2000.

[26] A. Ramakrishna, C.L.L. Gowda, C. Johansen, Management factors affecting legumes production in the Indo-Gangetic Plain. (2000) 156-165.

[27] A.K. Singh, S.S. Singh, V. Prakash, S. Kumar, S.K. Dwivedi, Pulses production in India: present status, bottleneck and way forward. J. of AgriSearch, 2(2) (2015) 75-83.

[28] M. Ali, P. K. Joshi, S. Pande, M. Asokan, S. M. Virmani, Ravi Kumar, B. K. Kandpal, Legumes in the Indo-Gangetic Plain of India. (2000) 35-70.

[29] P.K. Saha, M. Ishaque, M.A. Saleque, M.A.M. Miah, G.M. Panaullah, N.I. Bhuiyan, Long-Term Integrated Nutrient Management for Rice-Based Cropping Pattern: Effect on Growth, Yield, Nutrient Uptake, Nutrient Balance Sheet, and Soil Fertility. Communications in Soil Science and Plant Analysis, 38 (2007) 579-610.

[30] S.I. Hyder, S.A. Tariq Sultan, T. Tabssam, A. Ali, M.A. Ullah, Optimizing Yield and Nutrients Content in Peas by Integrated Use of Bio-Organic and Chemical Fertilizers. International Journal, 37 (2016).

[31] S.S. Tomar, A. Singh, A. Dwivedi, R. Sharma, R.K. Naresh, V. Kumar, S. Tyagi, A.S. Rahul, B.P. Singh, Effect of integrated nutrient management for sustainable production system of maize (Zea mays L.) in indo-gangetic plain zone of India. International J. of Chemical Studies, 5(2) (2017) 310-316.

[32] S.K. Kakraliya, R.D. Jat, S. Kumar, K.K. Choudhary, J. Prakash, L.K. Singh, Integrated nutrient management for improving, fertilizer use efficiency, soil biodiversity and productivity of wheat in irrigated rice wheat cropping system in Indo-Gangatic plains of India. International J. of Current Microbiology and Applied Sciences, 6(3) (2017) 152-63.

[33] B. Biswas, D.C. Ghosh, M.K. Dasgupta, N. Trivedi, J. Timsina, A. Dobermann, Integrated

assessment of cropping systems in the Eastern Indo-Gangetic plain. Field crops research. 99(1) (2006) 35-47.
[34] M.L. Jackson, Soil Chemical Analysis, Prentice Hall of India Pvt. Ltd. New Delhi, India, 1973.
[35] B.V. Subbiah, G.L. Asija, A rapid method for the estimation of nitrogen in soils. Current Science, 26 (1956) 259-260.
[36] S.R. Olsen, C.V. Cole, F.S. Watanabe, L.A. Dean, Estimation of available phosphorus in soils by extraction with sodium bicarbonate. US Department of Agriculture Circular, 939 (1954) 1-19.
[37] R. Koenig, C. Johnson, Colorimetric determination of phosphorus in biological materials. Industrial and Engineering Chemistry Analytical Edition, 14 (1942), 155-156.
[38] K.A. Gomez, A.A. Gomez, Statistical Procedures for Agricultural Research. John Wiley and Sons, New York, 1984.
[39] S. Dasgupta, A. Sarkar, A.K. Chaitanya, A. Saha, A. Dey, R. Mondal, Response of Potato Crop to Integrated Nutrient Management in the Indo-Gangetic Alluvial Soils of West Bengal, India. J. of Experimental Agriculture International, 16 (2017) 1-10.
[40] S. Matsushima, Nitrogen requirements at different stages of growth. In The Minerals Nutrition of the Rice Plant; John Hopkins University Press: Baltimore, MD, (1964) 199–218.
[41] N.K. Fageria. Mineral Nutrition of Rice. CRC Press, Taylor & Francis Group, (2014) 541.
[42] P.K. Bandyopadhyay, S. Saha, S. Mallick, Comparison of Soil Physical Properties betweena Permanent Fallow and a Long-Term Rice–Wheat Cropping with Inorganic and Organic Inputsin the Humid Subtropics of Eastern India. Communications in Soil Science and Plant Analysis, 42 (2011) 435-449.
[43] G.B. Singh, P.P. Biswas, Balanced and integrated nutrient management for sustainable crop production. Indian J. of Fertilizers, 45 (2000) 55-60.
[44] K.N. Devi, M.S. Singh, N.G. Singh, H.S. Athokpam, Effect of integrated nutrient management on growth and yield of wheat (Triticum aestivum L.). J. of Crop and Weed, 7(2) (2011) 23-27.
[45] R. Kumar, B.C. Deka, M. Kumar, S.V. Ngachan, Productivity, Quality and Soil Health as Influenced by Organic, Inorganic and Biofertilizer on Field Pea in Eastern Himalaya. J. of Plant Nutrition, 38 (2015) 2006-2027.
[46] A.S. Grandy, G.P. Robertson, Land use intensity effects on soil C accumulation rates and mechanisms. Ecosystems, 10(1) (2007) 58-73.

Table 1. *Initial physico-chemical properties of the experimental soil*

Particulars	
Sand (%)	36.8
Silt (%)	28.0
Clay (%)	35.2
Textural class	Clay-loam
Bulk density (g cm^{-3})	1.53
Soil pH	6.84
EC	0.24
Organic carbon (%)	0.66
Available N (kg ha^{-1})	147.84
Available P_2O_5 (kg ha^{-1})	18.24
Available K_2O (kg ha^{-1})	125.25

Table 2. *Details of the treatments employed in the experiment*

Vertical strips (Cropping system; C):	
C_1	Rice –Rapeseed – Fodder cowpea
C_2	Rice – Field pea – Fodder cowpea
C_3	Rice – Wheat – Fodder cowpea
Horizontal strips (Nutrient management; M):	
M_1	100% Recommended dose of Fertilizers (RDF) through chemical fertilizer (CF)
M_2	75% RDN through CF +25% N through FYM+ 100% RD of PK through CF
M_3	75% RDN through CF +25% N through Biogas Slurry + 100% RD of PK through CF
M_4	75% RDN through CF +25% N through Vermicompost + 100% RD of PK through CF
M_5	75% RDN through CF +25% N through Azolla+ 100% RD of PK through CF

Table 3. *Changes in nitrogen (N), phosphorus (P) and potassium (K) uptake with different agronomic practices (two years pooled data)*

Treatments	N uptake		P uptake		K uptake	
	Grain N (kg ha-1)	Straw N (kg ha^{-1})	Grain P (kg ha^{-1})	Straw P (kg ha^{-1})	Grain K (kg ha^{-1})	Straw K (kg ha^{-1})
Cropping system						
C1	90.16	79.98	18.11	7.95	24.32	67.13
C2	93.86	82.75	19.78	9.81	25.59	72.22
C3	84.52	73.45	16.72	8.02	23.03	67.58
SEm ±	1.51	1.89	0.34	0.20	0.50	1.80
CD (p=0.05)	4.93	6.18	1.12	0.64	1.64	5.86
Nutrient management						
M1	96.21	85.11	19.62	9.83	25.33	74.05
M2	99.05	86.33	22.72	11.20	29.12	76.93
M3	98.72	88.13	21.09	10.52	28.08	76.81
M4	80.00	68.99	14.70	6.61	20.41	62.39
M5	73.59	65.05	12.89	4.80	18.62	54.69
SEm ±	3.69	2.14	0.83	0.35	0.94	2.47
CD (p=0.05)	11.07	6.41	2.48	1.06	2.83	7.39

Table.4. *Variation in paddy yield parameter as influenced by various agronomic practices (two years pooled data)*

Treatments	Number of panicle m^{-2}	Number of filled grain $panicle^{-1}$	Panicle weight (g)	Panicle length (cm)	Grain yield (t ha^{-1})	Straw yield (t ha^{-1})	Harvest index (%)
Cropping system							
C1	249	155	2.55	26.8	4.66	6.64	41.08
C2	267	163	2.65	27.2	4.74	6.77	41.10
C3	249	147	2.47	26.9	4.42	6.37	40.82
SEm ±	3.1	1.3	0.03	0.07	0.05	0.07	0.28
CD (p=0.05)	10.2	4.3	0.11	0.24	0.15	0.24	NS
Nutrient management							
M1	264	168	2.63	27.2	4.84	6.96	40.89
M2	265	163	2.66	27.4	5.08	7.07	41.69
M3	267	163	2.66	27.2	5.01	7.15	41.08
M4	247	145	2.52	26.8	4.18	6.01	41.02
M5	231	134	2.33	26.3	3.91	5.77	40.33
SEm ±	4.9	3.4	0.05	0.17	0.17	0.12	0.53
CD (p=0.05)	14.7	8.6	0.16	0.50	0.50	0.37	NS

Table.5. *Correlation between NPK uptake and yield parameters*

	N Uptake	*P Uptake*	*K Uptake*	*Panicle m^{-2}*	*Filled grain $panicle^{-1}$*	*Panicle wt (g)*	*Panicle length (cm)*	*Test Weight (g)*	*Grain yield (t ha^{-1})*	*Straw yield (t ha^{-1})*	*Harvest Index*
N Uptake	1.00										
P Uptake	0.94[a]	1.00									
K Uptake	0.95[a]	0.93[a]	1.00								
Panicle m^{-2}	0.85[a]	0.86[a]	0.82[a]	1.00							
Filled grain $panicle^{-1}$	0.83[a]	0.85[a]	0.73[a]	0.84[a]	1.00						
Panicle wt (g)	0.75[a]	0.76[a]	0.64[a]	0.80[a]	0.80[a]	1.00					
Panicle length (cm)	0.63[a]	0.69[a]	0.70[a]	0.80[a]	0.54[b]	0.42	1.00				
Test Weight (g)	0.76[a]	0.86[a]	0.75[a]	0.69[a]	0.71[a]	0.71[a]	0.53[b]	1.00			
Grain yield (t ha^{-1})	0.98[a]	0.93[a]	0.96[a]	0.79[a]	0.77[a]	0.71[a]	0.62[a]	0.74[a]	1.00		
Straw yield (t ha^{-1})	0.98[a]	0.93[a]	0.95[a]	0.80[a]	0.77[a]	0.72[a]	0.57[a]	0.74[a]	0.98[a]	1.00	
Harvest Index	0.48[b]	0.49[b]	0.49[b]	0.42	0.40	0.32	0.58[a]	0.38	0.57[a]	0.39	1.00

'a' and 'b' indicates significance level at p <0.001 and 0.01 respectively (n= 30)

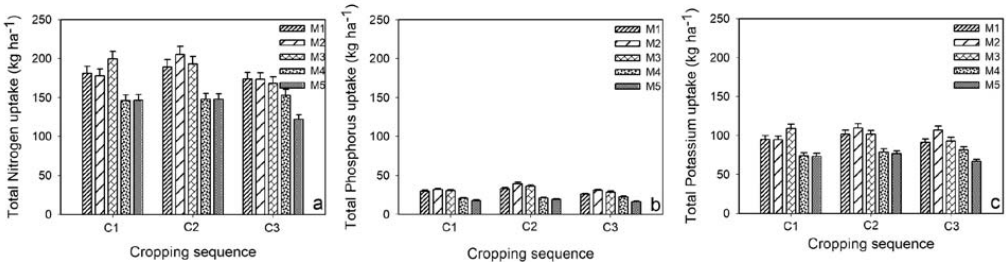

Fig. 1a, b, c. *Interaction effect between cropping sequence (C) and nutrient management (M) for N, P and K uptake respectively*

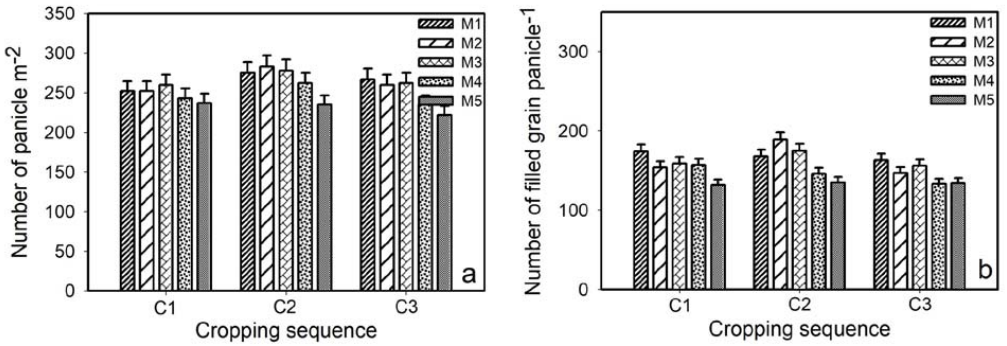

Fig. 2a, b. *Interaction effect between cropping sequence (C) and nutrient management (M) for number of panicle m^{-2} and number of filled grain $panicle^{-1}$ respectively*

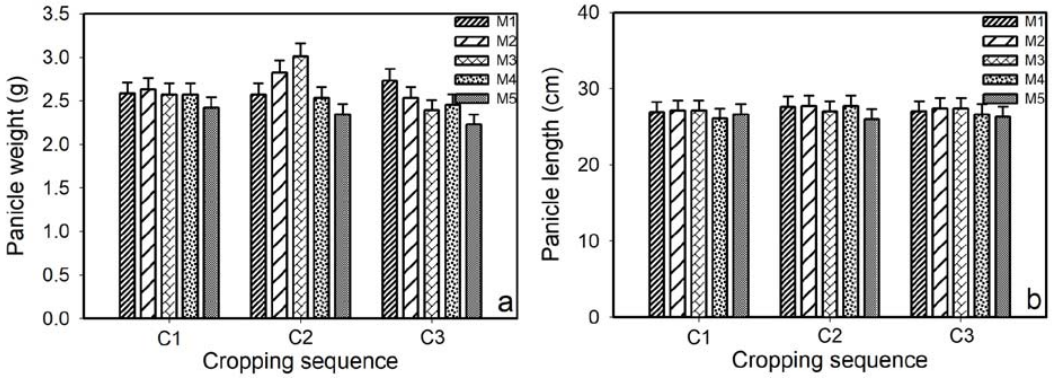

Fig. 3a, b. *Interaction effect between cropping sequence (C) and nutrient management (M) for panicle weight (g) and panicle length (cm) respectively*

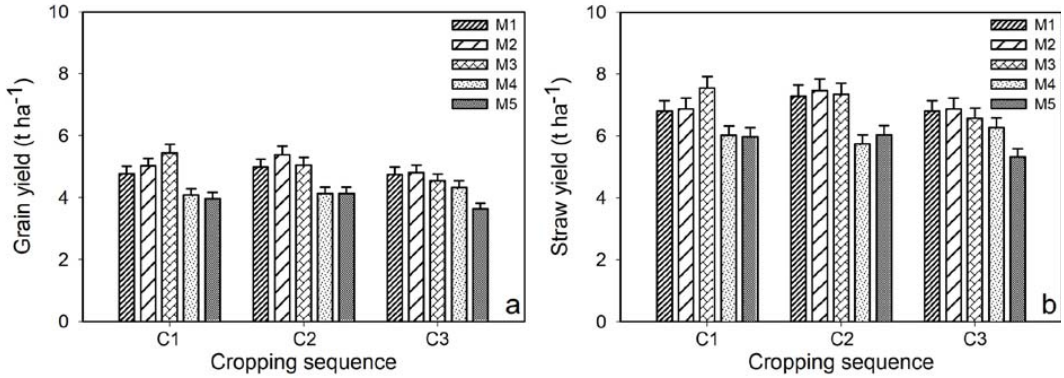

Fig. 4a, b. *Interaction effect between cropping sequence (C) and nutrient management (M) for grain yield and straw yield respectively*

Annals of Agrarian Science

Journal homepage: http://journals.org.ge/index.php

On the approach to the complex research into the vibratory technological process and some factors having an influence on the process regularity

Viktor Zviadauri

Dvali Institute of Machine Mechanics, 10, Mindeli Str., Tbilisi, 0187, Georgia

Received: 15 June 2018; accepted: 12 September 2018

A B S T R A C T

Vibratory transportation and technologic machines are widely used for transportation and processing of the friable materials in many spheres of industry (agriculture, mining industry, construction etc.). At the same time, many factors influencing the process are not thoroughly revealed; among them, influence of so called parasitic vibrations of the working member is not studied sufficiently. A three-mass vibratory system, an analogue of the vibratory transportation and technologic system "vibro-drive – working member – technologic load" was studied holistically. A relevant mathematical model of the spatial interconnected vibratory movement is drawn up in the form of the differential equations. The real possible reasons of generation of the spatial vibrations in the mentioned systems and possibility of their influence on the technologic process are considered. The influence of the constructional errors and resulting spatial (non-working) vibrations of the working member on the regularity of the friable material vibratory movement is studied by mathematical modeling. The researches have shown that some non-working (so called parasitic) vibrations in combination with the basic vibrations can improve the technological process - increase intensity of movement of the friable material. The graphical illustrations are presented.

Keywords: Vibratory system, Spatial vibrations, Vibratory displacement, Mathematical modeling, Friable material; Vibratory technology.

*Corresponding author: Viktor Zviadauri; E-mail addess: v_zviadauri@yahoo.com

1. INTRODUCTION

The vibratory technologic processes are in fact the useful movements of the friable materials and single small parts under influence of vibrations: transportation, metered feeding, sorting, mixing and etc.[1-4].

The vibratory technologic machines and processes are widely used in metallurgy, construction, mining industry, agriculture, chemical industry and confectionaries [5-7].

A vibratory technologic process is a dynamically sensitive process in which participate many physically different components: vibro-drive, elastic system, working member (absolutely rigid or of finite rigidity), diverse friable loads. Dynamical interaction of these components stipulates behavior of the friable material on the working member surface.

The mathematical models of vibratory transportation and technological processes presented in the existent researches [1, 2, 5] are mostly simplified. For example, non-linear excitation is replaced by harmonic vibrations; reaction of the material on the working member is provided by

so called coefficient of connection that is 1/3 of the whole mass; non-working vibrations that accompany vibratory technologic processes and have influence on them, are not often taken into account neither etc. Because of such approaches many nuances that could be important from the standpoint of influence on the process, are ignored.

Consequently, the attempt is made in the work to create a more or less universal model, where more perfect mathematical description of the vibratory transportation and technologic processes of the friable materials and study of influence of various parameters on the process would be possible.

2. A DYNAMICAL MODEL

Since a vibratory technologic process is in fact a vibratory movement of the system "vibro-drive – working member – technologic load" in space then it is evident that besides pre-determined working vibrations the working member and consequently technologic load can be subjected to non-working (spatial) vibrations [4, 8] not envisaged by the calculation.

This in the first place concerns the spatial, so called parasitic vibrations of the working member that can be caused by various factors such as inaccuracy of transmission of the exciting force, errors of relative disposition of the vibratory machine units, elastic specificity and etc.

In Fig.1 is presented a two-mass system "vibro-drive – working member" and are shown deviations of the working member caused by various possible errors: I – nominal (designed) position of the working member; II – position of the working member considering the errors including the eccentricities e_x, e_y, e_z of displacement of the center of gravity from position O_1 to point $O_1^{'}$; $\theta_0, \psi_0, \varphi_0$ - turnings of the coordinate axes caused by the assembly errors of the vibratory machine and transition from position $O_1x_1y_1z_1$ to position $O_1^{'}x_1^{'}y_1^{'}z_1^{'}$ (Fig.1 a, b); III – dynamical (working) position of the working member. System of coordinates $O_vx_vy_vz_v$ is connected to the vibro-drive; 1 – basic elastic system of the vibro-machine; 2 – suspensions of the vibro-machine; Q – exciting force; m_v, m_1 – masses of the vibro-drive and working member.

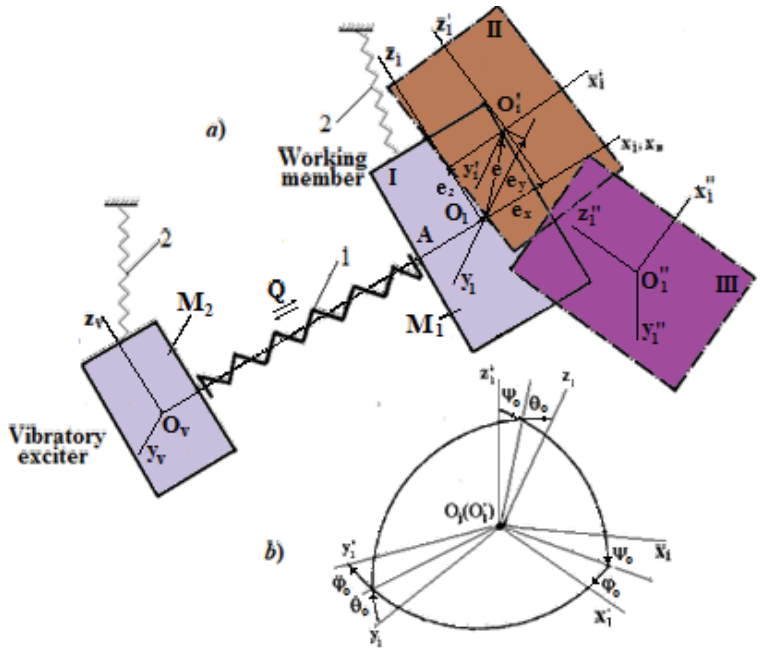

Fig. 1. *The Average Clinical Indicators of the Cows*

In the Fig.2 are shown spatial schemes of the three-mass spatial vibratory system, a generalized dynamical model of the vibratory technologic system "vibro-drive – working member – technologic load" (Fig.2a), elastic system of the vibro-drive – working member (Fig.2c) and conventional elastic system of the technologic load (Fig.2b). At that, the latter imitating phenomenological properties of the friable material is restricted unilaterally by the working member surface.

For full description of the spatial vibratory movement of the presented system it is expedient to use classical methods of relative movement of rigid bodies [8]. For this purpose a friction material (load) is presented as a rigid body in the form of cube where total mass of the load is located and which is provided with conventional elastic elements describing phenomenological properties and elastic and damping connections between layers as well as with surfaces of the working member [4, 9].

For obtaining general vector expressions of the kinetic energy of a body it is necessary to determine absolute movement of a free point of this body. Such points in Fig.2 are A_i (M_1), B_i (M_2), C_i (M_3) that are connected to the origins of the own coordinate axes as well as to the origins of coordinate axes inertial relative to them. Besides, mass M_3 is connected to mass M_2 at the center of gravity (at the origin of coordinate system).

Consider expressions of each component part of the three-mass system (Fig, 2a). Vector equations of absolute velocities of free points A_i, B_i, C_i of masses M_1, M_2 and M_3 have the form:

$$V_{Ai} = V_{01} + \omega_{01} \times r_{1i}\,;\;\; V_{Ci} = V_{02} + \omega_{02} \times r_{2i}\,;\; V_{Bi} = V_{01} + \omega_{01} \times R_{3i} + V_{03} + \omega_{03} \times r_{3i}, \quad (R_{3i} = R_3 + r_{3i}) \quad (1)$$

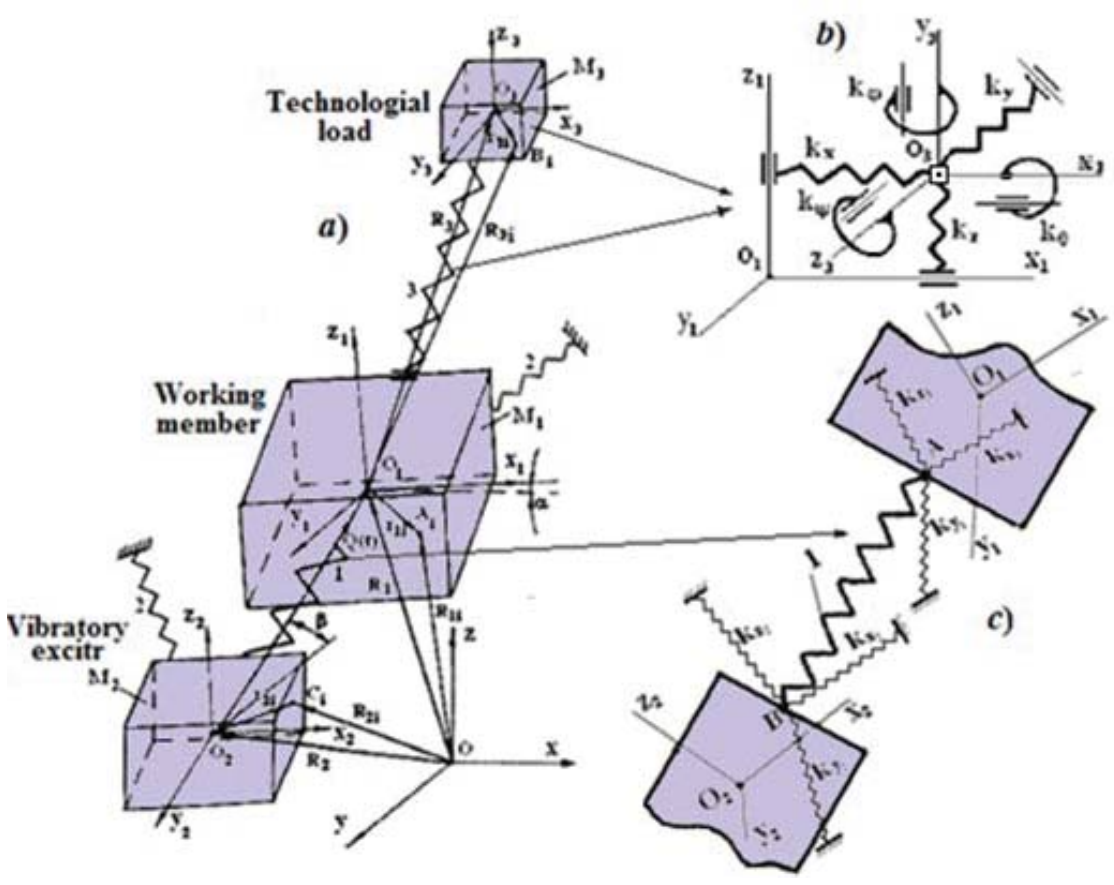

Fig. 2. *Three-mass spatial vibratory system – an analogue of the vibratory technologic system "vibro-drive – working member – technologic load"*

where V_{01}, V_{02} are translatory velocities of the particles A_i and C_i ; r_{1i}, r_{2i}, r_{3i} – position vectors of the particles A_i, B_i, C_i ; ω_{o1}, ω_{o2}, ω_{o3} – velocities of rotary movement of masses M_1, M_2 and M_3; V_{03} – velocity of relative movement of mass M_3; r_{1i}, r_{2i}, r_{3i} - position vectors of points A_i, B_i, C_i relative to the origins of the proper coordinate axes.

Consequently, the vector expressions of kinetic energies of masses M_1, M_2 and M_3 will have the form (is shown kinetic energy of mass M_1 only):

$$T_1 = \frac{1}{2}\sum_{i=1}^{n_1} M_{1i}[V_{01}^2 + (\omega_{01} \times r_{1i})^2 + V_{01}(\omega_{01} \times r_{1i})], \qquad (2)$$

where M_{1i}, M_{2i}, M_{3i} are masses of the particles A_i, B_i, C_i .

The vector expressions are converted into the analytical form with the help of the direction cosines and Euler's angles [8]**.** Then they (T_1, T_2, T_3) are reduced on the coordinate axes of the working member (M_1).

Kinetic energy of mass M_1 relative to the coordinate system $O_1'' x_1'' y_1'' z_1''$ has the following form:

$$\begin{aligned} T_1 = {} & \frac{1}{2}M_1(\dot{x}_1^2 + \dot{y}_1^2 + \dot{z}_1^2) + \frac{1}{2}[(J_{x1}\cos^2\alpha_1 + J_{z1}\sin^2\alpha_1)\dot{\theta}_1^2 + (J_{x1}\sin^2\alpha_1 + J_{z1}\cos^2\alpha_1)\dot{\varphi}_1^2 + \\ & + J_{y1}\dot{\psi}_1^2] + (J_{x1} - J_{z1})\sin\alpha_1\cos\alpha_1\dot{\theta}_1\dot{\varphi}_1 + (J_{x1}\cos^2\alpha_1 + J_{z1}\sin^2\alpha_1 - J_{y1})\dot{\theta}_1\dot{\psi}_1\varphi_1 + \\ & + (J_{z1} - J_{x1})\cos\alpha_1\sin\alpha_1\dot{\theta}_1\dot{\psi}_1\theta_1 + (J_{x1} - J_{z1})\cos\alpha_1\sin\alpha_1\dot{\varphi}_1\dot{\psi}_1\varphi_1 - \\ & - (J_{x1}\sin^2\alpha_1 + J_{z1}\cos^2\alpha_1)\dot{\varphi}_1\dot{\psi}_1\theta_1; \end{aligned} \qquad (3)$$

where $x_1, y_1, z_1, \theta_1, \psi_1, \varphi_1$ are linear and angular displacements of the center O_2 of mass M_2; J_{x1}, J_{y1}, J_{z1} - moments of inertia of mass M_2 about axes $O_1 x_1 y_1 z_1$.

Similar forms will have kinetic energies of masses M_2 and M_3.

3. EQUATIONS OF SPATIAL MOVEMENT OF THE WORKING MEMBER AND TECHNOLOGIC LOAD

The main difference between the system under research – vibratory technologic machine and classical n-mass system is stipulated by the following aspects: 1) Specificity of mass M_3 (load) performing relative movement with respect to mass M_1; 2) Predetermined location relative to each other of masses M_1, M_2, M_3 (vibro-drive, working member, load); 3) Pecularity of interaction of masses M_1 and M_3.

On the base of method of Lagrange we obtain the following differential equations of spatial movement of the system

$$\frac{d}{dt}\left(\frac{\partial T}{\partial \dot{q}} - \frac{\partial T}{\partial q}\right) = Q_q + Q_q', \qquad (4)$$

where T is the system kinetic energy; q – generalized coordinate that takes the values $x_1, y_1, z_1, \theta_1, \psi_1, \varphi_1$; $x_2, y_2, z_2, \theta_2, \psi_2, \varphi_2$; $x_3, y_3, z_3, \theta_3, \psi_3, \varphi_3$; Q_q - elastic and resistant forces stipulated by the machine elastic and damping system; Q_q' - forces that are not related with deformations of the elastic system or inertness of masses of the vibratory system under consideration (external exciting forces, forces of gravity, external forces resistant forces of the friction type and etc).

For illustration of the proposed approach consider a vibratory feeder with electromagnetic vibro-exciter (Fig.3) and its mathematical model with some assumptions. Namely, influence of the material on the working member dynamics will not be taken into account (kinetic and potential terms in the working member equations are presented in the linear form in contrast to the equations of the load, where kinetic terms are presented by the products of second order of the working member coordinates, their velocities and accelerations).

The research considers influence of the machine design errors and non-working spatial vibrations on the friable material vibratory movement.

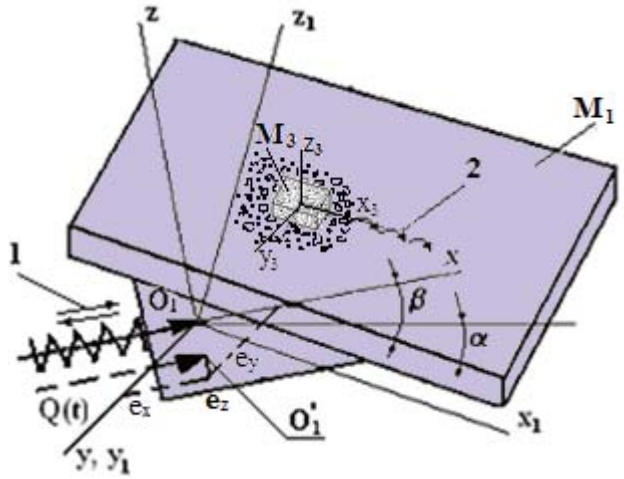

Fig. 3. *The errors of the force transmitted to the working member*

The equations of the working member will have the form

$$
\begin{aligned}
&M_1\ddot{x}_1 + c_x\dot{x}_1 + k_x x_1 - k_x'\theta_1 = Qf(\psi_0,\psi_1,\alpha_1);\\
&M_1\ddot{y}_1 + c_y\dot{y}_1 + k_y y_1 - k_y'\psi_1 = Qf(\varphi_0,\varphi_1,\theta_0,\theta_1,\alpha_1)\\
&M_1\ddot{z}_1 + c_z\dot{z}_1 + k_z z_1 - k_z'\varphi_1 = Qf(\psi_0,\psi_1,\alpha_1)\\
&J_\theta\ddot{\theta}_1 + c_\theta\dot{\theta}_1 + k_\theta\theta_1 - k_\theta'x_1 = Qf(e_y,e_z,\theta_0,\psi_0,\varphi_0,\alpha_1)\\
&J_\psi\ddot{\psi}_1 + c_\psi\dot{\psi}_1 + k_\xi\theta_1 - k_\theta'y_1 = Qf(e_x,e_z,\psi_0,\alpha_1)\\
&J_\varphi\ddot{\varphi}_1 + c_\varphi\dot{\varphi}_1 + k_\varphi\varphi_1 - k_\varphi'z_1 = Qf(e_x,e_y,\theta_0,\psi_0,\varphi_0,\alpha_1)
\end{aligned}
\qquad (5)
$$

where $C_x, C_y, C_z, C_\theta, C_\psi, C_\varphi, Q_q$ are coefficients of damping of the elastic system;

$k_x, k_y, k_z, k_\theta, k_\psi, k_\varphi$ - coefficients of rigidity; $k_x', k_y', k_z', k_\theta', k_\psi', k_\varphi'$ - coefficients relating lateral-rotary and longitudinal-torsional vibrations; $Q = Q_0 f(t)$, Q_0 – coefficient of the exciting forcr; $f(t)$ – regularity of variation of the exciting force.

Spatial vibratory movement along the coordinate axes will have the following form

$$
\begin{aligned}
&M_3[\ddot{y}_3 + \ddot{y}_1 + (\ddot{z}_1\theta_1 - \ddot{x}_1\varphi_1)\cos a_1 + (\ddot{x}_1\theta_1 + \ddot{z}_1\varphi_1)\sin a_1 - \theta_1 z_3 - 2\dot{\theta}_1\dot{z}_3 +\\
&+ 2\dot{\varphi}_1\dot{x}_3 - \ddot{x}_1(\varphi\cos a_1 - \theta_0\sin a_1) + \ddot{z}_1(\theta_0\cos a_1 + \varphi_0\sin a_1)] + B\dot{y}_3 - C'y_3 =\\
&= -fN_z sign(\dot{y}_3);\\
&M_3[\ddot{z}_3 + (\ddot{z}_1 + \ddot{x}_1\psi_1)\cos a_1 + (\ddot{x}_1 - \ddot{z}_1\psi_1)\sin a_1 - \theta_1\ddot{y}_1 + y_3\ddot{\theta}_1 + 2\dot{y}_3\dot{\theta}_1 -\\
&- 2\dot{x}_3\dot{\psi}_1 - \ddot{z}_1\psi_0\sin a_1 + \ddot{x}_1\psi_0\cos a_1 - \ddot{y}_1\theta_0] + D_1\dot{Z}_1 + E\dot{x}_1 + E'\dot{z}_3 + Cz_3 =\\
&= -fN_y sign(\dot{z}_3) - M_3 g\cos a_1,
\end{aligned}
\qquad (6)
$$

where coefficients A, B, B_1, C", D, E, E_1, C characterize state of the load relative to the working member surface (movement together with the surface or separately from it) and vary properly; $N_z = f(z_3, \dot{z}_3, \dot{z}_1)$, $N_y = f(y_3, \dot{y}_3, \dot{y}_1)$ - forces of the material normal reaction whose coefficients vary similarly to the above mentioned.

Equations (6) differ from generalized equations of the material spatial movement [4] by the terms generated from the errors of $\theta_0, \psi_0, \varphi_0$.

$$Q'_{x1} = Q(x,t); \tag{7}$$

where $Q(x,t)$ is a nonlinear exciting force;

$$Q = A\Phi^2;\ \dot{\Phi} = BF_1(t) - C(\delta - x_1)\Phi;$$

Φ – electromagnetic flow; A, B, C - coefficients depending on parameters of the electromagnetic vibro-exciter; δ – clearence of the electromagnet.

The system of equations was solved by the method of Runge-Kutta in the following limits of errors: for angular deviations $\theta_0, \psi_0, \varphi_0$ = (0 - 0,15) rad; for deviations of the force direction e_x, e_y, e_z = (0 – 0,015) m.

For greater visualization of influence of the mentioned deviations on the process the vibrations were enhanced in one concrete direction or another by resonating with the exciting force (in combination of variation of the errors).

Below are given some results of the modeling (Fig. 4-7), where are shown dependences of the material velocity V and other dynamical characteristics (z_3, y_3, N_z, N_y) on the non-working vibrations (y_1, φ_1, z_1, ψ_1) caused by the working member design errors ($\theta_0, \psi_0, \varphi_0, e_0, e_0, e_0$).

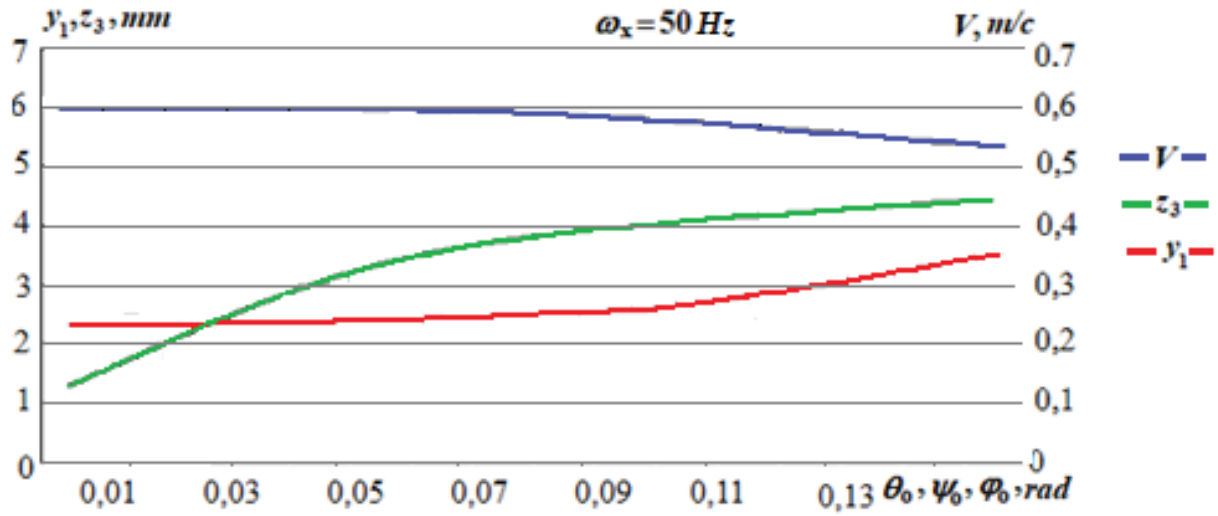

Fig. 4. *Dependences of V and z_3 on $\theta_0, \psi_0, \varphi_0$ and y_1.*

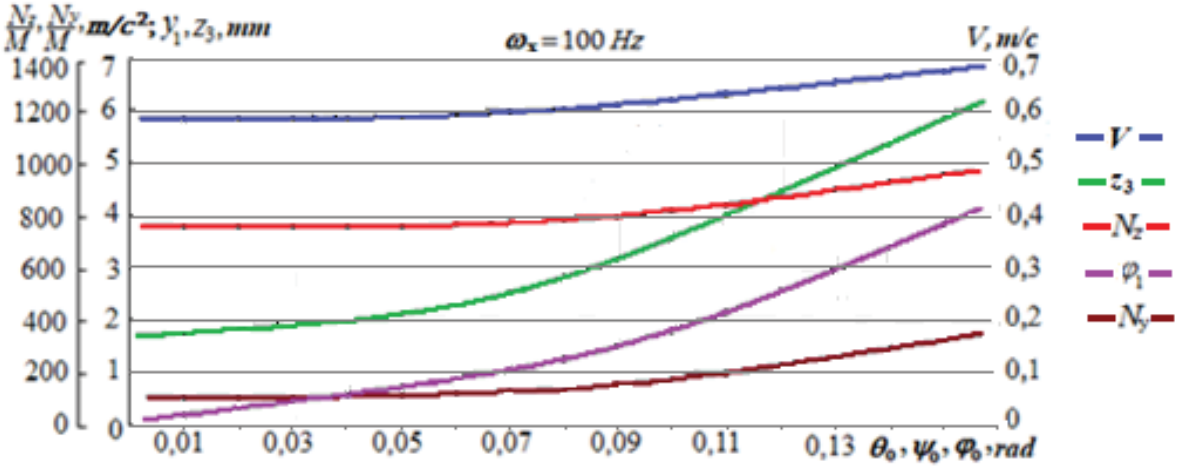

Fig. 5. *Dependences of V, z_3, N_z and N_y on $\theta_0, \psi_0, \varphi_0$ and ϕ_1*

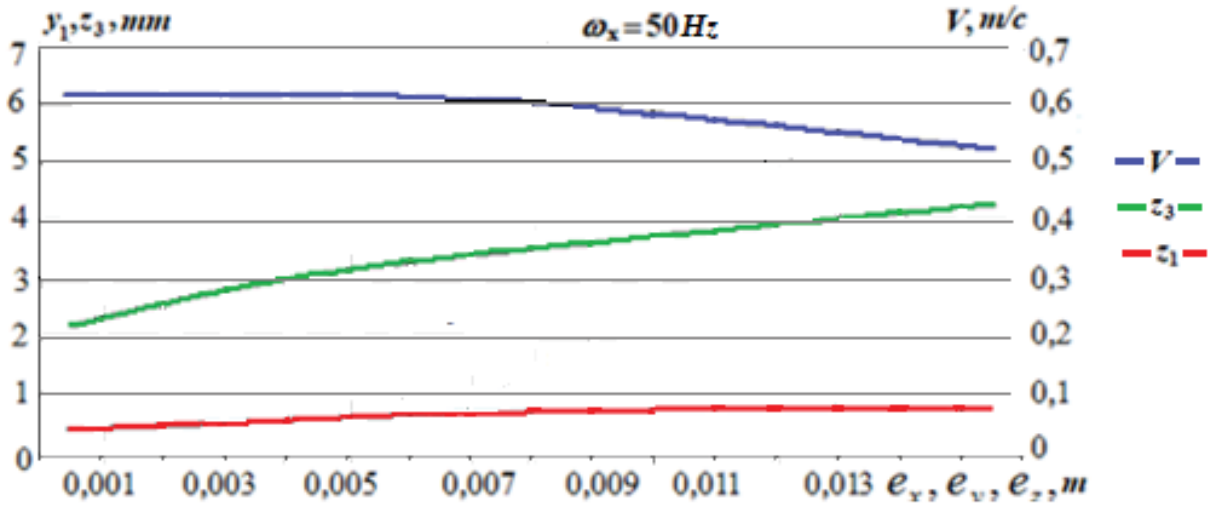

Fig. 6. *Dependences of V and z_3 on e_x, e_y, e_z and z_1*

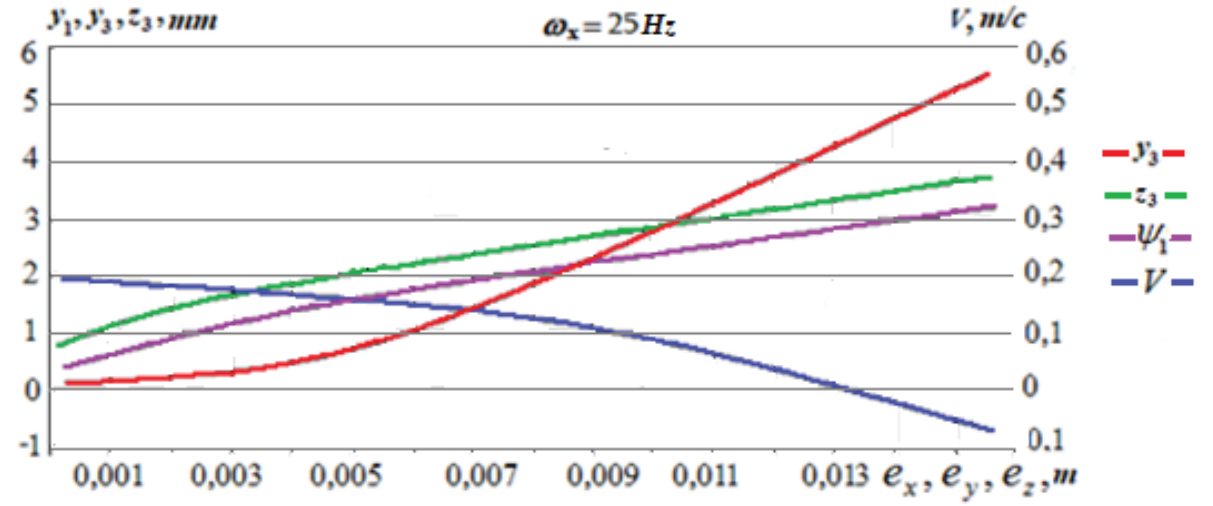

Fig. 7. *Dependences of V, y_3 and z_3 on e_x, e_y, e_z and ψ_1*

4. DISSCUSION

The design and assemblage errors in the vibratory transport and technologic machines (especially in the resonant ones) can cause a significant distortion of conformity with a law of the technologic process. Development of the spatial dynamical and corresponding mathematical models of the vibratory technologic system (vibrator – working member – load) was considered expedient for complex study of this problem.

The obtained mathematical model is universal and it ensures complex research into the technologic process. The results of influence of the spatial (non-working) vibrations (Fig.2) and eccentricity caused by the improper transfer of the force (Fig.3) on the process of vibratory displacement of the friable material are presented in the work.

The approach to the research envisaged enhancing of each non-working ("parasitic") spatial vibration at retaining other vibrations in the admissible limits. As the results of modeling have shown, in most cases, the non-working vibrations have a negative influence on the velocity of the material displacement (Fig. 4, 6, 7) but in some cases, increase of velocity takes place (Fig 5). It should also be noted that non-working spatial vibrations have a significant influence on the material displacement in the vertical direction (z3) (Fig.4, 5, 6, 7) or on the intensity of displacement.

The analysis of the research results have shown that improvement of the vibratory technologic process is mainly possible by combination of the basic working vibrations and some non-working, so called parasitic vibrations that implies design changes of the vibratory machine and will present the subject of the author's further research.

4.1. CONCLUSION

1. The considered approach and a mathematical model of spatial movement of the system "vibro-drive – working member – friable load" allows to realize complex research into the vibratory technologic process by the mathematical modeling;
2. Design errors of the vibratory transportation technologic machine have an influence on the process that is more expressed in the resonant machines;
3. The errors at their certain combination can promote improvement of the process indices (velocity for example, Fig.5) that may be realized in the machine.

Acknowledgements

This work was supported by Shota Rustaveli National Science Foundation of Georgia (SRNSFG) [N FR17_292, "Mathematical modeling of the vibratory technologic processes and design of the new, highly effective machines"

REFERENCES

[1]. I.I. Blekhman, Theory of Vibration Processes and Devices. Vibration mechanics and vibration technology, Ore and metals, SPB, 2013 (in Russian).
[2]. I. Goncharevich. Theory of Vibratory Technology. Hemisphere Publisher, 1990 (in Russian).
[3]. I. I. Fedorenko, Vibration processes and devices in the agroindustrial complex: monograph. RIO of the Altai State University, Barnaul, 2016 (in Russian). http://www.asau.ru/ru/mekhanizatsii-zhivotnovodstva?task=getfile&fileid=15612.
[4]. V. Zviadauri. Dynamics of the vibratory transportation and technological machines; "Mecniereba", 2001(in Russian).
[5]. L.Vaisberg, I. Demidov, K. Ivanov, Mechanics of granular materials under vibration action: Methods of description and mathematical modeling. Enrichment of ores. № 4 (2015) 21-31.

http://rudmet.net/media/articles/Article_OR_04_15_pp.21-31_1.pdf (in Russian).

[6]. V. S. Zviadauri, T. M. Natriashvili, G. I Tumanishvili, T. N. Nadiradze, The features of modeling of the friable material movement along the spatially vibrating surface of the vibratory machine working member. Mechanics of machines, mechanisms and materials, 1 (38), (2017) 21-26 (in Georgian).

[7]. V. S. Zviadauri, M. A. Chelidze, G. I. Tumanishvili, On the spatial dynamical model of vibratory displacement, Proceedings of the International Conference of Mechanical Engineering; London, U.K., 30 June - 2 July, (**2010)** 1567 – 1570.

[8]. R. Ganiev, V. Kononenko, Oscillations of solids. M. Nauka, 1976 (in Russian). http://stu.scask.ru/book_cst.php.

[9]. O. G. Loktionova, Dynamics of vibratory technological processes and machines for the processing of granular materials, Dissertation, 2008 (in Russian). http://www.dissercat.com/content/dinamika-vibratsionnykh-tekhnologicheskikh-protsessov-i-mashin-dlya-pererabotki-neodnorodnyk.

GUIDE FOR AUTHORS

Papers to be published in "Annals of Agrarian Science" must meet the following requirements:

1. A paper must deal with a temporary problem, methods of investigation and analysis of the received data. The title of a paper must completely reflect its content. The structure of a paper must be standardized by the following subtitles: Introduction, Objectives and Methods, Experimental Section, Results and Analysis, Conclusion, References.
2. Authors have to submit their manuscript to the journal's homepage: http://journals.org.ge/index.php

   Paper arrangement:
   - Field of science in top right-hand corner.
   - Title.
   - Surnames, first names and patronymics of the authors.
   - Name of the institution, address, positions and scientific degrees of the authors.
   - Annotation (10-12 lines, about 500 typographic units).
   - Body of a paper.
   - Pictures, graphs, photos on separate pages.
   - List of references in the order of citation; References in the text must be given in square brackets.
   - Summary (about 500 typographic units).
   - All the pages must be paginated.
   - Text must be in Times New Roman, prints 11,14.
   - A paper must contain about 15-20 typewritten pages including pictures, graphs, Tables, etc., in 1.5-2 spacing (about 20 thousand typographic units, prints 12, 14). White paper A-4, 25-30 mm margins from the four sides.
   - Language: English.
3. Arrangement of Figures:
   Tables must be numbered with Arabic numerals according to their appearance in a text. Tables must be titled.
   All the Figures and Tables must be titled and lined vertically.
   Words in Tables must not be abbreviated.
   Arrangement of figures in lines must be distinct.
   The same data must not be repeated in tables, graphs and a text.
4. Arrangement of illustrations:
   Pictures and photos must not be glued, they must be attached at the end of a paper.
   Pictures must be drawn in Indian ink on white paper or using computer graphics. Pictures must be very distinct. Legends must be placed according to a text.
   Comments on picture margins must be brief.
   Photos must be presented on glossy paper in two copies (xerox copies will not be accepted) not damaged.
   Pictures and photos must be numbered on back sides and the names of authors must be written in pencil.
   Comments to photos and pictures in a text must coincide with their contents.
5. Arrangement of illustrations and Tables in a text must be indicated on the margins with pencil.
6. Indication of references:
   For papers: surnames and initials of the authors, title of the article, journal, volume, number, year, pages.
   For books: surnames and initials of the authors, book, place of publishing, year, total number of pages.
7. Corrected version will not be returned to the authors.
8. Declined papers will not be returned to the authors.
9. The Editorial Board reserves the right not to consider papers which are arranged ignoring the instructions.
10. In the case of any questions, please feel free to contact us: editorial@agrscience.ge